frontiers | Research Topics

Ultrasound in rheumatology - a polyhedric imaging tool

Edited by
Andrea Di Matteo and Christian Dejaco

Published in
Frontiers in Medicine
Frontiers in Immunology

ISSN 1664-8714
ISBN 978-2-83251-724-6
DOI 10.3389/978-2-83251-724-6

About Frontiers

Frontiers is more than just an open access publisher of scholarly articles: it is a pioneering approach to the world of academia, radically improving the way scholarly research is managed. The grand vision of Frontiers is a world where all people have an equal opportunity to seek, share and generate knowledge. Frontiers provides immediate and permanent online open access to all its publications, but this alone is not enough to realize our grand goals.

Frontiers journal series

The Frontiers journal series is a multi-tier and interdisciplinary set of open-access, online journals, promising a paradigm shift from the current review, selection and dissemination processes in academic publishing. All Frontiers journals are driven by researchers for researchers; therefore, they constitute a service to the scholarly community. At the same time, the *Frontiers journal series* operates on a revolutionary invention, the tiered publishing system, initially addressing specific communities of scholars, and gradually climbing up to broader public understanding, thus serving the interests of the lay society, too.

Dedication to quality

Each Frontiers article is a landmark of the highest quality, thanks to genuinely collaborative interactions between authors and review editors, who include some of the world's best academicians. Research must be certified by peers before entering a stream of knowledge that may eventually reach the public - and shape society; therefore, Frontiers only applies the most rigorous and unbiased reviews. Frontiers revolutionizes research publishing by freely delivering the most outstanding research, evaluated with no bias from both the academic and social point of view. By applying the most advanced information technologies, Frontiers is catapulting scholarly publishing into a new generation.

What are Frontiers Research Topics?

Frontiers Research Topics are very popular trademarks of the *Frontiers journals series*: they are collections of at least ten articles, all centered on a particular subject. With their unique mix of varied contributions from Original Research to Review Articles, Frontiers Research Topics unify the most influential researchers, the latest key findings and historical advances in a hot research area.

Find out more on how to host your own Frontiers Research Topic or contribute to one as an author by contacting the Frontiers editorial office: frontiersin.org/about/contact

Ultrasound in rheumatology - a polyhedric imaging tool

Topic editors

Andrea Di Matteo — Leeds Teaching Hospitals NHS Trust, United Kingdom

Christian Dejaco — Medical University of Graz, Austria

Citation

Di Matteo, A., Dejaco, C., eds. (2023). *Ultrasound in rheumatology - a polyhedric imaging tool*. Lausanne: Frontiers Media SA. doi: 10.3389/978-2-83251-724-6

Table of contents

frontiers | Frontiers in Medicine

TYPE Editorial
PUBLISHED 07 February 2023
DOI 10.3389/fmed.2023.1150111

OPEN ACCESS

EDITED AND REVIEWED BY
João Eurico Fonseca,
University of Lisbon, Portugal

*CORRESPONDENCE
Andrea Di Matteo
✉ andrea.dimatteo@hotmail.com

SPECIALTY SECTION
This article was submitted to Rheumatology, a section of the journal Frontiers in Medicine

RECEIVED 23 January 2023
ACCEPTED 30 January 2023
PUBLISHED 07 February 2023

CITATION
Di Matteo A and Dejaco C (2023) Editorial: Ultrasound in rheumatology—A polyhedric imaging tool. *Front. Med.* 10:1150111. doi: 10.3389/fmed.2023.1150111

Editorial: Ultrasound in rheumatology—A polyhedric imaging tool

Andrea Di Matteo[1,2]* and Christian Dejaco[3,4]

[1]Rheumatology Unit, Department of Clinical and Molecular Sciences, Polytechnic University of Marche, "Carlo Urbani" Hospital, Ancona, Italy, [2]Faculty of Medicine and Health, Leeds Institute of Rheumatic and Musculoskeletal Medicine, University of Leeds, Leeds, United Kingdom, [3]Department of Rheumatology, Medical University Graz, Graz, Austria, [4]Department of Rheumatology, Hospital of Bruneck (ASAA-SABES), Teaching Hospital of the Paracelsus Medical University, Bruneck, Italy

KEYWORDS

ultrasound, rheumatology, joint, soft tissues, imaging

Editorial on the Research Topic
Ultrasound in rheumatology—A polyhedric imaging tool

In recent years, ultrasound (US) has become a pivotal tool in the diagnosis, differential diagnosis, follow-up and management of patients with rheumatic and musculoskeletal diseases (RMDs), such as rheumatoid arthritis (RA), spondylarthritis (SpA), crystal arthropathies and connective tissue diseases (CTDs) (1–4). Recent studies have also highlighted the potential value of this technique in the assessment of extra-articular "targets" of rheumatic diseases, such as muscles, salivary glands, nerves, skin and lungs. In large vessel vasculitis, the key diagnostic role of US has widely been recognized (5).

The articles included in the current Research Topic bring new insights into the application of US in the diagnosis and characterization of joint and extra-articular manifestations in a broad spectrum of RMDs. Although focused on US, research on other imaging techniques have been presented, as well as a comparison between US and other imaging methodologies, which is important for the understanding of the role of US in the assessment of RMDs.

Previous studies have shown the promising role of US in improving the prediction for the development of RA in individuals "at-risk" for this disease (6). In the current Research Topic, Harnden et al. reviewed the value of available imaging modalities for this purpose, including US, but also conventional radiography, magnetic resonance imaging (MRI), quantitative computed tomography (CT) and nuclear imaging, and the rationale for their use in the main populations "at-risk" of RA. According to the algorithm proposed for the use of imaging in these "at-risk" populations, US should be used as first line in "at-risk" individuals with musculoskeletal (MSK) symptoms (i.e., clinically suspect arthralgia or ACPA positive individuals with inflammatory MSK symptoms). If the US is negative, MRI may be used to identify sub-clinical inflammation, particularly at extracapsular structures. Radiographs should be used in "at-risk" individuals with non-inflammatory MSK symptoms to rule out alterative diagnoses. In "at-risk" individuals with no MSK symptoms (i.e., asymptomatic first-degree relatives or ACPA positive individuals), no imaging may be required given the absence of evidence suggesting the diagnostic or predictive value of any imaging techniques in this population.

Carbonell-Bobadilla et al. explored whether RA patients show a different phenotype according to the presence or absence of RA-related autoantibodies. The authors found that seronegative RA patients (i.e., negative for ACPA and rheumatoid factor) had a later disease onset and required less anti-rheumatic therapies than seropositive patients. In contrast, seropositive RA patients revealed more inflammation and joint damage on US.

In a study on human cadavers, Baksa et al. provided a high-resolution anatomical map on the arterial vasculature of healthy human metacarpophalangeal joints, thus providing an important basis for the evaluation of the vascularization of these joints by US.

Ventura-Rios et al. compared the extent of enthesitic changes in patients with SpA and gout using the US-based Madrid Sonographic Enthesis Index (MASEI). The overall MASEI was similar in both groups, however the prevalence and distribution of the US findings indicating inflammation and structural damage varied depending on the enthesis evaluated. While the prevalence of bone erosions and power Doppler signal was higher in patients with SpA in comparison with gout (especially at the Achilles tendon enthesis), gout patients had a higher prevalence of US structural damage, including calcifications/enthesophytes, especially at the proximal patellar tendon.

Geng et al. investigated the value of US detected tenosynovitis and/or enthesitis in improving the diagnosis of PsA according to the CASPAR criteria, using the clinically based diagnosis by the rheumatologist as the gold standard. In this study, 326 consecutive patients [164 with PsA and 162 with other conditions, such as psoriasis (PsO), osteoarthritis with PsO/family history of PsO, fibromyalgia with PsO, seronegative RA and undifferentiated arthritis] were consecutively enrolled. The diagnostic accuracy for CASPAR criteria increased from 89.3% to 93.6% when US was added to the clinical assessment in the included patients.

In a systematic literature review (SLR), Sakellariou et al. analyzed the evidence on the applications of US for the detection of subclinical involvement of joints and entheses in patients with inflammatory bowel diseases (IBD) with no previous history of inflammatory arthritis ("non-arthropathic IBD"). The main finding of this SLR was the high variability in the frequency of both chronic and acute inflammatory US lesions in patients with IBD, particularly in regard to the overall prevalence of the joint and entheseal abnormalities (mainly power Doppler signal). The limited evidence supporting the use of US in this population highlighted the need for more research on this topic.

Temporomandibular joint (TMJ) disorders are common in the general population as well as in patients with rheumatic diseases. In a narrative review, Maranini et al. discussed the role of US and MRI in the evaluation of TMJ disorders, proposing an imaging-based algorithm for the diagnosis of these conditions. According to the authors, US should be used as an "entry-criterion," given the high availability and relatively low costs of this imaging technique, including asymptomatic "at-risk" patients, such as those with RA. MRI (or CT scan in alternative) could be used in case of a non-conclusive US examination as well as during follow-up.

Barbosa-Cobos et al. developed a novel technique using pixel analysis (i.e., image J) for the interpretation of sono-elastography in the assessment major salivary glands. This methodology helped to discriminate between patients with Sjogren's syndrome and healthy subjects and revealed a significant association with patients' clinical features (i.e., "sicca symptoms"), objective evaluation of ocular and oral dryness, and histologic findings.

In a web-based multicentric study involving 42 rheumatologists and 2 radiologists from 13 countries, Di Matteo et al. highlighted the good inter and intra-rater reliability of two recently developed visual scales for the assessment of US muscle echogenicity using images and clips from patients with different rheumatic diseases. The scope of these scales is to detect (the often underestimated) sarcopenia "early" in patients with RMD (7).

Two articles focused on the role of US in giant cell arteritis (GCA). In a narrative review, Kirby et al. discussed the current use of US in routine clinical practice in patients with GCA, as well as the current evidence on the reliability and applicability of this imaging technique, highlighting the importance of incorporating US into diagnostic algorithms to improve the diagnosis of GCA. In a retrospective study, López-Gloria et al. developed new cut-off values for the measurement of intima-media thickness of cranial and extra-cranial arteries to discriminate between patients with and without GCA. These newly proposed cut-off values could potentially improve the diagnostic accuracy of US in this condition.

Finally, Zaottini et al. provided an overview on the role of US in the assessment of peripheral neuropathies of rheumatological interest, describing the different pathologic features and patterns of nerve involvement observed in the most common RMDs, such as Sjogren's syndrome, systemic sclerosis, RA, PsA, Behcet's syndrome, small and large vessels vasculitis, sarcoidosis and crystal arthropathies. The authors also described the potential advantages and limitations of using US for the assessment of peripheral neuropathies in comparison with other imaging techniques, such as MRI, and in addition to the diagnostic work-up that is routinely carried out in these conditions (e.g., nerve conduction study).

In conclusion, the current Research Topic provides a collection of papers, which highlights the recent advances, and potential applications of US in several RMDs. Several articles also showed the potential value of US in the assessment of extra-articular manifestations in patients with CTDs and large vessel vasculitis.

Author contributions

ADM and CD are guest editors of this Research Topic. All authors have made a substantial, direct, and intellectual contribution to the work and approved it for publication.

Conflict of interest

The authors declare that the research was conducted in the absence of any commercial or financial relationships that could be construed as a potential conflict of interest.

Publisher's note

References

1. Di Matteo A, Mankia K, Azukizawa M, Wakefield RJ. The role of musculoskeletal ultrasound in the rheumatoid arthritis continuum. *Curr Rheumatol Rep.* (2020) 22:41. doi: 10.1007/s11926-020-00911-w

2. Filippucci E, Smerilli G, Di Matteo A, Grassi W. Ultrasound definition of enthesitis in spondyloarthritis and psoriatic arthritis: arrival or starting point? *Ann Rheum Dis.* (2021) 80:1373–75. doi: 10.1136/annrheumdis-2021-220478

3. Cipolletta E, Filippucci E, Abhishek A, Di Battista J, Smerilli G, Di Carlo M, et al. In patients with acute mono-oligoarthritis, a targeted ultrasound scanning protocol shows great accuracy for the diagnosis of gout and CPPD. *Rheumatology (Oxford).* (2022) 23:keac479. doi: 10.1093/rheumatology/keac479

4. Cipolletta E, Filippou G, Scirè CA, Di Matteo A, Di Battista J, Salaffi F, et al. The diagnostic value of conventional radiography and musculoskeletal ultrasonography in calcium pyrophosphate deposition disease: a systematic literature review and meta-analysis. *Osteoarthr Cartil.* (2021) 29:619–32. doi: 10.1016/j.joca.2021.01.007

5. Dejaco C, Ramiro S, Duftner C, Besson FL, Bley TA, Blockmans D, et al. EULAR recommendations for the use of imaging in large vessel vasculitis in clinical practice. *Ann Rheum Dis.* (2018) 77:636–43. doi: 10.1136/annrheumdis-2017-212649

6. Di Matteo A, Corradini D, Mankia K. What is the value of ultrasound in individuals? 'at-risk' of rheumatoid arthritis who do not have clinical synovitis? *Healthcare (Basel).* (2021) 9:752. doi: 10.3390/healthcare9060752

7. Di Matteo A, Smerilli G, Cipolletta E, Wakefield RJ, De Angelis R, Risa AM, et al. Muscle involvement in systemic lupus erythematosus: multimodal ultrasound assessment and relationship with physical performance. *Rheumatology (Oxford).* (2022) 61:4775–85. doi: 10.1093/rheumatology/keac196

frontiers | Frontiers in Medicine

SYSTEMATIC REVIEW
published: 16 May 2022
doi: 10.3389/fmed.2022.919521

Musculoskeletal Ultrasound to Identify Subclinical Joint and Periarticular Involvement in Patients With Inflammatory Bowel Disease: A Systematic Literature Review

Garifallia Sakellariou[1,2*], *Annalisa Schiepatti*[2,3], *Davide Scalvini*[2,3], *Francesca Lusetti*[2,3], *Erica Fazzino*[2,3], *Federico Biagi*[2,3] *and Carlomaurizio Montecucco*[2,4]

[1] Istituti Clinici Scientifici Maugeri IRCCS, Pavia, Italy, [2] Department of Internal Medicine and Medical Therapy, University of Pavia, Pavia, Italy, [3] Gastroenterology Unit, Istituti Clinici Scientifici Maugeri IRCCS, Pavia, Italy, [4] Chair and Division of Rheumatology, IRCCS Policlinico San Matteo Foundation, Pavia, Italy

Background: Musculoskeletal ultrasonography identifies subclinical joint and entheseal inflammation, and it might be of value in patients with inflammatory bowel diseases (IBD), which are at higher risk of inflammatory arthropathy and disability. Our aim was to retrieve the evidence on the applications of ultrasound in patients with non-arthropathic IBD.

Methods: Studies enrolling patients with IBD without arthritis, undergoing ultrasound of joints, tendons or entheses were eligible. The outcomes of interest encompassed the frequency of ultrasound-detected lesions, their accuracy in diagnosing arthritis, their prognostic role and sensitivity to change. All study types, excluding case reports, case series and narrative reviews, were included. Search strategies were applied in PubMed and Embase. Abstract and full-texts were evaluated by pairs of reviewers. The risk of bias was evaluated through the Newcastle-Ottawa scale or the Quality Assessment of Diagnostic Accuracy Studies (QUADAS) 2. The protocol was registered in PROSPERO (CRD42021264972).

Results: Out of 2,304 records, eight studies were included, all reporting the frequency of lesions, while only three evaluated also the diagnostic accuracy. All studies had a cross-sectional design, with no evidence on prediction or follow-up. All studies evaluated the entheses, while only three the joints. The most common chronic lesions were entheseal thickening (up to 81.5%) and enthesophytes (67.9%), while entheseal erosions were present in 16%−17% of patients. Among inflammatory lesions, power Doppler was reported in 14%−67% of patients. There were no differences among Crohn's disease or ulcerative colitis and depending on disease activity, while there were contrasting results on different disease durations. When evaluating the diagnostic performance, the best specificity for a diagnosis if IBD was 0.88 (95%CI, 0.8–0.94) for joint abnormalities. Also, the best sensitivity was 0.88 (95%CI, 0.76–0.95) for entheseal lesions. No studies assessed of the combination of lesions. Due to the limited number of studies, meta-analyses were not performed.

OPEN ACCESS

Edited by:
Andrea Di Matteo,
Marche Polytechnic University, Italy

Reviewed by:
Marco Di Carlo,
Marche Polytechnic University, Italy
Gabriele De Marco,
University of Leeds, United Kingdom

****Correspondence:***
Garifallia Sakellariou
filiciasak@gmail.com

Specialty section:
This article was submitted to Rheumatology, a section of the journal Frontiers in Medicine

Received: *13 April 2022*
Accepted: *27 April 2022*
Published: *16 May 2022*

Citation:
Sakellariou G, Schiepatti A, Scalvini D, Lusetti F, Fazzino E, Biagi F and Montecucco C (2022) Musculoskeletal Ultrasound to Identify Subclinical Joint and Periarticular Involvement in Patients With Inflammatory Bowel Disease: A Systematic Literature Review. Front. Med. 9:919521. doi: 10.3389/fmed.2022.919521

Conclusions: Despite the possible value of ultrasound in IBD, there is limited evidence deriving from cross-sectional studies. Longitudinal studies are needed to clarify the role of this technique, while its current placement might be that of complementing clinical assessment, in particular in early intestinal disease.

Keywords: arthritis, disability, inflammatory bowel disease, imaging, ultrasonography, systematic literature review

INTRODUCTION

Inflammatory bowel diseases (IBD), which include Crohn's disease (CD) and ulcerative colitis (UC), are common chronic inflammatory diseases of the gastro-intestinal tract characterized by unknown etiology and heterogeneous clinical manifestations, both intestinal and extra-intestinal (1–4). The key diagnostic features of UC include diffuse mucosal inflammation extending proximally from the rectum, whereas in CD patchy and segmental transmural inflammation can occur in any site of the gastrointestinal tract (1–4). Among the extra-intestinal manifestations of IBD, inflammatory arthritis, pertaining to the group of spondyloenthesoarthritis (SpA), is undoubtedly the most common, with an estimated prevalence ranging from 13 to 39% of all IBD patients (5–11). The clinical phenotypes of IBD-associated SpA include peripheral arthritis and axial manifestations related to sacroiliitis with or without concomitant spondylitis, and imply a chronic joint involvement and increasing disability (12). Musculoskeletal symptoms leading to the diagnosis of SpA usually develop after the diagnosis of IBD, but in up to 20% of patients rheumatological involvement precedes the gastrointestinal symptoms and leads to the diagnostic suspicion of IBD (7, 13, 14).

In the last years, clinical interest has been dedicated to IBD patients who have undiagnosed SpA (5, 15), reflecting the promising results achieved in the similar field of patients with psoriasis (16). In fact, in patients affected by psoriasis without joint involvement, imaging-detected inflammation of joints and periarticular structures significantly predicted the subsequent development of arthritis (17).

Ultrasound assessment of entheseal and joint sites has been recognized as a powerful and reliable tool to evaluate subclinical joint involvement (15). In fact, ultrasound has shown a greater accuracy to identify musculoskeletal inflammation, compared to clinical evaluation (18), and this might even be of greater relevance in patients with IBD, as some immunosuppressive treatments might mask an underlying joint involvement. However, little is known on the prevalence of occult SpA in IBD patients and the diagnostic and prognostic relevance of ultrasonographic articular/enthesal findings in this subgroup of patients.

The aim of the present systematic literature review is to evaluate the available evidence on the prevalence of ultrasonographic abnormalities in IBD patients without a previous history of inflammatory arthritis and their diagnostic and prognostic role.

METHODS

The SLR was conducted following the PRISMA 2020 Checklist (19). The target population consisted of patients with a diagnosis of IBD and no previous diagnosis of inflammatory arthritis. Five clinical questions were identified, in order to drive the searches and the inclusion of the articles. The areas of interest encompassed the frequency of ultrasound-detectable abnormalities in the joints and tendons, the diagnostic performance of ultrasonographic variables in the diagnosis of arthritis, with clinical diagnosis as reference standard, the prognostic value of ultrasonographic findings in identifying patients at risk of development of arthritis, and the value of ultrasound in monitoring abnormalities. The research questions were transformed into the Patients, Intervention, Comparator, Outcome, Study Type (PICOs) format (**Table 1**), sharing pre-defined inclusion and exclusion criteria. Moreover, we planned subgroup assessments for each research question, comparing CD and UC, patients with and without arthralgia, patients with mechanical and inflammatory arthralgia, patients with active and inactive IBD, patients with different disease duration of IBD, patients with joint symptom duration of less or more than 12 months. The protocol of the SLR was shared among authors and registered in the PROSPERO database (registration number CRD42021264972).

Search strategies were applied to PubMed and Embase by one author (GS; January 1st 1980–July 29th 2021; **Supplementary Table S1**). The time interval was chosen to include all studies since the introduction of musculoskeletal ultrasound. The records retrieved were transferred into a bibliographic management software (Zotero) and duplicates removed. Four investigators (EF, FL, DS, AS) performed screening, selection, data extraction and Risk of Bias (RoB) assessment, working in pairs to assess titles and abstracts to define eligibility for detailed review. Full texts of the included records were retrieved, and eligibility for final inclusion was assessed. Disagreement was resolved by discussion within the pairs and, further, by involving a fifth reviewer (GS). Data from the included articles were extracted in pre-specified forms, including general information on the article, features of the population and, when available, 2 × 2 tables of diagnostic accuracy, 2 × 2 contingency tables, Odds Ratios or Risk Ratios. The references of the included studies were screened to look for further eligible articles. The RoB of the studies included

TABLE 1 | Research questions and corresponding PICOs, driving the literature search and the inclusion/exclusion of the articles. Population and Intervention are the same for all research questions.

Research question	Population	Intervention	Comparator/Reference standard	Outcome	Study type
What is the frequency of abnormalities, detected in the joints and in periarticular structures by ultrasonography, in patients with IBD without a diagnosis of arthritis?	Adult patients with IBD without a diagnosis of arthritis	Musculoskeletal US of joints and tendons, including entheses	Not required	Frequency of US abnormalities	Longitudinal or cross-sectional cohort studies, case-control studies, randomized clinical trials, systematic literature reviews, meta-analyses, diagnostic accuracy studies, case series
What is the value of ultrasonographic findings in making a diagnosis of arthritis in patients with IBD without a diagnosis of arthritis?			Clinical diagnosis of arthritis	Diagnostic accuracy: sensitivity, specificity, AUC, diagnostic Odds Ratio, LR+, LR–, PPV, NPV	Longitudinal or cross-sectional cohort studies, case-control studies, randomized clinical trials, systematic literature reviews (in order to review the references), meta-analyses, diagnostic accuracy studies, case series
What is the prognostic value of ultrasonographic findings against the development of arthritis in patients with IBD without a diagnosis of arthritis?			Other predictors of arthritis (not required)	Development of arthritis: OR, RR, HR	Longitudinal cohort studies, case-control studies, systematic literature reviews (in order to review the references), meta-analyses, case series
What is the value of ultrasonography in monitoring lesions in the joints and periarticular structures in patients with IBD without a diagnosis of arthritis?			Other means (clinical assessment, other imaging) to monitor the joints (not required)	Sensitivity to change	Longitudinal cohort studies, case-control studies, systematic literature reviews (in order to review the references), meta-analyses, case series

TABLE 2 | Summary of frequencies for each entheseal lesion.

	Any lesion	Chronic lesions	Acute lesions	Increased thickness	Hypoechogenicity	Power Doppler	Bursitis	Erosions	Entesophytes	Calcifications
All entheses	30*-87.9	83–83.8	31–43.8	81.5	–	14–67	27.1	15–16	67.9	–
CD	83.8	79.4	42.2	–	–	21.5	–	–	–	–
UC	90.2	87	45.3	–	–	31.6	–	–	–	–
Triceps tendon	–	–	–	73.3*	0*	0*	–	0*	0*	0*
Quadriceps	–	–	–	5.71*-40.7*	10.5*	2.3*-2.5	0–7.86*	0*-2.5	0*-38.2	0*
Proximal patellar	–	–	–	8.57*-42	4.7*	0–3.5*	0	0*-3.7	0*-2.4	1.2*
Distal patellar	–	–	–	6.43*-58	19.8*	3.7–16.3*	0*-21	0*-3.7	0*-7.4	1.2*
Achilles tendon	–	–	–	0.71*-23.3*	33.7*	0–20.9*	2.14*-7.4	0*-1.2	1.4*-56.8	2.3*
Plantar fascia	–	–	–	0*-16	1.2*	1.2	0	0*-2.5	0*-3.7	0*

*Results are presented as percentages and ranges, when available; * proportion of entheses; when not specified percentages refer to the proportion of patients.*

only in the analysis on the prevalence of abnormalities was assessed with the Newcastle-Ottawa scale (NOS) for cohort and case-control studies (20), while studies included in the diagnostic question were evaluated through the Quality Assessment of Diagnostic Accuracy Studies (QUADAS-2) tool for diagnostic studies (21). Results were presented in summary of evidence tables. Diagnostic accuracy meta-analyses could be considered in case data on a single variable were available from at least four clinically homogeneous studies. Summary graphs reporting sensitivities and specificities were created with Review Manager (RevMan) Version 5.4, The Cochrane Collaboration, 2020.

RESULTS

Of 2,304 abstracts evaluated, eight studies were finally included (15, 22–27). Of those, seven articles were retrieved from the electronic databases and one by hand search (**Figure 1**) (28). The total number of included patients was 679. All of these studies allowed to derive information on the frequency of lesions, while only three studies presented data on the diagnostic accuracy of ultrasonographic findings to identify patients with arthritis among patients with IBD (22, 24, 25). Three studies had a case-control design (15, 23, 24), while the remaining were cross-sectional studies. The absence of prospective studies, therefore, did not allow to retrieve any evidence on the value of musculoskeletal ultrasound to define prognosis and to monitor joint and entheseal lesions. All of the included studies assessed various entheseal sites (**Table 2**), while only three included also an evaluation of joints (22, 26, 28). A single study reported scanning synovial tendons (22). In particular, the quadriceps tendon, the proximal and distal patellar tendons, the Achilles tendon and plantar fascia were assessed in all of the studies, the insertion

TABLE 3 | Assessment of the risk of bias. Newcastle-Ottawa Scale: each asterisk refers to the fulfillment of the items of the different components of the scale. QUADAS-2: green refers to a low risk of bias, yellow to unclear risk of bias and red to high risk of bias.

What is the frequency of abnormalities, detected in the joints and in periarticular structures by ultrasonography, in patients with IBD without a diagnosis of arthritis? Newcastle-Ottawa Scale

Study	Selection	Comparability	Outcome/exposure
Bandinelli et al. (15)	***	**	***
Hsiao et al. (23)	*	*	***
Rodriguez-Caminero and Queiro (28)	****	*	*
Rovisco et al. (26)	***	*	*
Ureyen et al. (27)	***	*	*

What is the value of ultrasonographic findings in making a diagnosis of arthritis in patients with IBD without a diagnosis of arthritis? QUADAS-2

Study	Selection	Test	Standard	Flow/Timing
Bertolini et al. (22)				
Martinis et al. (25)				
Husic et al. (24)				

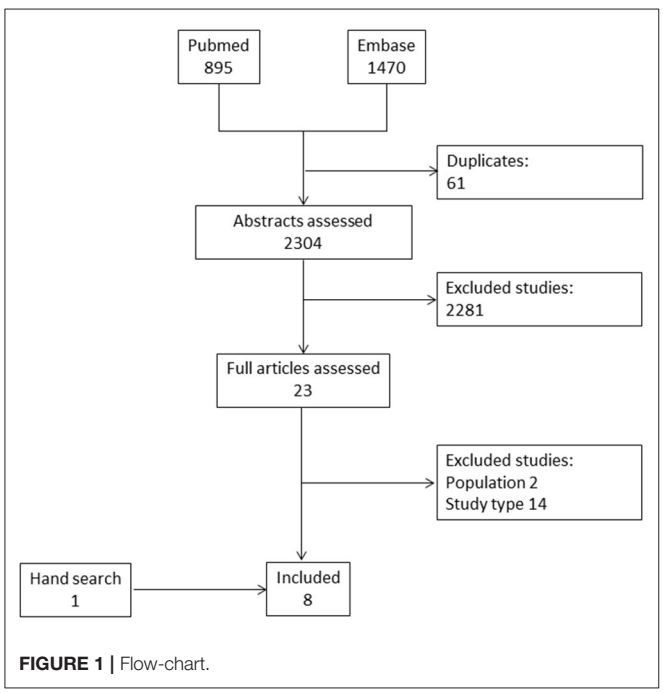

FIGURE 1 | Flow-chart.

of the common extensor tendon at the epicondyle in 4 studies (22, 24, 25, 28), the triceps tendon (27) and the insertion of the common flexor tendon at the medial epicondyle in one study each (28). Among the joints, the metacarpophalangeal joints (MCP) (28), the metatarsophalangeal joints (MTP) (26) were evaluated in one study, while the knees (22, 26) and the ankles (22, 26) were evaluated in two studies each.

Six studies applied semi-quantitative scoring systems to assesses entheses, in particular the Glasgow Ultrasound Enthesitis Scoring System (GUESS) (15, 22, 23, 25) and the Madrid Sonographic Enthesitis Index (MASEI) (22, 24, 25) were adopted by four and three studies, respectively. The use of high-end ultrasound equipment was reported by five studies (22, 24–27), all of the studies were performed after 2010, which likely implies technically comparable equipment. Three studies presented comparative data in CD and UC (15, 22, 26), while two studies compared active and inactive disease (15, 24). Information stratified based on IBD disease duration was obtained by three studies (15, 22, 27), while no studies addressed the influence of the presence of arthralgia, the type of arthralgia and the duration of joint symptoms.

The complete summary of findings of the included studies is reported in the **Supplementary Tables S2, S6**, in the online only supplement. The summary of the assessment of the Risk of Bias is shown in **Table 3**.

Frequency of Ultrasound-Detected Abnormalities

All of the eight included studies allowed to retrieve information on the prevalence of ultrasound-detectable lesions. The characteristics and results of the included studies are reported in **Supplementary Table S2**. Among the studies assessing entheseal involvement, four evaluated the presence of bone erosions, three entheseal thickening, enthesophytes and power Doppler, two evaluated bursitis, while a single study reported the prevalence of calcifications and hypoechogenicity.

The range of frequencies retrieved from the studies for each lesion is reported in **Table 2** and **Figure 2**.

Among the tested structures, entheseal involvement emerged as the most frequent lesion, with an overall range from 30 to 87.9% across studies. Specifically, chronic lesions were consistently found with a frequency ranging from 83 to 83.3%, while 31%−43.8% of entheses showed signs of acute inflammation. Joint involvement was reported with a lower frequency, from 19.7 to 48.8%. At entheseal level, among abnormalities in gray scale (GS), increased thickness was reported in 81.5% of patients, entesophytes in 67.9% and erosions with a frequency ranging from 16 to 17%, while bursitis was described in 27.1% of patients. The frequency of power Doppler (PD) was widely variable across studies, ranging from 14 to 67%.

When analyzing specific sites, the only lesion reported at the triceps tendon was increased thickness, while at the remaining

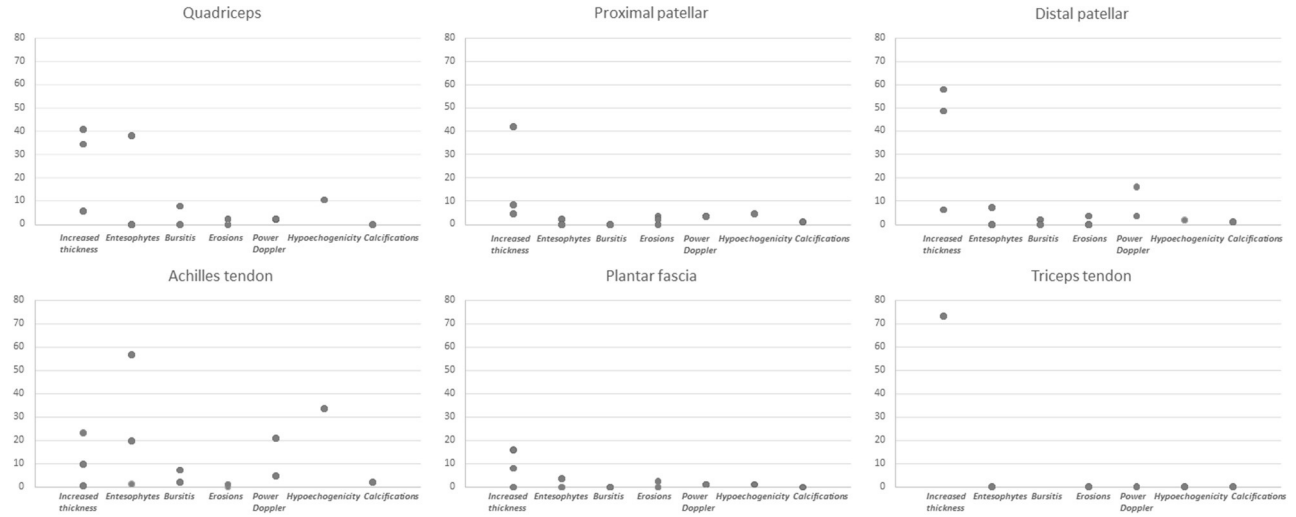

FIGURE 2 | Summary of frequencies for each lesion at entheseal sites.

sites for which frequency data were available in detail (quadriceps tendon, proximal and distal patellar tendon, Achilles tendon and plantar fascia) all lesions were assessed. Frequencies were reported based on the total number of patients in some studies (15, 22, 24–26, 28), while in some others on the number of assessed entheses (23, 27). Specifically, increased thickness was more frequently reported at the distal patellar tendon (range 6.43% of entheses to 58% of patients), hypoechogenicity was found more frequently at the Achilles tendon (33.7% of sites), as well as PD (from 0% of patients to 20.9% of sites), enthesophytes (from 1.42% of sites to 56.8% of patients) and calcifications (2.3% of sites). Bone erosions had a limited frequency at specific sites, with a maximal frequency of 3.7% of patients at the proximal and distal patellar tendon insertion. The frequencies for each lesion are displayed in **Figure 2**.

In studies comparing patients with CD and UC, no significant differences in terms of frequency of entheseal or joint involvement among diseases emerged (**Supplementary Table S3**) (15, 22, 26). Disease activity did not seem to be related to ultrasonographic findings: in fact, no association was found between clinical activity of IBD and entheseal involvement defined by MASEI (24) or GUESS (15), the presence of PD (15, 24), erosions and enthesophytes (**Supplementary Table S4**) (24). The evidence on the impact of disease duration, instead, was more contrasting. In fact, while two studies reported no differences in GUESS and PD (15, 27), a recent study reported a higher prevalence of entheseal abnormalities in patients with more than 1 year of IBD disease duration (90% vs. 72%, $P = 0.003$), and this applied particularly to bone erosions (7.4% vs. 0%, $P = 0.04$), while GUESS and MASEI did not significantly differ (**Supplementary Table S5**) (22).

Joint and tenosynovial involvement were less frequently assessed. A single study included synovial tendons in the scanning protocol, without however reporting the results of the assessment (22), while details on the prevalence of joint involvement were reported by two studies, with a frequency of 19.7 and 48.8%, depending on the sites (22, 26). The methodological quality of the included studies, assessed through the NOS, was mostly adequate for patient selection and comparability, while it was lower for outcome assessment in three studies.

Value of Ultrasound-Detected Lesions in Making a Diagnosis of Arthritis

Of the three studies reporting data on the diagnostic accuracy to detect arthritis, one had a case-control design (24), all described entheseal lesions (22, 24, 25), while a single study reported information on joint involvement (22). Of note, all of the studies were published after 2020, when a shared definition of enthesitis, proposed by the Outcome Measures in Rheumatology (OMERACT), was already available (29).

In detail, Bertolini et al. enrolled 148 consecutive patients with IBD, of which 27 were treated by biological drugs, assessing 12 entheseal sites to derive MASEI and GUESS, as well as synovitis and tenosynovitis at the knees and ankles. Husic and colleagues assessed 14 entheseal sites, in order to apply a modified version of MASEI, in 47 patients with IBD and 44 healthy controls. Finally, Martinis et al., evaluated a cohort of 158 IBD patients, with a median disease duration of about 10 years, assessing 12 entheseal sites to calculate MASEI.

The limited number of available studies did not allow any quantitative synthesis of the results. The features and findings of the included studies are summarized in **Supplementary Table S6**. The highest specificity for the detection of arthritis was provided by the overall presence of any joint abnormalities (specificity, 0.88, 95% CI 0.80–0.94), while the highest sensitivity by any entheseal lesion (sensitivity 0.88, 95% CI 0.76–0.95), although at the cost of a low specificity. Also, chronic entheseal lesions and erosions had a good sensitivity, however no single lesion or combination of lesions achieved an adequate compromise between sensitivity and specificity. The sensitivities and specificities of the primary studies are

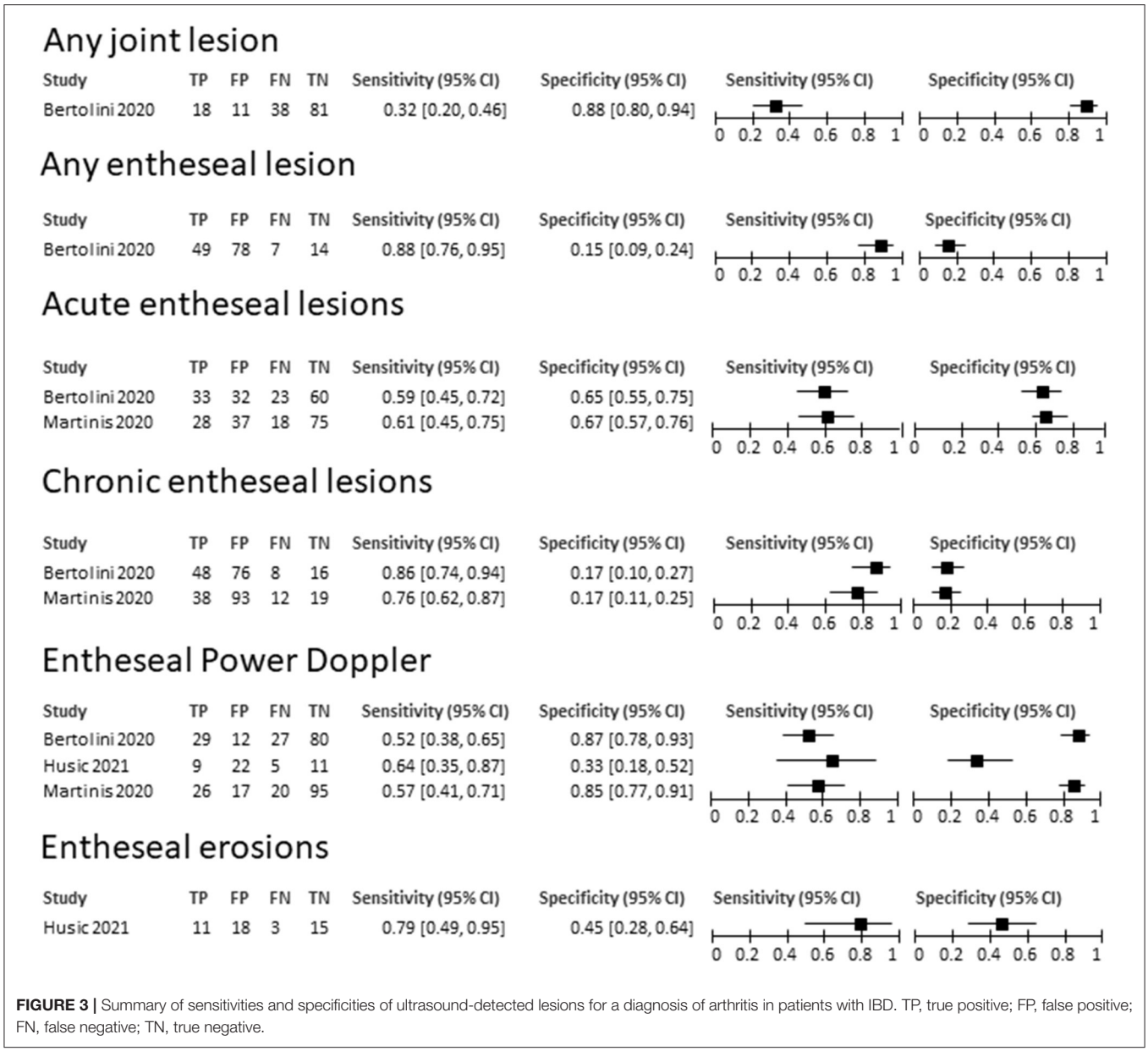

FIGURE 3 | Summary of sensitivities and specificities of ultrasound-detected lesions for a diagnosis of arthritis in patients with IBD. TP, true positive; FP, false positive; FN, false negative; TN, true negative.

summarized in **Figure 3**. The RoB of the included studies, assessed through the QUADAS2 tool, resulted to be low for two studies and high in one for selection, unclear for the test in all studies, and low for reference standard and flow and timing in all studies.

DISCUSSION

This systematic review provides an updated overview on the clinical applicability of musculoskeletal ultrasonography in patients with IBD without an overt joint involvement. In the field of rheumatology, ultrasonography has gained increasing success in the last two decades in light of the technical advances, the easy availability in an outpatient setting allowing an immediate application of the results to patient management, low cost and good acceptability (30). Ultrasonography has been proven to be more sensitive than clinical examination in identifying synovitis (31), and more specific than clinical examination in identifying entheseal involvement (32). For these reasons, ultrasonography has been considered an interesting imaging technique to evaluate patients at higher risk of developing arthritis, particularly in the field of psoriasis (17, 33), where a predictive value over the future development of arthritis has been demonstrated (34). While the amount of evidence for the application in psoriatic patients is already significant, with ongoing large prospective studies (16), in the field of IBD the interest on ultrasound is more recent.

We retrieved a total of 8 studies, all published after 2011, reflecting the growing and still evolving interest on this possible application of ultrasound. The main results pertain to the area

TABLE 4 | Research Agenda of US in IBD without a diagnosis of arthritis.

1. To evaluate the diagnostic performance of a combination of different entheseal lesions to identity patients with IBD and arthritis
2. To further assess the frequency and diagnostic value of tenosynovitis and synovitis
3. To investigate the prognostic value of ultrasound in identifying IBD patients at risk of developing arthritis by large prospective studies
4. To produce evidence on the value of ultrasound in monitoring joint involvement
5. To explore the value of ultrasound in specific populations (early disease, treatment with biological drugs)

of prevalence of ultrasound lesions, with some evidence also on their diagnostic value.

More precisely, we found a high variability in the frequency of both chronic and acute lesions in patients with IBD, in particular the overall prevalence of entheseal abnormalities, of entheseal PD as well as that of joint abnormalities were reported with a wide range across studies. This great heterogeneity could be related to populations under investigation, which largely differed, in terms of inclusion criteria, disease duration, clinical setting and type of treatment. The fact that the prevalence of lesions was calculated in some cases by using the number of patients and in others the number of entheses as statistical unit should be regarded as a possible further source of heterogeneity. The high degree of heterogeneity, however, seems to be in line with that found in patients with psoriasis and psoriatic arthritis (33).

As far as the gastroenterological setting is concerned, we found that only IBD disease duration correlated with a higher frequency of ultrasound abnormalities; however, this result emerged from a single study which enrolled patients with a very short disease duration (<12 months of disease duration). In this paper, patients with IBD from more than 1 year had a higher number of abnormal entheses and more entheses presenting bone erosions, compared to the early patients. Although it is known that articular manifestations in IBD patients can precede the onset of gastrointestinal symptoms, papers that evaluated the risk of developing arthritis after the diagnosis of IBD are scarce (1, 2, 5, 12).

On the other hand, we did not find any correlation between the type of IBD and the disease activity. Similarly, the remaining subgroup analyses did not provide any relevant result.

The three studies reporting information on the diagnostic accuracy allowed to retrieve data on the performance of single lesions, once again showing inconsistent results, with no information on the impact of a combination of lesions. None of the tested ultrasound-detectable lesions showed an acceptable compromise between sensitivity and specificity, although the limited number of included studies does not allow to draw solid conclusions. The highest sensitivity (0.88) was achieved considering any possible entheseal abnormality, at the cost of a poor specificity. The highest specificity, instead, was achieved by chronic entheseal lesions, with a range of specificities from 0.76 to 0.86. Given the paucity of studies, a quantitative summary of the results by a diagnostic accuracy meta-analysis was not possible. Once again, the lack of studies testing a combination of elementary lesions in cohorts reproducing a realistic clinical setting has already been described as a characteristic limitation of ultrasonographic studies in rheumatology, and represents a relevant issue to be addressed in future research (18, 35).

A major intrinsic limitation of our study is represented by the fact that most of the studies focused on the assessment of entheses, with limited information on the joints and no information on tenosynovitis. While in spondyloenthesoarthritis enthesitis has been identified as the primary lesion characterizing the disease process, tenosynovitis is emerging as a possible early lesion in new-onset peripheral inflammatory pain (36), and its low prevalence in healthy subjects suggests specificity for arthritis (37). In addition, tenosynovitis was the only lesion presenting with a different frequency in psoriatic patients with or without arthralgia (16), thus it might represent an interesting feature to assess also in IBD.

A further limitation of this review can be represented by potential evolutions in the field of ultrasound, since the data-driven validation of the definition of enthesitis is still ongoing, and the lesions included in the definition are frequently detected also in healthy subjects (38). The concept of ultrasonographic enthesitis might therefore change in the future, implying a different interpretation of our results (39). The development of new biological drugs for IBD, moreover, may change the clinical panorama of these disorders (40).

The absence of follow-up studies precluded the evaluation of the long-term prognostic role of ultrasound abnormalities over the occurrence of joint manifestations in IBD patients who do not show any joint involvement. The main difficulty in this field is related to the low incidence of inflammatory arthritis in patients with IBD, and the study of such process would require large samples, observed for a very long follow-up. This reduces the feasibility of valid prognostic studies. Moreover, a recent SLR has underpinned several methodological issues in existing cohorts of IBD and SpA, requiring a further effort in achieving a standardized assessment (41). In addition to this, the data we obtained derive from studies conducted on treated IBD patients, in which some drugs might have masked the possible joint involvement.

The implications for clinical practice of our results include the necessity of prioritizing accurate clinical assessment in patients with IBD, particularly at early stages, in order to timely detect a potential joint involvement, determining a decreased quality of life and the potential development of disability. In this setting, musculoskeletal ultrasonography can represent a valid complementary and easily available imaging technique to support clinical evaluation in the outpatient setting. Our work highlighted several existing gaps in the literature on this topic, and in particular the urge for future prospective studies (Research Agenda, **Table 4**), in order to identify clinical and imaging predictors of arthritis in patients with IBD without overt joint involvement.

DATA AVAILABILITY STATEMENT

The original contributions presented in the study are included in the article/**Supplementary Material**, further inquiries can be directed to the corresponding author.

AUTHOR CONTRIBUTIONS

GS, AS, FB, and CM contributed to conception and design of the study. GS performed the searches and organized the database. AS, DS, FL, and EF performed the screening of the abstracts and the extraction of the results. GS and AS wrote the first draft of the manuscript. All authors contributed to manuscript revision, read, and approved the submitted version.

FUNDING

This work was partially supported by the Ricerca Corrente funding scheme of the Ministry of Health, Italy.

SUPPLEMENTARY MATERIAL

The Supplementary Material for this article can be found online at: https://www.frontiersin.org/articles/10.3389/fmed.2022.919521/full#supplementary-material

REFERENCES

1. Maaser C, Sturm A, Vavricka SR, Kucharzik T, Fiorino G, Annese V, et al. ECCO-ESGAR guideline for diagnostic assessment in IBD Part 1: initial diagnosis, monitoring of known IBD, detection of complications. *J Crohns Colitis.* (2019) 13:144–64. doi: 10.1093/ecco-jcc/jjy113
2. Sturm A, Maaser C, Calabrese E, Annese V, Fiorino G, Kucharzik T, et al. ECCO-ESGAR guideline for diagnostic assessment in IBD part 2: IBD scores and general principles and technical aspects. *J Crohns Colitis.* (2019) 13:273–84. doi: 10.1093/ecco-jcc/jjy114
3. Rubin DT, Ananthakrishnan AN, Siegel CA, Sauer BG, Long MD. ACG. Clinical guideline: ulcerative colitis in adults. *Am J Gastroenterol.* (2019) 114:384–413. doi: 10.14309/ajg.0000000000000152
4. Lichtenstein GR, Loftus EV, Isaacs KL, Regueiro MD, Gerson LB, Sands BE, et al. Clinical guideline: management of crohn's disease in adults. *Am J Gastroenterol.* (2018) 113:481–517. doi: 10.1038/ajg.2018.27
5. Harbord M, Annese V, Vavricka SR, Allez M. Barreiro-de Acosta M, Boberg KM, et al. The first European evidence-based consensus on extra-intestinal manifestations in inflammatory bowel disease *J Crohns Colitis.* (2016) 10:239–54. doi: 10.1093/ecco-jcc/jjv213
6. Karreman MC, Luime JJ, Hazes JMW, Weel AEAM. The prevalence and incidence of axial and peripheral spondyloarthritis in inflammatory bowel disease: a systematic review and meta-analysis. *J Crohns Colitis.* (2017) 11:631–42. doi: 10.1093/ecco-jcc/jjw199
7. Olivieri I, Cantini F, Castiglione F, Felice C, Gionchetti P, Orlando A, et al. Italian Expert Panel on the management of patients with coexisting spondyloarthritis and inflammatory bowel disease. *Autoimmun Rev.* (2014) 13:822–30. doi: 10.1016/j.autrev.2014.04.003
8. Turkcapar N, Toruner M, Soykan I, Aydintug OT, Cetinkaya H, Duzgun N, et al. The prevalence of extraintestinal manifestations and HLA association in patients with inflammatory bowel disease. *Rheumatol Int.* (2006) 26:663–8. doi: 10.1007/s00296-005-0044-9
9. Salvarani C, Vlachonikolis IG, van der Heijde DM, Fornaciari G, Macchioni P, Beltrami M, et al. Musculoskeletal manifestations in a population-based cohort of inflammatory bowel disease patients. *Scand J Gastroenterol.* (2001) 36:1307–13. doi: 10.1080/003655201317097173
10. Fries W, Dinca M, Luisetto G, Peccolo F, Bottega F, Martin A. Calcaneal ultrasound bone densitometry in inflammatory bowel disease–a comparison with double x-ray densitometry of the lumbar spine. *Am J Gastroenterol.* (1998) 93:2339–44. doi: 10.1111/j.1572-0241.1998.00685.x
11. Hedin CRH, Vavricka SR, Stagg AJ, Schoepfer A, Raine T, Puig L, et al. The pathogenesis of extraintestinal manifestations: implications for IBD research, diagnosis, and therapy. *J Crohns Colitis.* (2019) 13:541–54. doi: 10.1093/ecco-jcc/jjy191
12. Atzeni F, Defendenti C, Ditto MC, Batticciotto A, Ventura D, Antivalle M, et al. Rheumatic manifestations in inflammatory bowel disease. *Autoimmun Rev.* (2014) 13:20–3. doi: 10.1016/j.autrev.2013.06.006
13. Salvarani C, Fries W. Clinical features and epidemiology of spondyloarthritides associated with inflammatory bowel disease. *World J Gastroenterol.* (2009) 15:2449–55. doi: 10.3748/wjg.15.2449
14. Peluso R, Di Minno MND, Iervolino S, Manguso F, Tramontano G, Ambrosino P, et al. Enteropathic spondyloarthritis: from diagnosis to treatment. *Clin Dev Immunol.* (2013) 631408. doi: 10.1155/2013/631408
15. Bandinelli F, Milla M, Genise S, Giovannini L, Bagnoli S, Candelieri A, et al. Ultrasound discloses entheseal involvement in inactive and low active inflammatory bowel disease without clinical signs and symptoms of spondyloarthropathy. *Rheumatology.* (2011) 50:1275–9. doi: 10.1093/rheumatology/keq447
16. Zabotti A, McGonagle DG, Giovannini I, Errichetti E, Zuliani F, Zanetti A, et al. Transition phase towards psoriatic arthritis: clinical and ultrasonographic characterisation of psoriatic arthralgia. *RMD Open.* (2019) 5:e001067. doi: 10.1136/rmdopen-2019-001067
17. Zabotti A, De Lucia O, Sakellariou G, Batticciotto A, Cincinelli G, Giovannini I, et al. Predictors, risk factors, and incidence rates of psoriatic arthritis development in psoriasis patients: a systematic literature review and meta-analysis. *Rheumatol Ther.* (2021) 8:1519–34. doi: 10.1007/s40744-021-00378-w
18. Sakellariou G, Scirè CA, Adinolfi A, Batticciotto A, Bortoluzzi A, Delle Sedie A, et al. Differential diagnosis of inflammatory arthropathies by musculoskeletal ultrasonography: a systematic literature review. *Front Med.* (2020) 7:141. doi: 10.3389/fmed.2020.00141
19. Page MJ, McKenzie JE, Bossuyt PM, Boutron I, Hoffmann TC, Mulrow CD, et al. The PRISMA 2020 statement: an updated guideline for reporting systematic reviews. *BMJ.* (2021) 372:n71. doi: 10.1136/bmj.n71
20. Ottawa Hospital Research Institute. Available online at: http://www.ohri.ca/programs/clinical_epidemiology/oxford.asp (accessed July 30, 2021).
21. Whiting PF, Rutjes AWS, Westwood ME, Mallett S, Deeks JJ, Reitsma JB, et al. QUADAS-2: a revised tool for the quality assessment of diagnostic accuracy studies. *Ann Intern Med.* (2011) 155:529–36. doi: 10.7326/0003-4819-155-8-201110180-00009
22. Bertolini E, Macchioni P, Rizzello F, Salice M, Vukatana G, Sandri G, et al. Ultrasonographic and clinical assessment of peripheral enthesitis and arthritis in an Italian cohort of inflammatory bowel disease patients. *Semin Arthritis Rheum.* (2020) 50:436–43. doi: 10.1016/j.semarthrit.2020.01.001
23. Hsiao Y-F, Wei S-C, Lu C-H, Wu C-H, Hsieh S-C, Li K-J. Patients with inflammatory bowel disease have higher sonographic enthesitis scores than normal individuals: Pilot study in Taiwan. *J Med Ultrasound.* (2014) 22:194–9. doi: 10.1016/j.jmu.2014.03.004
24. Husic R, Lackner A, Kump PK, Högenauer C, Graninger W, Dejaco C. High prevalence of ultrasound verified enthesitis in patients with inflammatory bowel disease with or without spondylarthritis. *Front Med.* (2021) 8:637459. doi: 10.3389/fmed.2021.637459
25. Martinis F, Tinazzi I, Bertolini E, Citriniti G, Variola A, Geccherle A, et al. Clinical and sonographic discrimination between fibromyalgia and spondyloarthopathy in inflammatory bowel disease with musculoskeletal pain. *Rheumatology.* (2020) 59:2857–63. doi: 10.1093/rheumatology/keaa036
26. Rovisco J, Duarte C, Batticcioto A, Sarzi-Puttini P, Dragresshi A, Portela F, et al. Hidden musculoskeletal involvement in inflammatory bowel disease: a multicenter ultrasound study. *BMC Musculoskelet Disord.* (2016) 17:84. doi: 10.1186/s12891-016-0932-z

27. Bakirci Ureyen S, Karacaer C, Toka B, Erturk Z, Eminler AT, Kaya M, et al. Similar subclinical enthesitis in celiac and inflammatory bowel diseases by ultrasound suggests a gut enthesis axis independent of spondyloarthropathy spectrum. *Rheumatology.* (2018) 57:1417–22. doi: 10.1093/rheumatology/key102
28. Rodríguez-Caminero S, Queiro R. Ultrasound subclinical musculoskeletal findings in inflammatory bowel disease: diagnostic value of positive Doppler signal. *Rheumatology.* (2020) 59:3571–2. doi: 10.1093/rheumatology/keaa320
29. Balint PV, Terslev L, Aegerter P, Bruyn GAW, Chary-Valckenaere I, Gandjbakhch F, et al. Reliability of a consensus-based ultrasound definition and scoring for enthesitis in spondyloarthritis and psoriatic arthritis: an OMERACT US initiative. *Ann Rheum Dis.* (2018) 77:1730–5. doi: 10.1136/annrheumdis-2018-213609
30. Ranganath VK, Hammer HB, McQueen FM. Contemporary imaging of rheumatoid arthritis: clinical role of ultrasound and MRI. *Best Pract Res Clin Rheumatol.* (2020) 34:101593. doi: 10.1016/j.berh.2020.101593
31. Colebatch AN, Edwards CJ, Østergaard M, van der Heijde D, Balint PV, D'Agostino M-A, et al. EULAR recommendations for the use of imaging of the joints in the clinical management of rheumatoid arthritis. *Ann Rheum Dis.* (2013) 72:804–14. doi: 10.1136/annrheumdis-2012-203158
32. Freeston JE, Coates LC, Helliwell PS, Hensor EMA, Wakefield RJ, Emery P, et al. Is there subclinical enthesitis in early psoriatic arthritis? A clinical comparison with power doppler ultrasound. *Arthritis Care Res.* (2012) 64:1617–21. doi: 10.1002/acr.21733
33. Zabotti A, Bandinelli F, Batticciotto A, Scirè CA, Iagnocco A, Sakellariou G, et al. Musculoskeletal ultrasonography for psoriatic arthritis and psoriasis patients: a systematic literature review. *Rheumatology.* (2017) 56:1518–32. doi: 10.1093/rheumatology/kex179
34. Tinazzi I, McGonagle D, Biasi D, Confente S, Caimmi C, Girolomoni G, et al. Preliminary evidence that subclinical enthesopathy may predict psoriatic arthritis in patients with psoriasis. *J Rheumatol.* (2011) 38:2691–2. doi: 10.3899/jrheum.110505
35. Sakellariou G, Iagnocco A, Delle Sedie A, Riente L, Filippucci E, Montecucco C. Ultrasonographic evaluation of entheses in patients with spondyloarthritis: a systematic literature review. *Clin Exp Rheumatol.* (2014) 32:969–78.
36. Molina Collada J, López Gloria K, Castrejón I, Nieto-González JC, Rivera J, Montero F, et al. Ultrasound in clinically suspect arthralgia: the role of power Doppler to predict rheumatoid arthritis development. *Arthritis Res Ther.* (2021) 23:299. doi: 10.1186/s13075-021-02685-7
37. Trickey J, Sahbudin I, Ammitzbøll-Danielsen M, Azzolin I, Borst C, Bortoluzzi A, et al. Very low prevalence of ultrasound-detected tenosynovial abnormalities in healthy subjects throughout the age range: OMERACT ultrasound minimal disease study. *Ann Rheum Dis.* (2022) 81:232–6. doi: 10.1136/annrheumdis-2021-219931
38. Di Matteo A, Filippucci E, Cipolletta E, Martire MV, Jesus D, Isidori M, et al. How normal is the enthesis by ultrasound in healthy subjects? *Clin Exp Rheumatol.* (2020) 38:472–8.
39. HÁnovÁ P, Faith N, Bruyn GA. Enthesitis: myth or reality? *J Rheumatol.* (2020) 47:945–6. doi: 10.3899/jrheum.200114
40. Harris C, Cummings JRF. JAK1 inhibition and inflammatory bowel disease. *Rheumatology.* (2021) 60:ii45–51. doi: 10.1093/rheumatology/keaa896
41. Schwartzman M, Ermann J, Kuhn KA, Schwartzman S, Weisman MH. Spondyloarthritis in inflammatory bowel disease cohorts: systematic literature review and critical appraisal of study designs. *RMD Open.* (2022) 8:e001777. doi: 10.1136/rmdopen-2021-001777

Conflict of Interest: The authors declare that the research was conducted in the absence of any commercial or financial relationships that could be construed as a potential conflict of interest.

frontiers | Frontiers in Medicine

ORIGINAL RESEARCH
published: 24 May 2022
doi: 10.3389/fmed.2022.871760

Entheseal Involvement in Spondyloarthritis (SpA) and Gout: An Ultrasound Comparative Study

Lucio Ventura-Ríos[1], Tomas Cazenave[2], Cristina Hernández-Díaz[1], Selma Gallegos-Nava[3], Citlallyc Gómez-Ruiz[4], Marcos Rosemffet[2], Karina Silva-Luna[5], Pedro Rodríguez-Henríquez[6], Janitzia Vázquez-Mellado[4], Julio Casasola-Vargas[4], Esteban Cruz-Arenas[7] and Eugenio M. de Miguel[8]*

[1] Laboratorio de Ultrasonido Musculoesquelético y Articular, Instituto Nacional de Rehabilitación Luis Guillermo Ibarra Ibarra, Mexico City, Mexico, [2] Department of Rheumatology, Instituto de Rehabilitación Psicofísica, Buenos Aires, Argentina, [3] Department of Rheumatology, Hospital General Dr. Darío Fernández Fierro, Mexico City, Mexico, [4] Department of Rheumatology, Hospital General de México, Mexico City, Mexico, [5] Service of Rheumatology, Hospital Universitario "Dr. JoséEleuterio González", Monterrey, Mexico, [6] Service of Rheumatology, Hospital General Dr. Manuel Gea González, México City, Mexico, [7] Instituto Nacional de Rehabilitación Luis Guillermo Ibarra Ibarra, Unidad de Vigilancia Epidemiológica Hospitalaria-Investigación Sociomédica, México City, Mexico, [8] Rheumatology Service, Hospital Universitario La Paz, Madrid, Spain

OPEN ACCESS

Edited by:
Christian Dejaco, Medical University of Graz, Austria

Reviewed by:
Luca Di Geso, Madonna del Soccorso Hospital, Italy
Xabier Michelena, Vall d'Hebron University Hospital, Spain
Jana Hurnakova, University Hospital in Motol, Czechia

***Correspondence:**
Lucio Ventura-Ríos
venturariosslucio@gmail.com

Specialty section:
This article was submitted to Rheumatology, a section of the journal Frontiers in Medicine

Received: *08 February 2022*
Accepted: *08 April 2022*
Published: *24 May 2022*

Citation:
Ventura-Ríos L, Cazenave T, Hernández-Díaz C, Gallegos-Nava S, Gómez-Ruiz C, Rosemffet M, Silva-Luna K, Rodríguez-Henríquez P, Vázquez-Mellado J, Casasola-Vargas J, Cruz-Arenas E and de Miguel EM (2022) Entheseal Involvement in Spondyloarthritis (SpA) and Gout: An Ultrasound Comparative Study. Front. Med. 9:871760. doi: 10.3389/fmed.2022.871760

Objective: To compare the assessment of entheses in subjects with spondyloarthritis (SpA) with patients with gout by the Madrid Sonographic Enthesis Index (MASEI).

Method: This cross-sectional study includes videos of entheses evaluated by ultrasound (US) of 30 patients with SpA diagnosed according to the ASAS criteria and 30 patients with gout established by the presence of monosodium urate crystals. Entheses were evaluated for MASEI in 2 Institutes located in two different countries. Demographic and clinical data were registered. Total MASEI score, MASEI-inflammatory, and MASEI-chronic damage were analyzed. Comparisons between groups were obtained by chi-square test and Student's *t*-test. An inter-reading US reliability was realized.

Results: Patients with gout were older and had significantly more comorbidities than those with SpA. The total MASEI score was not significantly different among diseases ($p = 0.07$). MASEI-inflammatory was significantly more prevalent at the Achilles tendon in SpA, while the proximal patellar tendon was in gout. Power Doppler was higher in SpA compared to gout ($p = 0.005$). MASEI-chronic damage related to calcification/enthesophytes predominated in gout ($p = 0.043$), while calcaneal erosions did in SpA ($p = 0.008$). The inter-reader concordance was excellent (0.93, CI 95% 0.87–0.96, $p = 0.001$).

Conclusions: SpA and gout similarly involve entheses according to MASE, however, some inflammatory and chronic lesions differ significantly depending on the underlying disease and tendon scanned.

Keywords: ultrasound, entheses, spondyloarthritis, gout, MASEI

INTRODUCTION

In patients with spondyloarthritis (SpA), enthesitis is one of the cornerstones of the etiopathogenesis of the disease (1). In axial SpA, the prevalence of peripheral enthesitis is around 25–58% (2). This manifestation is traditionally evaluated by clinical examination based on the presence of pain and/or swelling. However, neither the clinical examination's reliability nor accuracy is satisfactory enough (3–6). In this sense, ultrasound (US) has proven to be a promising imaging technique, since it allows the direct visualization of entheses and related structures (3–7), and it has been observed that it is very sensitive for the evaluation of morpho-structural alterations and changes in blood flow at the entheseal level. In SpA patients, the involvement of the entheses evaluated by the US has been found in up to 98% of cases, with the entheses of the lower limbs being the most frequently affected (3). The reliability of US enthesitis in patients with SpA using OMERACT definitions has been tested in a few studies (8–12).

On the other hand, gout is another inflammatory disease that also affects the entheses (13–15). Several studies have demonstrated the ability of US to differentiate it from other microcrystalline arthropathies in joints (16–18). However, little has been studied about the discriminant capacity of the US at the entheses level (19). In one study that evaluated the discriminant validity of US in SpA, rheumatoid arthritis, gout, chondrocalcinosis, and osteoarthritis in the Achilles tendon, the US shows a potential ability to differentiate between SpA and the other diseases, except for gout (19). So far, the ability of the US to discriminate between SpA and gout has not been evaluated through the identification of elemental lesions of each of these pathologies with MASEI. This index is the most complete and used scoring system, and it has been proven to be reliable and valid for the study of enthesis in diseases other than SpA (20). Although we know that each of these diseases has established diagnostic criteria, the objective of this study was to know if the MASEI in SpA is different compared to gout.

MATERIALS AND METHODS

Study Design

This is a cross-sectional and observational study conducted in México and Argentina. Videos of consecutive patients who were sent to realize MASEI from two rheumatology outpatient clinics to ultrasound units at the National Rehabilitation Institute in México and one rheumatology clinic to the Institute of Psychophysical Rehabilitation in Argentina. The study was approved by the local ethical committee, approval number 10/17, and conducted according to the Declaration of Helsinki. All participants gave written informed consent before realizing the US evaluation.

Inclusion and Exclusion Criteria

We included videos of 30 consecutive patients with axial or peripheral SpA according to the Assessment of Spondyloarthritis International Society (ASAS) classification criteria were included. Also, videos of 30 patients with gout with diagnosis established by the presence of monosodium urate crystals in synovial fluid or tophus were assessed. The diagnosis of all patients was established by the physician who referred the patients to the ultrasound units. All patients with gout were in an inter-critical period clinically. Patients with gout and psoriasis or inflammatory bowel disease were excluded. Patients who had received oral or injected corticosteroids within 4 weeks before inclusion in the study were also excluded. Demographic data such as age, gender, disease evolution time, comorbidities, and current treatment were recorded. BASDAI, BASFI, BASMI, and MASES were assessed in the case of SpA patients. Entheseal involvement was not an inclusion criterion in none of the diseases.

Ultrasound Assessment

The videos were obtained and recorded by 2 rheumatologist ultrasonographers (both with more than 10 years of experience), one in each ultrasound unit. The ultrasonographers were blinded to the clinical characteristics of the patients. The videos were recorded. Once all the videos were recorded, they were evaluated by the 5 readers. Triceps brachial, quadriceps tendon, proximal and distal patellar tendon, Achilles tendon, and proximal plantar fascia insertions were evaluated bilaterally, and each enthesis was scanned in longitudinal and transverse planes. The triceps enthesis was examined with the elbow flexed at 90°. Knee entheses evaluation was performed with the patient in supine position and knee flexed at 70° for grayscale and extended for power Doppler (PD). Achilles tendon and plantar fascia were evaluated with the patient in a prone position and their foot flexed at 90°. The US evaluation was blinded and realized independently of the pathology. We used two Esaote MyLab 70® equipment with a 7.5–12 MHz multifrequency linear probe. The vascularization was assessed using PD adjusted with a PRF of 500 Hz and gain from 50 to 55 dB.

According to MASEI, the following lesions were evaluated: pathologic structural change and thickening of the tendon at the site of insertion, calcification/enthesophyte, bursitis, bone erosion, and PD signal. The pathologic structural change was defined as a loss of a fibrillar pattern, hypoechoic appearance, or fusiform thickening; the following criteria were used for abnormal structure thickness: quadriceps tendon thickness >6.1 mm, proximal and distal patellar tendon >4.0 mm, Achilles tendon >5.29 mm, and plantar fascia >4.4 mm. Bone erosion was defined as cortical breakage with bone contour defects in 2 perpendicular planes. Calcification/enthesophyte was scored 0 if absent, 1 for small calcification or ossification with an irregularity of cortical bone, 2 if a clear presence of enthesophytes (hyperechoic spurs forming at a tendon insertion into the bone, growing in the direction of the natural pull of the tendon involved), or if medium-sized calcifications or ossification were seen and 3 for large calcifications or ossifications (21). According to OMERACT, merging some components like calcifications and enthesophytes is an adequate strategy to improve reliability, because sometimes they have the same appearance (22). Bursitis was defined as a well-circumscribed, localized anechoic or hypoechoic area at the site of an anatomical bursa, which was compressible by the transducer (21). The presence of PD signal was considered when seen at bone insertion (<2 mm from

TABLE 1 | Clinical and demographics characteristics among groups.

	Gout $n = 30$	SpA $N = 30$	p
Age years ± SD	54.1 (11.1)	45.7 (11.6)	0.005
Sex Men (%)	26 (86.7%)	21 (70.0%)	0.559
Women (%)	4 (13.3%)	9 (30.0%)	0.267
Disease duration years ± SD	10.2 (2.9)	9.7 (7.2)	0.324
Patients with comorbidities number (%)	25 (83.3%)	7 (23.3%)	0.002
Weight kg mean ± SD	75.7 + 9.5	70.6 ± 11.2	0.062
Height m mean ± SD	1.63 +1.6	1.64 ± 0.7	0.906
BMI mean ± SD	28.5 + 5.3	26.1 ± 4.3	0.059
Uric Acid level mg/dL mean ± SD	7.6 ± 1.7	5.5 ± 1.4	0.001
SpA axial / peripheral number (%)	NA	13 (43)/17 (56)	
Tophaceous gout *n* (%)	19 (63.3%)	NA	
Treatment			
Allopurinol	76%	NA	
Febuxostat	24%	NA	
Colchicine	53%	NA	
Non-steroidal anti-inflammatory drugs	48%	49%	
Methotrexate	NA	43%	
Sulphasalazin	NA	15%	
Anti-TNF	NA	23%	
BASDAI	NA	5.6 ± 3.8	
BASFI	NA	7.9 ± 3.9	
BASMI	NA	3.6 ± 1.2	
MASES median (min-max)	NA	4 (0–8)	

NA. Not Applicable.

the cortical bone), different from reflecting surface artifact or nutrition vessel signal, with or without cortical irregularities, erosions, or enthesophytes, according to OMERACT definition (22). The MASEI score was categorized in inflammatory lesions (thickening structural changes, bursitis, and vascularization) and chronic damage (calcifications/enthesophytes and bone erosions). The inter-reader agreement of total MASEI scores was performed among 5 ultrasonographers and the expert in the MASEI index (de Miguel E) online.

Statistical Analysis

Continuous data are described as the mean and standard deviation and categorical variables were expressed as frequencies and percentages. The normality of the continuous variables was probed by the Shapiro-Wilk test. The chi-square distribution was applied to compare categorical variables between groups. The student's *t*-test was used to contrast the total MASEI scores between groups. To analyze inter-reader agreement for continuous data we used intraclass correlation coefficient (ICC) with a 95% confidence interval. A $p < 0.05$ was considered statistically significant. Statistical analysis was performed in SPSS for Windows version 22.

RESULTS

Clinical and demographic characteristics are shown in **Table 1**. The average age of patients and prevalence of comorbidities were

TABLE 2 | Comparison of US findings of entheses between groups.

Enthesis	Gout 30 patients 60 entheses *n* (%)	Spondyloarthritis 30 patients 60 entheses *n* (%)	*P*
Quadriceps tendon			
Structural change	9 (15.0)	19 (31.6)	0.089
Thickening	8 (13.3)	13 (21.6)	0.382
Erosion	0 (0)	1 (1.6)	0.321
Calcification/enthesophyte (grade)			
0	35 (58.3)	40 (66.6)	0.644
1	19 (31.6)	5 (8.3)	**0.008**
2	6 (10.0)	9 (15.0)	0.605
3	0 (0)	6 (10.0)	0.130
Power Doppler signal	0 (0)	0 (0)	-
Proximal Patellar tendon			
Structural change	24 (40.0)	8 (13.3)	**0.008**
Thickening	21 (35.0)	9 (15.0)	**0.044**
Erosion	2 (3.3)	3 (3.3)	0.998
Calcification/enthesophyte			
0	39 (65.0)	45 (75.0)	0.585
1	19 (31.6)	10 (16.6)	0.137
2	2 (3.3)	2 (3.3)	1.000
3	0 (0.0)	1 (1.6)	0.321
Power Doppler signal	0 (0.0)	6 (10.0)	0.130
Distal patellar tendon			
Structural change	24 (40.0)	22 (36.6)	0.882
Thickening	21 (35.0)	22 (36.6)	0.998
Erosion	2 (3.3)	1 (1.6)	0.998
Calcification/enthesophyte			
0	42 (70.0)	49 (81.6)	0.529
1	14 (23.3)	7 (11.6)	0.190
2	4 (6.6)	2 (3.3)	0.683
3	0 (0.0)	0 (0.0)	-
Power Doppler signal	2 (3.3)	5 (8.3)	0.449
Bursitis infrapatelar	8 (13.3)	10 (16.6)	0.813
Achilles tendon			
Structural change	7 (11.6)	18 (30.0)	**0.045**
Thickening	4 (6.6)	14 (23.3)	**0.033**
Erosion	0 (0)	12 (20.0)	**0.005**
Calcification/enthesophyte			
0	39 (65.0)	35 (58.3)	0.727
1	13 (21.6)	5 (8.3)	0.099
2	6 (10.0)	16 (26.6)	0.055
3	2 (3.3)	3 (5.0)	0.998
Power Doppler signal	0 (0.0)	8 (13.3)	**0.045**
Retrocalcaneal bursa	0 (0.0)	9 (15.0)	**0.029**
Plantar fascia			
Structural change	20 (33.3)	14 (20.0)	0.391
Thickening	20 (33.3)	14 (20.0)	0.391
Erosion	2 (3.3)	2 (3.3)	1.000
Calcification/enthesophyte			
0	39 (65.0)	39 (65.0)	1.000

(Continued)

TABLE 2 | Continued

Enthesis	Gout 30 patients 60 entheses *n* (%)	Spondyloarthritis 30 patients 60 entheses *n* (%)	*P*
1	15 (25.0)	10 (16.6)	0.423
2	6 (10.0)	9 (15.0)	0.605
3	0 (0)	0 (0.0)	-
Power Doppler signal	0 (0)	1 (1.3)	0.321
Triceps tendon			
Structural change	14 (23.3)	9 (15.0)	0.404
Thickening	14 (23.3)	9 (15.0)	0.404
Erosion	9 (15.0)	12 (20.0)	0.662
Calcification/enthesophyte			
0	40 (66.6)	48 (80.0)	0.455
1	10 (16.6)	5 (8.3)	0.301
2	10 (16.6)	5 (8.3)	0.301
3	0 (0)	0 (0)	-
Power Doppler signal	0 (0.0)	1 (1.3)	0.321

The bold values indicate the values that were significantly different between groups.

significantly higher in the gout group than in the SpA. There was no significant difference in disease duration, weight, height, and body mass index (BMI) between groups. As expected, uric acid levels were significantly higher in patients with gout than with SpA. A high percentage had tophaceous gout. All patients with gout were receiving hypouricemic treatment; most of them had allopurinol. The SpA group received 43% methotrexate, 15% sulfasalazine, and 23% anti-TNF. A similar percentage of patients in both groups used non-steroidal anti-inflammatory drugs. The average BASDAI score was high suggesting SpA activity. BASFI and BASMI showed high dysfunction and decrease in spinal mobility, respectively. The median of MASES was 4.

Table 2 shows differences between groups related to lesions in the entheses evaluated. The site that was most frequently affected with structural change, thickness, erosion, bursitis, and PD signal was the Achilles tendon in patients with SpA (**Figures 1A–C**). In contrast with gout where the presence of structural change and thickening in the proximal patellar tendon was higher (**Figure 2**). The presence of small enthesophytes in the quadriceps tendon was significantly greater in gout than in SpA (**Figure 3**), whereas pathologic structural changes of the same tendon prevailed in gout. There was no significant difference in the distal patellar tendon, triceps tendon, and plantar fascia between groups.

Table 3 presents data related to MASEI. The total MASEI scores were higher in patients with SpA than gout, however, it was not significant. Regarding MASEI-inflammatory there were no differences in structural changes and thickening among groups, but the PD signal was significantly higher in SpA than gout. In respect of MASEI-chronic damage, the gout group had significantly higher calcifications/enthesophytes, nonetheless, bone erosions prevailed in the SpA group.

Inter-reader agreement for total MASEI score was excellent (0.93, 95% CI, 0.87–0.96, $p = 0.001$).

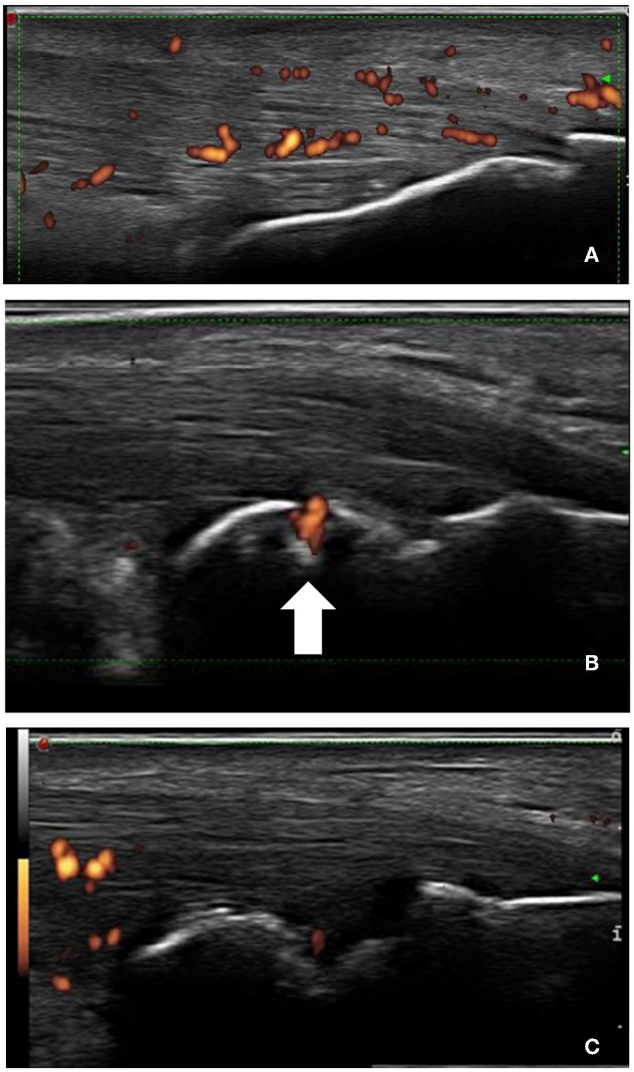

FIGURE 1 | Longitudinal scans of Achilles tendon in SpA. **(A)** Increased thickness of tendon insertion, enthesophyte (the step up of the bony prominence at the end of the normal bone contour), and power Doppler signal. **(B)** The arrow shows PD signal inside bone erosion and **(C)** arrowhead shows retrocalcaneal bursitis.

DISCUSSION

Although the US has proven to be a reliable and valid technique to evaluate enthesitis in SpA (23), little has been analyzed about its discriminant validity. In a study, the power of discrimination of US was evaluated by MASEI between different chronic diseases in the Achilles enthesis, showing that this index lacks validity to discriminate SpA from gout (19). Probably the fact that there is a single enthesis being assessed, limits the possibility of establishing the discriminant validity of an imaging technique. Other entheses different from the Achilles tendon are affected in gout, such as patellar tendon and quadriceps as observed in other studies (14, 15, 24). Therefore, in the present study, we decided to evaluate the 6 bilateral entheses included in the MASEI score.

FIGURE 2 | Longitudinal view of proximal patellar tendon shows increased thickness (> 4.0 mm) and hypoechogenicity in a patient with gout.

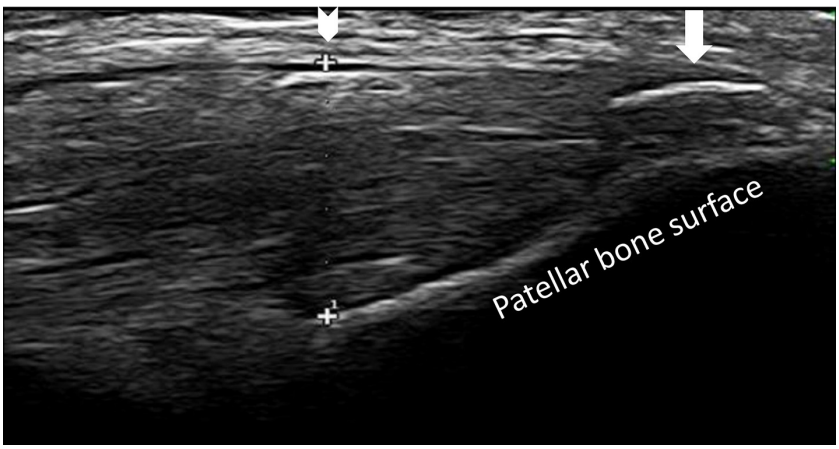

FIGURE 3 | Longitudinal scan of the distal patellar tendon in a patient with gout shows increased thickness, hypoechogenicity (arrowhead), and calcification (arrow).

As previously reported (19), we found significantly more structural changes/thickening and bone erosion in the Achilles tendon in SpA than in gout. This enthesis seems to be the most affected in SpA according to what has been reported (7, 25). de Miguel and cols, using MASEI had demonstrated that the presence of PD signal and bone erosion have a better predictive value for inflammatory enthesitis in SpA (21). Besides, as we have observed a higher prevalence of bone erosions in SpA than in gout, another study has found similar results (19). In a systematic review, significantly more erosions in the calcaneal enthesis were observed in SpA compared with the healthy population (26). Additionally, the presence of bursitis at the level of the calcaneal enthesis accompanying the inflammatory lesions can contribute to differentiating patients with SpA (27). By contrast, despite crystal deposition in gout, structural changes are infrequent in the Achilles tendon, as it has been shown in people with tophaceous gout where many of the characteristics observed were not disease-specific (28).

Structural change in the quadriceps tendon tended to be significantly greater in the SpA group than in gout, suggesting that it is one of the sites that could differentiate SpA from healthy subjects or other diseases (25, 29, 30). Moreover, patients with gout had a significantly greater presence of small calcifications/enthesophytes in quadriceps than those with SpA, as a recent study shows, where this tendon was the most involved in both diseases, therefore it is a site that requires more attention (31).

On the other hand, structural change in the proximal patellar tendon was significantly greater in gout than in SpA. In general,

TABLE 3 | MASEI score in 360 entheses in gout compared with SpA.

Total MASEI score means ± DS	26.0 ± 8.0	34.5 ± 14.8	***p*** 0.07
MASEI-inflammatory	*n* (%)	*n* (%)	
Structural change	99 (27.5%)	90 (25.0%)	0.560
Thickening	88 (24.4%)	81 (22.5%)	0.644
Power Doppler signal	2 (0.5%)	21 (5.8%)	**0.002**
Bursitis			
MASEI-chronic damage	8 (2.2%)	19 (5.2%)	0.054
Erosion	15 (4.1%)	41 (11.3%)	**0.008**
Calcification/enthesophyte	126 (35.0%)	95 (26.3%)	**0.043**

The bold values indicate the values that were significantly different between groups.

the patellar tendon seems to be the most affected in gout in several studies (1, 14, 15, 24). We did not find other significant differences in this tendon and the distal patellar tendon and plantar fascia because they are affected similarly in both diseases (31). Concerning the triceps tendon, there was a trend for a higher percentage of both inflammatory and chronic damage in the gout group, however, there were no significant differences among groups. It has been reported that it is the second tendon most affected in gout, affecting almost 50% of patients while, in SpA it is involved in around 12% of independent studies (14, 32). We consider that this is the first time that these entheses have been compared in these diseases.

Respecting the MASEI-Inflammatory index, we did not find significant differences in structural change and thickness because gout affects entheses as frequently as SpA does (31). Only the presence of PD was significantly present in patients with SpA and mainly observed in calcaneal enthesis (30, 33). The low prevalence of PD in the population with gout contrasts with other studies (28, 31). Factors associated with vascularization are advanced age and high uric acid levels. It has been shown that PD signal significantly decreased at 2 years of urate-lowering therapy (34).

In MASEI-chronic damage, the calcifications/enthesophytes were most frequently demonstrated in gout like the other study (19). It is probable that calcifications are a predominant characteristic associated with the deposit of MSU in entheses, as shown by animal models of enthesitis, where local injection of monosodium urate crystals into the metatarsal entheses of oxidative-burst-deficient (Ncf1**) mice developed chronic enthesitis accompanied by massive enthesophytes by resonance magnetic imaging (35). In addition, it has been observed that advanced age and belonging to the male sex are associated with greater structural damage, factors that prevailed in our gout group (20).

The total MASEI score was higher in SpA than gout but there were no significant differences. According to the original study, 18 points would be the best cut-off point to differentiate patients with SpA from controls (21). However, patients with longstanding gout develop a higher frequency of chronic damage, specifically calcifications/enthesophytes in multiple entheses, which increases the index. Therefore, the MASEI would have limitations to be used to differentiate between both groups. It is important to note that most of the patients with gout had the tophaceous variety, which could contribute to having a higher MASEI score (13). Discriminant validity of MASEI has been studied in other diseases like Behcet and Fibromyalgia in which, the entheses are often not affected, giving low scores, thus facilitating discrimination, in contrast, in diseases such as gout, the discrimination by this score can be more difficult (36, 37).

Finally, the inter-reading concordance was excellent. The performance of inter-reader exercise has a great influence to improve reliability and our group has carried out this type of exercise periodically (38, 39). The other study has shown excellent inter-observer agreement for quantitative data (37).

LIMITATIONS AND STRENGTHS

One of the main limitations of our study was a relatively low number of patients, however, 720 entheses is a good number to consider. Another limitation was the age difference which was greater in the gout group; a bias that is difficult to correct given that patients with gout start their disease later. This condition probably accounts for a higher frequency of calcifications in the gout group, however, for the analysis of differences between groups we are not exclusively based on this lesion. Another constraint is that all patients with gout were receiving hypouricemic treatment and more than 40% of the SpA group were receiving immunosuppressive therapy and just over 20% biological therapy, conditions that could reduce the presence of PD in the entheses. Another weakness of the study is that we did not record the physical activity of the patients because it has been described those individuals with a greater demand for physical activity develop more structural and inflammatory changes in entheses. Additionally, the comorbidities observed in patients with gout could have contributed to the entheseal condition. All the same, one of the strengths of the study is that it includes a binational multicenter sample and patients were of real life.

CONCLUSIONS

The total MASEI could not discriminate between SpA and gout, however, some inflammatory and chronic lesions differ significantly depending on the underlying disease and tendon explored. In the Achilles tendon, this index shows the ability to differentiate SpA from gout due to having a higher prevalence of structural change, thickness, bursitis, erosions, and PD signal. Gout induces the development of calcifications/enthesophytes which increases the total index. Entheseal involvement in gout is almost as frequent as in SpA, therefore its evaluation is necessary.

DATA AVAILABILITY STATEMENT

The original contributions presented in the study are included in the article/supplementary material, further inquiries can be directed to the corresponding authors.

ETHICS STATEMENT

The studies involving human participants were reviewed and approved by Research Committee of the National Institute of Rehabilitation. The patients/participants provided their written informed consent to participate in this study.

AUTHOR CONTRIBUTIONS

LV-R and EM contributed to study conception, design, data collection, and manuscript drafting. CH-D, TC, SG-N, CG-R, MR, KS-L, PR-H, JV-M, and JC-V participated in data collection and manuscript drafting. EC-A contributed to statistical analysis. All authors read and approved the final manuscript.

REFERENCES

1. Gandjbakhch F, Terslev L, Joshua F, Wakefield RJ, Naredo E, D'agostino MA, et al. Ultrasound in the evaluation of enthesitis: status and perspectives. *Arthritis Res Ther.* (2001) 13:R188. doi: 10.1186/ar3516
2. Olivieri I, Barozzi L, Padula A. Enthesopathy: clinical manifestations, imaging, and treatment. *Baillieres Clin Rheumatol.* (1998) 12:665–81. doi: 10.1016/S0950-3579(98)80043-5
3. Balint PV, Kane D, Wilson H, Mcinnes IB, Sturrock RD. Ultrasonography of entheseal insertions in the lower limb in spondyloarthropathy. *Ann Rheum Dis.* (2002) 61:905–10. doi: 10.1136/ard.61.10.905
4. Borman P, Koparal S, Babaoglu S, Bodur H. Ultrasound detection of entheseal insertions in the foot of patients with spondyloarthropathy. *Clin Rheumatol.* (2006) 25:373–7. doi: 10.1007/s10067-005-0036-x
5. D'Agostino MA, Aegerter P, Bechara K, Salliot C, Judet O, Chimenti MS, et al. How to diagnose spondyloarthritis early? Accuracy of peripheral enthesitis detection by power Doppler ultrasonography. *Ann Rheum Dis.* (2011) 70:1433–40. doi: 10.1136/ard.2010.138701
6. de Miguel E, Muñoz-Fernández S, Castillo C, Cobo-Ibáñez T, Martín-Mola E. Diagnostic accuracy of enthesis ultrasound in the diagnosis of early spondyloarthritis. *Ann Rheum Dis.* (2011) 70:434–9. doi: 10.1136/ard.2010.134965
7. D'agostino MA, Said-Nahal R, Hacquard-Bouder C, Brasseur JL, Dougados M, Breban M. Assessment of peripheral enthesitis in the spondyloarthropathies by ultrasonography combined with power Doppler: a cross-sectional study. *Arthritis Rheum.* (2003) 48:523–33. doi: 10.1002/art.10812
8. Filippucci E, Aydin S, Karadag O, Salaffi F, Gutiérrez M, Direskeneli H, et al. Reliability of high-resolution ultrasonography in the assessment of Achilles tendon enthesopathy in seronegative spondyloarthropathies. *Ann Rheum Dis.* (2009) 68:1850–55. doi: 10.1136/ard.2008.096511
9. Falcão S, De Miguel E, Castillo C, Branco JC, Martín-Mola E. Doppler ultrasound – a valid and reliable tool to assess spondyloarthritis. *Acta Rheumatol Port.* (2012) 37:212–7.
10. Terslev L, Naredo E, IagnoccoO A, Balint P, Wakefield J, Aegerter P, et al. Defining enthesitis in spondyloarthritis by ultrasound: results of a delphi process and of a reliability reading exercise. *Arthritis Care Res.* (2014) 66:741–48. doi: 10.1002/acr.22191
11. D'agostino MA, Aegerter P, Jousse-Jolin S, Chary-Valkenaere I, Lecoq B, Gaudin P, et al. How to evaluate and improve the reliability of power doppler ultrasonography for assessing enthesitis in spondyloarthritis. *Arthritis Care Res.* (2009) 1:61–9. doi: 10.1002/art.24369
12. Wakefield RJ, Balint PV, Szkudlarek M, Filippucci E, Backhaus M, D'Agostino MA, et al. Musculoskeletal ultrasound including definitions for ultrasonographic pathology. *J Rheumatol.* (2005) 32:2485–7.
13. Dalbeth N, Kalluru R, Aati O, Horne A, Doyle AJ, McQueen FM. Tendon involvement in the feet of patients with gout: a dual-energy CT study. *Ann Rheum Dis.* (2013) 72:1545–48. doi: 10.1136/annrheumdis-2012-202786
14. Naredo E, Uson J, Jiménez-Palop M, Martínez A, Vicente E, Brito E, et al. Ultrasound-detected musculoskeletal urate crystal deposition: which joints and what findings should be assessed for diagnosing gout? *Ann Rheum Dis.* (2014) 73:1522–28. doi: 10.1136/annrheumdis-2013-203487
15. Peiteado D, de Miguel E, Villalba A, Ordóñez MC, Castillo C, Martín-Mola E. Value of a short four-joint ultrasound test for gout diagnosis: a pilot study. *Clin Exp Rheum.* (2012) 30:830–7.
16. Filippucci E, Sciré CA, Delle Sedie A, Iagnocco A, RienteL, Meenagh G, et al. Ultrasound imaging for the rheumatologist. XXV. Sonographic assessment of the knee in patients with gout and calcium pyrophosphate deposition disease. *Clin Exp Rheumatol.* (2010) 28:2–5.
17. Filippou G, Adinolfi A, Iagnocco A, Filippucci E, Cimmino MA, Bertoldi I, et al. Ultrasound in the diagnosis of calcium pyrophosphate dihydrate deposition disease. A systematic literature review and a meta–analysis. *Osteoarthr Cartil.* (2016) 24:973–81. doi: 10.1016/j.joca.2016.01.136
18. Howard RG, Pillinger MH, Gyftopoulos S, Thiele RG, Swearingen CHJ, Samuels J. Reproducibility of musculoskeletal ultrasound for determining monosodium urate deposition: concordance between readers. *Arthritis Care Res.* (2011) 63:1456–62. doi: 10.1002/acr.20527
19. Expósito Molinero MR, de Miguel Mendieta E. Discriminant validity study of ultrasound achilles enthesis. *Reumatol Clin.* (2016) 12:206–9. doi: 10.1016/j.reumae.2015.08.002
20. Macia-Villa C, de Miguel E. Updating the use of the Madrid Sonographic Enthesis Index (MASEI): a systematic review of the literature. *Rheumatology.* (2020) 59:1031–40. doi: 10.1093/rheumatology/kez356
21. de Miguel E, Cobo T, Muñoz-Fernández S, Naredo E, Uson J, Acebes JC, et al. Validity of enthesis ultrasound assessment in Spondyloarthropathy. *Ann Rheum Dis.* (2009) 68:169–74. doi: 10.1136/ard.2007.084251
22. Balint PV, Terslev L, Aegerter Ph, Bruyn G, Chary-Valckenaere I, Gandjbakhch F, et al. Reliability of a consensus-based ultrasound definition and scoring for enthesitis in spondyloarthritis and psoriatic arthritis: an OMERACT US initiative. *Ann Rheum Dis.* (2018) 77:1730–5. doi: 10.1136/annrheumdis-2018-213609
23. Mata Arnaiz MC, de Miguel E. Usefulness of ultrasonography in the assessment of peripheral enthesis in spondyloarthritis. *Rheumatol Clin.* (2014) 10:113–9. doi: 10.1016/j.reumae.2013.11.008
24. Ventura-Ríos L, Sánchez-Bringas G, Pineda C, Hernández-Díaz C, Reginato A, Alva M, et al. Tendon involvement in patients with gout: an ultrasound study of prevalence. *Clin Rheumatol.* (2016) 35:2039–44. doi: 10.1007/s10067-016-3309-7
25. Seven S, Pedersen SJ, Østergaard M, Felbo SK, Sørensen IJ, Døhn UM, et al. Peripheral enthesitis detected by ultrasonography in patients with axial Spondyloarthritis—anatomical distribution, morphology, and response to Tumor Necrosis Factor-Inhibitor Therapy. *Front Med.* (2020) 7:341. doi: 10.3389/fmed.2020.00341
26. Carroll M, Dalbeth N, Boocockd M, Romea K. The assessment of lesions of the Achilles tendon by ultrasound imaging in inflammatory arthritis: a systematic review and meta-analysis. *Sem Arthritis Rheum.* (2015) 45:103–14. doi: 10.1016/j.semarthrit.2015.03.001
27. Falcao S, de Miguel E, Castillo-Gallego C, Peiteado D, Branco J, Martin Mola E. Achilles enthesis ultrasound: the importance of the bursa in spondyloarthritis. *Clin Exp Rheum.* (2013) 31:422–7.
28. Carroll M, Dalbeth N, Allen B, Stewart S, House T, Boocock M, et al. Ultrasound characteristics of the achilles tendon in tophaceous gout: a comparison with age- and sex-matched controls. *J Rheumatol.* (2017) 44:1487–92. doi: 10.3899/jrheum.170203
29. Aydin SZ, Tan AL, Hodsgon R, Grainger A, Emery P, Wakefield RJ, et al. Comparison of ultrasonography and magnetic resonance imaging for the assessment of clinically defined knee enthesitis in spondyloarthritis. *Clin Exp Rheumatol.* (2013) 31:933–6.
30. Narimatsu Ishida S, Vilar Furtado RN, Rosenfeld A, Passos Proglhof JE, Queiroga Estrela GB, NatourI J. Ultrasound of entheses in ankylosing spondylitis patients: The importance of the calcaneal and quadriceps entheses for differentiating patients from healthy individuals. *Clinics.* (2019) 74:e727. doi: 10.6061/clinics/2019/e727
31. Xu G, Lin J, Liang J, Yang Y, Ye Z, Zhu G, et al. Entheseal involvement of the lower extremities in gout: an ultrasonographic descriptive observational study. *Clin Rheumatol.* (2021) 40:4649–57. doi: 10.1007/s10067-021-05826-0
32. Ebsteina E, Coustet B, Masson-Behar V, Foriena M, Palazzo E, Dieudéa P, et al. Enthesopathy in rheumatoid arthritis and spondyloarthritis: an ultrasound study. *Joint Bone Spine.* (2017) 85:577–81. doi: 10.1016/j.jbspin.2017.11.014
33. Aydin SZ, Bakirci S, Kasapoglu E, Castillo-Gallego C, Alhussain FA, Ash ZR, et al. The relationship between physical examination and ultrasonography for large entheses is best for the Achilles tendon and patellar tendon origin. *J Rheumatol.* (2020) 47:1026–30. doi: 10.3899/jrheum.190169
34. Peiteado D, Villalba A, Martín-Mola E, de Miguel E. Reduction but not the disappearance of Doppler signal after two years of treatment for gout. Do we need a more intensive treatment? *Clin Exp Rheumatol.* (2015) 33:385–90.
35. Czegley Ch, Gillmann C, Schauer Ch, Seyler S, Reinwald Ch, Hahn M, et al. A model of chronic enthesitis and new bone formation characterized by multimodal imaging. *Dis Model Mech.* (2018) 11:dmm034041. doi: 10.1242/dmm.034041
36. Ozkan F, Cetin GY, Bakan B, Kalender AM, Yuksel M, Ekerbice HC, et al. Sonographic evaluation of subclinical entheseal involvement in patients with Behcet disease. *Am J Roentgenol.* (2012) 199:W723–9. doi: 10.2214/AJR.12.8576

37. Ozkan F, Bakan B, Inci MF, Kocturk F, Cetin GY, Yuksel M, et al. Assessment of enthesopathy in patients with fibromyalgia by using new sonographic enthesitis index. *Rev Bras Reumatol.* (2013) 53:335–40. doi: 10.1016/S2255-5021(13)70045-2
38. Ventura-Ríos L, Navarro-Compan V, Aliste M, Linares MA, Areny R, Audisio M, et al. Is entheses ultrasound reliable? A reading Latin American exercise. *Clin Rheumatol.* (2016) 35:1353–7. doi: 10.1007/s10067-015-3007-x
39. Cazenave T, Martire V, Reginato AM, Gutierrez M, Waimann CA, Pineda C, et al. Reliability of OMERACT ultrasound elementary lesions in gout: results from a multicenter exercise. *Rheumatol Int.* (2019) 39:707–13. doi: 10.1007/s00296-018-4220-0

Conflict of Interest: The authors declare that the research was conducted in the absence of any commercial or financial relationships that could be construed as a potential conflict of interest.

frontiers | Frontiers in Medicine

BRIEF RESEARCH REPORT
published: 31 May 2022
doi: 10.3389/fmed.2022.913589

A Novel Technique for the Evaluation and Interpretation of Elastography in Salivary Gland Involvement in Primary Sjögren Syndrome

*Rosa Elda Barbosa-Cobos[1], Rubén Torres-González[2], Ana Victoria Meza-Sánchez[3,4], Lucio Ventura-Ríos[4], Luz Elena Concha-Del-Río[5], Julián Ramírez-Bello[6], Everardo Álvarez-Hernández[7], Claudia Irene Meléndez-Mercado[8], Favio Edmundo Enríquez-Sosa[9], Cinthia Jahoska Samuria-Flores[1], Gustavo Esteban Lugo-Zamudio[1] and Cristina Hernández-Díaz[4]**

[1] Servicio de Reumatología, Hospital Juárez de México, Centro Médico ABC y Grupo "Manifestaciones Oculares en Reumatología" MOR, Mexico City, Mexico, [2] Dirección de Educación e Investigación en Salud, Unidad Médica de Alta Especialidad (UMAE) de Traumatología, Ortopedia, Rehabilitación "Dr. Victorio de la Fuente Narváez," Instituto Mexicano del Seguro Social (IMSS) y Grupo "Manifestaciones Oculares en Reumatología" MOR, Mexico City, Mexico, [3] Escuela Superior de Medicina, Instituto Politécnico Nacional, Mexico City, Mexico, [4] División de Reumatología, Instituto Nacional de Rehabilitación "Luis Guillermo Ibarra Ibarra," Mexico City, Mexico, [5] Clínica de Enfermedades Inflamatorias Oculares, Asociación Para Evitar la Ceguera en México (APEC), Hospital de la Ceguera "Dr. Luis Sánchez Bulnes," y Grupo "Manifestaciones Oculares en Reumatología" MOR, Mexico City, Mexico, [6] Departamento de Endocrinología, Instituto Nacional de Cardiología, Mexico City, Mexico, [7] Servicio de Reumatología, Hospital General de México, "Dr. Eduardo Liceaga," Mexico City, Mexico, [8] Servicio de Reumatología, Centro Médico ISSEMYM "Lic. Arturo Montiel Rojas" Toluca, Mexico City, Mexico, [9] Servicio de Reumatología, Hospital Regional "General Ignacio Zaragoza," ISSSTE, Mexico City, Mexico*

OPEN ACCESS

Edited by:
Andrea Di Matteo,
Marche Polytechnic University, Italy

Reviewed by:
Antonella Adinolfi,
Niguarda Ca' Granda Hospital, Italy
Lene Terslev,
Copenhagen University Hospital, Denmark
Edoardo Cipolletta,
Marche Polytechnic University, Italy

***Correspondence:**
Cristina Hernández-Díaz
cristy_hernandez@hotmail.com

Specialty section:
This article was submitted to Rheumatology, a section of the journal Frontiers in Medicine

Received: *05 April 2022*
Accepted: *11 May 2022*
Published: *31 May 2022*

Citation:
Barbosa-Cobos RE, Torres-González R, Meza-Sánchez AV, Ventura-Ríos L, Concha-Del-Río LE, Ramírez-Bello J, Álvarez-Hernández E, Meléndez-Mercado CI, Enríquez-Sosa FE, Samuria-Flores CJ, Lugo-Zamudio GE and Hernández-Díaz C (2022) A Novel Technique for the Evaluation and Interpretation of Elastography in Salivary Gland Involvement in Primary Sjögren Syndrome. Front. Med. 9:913589. doi: 10.3389/fmed.2022.913589

Ultrasound (US) of major salivary glands (MSG) evaluates echogenicity, border features and vascularization, with elastography, it can detect tissue elasticity and glandular fibrosis, related to inflammation in Primary Sjögren's syndrome (pSS). This study aimed to develop a novel technique by pixel analysis for evaluation and interpretation of elastography in MSG in pSS. A cross-sectional and observational multicenter study was conducted. The US of MSG performed in orthogonal planes in grayscale, Doppler, and shear-wave elastography. For elastography images of each gland were analyzed with the open-source program ImageJ to perform a pixel analysis. Statistical analysis was performed with the IBM-SPSS v25 program. Fifty-nine women with a mean age of 57.69 (23–83) years were recruited; pSS mean duration of 87 (5–275) months, and 12 healthy women without sicca symptoms as a control group with a mean age of 50.67 (42–60) years. Intragroup analysis showed p-values >0.05 between sicca symptoms, ocular/dryness tests, biopsy, US, and pixel analysis; correlation between Hocevar and pixel analysis was not found (rho < 0.1, $p > 0.5$). MSG anatomical size was 41.7 ± 28.2 mm vs. 67.6 ± 8.8 mm ($p \leq 0.0001$); unstimulated whole saliva flow rate was 0.80 ± 0.80 ml/5 min vs. 1.85 ± 1.27 ml/5 min ($p = 0.016$). The elastography values (absolute number of pixels) were 572.38 ± 99.21 vs. 539.69 ± 93.12 ($p = 0.290$). A cut-off point risk for pSS identified with less than 54% of red pixels in the global MSG mass [OR of 3.8 95% CI (1.01–15.00)]. Pixel analysis is a new tool that could lead to a better understanding of the MSG chronic inflammatory process in pSS.

Keywords: major salivary glands, ultrasound, elastography, pixel analysis, primary Sjögren syndrome

INTRODUCTION

Primary Sjögren's syndrome (pSS) is a chronic, systemic, and autoimmune exocrinopathy involving mainly the salivary and lacrimal glands, which are progressive destructed by an immune-mediated process. Xerostomia and xeropthalmia are the main complaints, but other sicca symptoms and extra-glandular manifestations may be present (1). pSS confirmation of depends on objective measures of dysfunctional salivary or lacrimal glands in addition to serological or salivary gland histopathology of MSG to evidence autoimmunity. Salivary gland correct evaluation of involvement provides data for the pSS diagnosis (2, 3).

The major salivary glands (MSG) are the parotid, submandibular and sublingual. Meanwhile, the minor salivary glands are located throughout the mouth and the aerodigestive tract.

The glands, especially parotid, are also composed of abundant fatty tissue with a ratio of adipose-acinar tissue 1:1 (4). All salivary glands can be affected by pSS (4, 5). The parotid and submandibular glands, if affected by inflammation, contribute little to saliva production. Acini atrophy can derive from ductal system failure and influence xerostomia. In the beginning, the affection in pSS is related to peripheral intraglandular ducts and acini, due to inflammation associated with lymphocytic infiltrate (foci) located around the ducts, with the capacity to carry out effective immune responses (5).

Although imaging techniques contribute to the diagnosis by avoiding invasive procedures, such as biopsies, there is no gold standard technique to evaluate MSG. Due to its accessible location, it is easier to determine structural damage. Magnetic resonance imaging (MRI) has proven good performance, with a specificity of up to 98%, but it is expensive, whereas scintigraphy and sialography with specificities of up to 50 and 82%, respectively, are not widely used due to their invasiveness and high cost (6, 7). Ultrasound (US) has proven good sensitivity and very good specificity when compared to sublingual biopsies, using different scoring systems, equipment, and transducers (8, 9). US is non-invasive, non-expensive, non-ionizing radiation-related, and easy-going for patients. MSG US evaluates echogenicity, border features in B mode, and vascularization with power Doppler, with high specificity (between 83 and 98%) (9). Today, MSG US is used to describe glandular homogeneity, echogenicity, and parenchymal characterization, with good performance when compared to labial biopsies, minor salivary gland focus score and other autoimmune diseases (10), and provides accurate information about intraglandular vascularization.

Recently, elastography has been used to detect tissue elasticity and glandular fibrosis (11–13); there is scarce information in elderly pSS patients in which MSG US is associated with glandular atrophy (14). There is no valid scoring system to interpret elastography in MSG, however, a four-grade score has been used, which gives an interpretation related to the main color in the area of interest. To achieve better objective evaluation, with qualitative elastography, some image visualization software has been used, one of them, Image J (NIH®) (15), allows delimiting the area of interest by obtaining a histogram of the color map, with which you can get obtained a quantitative analysis of the pixels in general and each color.

However, there is still the need for a better approach to evaluate MSG involvement in daily clinical settings that could be easily applied and learned.

This study aimed to develop a novel technique by pixel analysis for evaluation and interpretation of elastography in MSG in pSS.

PATIENTS AND METHODS

Subjects and Study Design

A cross-sectional and observational multicenter study was conducted. The study was done according to the ethics guidelines of the Declaration of Helsinki and approved by the ethics, research, and biosecurity Committees of Hospital Juárez de México (HJM0323/17-R) and Instituto Nacional de Rehabilitación "Luis Guillermo Ibarra Ibarra" (INRLGII 01/21/SP-1). All participants signed a written informed consent letter.

Clinical Assessment

Epidemiological, clinical, serological, histological, and therapeutic data were abstracted from clinical records. Patients with pSS (who fulfilled the 2016 American College of Rheumatology-European League Against Rheumatism classification criteria for Sjögren syndrome) enrolled consecutively, and the control group was integrated by healthy women (without sicca symptoms). All subjects were examined to evaluate sicca symptoms, clinical parotid gland enlargement, systemic manifestations, and ocular and oral dryness, last assessed with unstimulated whole saliva flow rate for salivary flow measurement according to Navazesh et al. (16). Labial salivary gland biopsy was only performed in pSS group for ethical issues. The exclusion criteria were the coexistence of another autoimmune disease.

Major Salivary Glands Ultrasound and Elastography

After clinical evaluation, all participants were sent to the US unit.

US and elastography were performed by the same ultrasonographer (HDC) with 18 years of experience, blinded to subject data in a mean time of 15 min.

Grayscale and elastography from parotid and submandibular gland were assessed, with subject in sitting position and the neck slightly extended backward, in orthogonal planes bilaterally. A GE Logic P7 unit was used with a 6–12 MHz multifrequency linear transducer for grayscale and a 10 MHz frequency power Doppler with PRF 0.6; color gain was adjusted when sound artifacts disappeared below cortical bone. Shear wave elastography of each gland took in the same position as the grayscale, displaying images simultaneously, showing the region of interest (ROI) when the compressibility limit come to green in the visual indicator scale on the screen. The softest component was described in red, whereas the hardest was depicted in blue,

and green showed intermediate elasticity. A total of thirty-six images of each subject were saved and subsequently evaluated to determine the grayscale MSG structural changes using the Hocevar scoring system (0–48, cut-off score 18 points) and the presence of Doppler signal excluding normal vessels (17). The open-source program ImageJ was used for image pixel analysis, both in greyscale and elastography.

Statistical Analysis

A specific integrated database was used for our study with Excel and IBM-SPSS v25. Description of variables made with measures of central tendency and dispersion. Homogeneity variable analysis with Chi-square for nominal and Levene's statistic for numerical carried out, p-values > 0.05. Variables compared between groups (pSS patients and healthy subjects) and intragroup (pSS patients) with chi-square and means with Student's t-test, ANOVA, Pearson and Spearman correlation; with statistical significance p-values ≤ 0.05, with the calculation of impact measure through risks with OR, and identification of cut-off point with statistical significance through CI at 95%.

TABLE 1 | Characteristics and treatment of 59 women with primary Sjögren syndrome.

Variable	Frequency	(%)
Sicca symptoms		
Xeropthalmia	59	100
Xerostomia	42	71
Nasal dryness	16	27
Non-productive cough	5	8.5
Vaginal dryness	11	18.6
Cutaneous dryness	17	28.8
Ocular dryness tests		
Positive schirmer-1 test[#]	30	50.8
Ocular staining score[&]	33	55.9
Tear break-up time[*]	56	94.9
Oral dryness tests		
Unstimulated whole saliva flow rate[$]	35	59.3
Systemic manifestations		
Fatigue	14	23.7
Fever	1	1.7
Night sweats	13	22
Involuntary weight loss	5	8.5
Arthralgias	13	22
Synovitis	5	8.5
Raynaud phenomenon	3	5.1
Anti-SSA (Ro)$^{+}$	51	86
Anti-SSB (La)$^{+}$	31	52.5
Labial salivary gland biopsy[‡]		
Positive	50	84.7
Negative	3	5.3
Not performed	6	10
Symptomatic treatment		
Ocular	58	98
Oral	17	28.8
Vaginal	13	22
Cutaneous	38	64
Comorbidity		
Smoking	8	13.6
Diabetes	2	3.4
Hypertension	9	15.3
Dyslipidemia	16	27.1
Hypothyroidism	14	23.7

[#] *≤5 mm/5 min on at least one eye,* [&] *≥ 5 on at least one eye,* [*] *<10 s,* [$] *≤ 0.1 ml/min,* [‡] *with focal lymphocytic sialadenitis and focus score ≥ 1 foci/4 mm^2. +, Positive.*

RESULTS

The study group 59 women with a mean age of 57.69 (23–83) years, mean disease duration of 87 (5–275) months, and the control group was 12 healthy women with a mean age of 50.67 (42–60) years.

Clinical, serological, and histological characteristics of pSS group are depicted in **Table 1**. No clinical parotidomegaly was found among the patients or healthy subjects. Systemic treatment of the patients consisted in hydroxychloroquine 30 (50.8%), glucocorticoids 22 (37.3%), methotrexate 20 (33.9%), rituximab 3 (5.1%), cyclophosphamide 1 (1.7%), and mycophenolate 1 (1.75%).

Intragroup analysis showed p-values > 0.05 between sicca symptoms, ocular and dryness tests, systemic manifestations, labial salivary gland biopsy, US glandular size, and pixel analysis. Correlation between Hocevar and pixel analysis was not found (rho < 0.1, $p > 0.5$).

The anatomical size of all MSG identified were 41.7 ± 28.2 mm for Sjögren patients and 67.6 ± 8 mm for healthy subjects (group 1: 38.8% smaller), with a p-value < 0.0001; unstimulated whole saliva flow rate was 0.80 ± 0.80 ml/5 min for group 1 and 1.85 ± 1.27 ml/5 min for group 2, with a p-value of 0.016. The elastography values by an absolute number of pixels were 572.38 ± 99.21 in group 1 and 539.69 ± 93.12 in group 2 (p-value of 0.290). A cut-off point risk was identified for pSS with less than 54% of Red Pixels in the global salivary gland mass, with OR of 3.8 95% CI (1.01–15.00) (**Figure 1**).

When comparing elastography values between groups, with and without sicca symptoms, they showed p-values > 0.005.

DISCUSSION

We explored a new face of US using elastography to evaluate pSS. US and elastography gave us a new non-invasive approach to possibly integrate these features into pSS diagnosis.

By using pixel analysis, we demonstrated that global salivary gland mass was $< 54\%$ red without a predominant stiffness, as also shown by Zhang et al., which used a global score derived from the one used for hepatic fibrosis with chronic hepatitis C (18, 19). In this study, Zhang et al. also demonstrated that elastography scores of bilateral parotids correlated significantly with dental loss and disease duration.

In our study, we found by elastography stiffer tissue in both parotid and submandibular glands by pixel analysis, the finding was associated significantly with minor glands and low

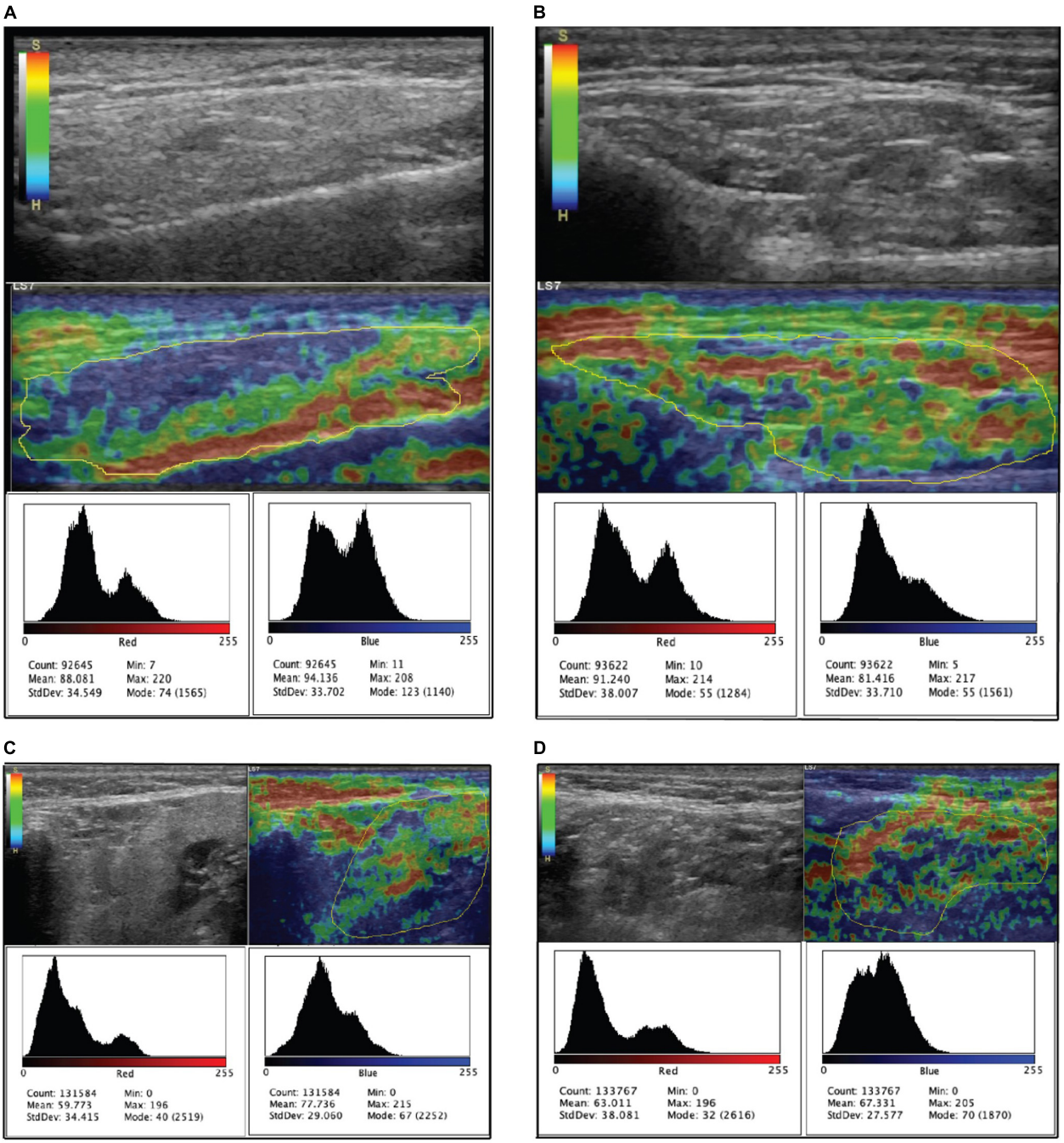

FIGURE 1 | Shows the B-mode ultrasound and elastography of major salivary glands. Below each ultrasound figure are the histograms for soft (red) and hard (blue) tissues. **(A,C)** Are the parotid and submandibular glands of a patient with a Hocevar score of 1, and **(B,D)** are the glands of a patient with a Hocevar score of 33.

unstimulated whole saliva flow rate; it can translate as chronic damage or its consequences; differing to what Zhang et al. found in their study in which the parotid was the most involved gland (20, 21).

This finding could be related to fatty tissue infiltration in the glands. Additionally, it accompanies the initial inflammatory and fibrotic process, which is not evaluated adequately since parotid or submandibular biopsies are not recommended (22). However, fatty tissue is an inflammatory tissue, so detecting initial changes with elastography, especially with pixel analysis leads to early diagnosis of inflammation or fibrosis and fatty infiltrate in the gland; as has been done in other studies in which elasticity index has been used (13, 20), but not this novel pixel analysis technique. Our finding suggests a path, possibly related to fatty tissue

inflammation, to evaluate early damage, as Skarstein et al. (22) previously showed. They performed a biopsy of labial salivary glands, finding that the fatty tissue that replaced glandular tissue was rich in interleukin 6, especially in areas in which adipocytes were about focal infiltrates. This hypothesis should be further studied for MSG without invasive procedures, so elastography is a good possibility.

Jimenez-Royo et al. (23) have demonstrated by MRI that there is a fatty infiltrate in the MSG, possibly resembling functional glandular tissue substitution, even though salivary flow rate has a weak correlation with the imaging technique, as in our study.

Despite the small number of patients, we found that pixel analysis gives accurate information related to MSG structural glandular changes.

US allows us to explore new tissue characteristics such as elasticity, picturing new ways to analyze MSG structural damage, by exploring the fat deposit role during pSS natural history.

CONCLUSION

Even though in the pSS group, mass in the MSG is 38.3% smaller, the global number of pixels is similar in both groups, contrasting with the lower saliva production and less elastic tissue; that is shown by the lower proportion of red pixels in the pSS group. The identified cut-off point could function as a new screening test in this group of patients.

Pixel analysis is a new tool that could lead to a better understanding of the chronic inflammatory process in pSS by showing the role that fat tissue deposition plays in the fibrotic process of the major salivary glands.

DATA AVAILABILITY STATEMENT

The raw data supporting the conclusions of this article will be made available by the authors, without undue reservation.

ETHICS STATEMENT

The studies involving human participants were reviewed and approved by the Hospital Juárez de México (HJM0323/17-R) and Instituto Nacional de Rehabilitación "Luis Guillermo Ibarra Ibarra" (INRLGII 01/21/SP-1). The patients/participants provided their written informed consent to participate in this study.

AUTHOR CONTRIBUTIONS

RB-C, RT-G, AM-S, LV-R, and CH-D: manuscript elaboration, conception and edition, statistical analysis, and final review. RB-C and RT-G: patient recruitment and data-based review. LC-D-R, JR-B, EÁ-H, CM-M, FE-S, CS-F, and RB-C: patient recruitment. RB-C, RT-G, LV-R, and CH-D: final draft review and edition. All authors contributed to the article and approved the submitted version.

ACKNOWLEDGMENTS

We thank the enrolment contribution of Carrillo-Vázquez Sandra, Diaz-Ceballos Moreno María de los Ángeles, and Vargas Angélica.

REFERENCES

1. Generali E, Costanzo A, Mainetti C, Selmi C. Cutaneous and mucosal manifestations of Sjögren's syndrome. *Clin Rev Allergy Immunol.* (2017) 53:357–70. doi: 10.1007/s12016-017-8639-y
2. Rischmueller M, Spurrier A. Can Sjögren's syndrome diagnosis and evaluation be stretched by elastography? *Int J Rheum Dis.* (2019) 22:172–4.
3. Shiboski CH, Shiboski SC, Seror R, Criswell LA, Labetoulle M, Lietman TM, et al. 2016 American college of rheumatology/European league against rheumatism classification criteria for primary Sjogren's syndrome: a consensus and data-driven methodology involving three international patient cohorts. *Arthritis Rheumatol.* (2017) 69:35–45.
4. Silvers AR, Som PM. Salivary glands. *Radiol Clin North Am.* (1998) 36:941–66.
5. Kroese FGM, Haacke EA, Bombardieri M. The role of salivary gland histopathology in primary Sjögren's syndrome promises and pitfalls. *Clin Exp Rheumatol.* (2018) 36(Suppl. 112):222–33.
6. Van Ginkel M, Glaudemans A, Van del Vegt B, Mossel E, Kroese F, Bootsma H, et al. Imaging in primary Sjögren's syndrome. *J Clin Med.* (2020) 9:2492. doi: 10.3390/jcm9082492
7. Świecka M, Maślińska M, Paluch Ł, Zakrzewski J, Kwiatkowska B. Imaging methods in primary Sjögren's syndrome as potential tools of disease diagnostics and monitoring. *Reumatologia.* (2019) 57:336–42. doi: 10.5114/reum.2019.91273
8. Mossel E, Delli K, van Nimwegen JF, Stel AJ, Kroese FGM, Spijkervet FK, et al. Ultrasonography of major salivary glands compared with parotid and labial gland biopsy and classification criteria in patients with clinically suspected primary Sjögren's syndrome. *Ann Rheum Dis.* (2017) 76:1883–9. doi: 10.1136/annrheumdis-2017-211250
9. Cornec D, Jousse-Joulin S, Marhadour T, Pers JO, Boisramé-Gastrin S, Renaudineau Y, et al. Salivary gland ultrasonography improves the diagnostic performance of the 2012 American college of rheumatology classification criteria for Sjögren's syndrome. *Rheumatology (Oxford).* (2014) 53:1604–7. doi: 10.1093/rheumatology/keu037
10. Baldini C, Zabotti A, Filipovic N, Vukicevic A, Luciano N, Ferro F, et al. Imaging in primary Sjögren's syndrome: the "obsolete and the new". *Clin Exp Rheumatol.* (2018) 36(Suppl. 112):S215–21.
11. López-Jornet P, Berna Mestre J, Pina F, Aniorte Alegria A, Gálvez J, Berna Serna JD. Is sonoelastography a helpful method of evaluation to diagnose Sjögren's syndrome? *Int J Rheum Dis.* (2019) 22:175–81.
12. Sigrist R, Liau J, Kaffas A, Chamas M, Willmann J. Ultrasound elastography: review of techniques and clinical applications. *Theranostics.* (2017) 7:1303–29.
13. Cindil E, Oktar SO, Akkan K, Sendur HN, Mercan R, Tufan A, et al. Ultrasound elastography in assessment of salivary glands involvement in primary Sjogren's syndrome. *Clin Imaging.* (2018) 50:229–34. doi: 10.1016/j.clinimag.2018.04.011
14. Lee K-A, Choi W, Kim JS, Lee S-H, Kim H-R. Elderly-onset primary Sjögren's syndrome focus on clinical and salivary gland ultrasonographic features. *Joint Bone Spine.* (2021) 88:105132.
15. Image J. *Java-Based Image Processing Program Developed at the National Institutes of Health and the Laboratory for Optical and Computational Instrumentation.* LOCI, University of Wisconsin (1997). Available online at: http://rsbweb.nih.gov/ij/
16. Navazesh M, Kumar SK, University of Southern California School of Dentistry. Measuring salivary flow: challenges and opportunities. *J Am Dent Assoc.* (2008) 139(Suppl):35S–40S. doi: 10.14219/jada.archive.2008.0353

17. Hocevar A, Ambrozic A, Rozman B, Kveder T, Tomsic M. Ultrasonographic changes of major salivary glands in primary Sjogren's syndrome. Diagnostic value of a novel scoring system. *Rheumatology.* (2005) 44:768–72. doi: 10.1093/rheumatology/keh588
18. Zhang X, Zhang S, Feng R, Yao H, Tang S, He J. Sonoelastography of salivary glands for diagnosis and clinical evaluation in primary Sjögren's syndrome. *Clin Exp Rheumatol.* (2021) 39(Suppl. 133):184–9.
19. Fujimoto K, Kato M, Kudo M, Yada N, Shiina T, Ueshima K, et al. Novel image analysis method using ultrasound elastography for noninvasive evaluation of hepatic fibrosis in patients with chronic hepatitis C. *Oncology.* (2013) 84(Suppl. 1):3–12. doi: 10.1159/000345883
20. Oruk YE, Çildağ MB, Karaman CZ, Çildağ S. Effectiveness of ultrasonography and shear wave sonoelastography in Sjögren syndrome with salivary gland involvement. *Ultrasonography.* (2021) 40:584–93. doi: 10.14366/usg.21014
21. Kimura-Hayama E, Criales-Vera S, Azpeitia-Espinosa L, Pacheco-Molina C, Reyes E, Lima G, et al. Elastographic ultrasound: an additional image tool in Sjögren's syndrome. *Int J Rheum Dis.* (2018) 21:1293–300. doi: 10.1111/1756-185X.13292
22. Skarstein K, Aqrawi LA, Øijordsbakken G, Jonsson R, Liaaen Jensen J. Adipose tissue is prominent in salivary glands of Sjögren's syndrome patients and appears to influence the microenvironment in these organs. *Autoimmunity.* (2016) 49:338–46. doi: 10.1080/08916934.2016.1183656
23. Jimenez-Royo P, Bombardieri M, Curtin C, Kostapanos M, Tappuni AR, Jordan N, et al. Advanced imaging for quantification of abnormalities in the salivary glands of patients with primary Sjogren's syndrome. *Rheumatology.* (2021) 60:2396–408. doi: 10.1093/rheumatology/keaa624

Conflict of Interest: The authors declare that the research was conducted in the absence of any commercial or financial relationships that could be construed as a potential conflict of interest.

Publisher's Note: All claims expressed in this article are solely those of the authors and do not necessarily represent those of their affiliated organizations, or those of the publisher, the editors and the reviewers. Any product that may be evaluated in this article, or claim that may be made by its manufacturer, is not guaranteed or endorsed by the publisher.

frontiers | Frontiers in Medicine

REVIEW
published: 20 June 2022
doi: 10.3389/fmed.2022.926573

The Role of Ultrasound in Temporomandibular Joint Disorders: An Update and Future Perspectives

Beatrice Maranini[1]*, *Giovanni Ciancio*[1], *Stefano Mandrioli*[2], *Manlio Galiè*[2] and *Marcello Govoni*[1]

[1] Rheumatology Unit, Department of Medical Sciences, University of Ferrara, Ferrara, Italy, [2] Department of Cranio-Maxillofacial Surgery, Unit of Cranio-Maxillofacial Surgery, University of Ferrara, Ferrara, Italy

Temporomandibular joint (TMJ) disorder is the second most common chronic pain condition affecting the general population after back pain. It encompasses a complex set of conditions, manifesting with jaw pain and limitation in mouth opening, influencing chewing, eating, speaking, and facial expression. TMJ dysfunction could be related to mechanical abnormalities or underlying inflammatory arthropathies, such as rheumatoid arthritis (RA) or juvenile idiopathic arthritis (JIA). TMJ exhibits a complex anatomy, and thus a thorough investigation is required to detect the TMJ abnormalities. Importantly, TMJ involvement can be completely asymptomatic during the early stages of the disease, showing no clinically detectable signs, exposing patients to delayed diagnosis, and progressive irreversible condylar damage. For the prevention of JIA complications, early diagnosis is therefore essential. Currently, magnetic resonance imaging (MRI) is described in the literature as the gold standard method to evaluate TMJ. However, it is a high-cost procedure, not available in all centers, and requires a long time for image acquisition, which could represent a problem notably in the pediatric population. It also suffers restricted usage in patients with claustrophobia. Ultrasonography (US) has emerged in recent years as an alternative diagnostic method, as it is less expensive, not invasive, and does not demand special facilities. In this narrative review, we will investigate the power of US in TMJ disorders based on the most relevant literature data, from an early screening of TMJ changes to differential diagnosis and monitoring. We then propose a potential algorithm to optimize the management of TMJ pathology, questioning what would be the role of ultrasonographic study.

Keywords: ultrasonography, temporomandibular joint, temporomandibular joint disorders, diagnostic imaging, articular disc, capsular width, joint pain

OPEN ACCESS

Edited by:
Christian Dejaco,
Medical University of Graz, Austria

Reviewed by:
Stephanie Finzel,
University of Freiburg, Germany
Rusmir Husic,
Medical University of Graz, Austria

***Correspondence:**
Beatrice Maranini
beatrice.maranini@edu.unife.it

Specialty section:
This article was submitted to Rheumatology, a section of the journal Frontiers in Medicine

Received: *22 April 2022*
Accepted: *24 May 2022*
Published: *20 June 2022*

Citation:
Maranini B, Ciancio G, Mandrioli S, Galiè M and Govoni M (2022) The Role of Ultrasound in Temporomandibular Joint Disorders: An Update and Future Perspectives. Front. Med. 9:926573. doi: 10.3389/fmed.2022.926573

INTRODUCTION

The temporomandibular joint (TMJ) is a bicondylar articulation of the ellipsoid variety (1). It is a synovial joint and thus it is susceptible to arthritis and related inflammatory conditions (2).

Following chronic low back pain, TMJ disorders (TMD) are the second most common musculoskeletal condition affecting approximately 5–12% of the population (3), causing chronic pain and even disability if untreated. Thus, a prompt diagnosis, before morphological degeneration occurs, is crucial (4, 5).

The Research Diagnostic Criteria for TMD classifies patients into three groups: (a) myogenous (sustained by muscular dysfunction, bruxism, abnormal posture, and myofascial conditions); (b) disk displacement or articular disk derangement; (c) articular causes (arthralgia, inflammatory arthritis, osteoarthritis, and less commonly ankylosis and neoplastic conditions) (6).

Although the most frequent causes of TMD are dental or orofacial phenomena, clinicians should not neglect inflammatory arthritis as a source of arthropathy (6), mainly rheumatoid arthritis (RA), psoriatic arthritis (PsA), and ankylosing spondylitis (AS) (7–9). Consequently, patients with known rheumatological conditions should be regularly screened for TMD, even if this assessment is not currently included in the routine screening and monitoring protocols (2).

Inflammation and increased vascularity are supposed to play a pivotal role in the pathogenesis of TMJ painful dysfunction (10). Moreover, TMJ represents a unique model to study bone changes in osteoarthritis (OA), because TMJ condylar articular surface is covered only by a thin layer of fibrocartilage, and the bone of the mandibular condyle is located just beneath the fibrocartilage, making it particularly vulnerable to inflammatory damage (11, 12).

The typical physical examination comprises evaluation for pain, stiffness, joint noises, and asymmetric or reduced mouth opening (13). Recently, published recommendations also encouraged detailed examination of masticatory muscles by palpation, as muscle tenderness may reveal an active disease (7, 14).

However, TMJ configures one of the most challenging joints to evaluate clinically, due to relatively uncommon evidence of swelling and paucisymptomatic conditions occurring during the early stage of the disease (15, 16). Thus, while certain abnormalities at the physical examination are strongly suggestive of TMJ involvement, their absence does not exclude it.

As there are no treatments to reverse the TMJ chronic damage once established, early diagnosis represents the only opportunity to prevent extensive and permanent joint derangements. Nonetheless, the current diagnosis, based on the Diagnostic Criteria for Temporomandibular Disorders (DC/TMD), confirms that TMJ degradation has already occurred, as documented in the standard imaging recommended protocols (computed tomography, CT, and magnetic resonance imaging, (MRI) (17). Therefore, the DC/TMD criteria are based on pre-existent condylar damage, namely surface erosions, osteophytes, or generalized sclerosis, mainly present in the later stages of the disease.

The purpose of this narrative review is to outline the role of ultrasonography (US) in the early diagnosis, differential diagnosis, patient reassessment, and monitoring of TMD. Furthermore, we want to explore the place of US in disease detection and follow-up appraisal, alongside the MRI and CT investigations.

To ensure a comprehensive update on the recent developments in this field, search strategies were adopted complying with recommendations for narrative reviews (18). We searched the PubMed and Embase databases up to March 2022.

Temporomandibular joint disorders, temporomandibular joint arthritis, temporomandibular joint dysfunction, temporomandibular joint osteoarthritis, temporomandibular joint disk, jaw disease, temporomandibular pain, temporomandibular joint ultrasound, ultrasound, sonography, and their respective MeSH terms were used as keywords. Specifically, we selected studies addressing the contribution of US in the diagnosis and prognostic outcomes, compared to the other imaging techniques, analyzing the advantage of US employment over MRI or CT. Only studies published in the English language were included, and the additional references quoted in these articles were also included when relevant.

METHODS

Our work is a narrative review. A comprehensive search of the literature published from inception to March 2022 was conducted. Two databases, PubMed and Embase, were utilized. Abstracts and titles were searched using keywords, MeSH terms as aforementioned, and subject headings, which were selected as they corresponded to the key characteristics of TMD, TMJ examination, and TMJ US that have been described in the introduction. The papers were then screened for eligibility: to be included, items needed to report studies that involved people with TMJ derangement or populations at risk for TMD. Papers that did not fit into the conceptual framework of this review or did not deal with the examination experience of TMD were excluded.

We grouped the studies according to the topic: imaging examination in TMD, US in TMD, TMD manifestations and differential diagnosis, and US in invasive procedures.

In addition, the references of relevant papers were hand-searched and their citations were examined. Only publications in English were considered.

Data from the selected papers were extracted. **Figure 1** summarizes the selection and screening process: in total 43 articles were critically reviewed and consolidated for this literature review.

In **Table 1**, we summarize the key findings of the main articles employed for this narrative review.

Imaging Examination Techniques in TMJ Disorders: What Is the Current State of the Art in Ultrasound?

Although a large proportion of patients affected by TMJ arthritis are completely asymptomatic during the early stages of the disease (complaining of neither pain nor impaired TMJ function) and present a normal TMJ clinical examination (23), radiographic signs of TMJ damage may still be revealed even in the early phases of the disease.

Therefore, imaging acquires a pivotal role in the early assessment of TMJ changes, trying to prevent further impairment of TMJ. Additionally, a frequent instrumental follow-up is essential to evaluate the progression of the disease and response to the therapeutic approaches.

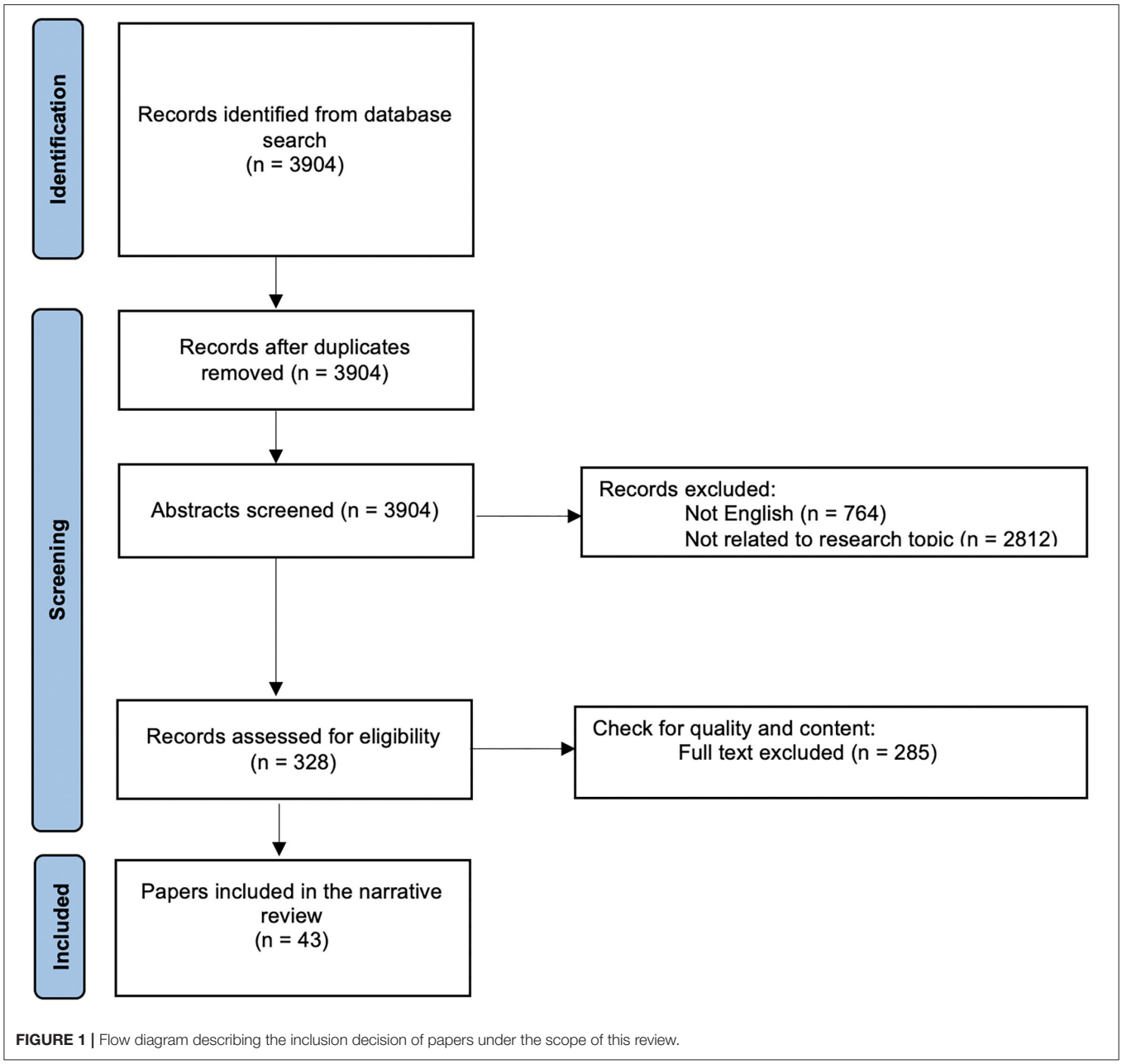

FIGURE 1 | Flow diagram describing the inclusion decision of papers under the scope of this review.

Conventional X-ray and CT scans reveal only advanced damage of TMJ arthropathy, but do not properly analyze the soft tissues, articular disk changes, and early or active signs of arthritis. Furthermore, even if CT provides accurate anatomic detail and it is thus beneficial in identifying surgical candidates (62), it lacks the dynamic imaging potential, and it employs a high radiation dose.

Therefore, MRI is now regarded as the current imaging "gold standard" for the evaluation of inflammatory processes in TMJ pathology, as it can identify both active arthritis changes as well as arthritic sequelae, showing a moderate-to-good reliability (21, 25, 26, 28, 41, 63–65).

MRI technique can detect acute signs of TMJs involvement, such as the presence of synovitis, which is better demonstrated by contrast-enhanced (CE) MRI sequences, joint effusion, and bone marrow edema. In addition, it reveals chronic signs of TMJs involvement, such as condylar changes, erosion, and abnormalities pertaining to the disk (28).

Despite many advantages, MRI also suffers some drawbacks. Namely, the time for image acquisition ranges from 20 to 45 min on average, and the exam requires an open-mouth position, which is particularly troublesome in patients experiencing TMJ pain. Besides, MRI allows mostly static image study, it necessitates the patient's collaboration, which may be difficult

TABLE 1 | Key features of the studies.

First author and reference in the manuscript	Year	Study population	Type of study	Topic	Main statement
IMAGING IN ASYMPTOMATIC / EARLY SYMPTOMS PATIENTS					
Hayashi et al. (19)	2001	Elementary school children	Prospective	US vs. MRI and CT in early detecting TMJ involvement in JIA	Although US accuracy for the diagnosis of disk displacement is slightly inferior to that of MR or CT, authors assert US as a useful imaging method for longitudinal investigations of elementary school children.
Melchiorre et al. (20)	2010	JIA	Prospective	Clinical examination vs. US in early detecting TMJ involvement	Early stage oligoarticular JIA children are likely to have inflammation of the TMJs even in the absence of symptoms. US is a simple-to-use, noninvasive, radiation-free tool for the assessment and follow-up of TMD.
Muller et al. (21)	2009	JIA	Prospective	Clinical examination and US vs. MRI in early detecting TMJ involvement	None of the methods tested is able to reliably predict the presence or absence of MRI-proven inflammation of the TMJs.
Von Kalle et al. (22)	2015	JIA	Retrospective	CE-MRI in early detecting TMJ involvement	The degree of CE alone do not allow differentiation between TMJs with and without signs of inflammation. Thickening of the soft joint tissue seems to remain the earliest sign to reliably indicate TMJ arthritis.
Weiss et al. (23)	2008	JIA	Prospective	MRI vs. US in early detecting TMJ involvement	TMD are present in the majority of patients with new-onset JIA, even if normal jaw examination is present. MRI and US findings are not well correlated, and MRI is preferable for the detection of TMJ disease in new-onset JIA.
IMAGING TECHNIQUES AND COMPARISON IN TMD					
Ahmad et al. (24)	2009	TMD	Diagnostic criteria establishment	Development of image analysis criteria	Authors suggest assessing osteoarthritis using CT, and disc position and effusion using MRI. No mention on US.
Al-Saleh et al. (25)	2016	TMD	Systematic review	MRI vs. CT in detecting TMJ involvement	Very limited studies of MRI and CT to reach a conclusion. MRI better at disk position visualization.
Dong et al. (26)	2021	TMD	Prospective	Determining the optimal MRI sequences for TMD	The three optimal MRI sequences are oblique sagittal proton density-weighted imaging, oblique coronal T2-weighted imaging with closed mouth, and oblique sagittal T2-weighted imaging with opened mouth.
Friedman et al. (27)	2020	TMD	Prospective	US vs. MRI in detecting TMJ involvement	US is both a sensitive and a specific screening tool for TMD when used by an appropriately trained operator, with the exception of medially displaced discs. If TMJ assessment is found to be abnormal, the patient should be referred for MRI. If a component of medial disc displacement is suspected, MRI should be performed despite a normal screening US.
Hechler et al. (28)	2018	JIA	Systematic review	MRI vs. US in detecting TMJ involvement	Dynamic HR-US improves sensitivity and specificity compared to static, low-resolution US. Among TMJ changes (disk displacement, joint effusion, bony deformity), only joint effusion was appropriately assessed by multiple authors. US imaging following a baseline MRI can increase US sensitivity and specificity.
Kulkarni et al. (29)	2013	PsA	Case report	CT and X-ray in detecting TMJ involvement	CT and X-ray show erosion and resorption of the mandibular condyles, as well as calcification and osteophytic spurs in the joint space.
Landes et al. (30)	2007	TMD	Prospective	2D and 3D-US vs MRI in detecting TMJ involvement	3D-US in closed mouth position appears superior in diagnosing disk dislocation, and in overall joint degeneration. Sensitivity, accuracy and positive predictive value ameliorate if US is clinically applied prior to MRI.
Manfredini et al. (31)	2009	TMD	Systematic review	US vs. MRI, CT and clinical assessment in detecting TMJ involvement	US remains potentially useful as an alternative imaging technique for monitoring TMJ disorders, particularly the presence of intrarticular effusion (good accuracy). Better standardization of the technique is required, and normal parameters must be set.
Melchiorre et al. (32)	2003	RA, PsA	Prospective	MRI vs US in detecting TMJ involvement	US imaging can detect different pathological changes of TMJs and may be considered an important diagnostic tool.
Mupparapu et al. (33)	2019	RA	Systematic review	MRI vs. CT vs. PET in detecting TMJ involvement	PET used in conjunction with CT is the only imaging modality that can quantify TMJ inflammation in active RA disease.
Navallas et al. (34)	2017	JIA	ND	MRI in detecting TMJ involvement	MRI is the technique of choice for the study of TMJ arthritis. MRI is the only TMJ exam able to demonstrate bone marrow edema.

(Continued)

TABLE 1 | Continued

First author and reference in the manuscript	Year	Study population	Type of study	Topic	Main statement
Sodhi et al. (35)	2015	RA	Case report	CT in early diagnosis	CT is a useful technique in diagnosing the bony changes (erosions) in the early phase of the disease.
Zwir et al. (36)	2020	JIA	Prospective	PDUS vs. MRI in detecting TMJ involvement	PDUS could be a useful screening exam to identify TMJ inflammatory activity. However, PDUS cannot replace MRI for the detection of TMJ inflammatory involvement.
TMJ DISC DISPLACEMENT					
Dong et al. (37)	2015	TMJ disc displacement	Meta-analysis	HR-US in detecting TMJ involvement	HR-US delivers acceptable performance when used to diagnose anterior disc displacement, being superior for the detection of anterior disc displacement without reduction rather than with reduction.
Emshoff et al. (38)	1997	TMD	Prospective	US in TMJ disc displacement	Both static and dynamic US modalities are insufficient in establishing a correct diagnosis of disk displacement.
Landes et al. (39)	2006	TMD	Prospective	3D-US vs. MRI in TMJ disc displacement	3D-US proves to be reliable for exclusion of disk degeneration compared with MRI, whereas the presence of such finding cannot be reliably diagnosed by 3D-US.
Li et al. (40)	2012	TMD	Systematic review and meta-analysis	US vs. MRI in TMJ disc displacement	The diagnostic efficacy of US is acceptable and can be used as a rapid preliminary diagnostic method to exclude some clinical suspicions. However, positive US findings should be confirmed by MRI. The ability of US to detect lateral and posterior displacements is still unclear.
Pupo et al. (41)	2016	TMJ disc displacement	Meta-analysis	Clinical examination vs. MRI in TMJ disc displacement	Clinical examination protocols have poor validity to diagnose disc displacement. MRI shows better results.
Severino et al. (42)	2021	TMD	ND	Clinical examination and MRI vs. US in TMJ disc displacement	US shows acceptable results in identifying bone structures. However, lower values of diagnostic efficacy were obtained for disc position during joint movements with respect to MRI images.
Tognini et al. (43)	2005	TMJ disc displacement	Prospective	US vs. MRI in TMJ disc displacement	US proves to be accurate in detecting normal disc position and the presence of abnormalities in disc-condyle relationship. US is not so useful for the distinction between disc displacement with and without reduction.
Westesson et al. (44)	1992	TMD	Prospective	Relationship between MRI effusion and clinical examination	TMJ effusion primarily occurs in joints with disk displacement and is strongly associated with joint pain.
US IN TMD					
Almeida et al. (45)	2019	TMD	Systematic review and meta-analysis	US in detecting TMJ involvement	US has acceptable capability to screen for disk displacement and joint effusion in TMD patients. For screening of condylar changes, ultrasound needs further studies using CT. More advanced imaging such as MRI can thereafter be used to confirm the diagnosis if deemed necessary.
Assaf et al. (46)	2013	JIA	Prospective	HR-US in detecting TMJ involvement	HR-US improves sensitivity and specificity in the detection of TMJ involvement, especially for the detection of condylar involvement in children with JIA (even if not all parts of the TMJ are visible on US).
Emshoff et al. (47)	2003	TMD	Prospective	HR-US in detecting TMJ involvement	US is an insufficient imaging technique for the detection of condylar erosion. Assessment of disc displacement without reduction may be reliably made with US.
Hu et al. (48)	2020	TMD	Systematic review and meta-analysis	US-guided arthrocentesis vs. conventional arthrocentesis in TMD	US-guided arthrocentesis may not improve postoperative pain and maximal mouth opening in the short term.
Jank et al. (49)	2007	JIA	Prospective	Clinical examination vs. US in detecting TMJ involvement	The significant correlation between pathologic US findings, duration of JIA, and the number of affected peripheral joints make US technique interesting for use as a diagnostic screening method.
Kim et al. (50)	2021	TMD	Prospective	US in detecting TMJ involvement	Capsular width is a risk factor for TMJ pain after adjusting for confounders. A refined and established protocol for standard examinations is needed.
Kundu et al. (51)	2013	TMD	Narrative review	US in detecting TMJ involvement	US is overall an acceptable diagnostic tool for detection of disc displacement (but MRI remains gold standard), condylar erosion and articular effusion.

(Continued)

TABLE 1 | Continued

First author and reference in the manuscript	Year	Study population	Type of study	Topic	Main statement
Manfredini et al. (52)	2003	TMD	Prospective	US measures of TMJ capsular width (in mm) and MRI diagnosis of TMJ effusion	The critical US area is around 2 mm value for TMJ capsular width.
Parra et al. (53)	2010	JIA	Retrospective	US in joint injections	TMJ injections using sonographic guidance is a safe, effective and accurate procedure.
Rudisch et al. (54)	2006	TMD	Autopsy specimens	HR-US in detecting TMJ involvement	Condylar erosion is reliably assessed by HR-US, but the evaluation of disk position is less accurate.
Tonni et al. (55)	2021	JIA	Pilot study (TMD vs. healthy controls)	US in detecting TMJ involvement	Ultrasound can detect differences in the TMJ features between JIA patients and healthy patients. US might be used as a follow-up tool.
Varol et al. (56)	2008	TMD	Prospective	PDUS in TMJ internal derangements (vs. arthroscopic findings)	Arthroscopic synovitis with varying degrees of synovial vascularization was detected in all patients with positive PDUS exam.
DIFFERENTIAL DIAGNOSIS IN TMD					
Fan et al. (57)	2019	Pseudogout	Case report	Differential diagnosis of TMD, role of US-guided procedures	US-guided fine-needle aspiration is a reliable tool for diagnosing tophaceous pseudogout of TMJs.
Imanimoghaddam et al. (58)	2013	Myofascal pain	Case-control	Differential diagnosis of TMD	There is a significant difference between control and myofascial pain disorders groups in terms of visibility, widths, and echogenicity of masseter bands, which might be related to muscle inflammation.
Klasser et al. (59)	2009	Parotid gland tumor	Case report	Differential diagnosis of TMD	Parotid gland masses can be accompanied by pain and TMJ dysfunction, mimicking TMD, which may delay definitive diagnosis.
Matsumura et al. (60)	2012	Pseudogout	Case report	Differential diagnosis of TMD	Synovial chondromatosis with deposition of calcium pyrophosphate dihydrate may affect TMJs.
Poveda-Roda et al. (61)	2018	Myofascal pain	Case-control	Differential diagnosis of TMD	There is no statistically significant differences in masseter muscle width between chronic myofascial pain subjects and control subjects. The increase in width under maximum contraction is not significantly different between the groups.

2D, two-dimensional; 3D, three-dimensional; CE, contrast enhancement; CT, computed tomography; HR-US, high-resolution ultrasound; JIA, juvenile idiopathic arthritis; MRI, magnetic resonance imaging; ND, not defined/not deductible; PDUS, power Ddoppler ultrasound; PET, positron emission tomography; PsA, psoriatic arthritis; RA, rheumatoid arthritis; TMD, temporomandibular disorders; TMJ, temporomandibular joint; US, ultrasonography/ultrasound.

in the pediatric population or claustrophobic patients, and it is a high-cost procedure, not available in all centers. Moreover, MRI is contraindicated for patients with pacemakers, implantable cardiac defibrillators, and in the case of metallic foreign bodies (66).

Additionally, positron emission tomography (PET) and PET/CT represent novel technologies, which have shown good promises for the diagnosis and follow-up evaluation of TMD (33, 67). In fact, the maximum standardized uptake value (SUVmax) tends to be higher in the TMJ symptomatic patient or in the disease aggravation and decreases when TMD improves. In this regard, SUVmax may play a significant role, not only in detecting TMD, but also in evaluating the treatment response and measuring the TMD activity (68). However, the inflammatory activity in small joints such as TMJs has not been studied as extensively as in the large joints in PET studies (69), thus a careful interpretation is required.

To overcome these limitations, a promising alternative diagnostic tool seems to be represented by US, which is relatively inexpensive and potentially accessible in most outpatient clinics, after an adequate operator's training (51). The examination only takes 10–15 min ordinarily, a tolerable time even for the youngest patients; in the absence of radiation or any other risk, it is pain-free, and it allows dynamic real-time assessment, while the mouth is closed or opened, with the option of direct communication with the patient that can guide examination to painful regions. Furthermore, it does not require any sedation in children. However, it is unclear whether it can identify the active inflammation and arthritic sequelae as accurately as CE-MRI.

Consequently, there has been an intense effort to identify the sensibility and specificity of US as compared to MRI, particularly in the pediatric population, as several recent studies have shown that non-arthritic children can still present subtle findings on MRI consistent with TMJ arthritis, such as joint effusion and contrast enhancement, which may be possibly more easily and rapidly detected by US (16).

Ultrasound Protocol

A common feature of TMJ involvement is synovitis, defined as a thickened synovia, joint effusion, and with or without an active synovial inflammation (55) (**Figure 2**). Afterward, arthritic changes may occur as reparative or destructive signs, cystic lesions, erosions, flattening of the articular condyle, as well as destructive changes of the articular disk and synovial structures (32, 46, 47, 49, 54). Currently, no different TMJ US findings characterizing condylar inflammation or damage have

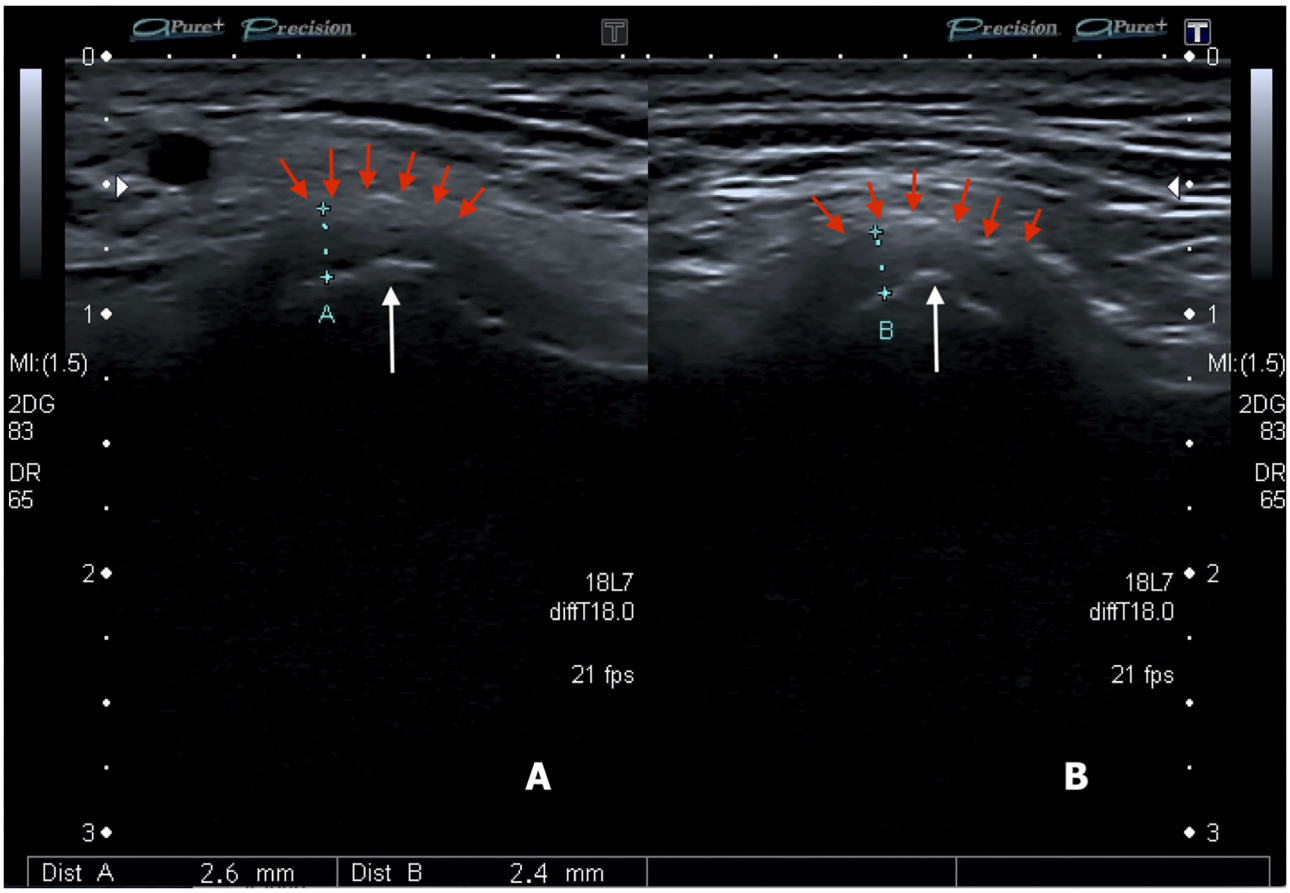

FIGURE 2 | Transverse image of the right **(A)** and left **(B)** TMJs showing the condyle and capsular width (distance between markers). White arrows show the condylar process and red arrows show the articular capsule (Personal archive).

been described, as they may coexist. Moreover, to date, no defined TMJ US pattern has been reported to be peculiar to different TMD. The traditional US imaging protocol includes axial and coronal scans at closed- and open-mouth (55) (**Figure 3**).

The surface of the condyle is hyperechoic (high reflection of sound waves) and it appears white in the US images. The connective tissues, represented by a joint capsule, retrodiscal tissue, and muscles (lateral pterygoid and masseter), are isoechoic (intermediate reflection of sound waves) and appear heterogeneously gray in the US images.

However, the margin of the joint capsule highly reflects the US waves, generating a hyperechoic white line. These anatomic cavities are virtual because the opposite surfaces are in contact and usually not detectable unless effusion occurs (51).

Thus, the width of the synovial joint space is particularly relevant, because it may indirectly indicate the presence of a joint effusion, which is usually regarded as a sign of synovitis (46, 70).

The joint space width is measured from the cortical contour of the condyle to the articular capsule at different levels over the condylar cortical line (anterior and lateral levels). The coronal scan position is the most suitable to assess this measurement (46, 55, 70).

The US diagnosis of effusion has been favorably compared to the gold standard MRI technique, especially when the capsular width is above 1.950 mm in the adult population (52). In fact, current studies identify a critical TMJ capsular width of around 2 mm (31) and therefore focus attention on interobserver reliability. Moreover, the capsular width has been documented to be a risk factor for TMJ pain when adjusted for other confounders, thus it is an estimation with consequent clinical correlation (50).

In a pediatric study, Muller et al. (21) employed the same capsular width cut-off for the assessment of TMJ effusion, as had been applied for adults (2 mm), and this could explain a weak correlation observed between US and MRI. Thus, for the pediatric population, a cut-off level of 1.2 mm has been proposed (70), with better results in terms of the correlation between the US-assessed capsular width and MRI-assessed synovitis. In fact, a correct cut-off level is essential to avoid wrong discredit of US as an instrumental exam tool in TMD.

Conversely, only a few efforts have been made on MRI images to differentiate between the normal and abnormal TMJ effusions, defined as an area of high-signal intensity within the joint space on T2-weighted images (24). Only two studies attempted to address this question, defining the abnormal synovial joint

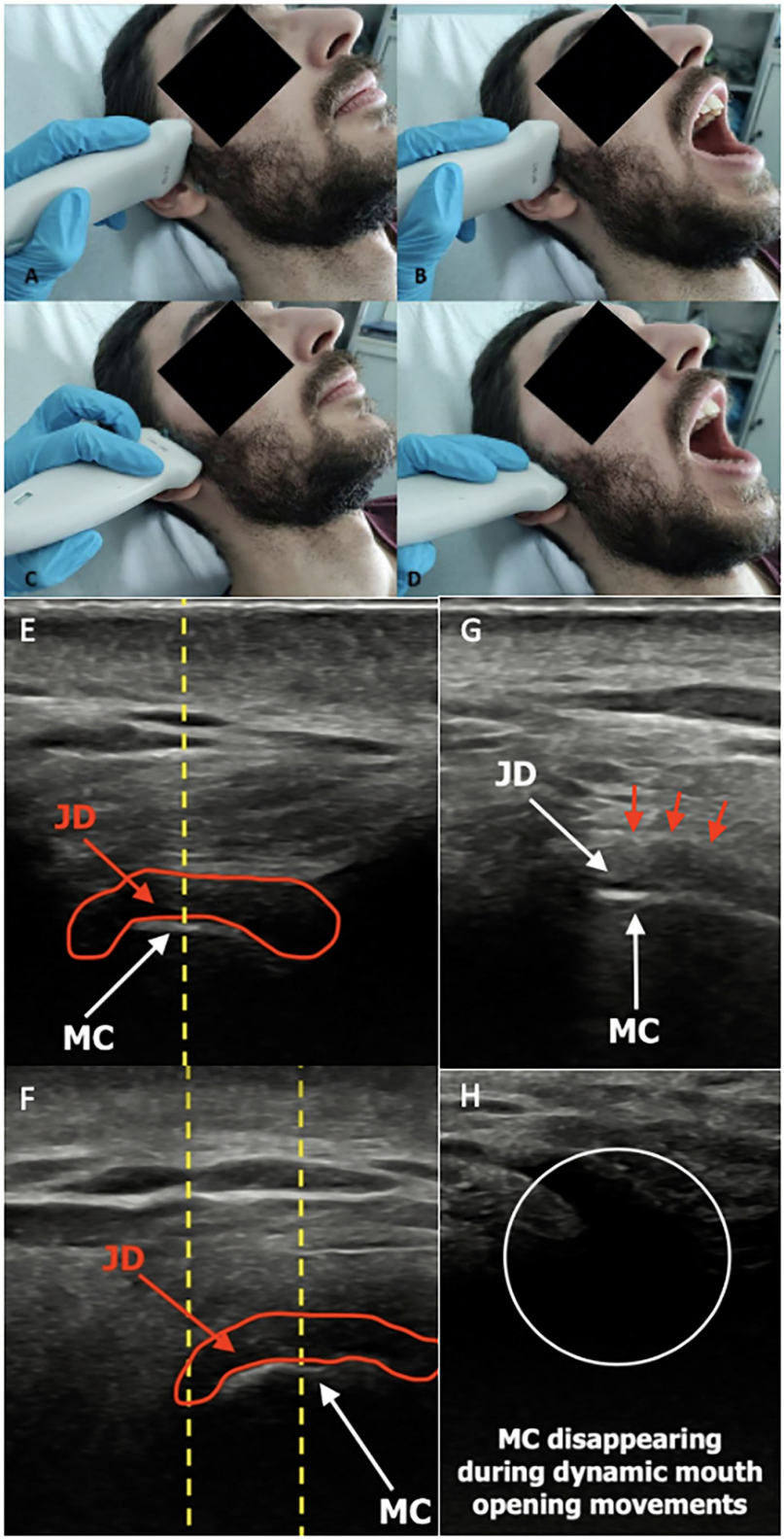

FIGURE 3 | Conventional US transducer positions are parallel to the Frankfort horizontal plane (a plane connecting the highest point of the opening of the external auditory canal with the lowest point on the lower margin of the orbit) in closed-mouth **(A)** position and open-mouth **(B)** position, as well as parallel to the ramus of mandible, both in closed-mouth **(C)** and open-mouth **(D)** positions. Normal ultrasound image of TMJ in transverse sections in closed- **(E)** and open-mouth

(Continued)

FIGURE 3 | positions **(F)**. The normal ultrasound appearance of the articular disk in the sagittal plane is an inverted hypoechoic C-shaped structure, outlined by the red circle. During the mouth opening, the mandibular condyle translates anteriorly as defined by the distance between the center of the condylar oval at the two positions (yellow dotted line). Notably, the disk maintains a constant central appearance with respect to the center of the mandibular condyle in normal anatomy, while it may be displaced anteriorly or posteriorly in the pathological findings. Normal ultrasound image of TMJ in longitudinal closed-mouth **(G)** and open-mouth position **(H)**. Red arrows show the articular capsule. JD, joint disk; MC, mandibular condyle (Personal archive).

space to be more than a line of high T2-signal along the joint surface (44, 71). A more recent study calculated a ratio of pixel intensity between TMJ synovia and the longus capitis muscle, suggesting this measure to be a reliable way to quantify synovial enhancement (72).

Importantly, the identification of synovial thickening alone in TMJ US might not indicate an ongoing active inflammation, but might rather represent a quiescent chronic disease. Considerably, the power Doppler (PD) images enable the diagnosis of an active TMJ inflammation through the detection of increased synovial vascularization that, while theoretically possible if contrast is used, is unlikely in MRI when performed with the standard practices (73). Additionally, the gadolinium-based contrast medium is generally considered safe, but it may be associated with adverse reactions, such as the idiosyncratic allergy-like reactions (74).

Few studies concluded that power Doppler US is a good technique for the assessment of synovial changes by microvascularization. A study by Varol and colleagues (56) assessed and confirms TMJ synovial vascularization both on US and arthroscopy.

Conversely, other studies showed no considerable differences between synovial inflammation obtained using power Doppler US or determined through MRI images, as the sensitivity is very low even in cases of the obvious inflammatory process, mainly because the deepest part of the TMJ cannot be assessed with this technique (34, 36). Nonetheless, the issue is not fully elucidated, as a lack of synovial enhancement on MRI may not exclude the joint inflammation as well (22).

Awareness should be raised regarding the increased signals of vascularity in pathological conditions aside from TMD. For instance, the majority of cases of pleomorphic adenoma present with color peripheral Doppler signal (75), and because TMJs are adjacent to the parotid gland, this element acquires particular relevance. At the same time, post-radiotherapy nasopharyngeal carcinomas patients showed a reduction in the TMJ disk thickness, an increase in condyle irregularity, and joint vascularity (76).

The main disadvantages of the US technique remain the long-learning curve and the fact that the examination is operator-dependent. Furthermore, ultrasound images present questionable anatomical validity, mainly because of the bone blockade barrier and the consequent inability of the US beam to identify all the local structures. Additionally, currently, only a few studies have been published upon this argument, limiting the evidence of data discussion. More recent works provide strong support for the use of conventional US techniques, and hopefully, future research will contribute to better knowledge on this topic, possibly reaching a definite consensus.

Ultrasound Sensitivity and Specificity

Far from being clarified, the sensitivity and specificity of US in recognizing TMJ changes are still debatable, due to the performance of US as compared to MRI (28, 51).

The main reason for this ongoing discussion is the wide heterogeneity of the study designs, in terms of the population [juvenile idiopathic arthritis (JIA), adult rheumatic conditions, non-rheumatic patients, and other TMJ derangements], US protocols, and considered parameters of specific acute and chronic TMJ changes (recognized as disk displacement, joint effusion, condylar deformity, even if only joint effusion has been appropriately investigated by multiple authors) (28). In addition to the above-mentioned aspects, there is a relative paucity of studies about the topic, which makes the comparison difficult and subject to possible biases.

Emshoff et al. (38) employed a transducer of 7.5 MHz, with a revealed sensitivity of 40–50%, and specificity of 70%. Sensitivity was found to decrease from closed- to open-mouth position, conversely, specificity increased from closed- to open-mouth position, but in both positions, the diagnostic accuracy was found acceptable.

Such findings may be explained by the medial disk displacement occurring after mouth opening, as the mandibular condyle and the glenoid cavity do not allow proper US propagation without appropriate adjustment of the probe in different planes, thus impairing the visualization of the articular disk. Nonetheless, this consideration does not apply to an ultimate 3D US, where the TMJ can be evaluated in different planes within the scan volume. The 3D US has also been found to have acceptable sensitivity and accuracy (39), but according to recent findings, it does not seem to significantly increase the reliability of the examination (51).

Similar results were found in other studies (77), and in particular, following progressive employment of transducer with higher frequency, of 10 MHz or more, allow a better sensitivity, ranging from 60% to 90% (30, 40, 42, 45). Specifically, a recent review (28) found that high-resolution US (HR-US), defined as a US resolution of 12 MHz or more, improves sensitivity and specificity in the detection of TMJ involvement as compared to low-resolution US (LR-US), defined as a US resolution of $<$12 MHz (28, 31). Moreover, a study by Jank et al. (49) found that HR-US is able to detect TMJ pathology even before clinical symptoms appeared, which is particularly relevant in the younger population to avoid damage accumulation. Melchiorre et al. (32) have found US quite useful even for the diagnosis of TMD in adult RA patients.

Few studies also illustrated the benefit of executing a baseline MRI to increase US accuracy, which can be reassessed during the

follow-up, as attested by a reported increased US sensitivity and specificity parameters (28).

To the best of our knowledge, only one study compared the power of clinical examinations, MRI, and US imaging in TMD (21). The population study included JIA patients, and US was found to be the most specific of all tested methods, but the least sensitive, detecting only the most severely affected joints.

The studies comparing US with MRI in TMJ arthritis have determined a poor correlation between these modalities, with US potentially missing from 67% up to 75% of TMJ MRI-detected inflammatory changes (23, 78). Alongside, MRI contrast enhancement improves the detection of MRI TMJ inflammation from 35.7% to 86.7% (79).

A study by Weiss et al. (23), carried out on a population of children affected by JIA, compared MRI and US in detecting both the acute and chronic TMJ arthritic signs. For the acute inflammatory TMJ changes, the agreement between these two techniques was only 23%, and for chronic TMJ changes, the agreement reached 50%. These results indicate that MRI and US findings are not well correlated and that MRI shows a greater sensitivity for the detection of TMD.

Because of all the above-illustrated reasons, US is currently neither recommended as a screening method for early TMJ involvement nor for the monitoring purpose in the recent European League Against Rheumatism (EULAR) guidelines for JIA management (80), which claims MRI for both diagnosis and follow-up schedule.

However, the latter aspect has been debated in a recent review of the literature; although the paper concludes that US has low sensitivity in detecting joint effusion, its employment during follow-up monitoring is advocated by authors (28), highlighting again how current data do not answer the question whether US can assist MRI.

TMJ Ultrasonography: Who, When, and What

Asymptomatic Patients

As previously mentioned, many patients affected by TMD can be totally asymptomatic during the early stages of the disease.

This is particularly remarkable in JIA, which is the most common childhood chronic rheumatic disease, encompassing different joint arthritis subsets, with an onset before the age of 16 years (81). TMJ dysfunction has been frequently reported in association with JIA (82, 83), with a prevalence of 17–87% according to different studies (84–87). Undiagnosed and consequently untreated disease can result in a variety of serious sequelae, particularly relevant for a population of growing children, including impaired facial development, dysmorphic facial features, mandibular asymmetry, micrognathia and retrognathia, and, in most severe cases, even condylar resorption, eventually require a total joint replacement. Melchiorre et al. (20) found that in the newly diagnosed JIA patients with US evidence of joint effusion, more than 95% did not complain of any joint pain. Remarkably, many of these patients were under the influence of anti-rheumatic drugs, which may hide the TMJ symptoms.

Even other inflammatory chronic arthropathies may present rather asymptomatic during the early stages of the disease.

RA is a chronic inflammatory joint disease, affecting mostly women. Clinical manifestations encompass symmetrical joint polyarthritis, possibly leading to progressive joint damage and irreversible disability (88). Thus, early diagnosis is deemed essential against the most undesirable outcomes. Albeit RA mainly affects the joints of the hands, wrists, elbows, knees, ankles, and feet, TMJ may be involved as well, even if less frequently. The literature data report from 4% up to 80% of RA patients clinically exhibit TMJ involvement (35). Morning stiffness may be present even at the TMJ site, along with decreased masticatory force (15). Morphologic alterations may be documented on conventional radiographs of the TMJ, ranging from 19% to 86% of RA patients (89). Occasionally, TMD may be the presenting manifestation of RA (90). Nevertheless, there are only few studies concerning TMJ and masticatory muscles involvement in patients with early RA; therefore, the relationship between TMD and the rheumatological condition remains unclear (15).

Interestingly, Crincoli et al. (15) carried out an early RA cohort (defined as patients who received RA diagnosis within 12 months); despite TMJ involvement, the study group complained less frequently about the TDM symptoms as compared to the healthy controls. Similarly, TMJ noises and opening derangement were significantly lower in the study group compared to the controls. These phenomena are probably explained by drug therapy, corticosteroids, or conventional/biological disease-modifying anti-rheumatic drugs (DMARDs), promoting downregulation of pro-inflammatory chemokines, and therefore masking the clinical picture.

Moreover, a study by Kroese et al. (91) demonstrated an increased risk of TMD in individuals with early RA, defined as a time limit of <3 years from symptoms onset (92), and at-risk of RA, as defined by the EULAR guidelines (93) (including joint symptoms <1 year, mainly located at metacarpophalangeal joints, with early morning stiffness and difficulties in making a fist, showing a positive squeeze test at joint examination), who should benefit from further TMJ examination and management.

Additionally, patients with PsA and, to a lesser extent, those with psoriasis (PsO) are equally more frequently affected by TMD as compared to the healthy subjects, and again, TMD may be the presenting manifestation of the rheumatic condition (8, 29, 94). Dervis et al. (95) showed TMJ dysfunction in 29% and 35% of patients with PsO and PsA, respectively.

TMJ involvement is also possible in AS, and it occurs in 22% of patients, but frequently most patients complain of no symptoms, so this is likely to be an underestimation (96).

Today, to the best of our knowledge, there are no conclusive data on TMJ involvement in the asymptomatic patients, nor in pediatric or in adult population affected by rheumatological conditions. Currently, TMJs are not included in routine rheumatological ultrasound screening protocols. The clinimetric questionnaires present no specific questions for TMJs, and patients very often underestimate the early symptoms in terms of pain and joint clicks and do not tell physicians about them.

Therefore, TMJ involvement may undergo underreporting. This is a huge gap that hopefully will be conceivably investigated in future research.

As early functional disorders of TMJ are often preclinical, in all the above-mentioned populations of patients, and particularly in children, US would be beneficial as an entry-level diagnostic screening tool, which is rapidly accessible and of relatively low cost. Patients found with suspicious TMJ alterations would then be directed to complete second-level investigations, such as MRI and CT. Due to the low sensitivity of US method, some patients will be considered devoid of TMJ changes at first US screening procedure, but would anyway be undiagnosed due to the current absence of guidelines suggesting MRI or CT early screening in these populations, while, for example, ultrasound and X-ray imaging is now considered the gold standard both for the early diagnosis and progression monitoring in many forms of osteoarthritis regarding other anatomical joints (97–99).

Remarkably, currently, as for US, no differences in MRI findings have been documented in JIA, RA, PsA, or PsO patients in the literature.

TMJ Ultrasound: Is a "Point-of-Care Ultrasonography" Possible?

As already explained, TMD is a frequent cause of orofacial pain, derived from trauma, rheumatoid disorders, and dental- and non-dental-origin causes. The reported TMJ pain can be regionally localized or generalized as myofascial pain (100), and sometimes other clinical conditions may mimic TMD.

As clinicians, we search for a quick precise diagnosis; therefore, we collect a careful anamnesis of pain characteristics and a complete clinical examination, but sometimes, we are still doubtful about the diagnosis. In some cases, US would come to the rescue, adding precious clues to address the diagnosis.

For example, heterotopic ossification has been reported to be associated with crystalline arthropathies and secondary systemic illnesses such as gout and chondrocalcinosis (101, 102). Deposition of calcium pyrophosphate dihydrate crystals occurs within and around TMJ, especially involving the articular cartilage and fibrocartilage, appearing as spotted hyperechoic signals on US images. Sometimes a marked destruction of the condyle with erosive changes may be observed in association (60).

Occasionally, especially in long-term gout disease, a TMJ palpable mass may be appreciated, and US may evidence a TMJ adjacent hypoechoic mass, corresponding to the tophaceous material (57, 103). In these cases, US can guide fine-needle aspiration for the histological confirmation of diagnosis (57).

The US-documented involvement of other joints with chondrocalcinosis is a clue to the diagnosis, while differential diagnosis includes synovial chondromatosis, synovial osteochondroma, and osteosarcoma (104).

Even in JIA children, it has been reported few cases with new bone formation rather than proper crystal deposition, and the new bone formation is frequently heterotopic, rather than condylar. In addition, in these cases, the heterotopic ossification appears to be intra-articular, rather than in the periarticular soft tissues (83).

TMJ referred pain may also be caused by salivary glands pathology, which is particularly relevant in the rheumatological population, as connective tissue diseases (CTD) may be associated with the enlargement of these glands. Indeed, salivary glands US is now advocated as a meaningful tool to be incorporated into the clinical evaluation among these patients, therefore many clinics are still performing it on patients with CTD (105).

A parotid gland swelling located in the deep lobe is a possible cause of TMD symptoms (59). This is due to the common vegetative innervation of the salivary glands and components of the TMJ. US is a dynamic exam, scanning different planes, therefore it may reveal a proximal enlarged parotid gland, or TMJ adjacent mass within the parotid gland presenting as a hypoechoic or heterogeneous US pattern, enabling further investigations to exclude possible tumor masses, such as pleomorphic adenoma of the parotid gland (106, 107). Therefore, even if the physician is not particularly skilled at salivary gland US, he or she can anyhow quickly identify a suspicious lesion, as it presents with a different echogenicity compared to the surrounding tissue, addressing the patient to further analysis.

TMJ tumors and pseudotumors are relatively infrequent, but usually present as orofacial pain, with a similar presentation to TMJ internal derangement. According to the literature, in adults, benign tumors primarily include chondroblastomas, osteoblastomas, osteochondromas, and osteomas, while metastatic tumors and sarcomas are the main malignant tumors (108). US may reveal a solid lesion, destroying the TMJ profile (109). Again, US may be considered a beginning examination, not necessarily requiring experienced ultrasonographers for justifying further investigations.

Rarely, temporal arteritis headache may mimic TMJ irradiated pain. In this case, only an expert rheumatologist in temporal arteries US is qualified to discern a halo sign, as a hallmark of giant cell arteritis, from TMJ derangement (110).

Focal myalgia caused by TMJ parafunction or myofascial pain may be another cause of regional pain (100). In recent years, studies using MRI and US in patients with masticatory muscle myalgia have frequently been reported (111). Few studies showed no statistically significant differences in the masseter muscle width between myofascial patients and control subjects (61), while others showed obvious US changes in the masseter muscle, especially in female myofascial syndrome patients (58). Muscle visualization technique is not currently performed in TMJ US, but would help in differential diagnosis, mainly in cases when maxillofacial surgeons find no conclusive elements at clinical evaluation, MRI or CT exams in patients reporting TMJ disturbs.

TMJ Disk Displacement

Features of TMD could derive from the articular disk changes.

In addition to the prior discussed disadvantages of US, another relevant one is the limited access to deep structures and in particular to the articular disk, derived by sound waves absorption by the head of the condyle and the zygomatic process of the temporal bone (31). Moreover, because the internal echoes of the articular disk are similar to those of the articular capsule,

it is difficult to discriminate the articular disk from the articular capsule in the US images (19).

The evaluation of condylar and disk irregularities is a standard procedure in any assessment of MRI scans or conventional radiographs (19, 112). Some authors suggest that, with a few shrewdness by appropriately constantly adjusting the position of the transducer over examined structures, evaluation of the articular disk can be captured; however, US alone is likely to underestimate disk changes (46).

The disk is visualized only through a small space between the zygomatic process of the temporal bone and the head of the condyle. It is challenging to obtain satisfactory images, especially when the condyle rotates and translates from the closed-mouth position to the open-mouth position (51).

With the adjustment of probe position, disk thickness and shape can be assessed with US, and derangement may present as a hypoechoic inhomogeneity in the range of the articular disc. However, perforations and adhesions are not adequately visualized by US, nor is the medially displaced disk (27). Then, if a component of medial disk displacement is suspected, MRI should be performed directly, despite a normal screening US (27).

To the best of our knowledge, only one study in literature summarized the US power in the evaluation of condylar disk displacement: the overall sensitivity of HR-US compared to MRI across studies ranged from 0% to 100% and the specificity ranged from 63% to 100% (43). Sensitivity was found to be directly proportional to the resolution of the probe, as it increases following the increase of US resolution (37, 40, 47).

Invasive Procedures

Although US TMJ is mainly employed for the diagnosis of degenerative changes and synovitis, in recent years, US is growing as a supporting technique in therapeutic procedures, such as arthrocentesis procedures (sodium hyaluronate or steroid injections) to detect the disk and bone structures (113).

A study by Parra et al. (53) compared CT vs. US-guided TMJ injections. Needle placement was shown to be acceptable in 91% of US-guided procedures (75% required no needle adjustment, 16% only minor adjustment) and unacceptable in 9%, which means the needle required major readjustment.

A similar study using post-injection MRI to assess needle placement accuracy described a technical success of 100% (114).

Certainly, the US-guided procedures do not contain as much detail as the other advanced imaging techniques. A recent meta-analysis, in fact, showed that US may not improve postoperative pain and maximal mouth opening in short term after TMJ arthrocentesis, presenting scarce and conflicting results for any definite conclusion (48). On the contrary, US has no harmful effects and could be employed even in children and pregnant women, and this aspect may be considered in everyday practice.

Monitoring TMJ Disease

A survey of the American Association of Oral and Maxillofacial Surgeons in managing and monitoring JIA patients suggests that once the inflammatory arthritic patients are judged to be in remission, most of them are monitored at 6–12 month intervals (115). This study also revealed that the assessment of remission relies more on the symptoms and plain radiography rather than MRI when following these patients over time, while, as already mentioned, the EULAR guidelines for JIA management claim MRI for both the diagnosis and follow-up monitoring (80). This supports the potential need for ongoing discussions between the Rheumatologist and Maxillofacial surgeons to determine the best imaging modality for individual patients (2, 115).

US may be possibly employed for monitoring scope through treatment course, even if, of note, randomized clinical trials of conventional and biologic disease-modifying anti-rheumatic drugs generally do not include TMJ as an outcome (16).

Conceivably, an association of clinical parameters and US details can be proposed as an integrative model.

A recent study by Johnston et al. (116) explored the link between TMJ inflammation as measured by US and patient disability as assessed by the Steigerwald Maher TMD Disability Index (SMTDI). This is the first study in which capsular width was integrated into a functional disability questionnaire.

CONCLUSION

MRI is currently regarded as the gold standard imaging technique for the evaluation of TMJ pathology, as it can accurately identify both the active and chronic arthritic sequelae (65). This opinion is based on reliable parameters in terms of sensitivity and specificity from numerous studies and systematic reviews of the literature (21, 25, 28, 64); only the EULAR guidelines for JIA management recommend MRI for the diagnosis and follow-up evaluation of TMJ (80).

Regardless, US can be suggested as a useful examination tool in the assessment of TMD due to several advantages over MRI: low cost, large availability, and real-time quick assessment, the last two being favorable features, especially for claustrophobic patients and the pediatric population. Furthermore, US allows a dynamic and direct investigation of the surrounding structures (muscles, tendons, and ligaments), which is essential for an exhaustive understanding of the pathophysiological aspects of TMD and to obtain a first diagnostic approach to address a patient to more advanced imaging such as MRI after a positive screening when US is suspicious for TMD diagnosis (45).

However, as previously stated, given the potential for active and erosive TMJ arthritis in asymptomatic or minimally symptomatic patients, we should not disregard the value of suspicious US features (when the examination is not frankly positive for pathology but presents some unclarified signs). This situation can of course lead to unnecessary examination if MRI images do not confirm any pathological change, but reversely may earlier address the patient to appropriate management and early diagnosis of the pathological condition.

Noteworthy, the US survey is repeatable within a short time without any risk, allowing frequent monitoring of the pathology during the course of therapy, which is of particular relevance especially in children, avoiding the accumulation of TMJ damage.

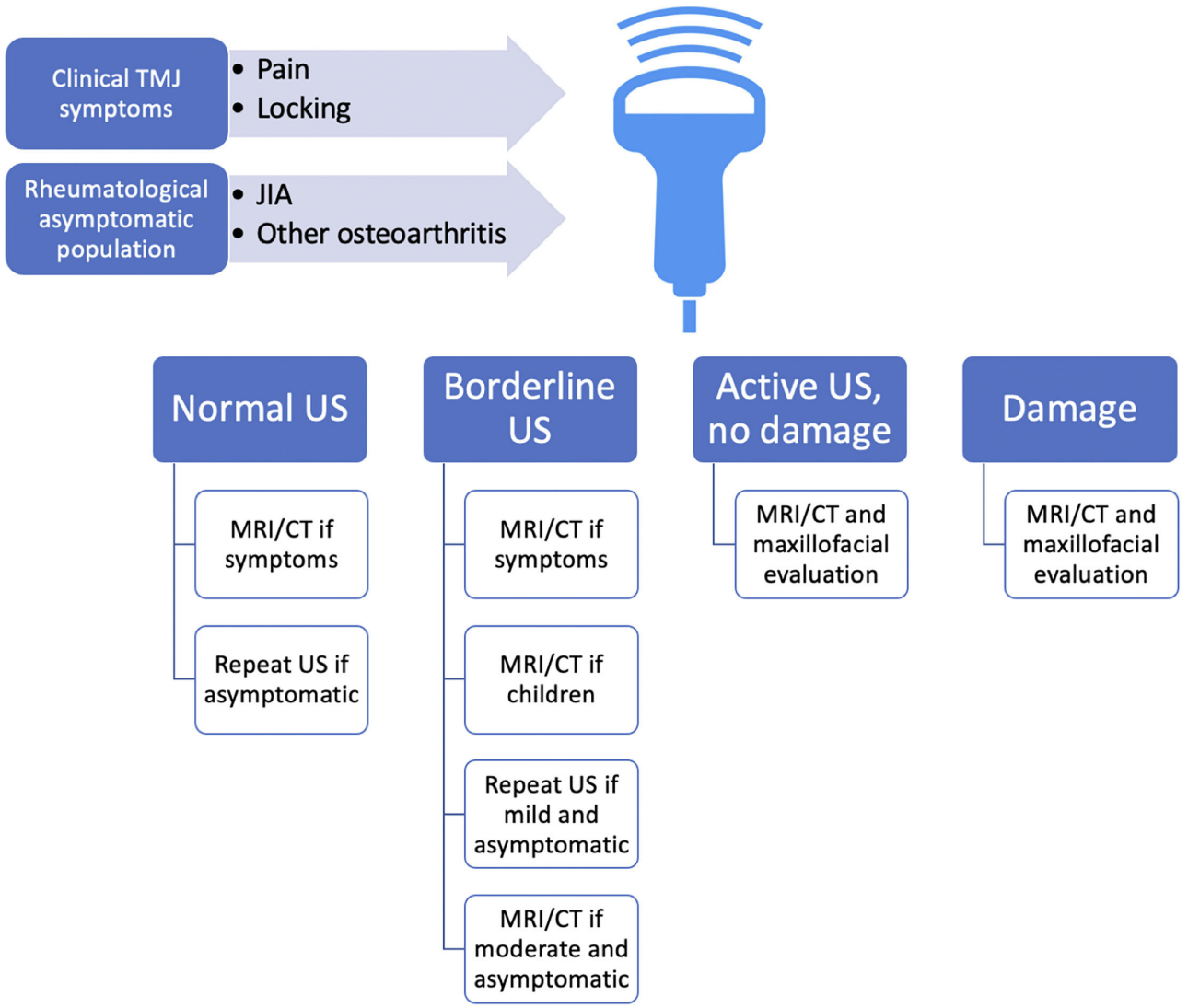

FIGURE 4 | Overview of possible proposed employment of US in TMJ pathology screening as a first-level examination, guiding choice on the follow-up methods. As no validated protocol suggests any early imaging methodic screening in the rheumatological population at-risk for TMD, and also TMD may present rather asymptomatic during the early stages of the disease, we propose US as an "entry-level" method, which is rapidly accessible and of relatively low cost. US could approach all the patients with rheumatic conditions and hopefully also RA-at-risk patients, even if asymptomatic, and of course those with TMJ symptoms. Because US was found to be specific, but not particularly sensitive, we advocate MRI execution even for borderline suspicious findings at US, as baseline MRI could improve anatomic US accuracy during the follow-up. CT, computed tomography; JIA, juvenile idiopathic arthritis; MRI, magnetic resonance imaging; RA, rheumatoid arthritis; TMJ, temporomandibular joint; US, ultrasonography.

We have proposed a possible algorithm for US employment in TMJ pathology (**Figure 4**), which has no claim other than laying the groundwork for further reflection and development of studies that may hopefully clarify the importance of a preliminary analysis of TMJ through a non-invasive methodic such as US.

AUTHOR CONTRIBUTIONS

BM: conceptualization and writing the original draft preparation. BM, GC, SM, MGa, and MGo: methodology, investigation, data curation, writing, reviewing, and editing. MGa and MGo: supervision. All the authors have read and agreed to the published version of the manuscript.

FUNDING

The APC was funded by the University of Ferrara.

ACKNOWLEDGMENTS

The authors thank the colleague Samuel Marturano for image consent and for helping with ultrasound probe position pictures.

REFERENCES

1. Alomar X, Medrano J, Cabratosa J, Clavero JA, Lorente M, Serra I, et al. Anatomy of the temporomandibular joint. *Semin Ultrasound CT MR.* (2007) 28:170–83. doi: 10.1053/j.sult.2007.02.002
2. Covert L, Mater HV, Hechler BL. Comprehensive management of rheumatic diseases affecting the temporomandibular joint. *Diagnostics (Basel).* (2021) 11:409. doi: 10.3390/diagnostics11030409
3. Research NIoDaC. *Facial Pain*. Available online at: https://www.nidcr.nih.gov/research/data-statistics/facial-pain (accessed March 22, 2022).
4. Hunter DJ, Bierma-Zeinstra S. Osteoarthritis. *Lancet.* (2019) 393:1745–59. doi: 10.1016/S0140-6736(19)30417-9
5. Song H, Lee JY, Huh KH, Park JW. Long-Term changes of temporomandibular joint osteoarthritis on computed tomography. *Sci Rep.* (2020) 10:6731. doi: 10.1038/s41598-020-63493-8
6. Dworkin SF, LeResche L. Research diagnostic criteria for temporomandibular disorders: review, criteria, examinations and specifications, critique. *J Craniomandib Disord.* (1992) 6:301–55.
7. Aliko A, Ciancaglini R, Alushi A, Tafaj A, Ruci D. Temporomandibular joint involvement in rheumatoid arthritis, systemic lupus erythematosus and systemic sclerosis. *Int J Oral Maxillofac Surg.* (2011) 40:704–9. doi: 10.1016/j.ijom.2011.02.026
8. Crincoli V, Di Comite M, Di Bisceglie MB, Fatone L, Favia G. Temporomandibular disorders in psoriasis patients with and without psoriatic arthritis: an observational study. *Int J Med Sci.* (2015) 12:341–8. doi: 10.7150/ijms.11288
9. Kononen M, Wenneberg B, Kallenberg A. Craniomandibular disorders in rheumatoid arthritis, psoriatic arthritis, and ankylosing spondylitis. a clinical study. *Acta Odontol Scand.* (1992) 50:281–7. doi: 10.3109/00016359209012774
10. Tasali N, Cubuk R, Aricak M, Ozarar M, Saydam B, Nur H, et al. Temporomandibular joint (Tmj) pain revisited with dynamic contrast-enhanced magnetic resonance imaging (Dce-Mri). *Eur J Radiol.* (2012) 81:603–8. doi: 10.1016/j.ejrad.2011.01.044
11. Bianchi J, de Oliveira Ruellas AC, Goncalves JR, Paniagua B, Prieto JC, Styner M, et al. Osteoarthritis of the temporomandibular joint can be diagnosed earlier using biomarkers and machine learning. *Sci Rep.* (2020) 10:8012. doi: 10.1038/s41598-020-64942-0
12. Cevidanes LH, Gomes LR, Jung BT, Gomes MR, Ruellas AC, Goncalves JR, et al. 3d superimposition and understanding temporomandibular joint arthritis. *Orthod Craniofac Res.* (2015) 18 Suppl 1:18–28. doi: 10.1111/ocr.12070
13. Mejersjo C, Bertilsson O, Back K. Short clinical examination for temporomandibular symptoms in general practice. *Acta Odontol Scand.* (2018) 76:183–7. doi: 10.1080/00016357.2017.1401657
14. Stoustrup P, Twilt M, Spiegel L, Kristensen KD, Koos B, Pedersen TK, et al. Clinical orofacial examination in juvenile idiopathic arthritis: international consensus-based recommendations for monitoring patients in clinical practice and research studies. *J Rheumatol.* (2017) 44:326–33. doi: 10.3899/jrheum.160796
15. Crincoli V, Anelli MG, Quercia E, Piancino MG, Di Comite M. Temporomandibular disorders and oral features in early rheumatoid arthritis patients: an observational study. *Int J Med Sci.* (2019) 16:253–63. doi: 10.7150/ijms.28361
16. Stoll ML, Kau CH, Waite PD, Cron RQ. Temporomandibular joint arthritis in juvenile idiopathic arthritis, now what? *Pediatr Rheumatol Online J.* (2018) 16:32. doi: 10.1186/s12969-018-0244-y
17. Schiffman E, Ohrbach R, Truelove E, Look J, Anderson G, Goulet JP, et al. Diagnostic criteria for temporomandibular disorders (Dc/Tmd) for clinical and research applications: recommendations of the international Rdc/Tmd consortium network* and orofacial pain special interest groupdagger. *J Oral Facial Pain Headache.* (2014) 28:6–27. doi: 10.11607/jop.1151
18. Gasparyan AY, Ayvazyan L, Blackmore H, Kitas GD. Writing a narrative biomedical review: considerations for authors, peer reviewers, and editors. *Rheumatol Int.* (2011) 31:1409–17. doi: 10.1007/s00296-011-1999-3
19. Hayashi T, Ito J, Koyama J, Yamada K. The accuracy of sonography for evaluation of internal derangement of the temporomandibular joint in asymptomatic elementary school children: comparison with Mr and Ct. *AJNR Am J Neuroradiol.* (2001) 22:728–34.
20. Melchiorre D, Falcini F, Kaloudi O, Bandinelli F, Nacci F, Matucci Cerinic M. Sonographic evaluation of the temporomandibular joints in juvenile idiopathic arthritis(). *J Ultrasound.* (2010) 13:34–7. doi: 10.1016/j.jus.2009.09.008
21. Muller L, Kellenberger CJ, Cannizzaro E, Ettlin D, Schraner T, Bolt IB, et al. Early diagnosis of temporomandibular joint involvement in juvenile idiopathic arthritis: a pilot study comparing clinical examination and ultrasound to magnetic resonance imaging. *Rheumatology (Oxford).* (2009) 48:680–5. doi: 10.1093/rheumatology/kep068
22. von Kalle T, Stuber T, Winkler P, Maier J, Hospach T. Early detection of temporomandibular joint arthritis in children with juvenile idiopathic arthritis - the role of contrast-enhanced Mri. *Pediatr Radiol.* (2015) 45:402–10. doi: 10.1007/s00247-014-3143-5
23. Weiss PF, Arabshahi B, Johnson A, Bilaniuk LT, Zarnow D, Cahill AM, et al. High prevalence of temporomandibular joint arthritis at disease onset in children with juvenile idiopathic arthritis, as detected by magnetic resonance imaging but not by ultrasound. *Arthritis Rheum.* (2008) 58:1189–96. doi: 10.1002/art.23401
24. Ahmad M, Hollender L, Anderson Q, Kartha K, Ohrbach R, Truelove EL, et al. Research diagnostic criteria for temporomandibular disorders (Rdc/Tmd): development of image analysis criteria and examiner reliability for image analysis. *Oral Surg Oral Med Oral Pathol Oral Radiol Endod.* (2009) 107:844–60. doi: 10.1016/j.tripleo.2009.02.023
25. Al-Saleh MA, Alsufyani NA, Saltaji H, Jaremko JL, Major PW. Mri and Cbct image registration of temporomandibular joint: a systematic review. *J Otolaryngol Head Neck Surg.* (2016) 45:30. doi: 10.1186/s40463-016-0144-4
26. Dong M, Sun Q, Yu Q, Tao X, Yang C, Qiu W. Determining the optimal magnetic resonance imaging sequences for the efficient diagnosis of temporomandibular joint disorders. *Quant Imaging Med Surg.* (2021) 11:1343–53. doi: 10.21037/qims-20-67
27. Friedman SN, Grushka M, Beituni HK, Rehman M, Bressler HB, Friedman L. Advanced ultrasound screening for temporomandibular joint (Tmj) internal derangement. *Radiol Res Pract.* (2020) 2020:1809690. doi: 10.1155/2020/1809690
28. Hechler BL, Phero JA, Van Mater H, Matthews NS. Ultrasound versus magnetic resonance imaging of the temporomandibular joint in juvenile idiopathic arthritis: a systematic review. *Int J Oral Maxillofac Surg.* (2018) 47:83–9. doi: 10.1016/j.ijom.2017.07.014
29. Kulkarni AU, Gadre PK, Kulkarni PA, Gadre KS. Diagnosing psoriatic arthritis of the temporomandibular joint: a study in radiographic images. *BMJ Case Rep.* (2013) 2013:010301. doi: 10.1136/bcr-2013-010301
30. Landes CA, Goral WA, Sader R, Mack MG. Three-dimensional versus two-dimensional sonography of the temporomandibular joint in comparison to Mri. *Eur J Radiol.* (2007) 61:235–44. doi: 10.1016/j.ejrad.2006.09.015
31. Manfredini D, Guarda-Nardini L. Ultrasonography of the temporomandibular joint: a literature review. *Int J Oral Maxillofac Surg.* (2009) 38:1229–36. doi: 10.1016/j.ijom.2009.07.014
32. Melchiorre D, Calderazzi A, Maddali Bongi S, Cristofani R, Bazzichi L, Eligi C, et al. A comparison of ultrasonography and magnetic resonance imaging in the evaluation of temporomandibular joint involvement in rheumatoid arthritis and psoriatic arthritis. *Rheumatology (Oxford).* (2003) 42:673–6. doi: 10.1093/rheumatology/keg181
33. Mupparapu M, Oak S, Chang YC, Alavi A. Conventional and functional imaging in the evaluation of temporomandibular joint rheumatoid arthritis: a systematic review. *Quintessence Int.* (2019) 50:742–53. doi: 10.3290/j.qi.a43046
34. Navallas M, Inarejos EJ, Iglesias E, Cho Lee GY, Rodriguez N, Anton J. Mr imaging of the temporomandibular joint in juvenile idiopathic arthritis: technique and findings. *Radiographics.* (2017) 37:595–612. doi: 10.1148/rg.2017160078
35. Sodhi A, Naik S, Pai A, Anuradha A. Rheumatoid arthritis affecting temporomandibular joint. *Contemp Clin Dent.* (2015) 6:124–7. doi: 10.4103/0976-237X.149308
36. Zwir LF, Terreri MT. do Amaral ECA, Rodrigues WDR, Fernandes ARC. Is power doppler ultrasound useful to evaluate temporomandibular joint

inflammatory activity in juvenile idiopathic arthritis? *Clin Rheumatol.* (2020) 39:1237–40. doi: 10.1007/s10067-019-04731-x
37. Dong XY, He S, Zhu L, Dong TY, Pan SS, Tang LJ, et al. The diagnostic value of high-resolution ultrasonography for the detection of anterior disc displacement of the temporomandibular joint: a meta-analysis employing the hsroc statistical model. *Int J Oral Maxillofac Surg.* (2015) 44:852–8. doi: 10.1016/j.ijom.2015.01.012
38. Emshoff R, Bertram S, Rudisch A, Gassner R. The diagnostic value of ultrasonography to determine the temporomandibular joint disk position. *Oral Surg Oral Med Oral Pathol Oral Radiol Endod.* (1997) 84:688–96. doi: 10.1016/S1079-2104(97)90374-7
39. Landes CA, Goral W, Mack MG, Sader R. 3-D sonography for diagnosis of osteoarthrosis and disk degeneration of the temporomandibular joint, compared with Mri. *Ultrasound Med Biol.* (2006) 32:627–32. doi: 10.1016/j.ultrasmedbio.2006.01.014
40. Li C, Su N, Yang X, Yang X, Shi Z, Li L. Ultrasonography for detection of disc displacement of temporomandibular joint: a systematic review and meta-analysis. *J Oral Maxillofac Surg.* (2012) 70:1300–9. doi: 10.1016/j.joms.2012.01.003
41. Pupo YM, Pantoja LL, Veiga FF, Stechman-Neto J, Zwir LF, Farago PV, et al. Diagnostic validity of clinical protocols to assess temporomandibular disk displacement disorders: a meta-analysis. *Oral Surg Oral Med Oral Pathol Oral Radiol.* (2016) 122:572–86. doi: 10.1016/j.oooo.2016.07.004
42. Severino M, Caruso S, Rastelli S, Gatto R, Cutilli T, Pittari L, et al. Hand-Carried ultrasonography instrumentation in the diagnosis of temporomandibular joint dysfunction. *Methods Protoc.* (2021) 4:81. doi: 10.3390/mps4040081
43. Tognini F, Manfredini D, Melchiorre D, Bosco M. Comparison of ultrasonography and magnetic resonance imaging in the evaluation of temporomandibular joint disc displacement. *J Oral Rehabil.* (2005) 32:248–53. doi: 10.1111/j.1365-2842.2004.01410.x
44. Westesson PL, Brooks SL. Temporomandibular joint: relationship between mr evidence of effusion and the presence of pain and disk displacement. *AJR Am J Roentgenol.* (1992) 159:559–63. doi: 10.2214/ajr.159.3.1503025
45. Almeida FT, Pacheco-Pereira C, Flores-Mir C, Le LH, Jaremko JL, Major PW. Diagnostic ultrasound assessment of temporomandibular joints: a systematic review and meta-analysis. *Dentomaxillofac Radiol.* (2019) 48:20180144. doi: 10.1259/dmfr.20180144
46. Assaf AT, Kahl-Nieke B, Feddersen J, Habermann CR. Is high-resolution ultrasonography suitable for the detection of temporomandibular joint involvement in children with juvenile idiopathic arthritis? *Dentomaxillofac Radiol.* (2013) 42:20110379. doi: 10.1259/dmfr.20110379
47. Emshoff R, Brandlmaier I, Bodner G, Rudisch A. Condylar erosion and disc displacement: detection with high-resolution ultrasonography. *J Oral Maxillofac Surg.* (2003) 61:877–81. doi: 10.1016/S0278-2391(03)00247-7
48. Hu Y, Zhang X, Liu S, Xu F. Ultrasound-Guided vs conventional arthrocentesis for management of temporomandibular joint disorders: a systematic review and meta-analysis. *Cranio.* (2020) 12:1–10. doi: 10.1080/08869634.2020.1829870
49. Jank S, Haase S, Strobl H, Michels H, Hafner R, Missmann M, et al. Sonographic investigation of the temporomandibular joint in patients with juvenile idiopathic arthritis: a pilot study. *Arthritis Rheum.* (2007) 57:213–8. doi: 10.1002/art.22533
50. Kim JH, Park JH, Kim JW, Kim SJ. Can ultrasonography be used to assess capsular distention in the painful temporomandibular joint? *BMC Oral Health.* (2021) 21:497. doi: 10.1186/s12903-021-01853-0
51. Kundu H, Basavaraj P, Kote S, Singla A, Singh S. Assessment of Tmj disorders using ultrasonography as a diagnostic tool: a review. *J Clin Diagn Res.* (2013) 7:3116–20. doi: 10.7860/JCDR/2013/6678.3874
52. Manfredini D, Tognini F, Melchiorre D, Zampa V, Bosco M. Ultrasound assessment of increased capsular width as a predictor of temporomandibular joint effusion. *Dentomaxillofac Radiol.* (2003) 32:359–64. doi: 10.1259/dmfr/25091144
53. Parra DA, Chan M, Krishnamurthy G, Spiegel L, Amaral JG, Temple MJ, et al. Use and accuracy of Us guidance for image-guided injections of the temporomandibular joints in children with arthritis. *Pediatr Radiol.* (2010) 40:1498–504. doi: 10.1007/s00247-010-1581-2
54. Rudisch A, Emshoff R, Maurer H, Kovacs P, Bodner G. Pathologic-Sonographic correlation in temporomandibular joint pathology. *Eur Radiol.* (2006) 16:1750–6. doi: 10.1007/s00330-006-0162-0
55. Tonni I, Borghesi A, Tonesi S, Fossati G, Ricci F, Visconti L. An ultrasound protocol for temporomandibular joint in juvenile idiopathic arthritis: a pilot study. *Dentomaxillofac Radiol.* (2021) 50:20200399. doi: 10.1259/dmfr.20200399
56. Varol A, Basa S, Topsakal A, Akpinar I. Assessment of synovial vascularization by power doppler ultrasonography in tmj internal derangements treated arthroscopically. *Br J Oral Maxillofac Surg.* (2008) 46:625–30. doi: 10.1016/j.bjoms.2008.04.022
57. Fan J, Heimann A, Wu M. Temporal mandibular joint chondrocalcinosis (Tophaceous Pseudogout) diagnosed by ultrasound-guided fine-needle aspiration. *Diagn Cytopathol.* (2019) 47:803–7. doi: 10.1002/dc.24181
58. Imanimoghaddam M, Davachi B, Madani AS, Nemati S. Ultrasonographic findings of masseter muscle in females with temporomandibular disorders. *J Craniofac Surg.* (2013) 24:e108–12. doi: 10.1097/SCS.0b013e3182646af0
59. Klasser GD, Epstein JB, Utsman R, Yao M, Nguyen PH. Parotid gland squamous cell carcinoma invading the temporomandibular joint. *J Am Dent Assoc.* (2009) 140:992–9. doi: 10.14219/jada.archive.2009.0309
60. Matsumura Y, Nomura J, Nakanishi K, Yanase S, Kato H, Tagawa T. Synovial chondromatosis of the temporomandibular joint with calcium pyrophosphate dihydrate crystal deposition disease (Pseudogout). *Dentomaxillofac Radiol.* (2012) 41:703–7. doi: 10.1259/dmfr/24183821
61. Poveda-Roda R, Moreno P, Bagan J, Margaix M. Myofascial pain: ultrasound width of the masseter muscle. *J Oral Facial Pain Headache.* (2014) 32:298–303. doi: 10.11607/ofph.1944
62. da Motta AT, de Assis Ribeiro Carvalho F, Oliveira AE, Cevidanes LH, de Oliveira Almeida MA. Superimposition of 3d cone-beam Ct models in orthognathic surgery. *Dental Press J Orthod.* (2010) 15:39–41. doi: 10.1590/S2176-94512010000200005
63. De Boever JA, Nilner M, Orthlieb JD, Steenks MH. Educational committee of the European academy of craniomandibular D. recommendations by the eacd for examination, diagnosis, and management of patients with temporomandibular disorders and orofacial pain by the general dental practitioner. *J Orofac Pain.* (2008) 22:268–78.
64. Gibbs SJ, Simmons HC. 3rd. A protocol for magnetic resonance imaging of the temporomandibular joints. *Cranio.* (1998) 16:236–41. doi: 10.1080/08869634.1998.11746063
65. Tolend M, Doria AS, Meyers AB, Larheim TA, Abramowicz S, Aguet J, et al. Assessing the reliability of the omeract juvenile idiopathic arthritis magnetic resonance scoring system for temporomandibular joints (Jamris-Tmj). *J Clin Med.* (2021) 10:4047. doi: 10.3390/jcm10184047
66. Jabehdar Maralani P, Schieda N, Hecht EM, Litt H, Hindman N, Heyn C, et al. Mri safety and devices: an update and expert consensus. *J Magn Reson Imaging.* (2020) 51:657–74. doi: 10.1002/jmri.26909
67. Lee JW, Lee SM, Kim SJ, Choi JW, Baek KW. Clinical utility of fluoride-18 positron emission tomography/Ct in temporomandibular disorder with osteoarthritis: comparisons with 99mtc-Mdp bone scan. *Dentomaxillofac Radiol.* (2013) 42:29292350. doi: 10.1259/dmfr/29292350
68. Suh MS, Park SH, Kim YK, Yun PY, Lee WW. (18)F-Naf Pet/Ct for the evaluation of temporomandibular joint disorder. *Clin Radiol.* (2018) 73:414 e7–13. doi: 10.1016/j.crad.2017.11.008
69. Alavi A, Lakhani P, Mavi A, Kung JW, Zhuang H. Pet: a revolution in medical imaging. *Radiol Clin North Am.* (2004) 42:983-1001. doi: 10.1016/j.rcl.2004.08.012
70. Kirkhus E, Gunderson RB, Smith HJ, Flato B, Hetlevik SO, Larheim TA, et al. Temporomandibular joint involvement in childhood arthritis: comparison of ultrasonography-assessed capsular width and mri-assessed synovitis. *Dentomaxillofac Radiol.* (2016) 45:20160195. doi: 10.1259/dmfr.20160195
71. Murakami K, Nishida M, Bessho K, Iizuka T, Tsuda Y, Konishi J. Mri evidence of high signal intensity and temporomandibular arthralgia and relating pain. does the high signal correlate to the pain? *Br J Oral Maxillofac Surg.* (1996) 34:220–4. doi: 10.1016/S0266-4356(96)90273-9
72. Resnick CM, Vakilian PM, Breen M, Zurakowski D, Caruso P, Henderson L, et al. Quantifying temporomandibular joint synovitis in children with juvenile idiopathic arthritis. *Arthritis Care Res (Hoboken).* (2016) 68:1795–802. doi: 10.1002/acr.22911

73. Chauvin NA, Doria AS. Ultrasound imaging of synovial inflammation in juvenile idiopathic arthritis. *Pediatr Radiol.* (2017) 47:1160–70. doi: 10.1007/s00247-017-3934-6
74. Granata V, Cascella M, Fusco R. dell'Aprovitola N, Catalano O, Filice S, et al. Immediate adverse reactions to gadolinium-based mr contrast media: a retrospective analysis on 10,608 examinations. *Biomed Res Int.* (2016) 2016:3918292. doi: 10.1155/2016/3918292
75. Yousem DM, Kraut MA, Chalian AA. Major salivary gland imaging. *Radiology.* (2000) 216:19–29. doi: 10.1148/radiology.216.1.r00jl4519
76. Wu VW, Ying MT, Kwong DL, A. Study on the post-radiotherapy changes of temporomandibular joint in nasopharyngeal carcinoma patients. *Br J Radiol.* (2017) 90:20170375. doi: 10.1259/bjr.20170375
77. Jank S, Rudisch A, Bodner G, Brandlmaier I, Gerhard S, Emshoff R. High-Resolution ultrasonography of the Tmj: helpful diagnostic approach for patients with tmj disorders? *J Craniomaxillofac Surg.* (2001) 29:366–71. doi: 10.1054/jcms.2001.0252
78. Stabrun AE, Larheim TA, Hoyeraal HM. Temporomandibular joint involvement in juvenile rheumatoid arthritis. clinical diagnostic criteria scand. *J Rheumatol.* (1989) 18:197–204. doi: 10.3109/03009748909099929
79. Kuseler A, Pedersen TK, Herlin T, Gelineck J. Contrast enhanced magnetic resonance imaging as a method to diagnose early inflammatory changes in the temporomandibular joint in children with juvenile chronic arthritis. *J Rheumatol.* (1998) 25:1406–12.
80. Colebatch-Bourn AN, Edwards CJ, Collado P, D'Agostino MA, Hemke R, Jousse-Joulin S, et al. Eular-Pres points to consider for the use of imaging in the diagnosis and management of juvenile idiopathic arthritis in clinical practice. *Ann Rheum Dis.* (2015) 74:1946–57. doi: 10.1136/annrheumdis-2015-207892
81. Prakken B, Albani S, Martini A. Juvenile idiopathic arthritis. *Lancet.* (2011) 377:2138–49. doi: 10.1016/S0140-6736(11)60244-4
82. Martini A, Ravelli A, Avcin T, Beresford MW, Burgos-Vargas R, Cuttica R, et al. Toward new classification criteria for juvenile idiopathic arthritis: first steps, pediatric rheumatology international trials organization international consensus. *J Rheumatol.* (2019) 46:190–7. doi: 10.3899/jrheum.180168
83. Ringold S, Cron RQ. The temporomandibular joint in juvenile idiopathic arthritis: frequently used and frequently arthritic. *Pediatr Rheumatol Online J.* (2009) 7:11. doi: 10.1186/1546-0096-7-11
84. Argyropoulou MI, Margariti PN, Karali A, Astrakas L, Alfandaki S, Kosta P, et al. Temporomandibular joint involvement in juvenile idiopathic arthritis: clinical predictors of magnetic resonance imaging signs. *Eur Radiol.* (2009) 19:693–700. doi: 10.1007/s00330-008-1196-2
85. Cedstromer AL, Ahlqwist M, Andlin-Sobocki A, Berntson L, Hedenberg-Magnusson B, Dahlstrom L. Temporomandibular condylar alterations in juvenile idiopathic arthritis most common in longitudinally severe disease despite medical treatment. *Pediatr Rheumatol Online J.* (2014) 12:43. doi: 10.1186/1546-0096-12-43
86. Cannizzaro E, Schroeder S, Muller LM, Kellenberger CJ, Saurenmann RK. Temporomandibular joint involvement in children with juvenile idiopathic arthritis. *J Rheumatol.* (2011) 38:510–5. doi: 10.3899/jrheum.100325
87. Stoll ML, Sharpe T, Beukelman T, Good J, Young D, Cron RQ. Risk factors for temporomandibular joint arthritis in children with juvenile idiopathic arthritis. *J Rheumatol.* (2012) 39:1880–7. doi: 10.3899/jrheum.111441
88. Guo Q, Wang Y, Xu D, Nossent J, Pavlos NJ, Xu J. Rheumatoid arthritis: pathological mechanisms and modern pharmacologic therapies. *Bone Res.* (2018) 6:15. doi: 10.1038/s41413-018-0016-9
89. Delantoni A, Spyropoulou E, Chatzigiannis J, Papademitriou P. Sole radiographic expression of rheumatoid arthritis in the temporomandibular joints: a case report. *Oral Surg Oral Med Oral Pathol Oral Radiol Endod.* (2006) 102:e37–40. doi: 10.1016/j.tripleo.2005.12.024
90. Ruparelia PB, Shah DS, Ruparelia K, Sutaria SP, Pathak D. Bilateral Tmj involvement in rheumatoid arthritis. *Case Rep Dent.* (2014) 2014:262430. doi: 10.1155/2014/262430
91. Kroese JM, Volgenant CMC, Crielaard W, Loos B, van Schaardenburg D, Visscher CM, et al. Temporomandibular disorders in patients with early rheumatoid arthritis and at-risk individuals in the dutch population: a cross-sectional study. *RMD Open.* (2021) 7:e001485. doi: 10.1136/rmdopen-2020-001485
92. Demoruelle MK, Deane KD. Treatment strategies in early rheumatoid arthritis and prevention of rheumatoid arthritis. *Curr Rheumatol Rep.* (2012) 14:472–80. doi: 10.1007/s11926-012-0275-1
93. van Steenbergen HW, Aletaha D. Beaart-van de Voorde LJ, Brouwer E, Codreanu C, Combe B, et al. Eular definition of arthralgia suspicious for progression to rheumatoid arthritis. *Ann Rheum Dis.* (2017) 76:491–6. doi: 10.1136/annrheumdis-2016-209846
94. Falisi G, Gatto R, Di Paolo C, De Biase A, Franceschini C, Monaco A, et al. A female psoriatic arthritis patient involving the Tmj. *Case Rep Dent.* (2021) 2021:6638638. doi: 10.1155/2021/6638638
95. Dervis E, Dervis E. The prevalence of temporomandibular disorders in patients with psoriasis with or without psoriatic arthritis. *J Oral Rehabil.* (2005) 32:786–93. doi: 10.1111/j.1365-2842.2005.01521.x
96. Locher MC, Felder M, Sailer HF. Involvement of the temporomandibular joints in ankylosing spondylitis (Bechterew's Disease). *J Craniomaxillofac Surg.* (1996) 24:205–13. doi: 10.1016/S1010-5182(96)80003-5
97. Sakellariou G, Conaghan PG, Zhang W, Bijlsma JWJ, Boyesen P, D'Agostino MA, et al. Eular recommendations for the use of imaging in the clinical management of peripheral joint osteoarthritis. *Ann Rheum Dis.* (2017) 76:1484–94. doi: 10.1136/annrheumdis-2016-210815
98. D'Agostino MA, Terslev L, Aegerter P, Backhaus M, Balint P, Bruyn GA, et al. Scoring ultrasound synovitis in rheumatoid arthritis: a eular-omeract ultrasound taskforce-part 1: definition and development of a standardised, consensus-based scoring system. *RMD Open.* (2017) 3:e000428. doi: 10.1136/rmdopen-2016-000428
99. Terslev L, Naredo E, Aegerter P, Wakefield RJ, Backhaus M, Balint P, et al. Scoring ultrasound synovitis in rheumatoid arthritis: a eular-omeract ultrasound taskforce-part 2: reliability and application to multiple joints of a standardised consensus-based scoring system. *RMD Open.* (2017) 3:e000427. doi: 10.1136/rmdopen-2016-000427
100. De Rossi SS, Greenberg MS, Liu F, Steinkeler A. Temporomandibular disorders: evaluation and management. *Med Clin North Am.* (2014) 98:1353–84. doi: 10.1016/j.mcna.2014.08.009
101. Laviv A, Sadow PM, Keith DA. Pseudogout in the temporomandibular joint with imaging, arthroscopic, operative, and pathologic findings. report of an unusual case. *J Oral Maxillofac Surg.* (2015) 73:1106–12. doi: 10.1016/j.joms.2014.12.041
102. Kwon KJ, Seok H, Lee JH, Kim MK, Kim SG, Park HK, et al. Calcium pyrophosphate dihydrate deposition disease in the temporomandibular joint: diagnosis and treatment. *Maxillofac Plast Reconstr Surg.* (2018) 40:19. doi: 10.1186/s40902-018-0158-0
103. Oliveira IN, Gomes RC, Dos Santos RR, Oliveira Tde P, Pereira LL, Mainenti P. Gout of the temporomandibular joint: report of a case. *Int Arch Otorhinolaryngol.* (2014) 18:316–8. doi: 10.1055/s-0033-1363464
104. Bag AK, Gaddikeri S, Singhal A, Hardin S, Tran BD, Medina JA, et al. Imaging of the temporomandibular joint: an update. *World J Radiol.* (2014) 6:567–82. doi: 10.4329/wjr.v6.i8.567
105. van Nimwegen JF, Mossel E, Delli K, van Ginkel MS, Stel AJ, Kroese FGM, et al. Incorporation of salivary gland ultrasonography into the American college of Rheumatology/European league against rheumatism criteria for primary sjogren's syndrome. *Arthritis Care Res (Hoboken).* (2020) 72:583–90. doi: 10.1002/acr.24017
106. Makdissi J, Pawar RR, Radon M, Holmes SB. Incidental findings on Mri of the temporomandibular joint. *Dentomaxillofac Radiol.* (2013) 42:20130175. doi: 10.1259/dmfr.20130175
107. Rybalov OV, Yatsenko PI, Andriyanova OY, Ivanytska ES, Korostashova MA. Functional disordersof the salivary glands in patients with compression and dislocation dysfunction of the temporomandibular joint and their correction. *Wiad Lek.* (2021) 74:1695–8. doi: 10.36740/WLek202107124
108. Poveda-Roda R, Bagan JV, Sanchis JM, Margaix M. Pseudotumors and tumors of the temporomandibular joint. a review. *Med Oral Patol Oral Cir Bucal.* (2013) 18:e392–402. doi: 10.4317/medoral.18799
109. Yang CY. Diagnosis of giant cell tumor of temporomandibular joint with ultrasound-guided core needle biopsy. *J Med Ultrasound.* (2014) 22:164–6. doi: 10.1016/j.jmu.2014.06.002
110. Austin D, O'Donnell F, Attanasio R. Temporal arteritis mimics Tmj/myofascial pain syndrome. *Ohio Dent J.* (1992) 66:44–7.

111. Ariji Y, Ariji E. Magnetic resonance and sonographic imagings of masticatory muscle myalgia in temporomandibular disorder patients. *Jpn Dent Sci Rev.* (2017) 53:11–7. doi: 10.1016/j.jdsr.2016.05.001
112. Kuseler A, Pedersen TK, Gelineck J, Herlin T, A. 2 year followup study of enhanced magnetic resonance imaging and clinical examination of the temporomandibular joint in children with juvenile idiopathic arthritis. *J Rheumatol.* (2005) 32:162–9.
113. Orhan K. Ultrasonography-Guided invasive procedures of the temporomandibular joint. *Clin Dent Rev.* (2021) 5:3. doi: 10.1007/s41894-020-00091-x
114. Fritz J, Tzaribachev N, Thomas C, Carrino JA, Claussen CD, Lewin JS, et al. Evaluation of Mr imaging guided steroid injection of the sacroiliac joints for the treatment of children with refractory enthesitis-related arthritis. *Eur Radiol.* (2011) 21:1050–7. doi: 10.1007/s00330-010-1994-1
115. Kinard BE, Abramowicz S. Juvenile idiopathic arthritis practice patterns among oral and maxillofacial surgeons. *J Oral Maxillofac Surg.* (2017) 75:2333 e1–8. doi: 10.1016/j.joms.2017.07.159
116. Johnston K, Bird L, Bright P. Temporomandibular joint effusion and its relationship with perceived disability assessed using musculoskeletal ultrasound and a patient-reported disability index. *Ultrasound.* (2015) 23:90–6. doi: 10.1177/1742271X14568608

Conflict of Interest: The authors declare that the research was conducted in the absence of any commercial or financial relationships that could be construed as a potential conflict of interest.

Publisher's Note: All claims expressed in this article are solely those of the authors and do not necessarily represent those of their affiliated organizations, or those of the publisher, the editors and the reviewers. Any product that may be evaluated in this article, or claim that may be made by its manufacturer, is not guaranteed or endorsed by the publisher.

frontiers | Frontiers in Medicine

TYPE Original Research
PUBLISHED 16 August 2022
DOI 10.3389/fmed.2022.978351

OPEN ACCESS

EDITED BY
Andrea Di Matteo,
Marche Polytechnic University, Italy

REVIEWED BY
Reem Hamdy A. Mohammed,
Cairo University, Egypt
João Rovisco,
Centro Hospitalar e Universitário de Coimbra, Portugal

*CORRESPONDENCE
Carlos Pineda
carpineda@yahoo.com

†These authors have contributed equally to this work

SPECIALTY SECTION
This article was submitted to Rheumatology, a section of the journal Frontiers in Medicine

RECEIVED 25 June 2022
ACCEPTED 27 July 2022
PUBLISHED 16 August 2022

CITATION
Carbonell-Bobadilla N, Soto-Fajardo C, Amezcua-Guerra LM, Batres-Marroquín AB, Vargas T, Hernández-Diazcouder A, Jiménez-Rojas V, Medina-García AC, Pineda C and Silveira LH (2022) Patients with seronegative rheumatoid arthritis have a different phenotype than seropositive patients: A clinical and ultrasound study. *Front. Med.* 9:978351. doi: 10.3389/fmed.2022.978351

Patients with seronegative rheumatoid arthritis have a different phenotype than seropositive patients: A clinical and ultrasound study

Natalia Carbonell-Bobadilla[1†], Carina Soto-Fajardo[2†], Luis M. Amezcua-Guerra[3,4†], Ana Beatriz Batres-Marroquín[2], Tania Vargas[1], Adrian Hernández-Diazcouder[3], Valentin Jiménez-Rojas[3], Ana Cristina Medina-García[2], Carlos Pineda[2*] and Luis H. Silveira[1]

[1]Department of Rheumatology, Instituto Nacional de Cardiología Ignacio Chávez, Mexico City, Mexico, [2]Rheumatology Division, Instituto Nacional de Rehabilitación Luis Guillermo Ibarra Ibarra, Mexico City, Mexico, [3]Department of Immunology, Instituto Nacional de Cardiología Ignacio Chávez, Mexico City, Mexico, [4]Department of Health Care, Universidad Autónoma Metropolitana-Xochimilco, Mexico City, Mexico

Introduction: Rheumatoid arthritis (RA) is an inflammatory disease whose clinical phenotype largely depends on the presence of rheumatoid factor (RF) and anti-citrullinated protein antibodies (ACPA). Seronegative RA appears to be a less severe disease, but this remains controversial. This study aimed to assess whether seronegative patients show a less severe disease than seropositive patients.

Methods: A cross-sectional study was conducted on RA outpatients from a single center. Clinical activity scales, laboratory evaluations, and cardiovascular risk scores were assessed. Musculoskeletal ultrasound (US) examinations were performed.

Results: One hundred and fourteen patients were enrolled. Eighty-five were seropositive (76% women) and 29 seronegative (93% women). Seropositive patients had a younger age at disease onset (43 ± 14 vs. 54 ± 11; $p = 0.001$) and used sulfasalazine (47 vs. 17%; $p = 0.004$) and glucocorticoids (36 vs. 10%; $p = 0.007$) more frequently. No differences in clinical activity scales and in 10-year cardiovascular risk were observed. Pathological US data were found more frequently in seropositive patients in the 2nd metacarpophalangeal (MCP) joint, both in grayscale (71 vs. 38%; $p = 0.008$) and in power Doppler (PD; 53 vs. 9%; $p < 0.001$); erosions (36 vs. 9%; $p = 0.020$) were also more frequent. We found greater severity of PD signals in the 2nd MCP and 3rd MCP joints of the seropositive patients, while synovitis severity was higher only in the 2nd MCP joints. The percentage of total joints with erosions (9 vs. 1%; $p < 0.001$) and 2nd MCP joints with erosions (25 vs. 7%; $p < 0.001$) was higher in seropositive patients.

Conclusion: RA patients show a differentiated phenotype according to their ACPA and RF status. In seronegative patients, RA begins later in life and has a

lower requirement for antirheumatic therapies. On US evaluation, seropositive patients show more joint damage, especially in MCP joints. Despite this, long-term cardiovascular risk is similar among RA patients, regardless of their RF and ACPA status.

KEYWORDS

rheumatoid arthritis, ultrasound, rheumatoid factor, anti-citrullinated protein antibodies, cardiovascular risk, seronegative rheumatoid arthritis

Introduction

Rheumatoid arthritis (RA) is a chronic disease that affects ∼1% of the population. In Mexico, the prevalence has been estimated at 1.6%, according to the COPCORD methodology (1). RA is classified according to seropositivity for rheumatoid factor (RF) and anti-citrullinated protein antibodies (ACPA). Although seronegative RA (SNRA) appears to be less severe in its presentation and clinical course than seropositive RA (SPRA), there are still controversies because there are studies in which these differences do not exist. Furthermore, 20–30% of RA patients do not have ACPA and RF, and erosive RA can occur without these antibodies. Mouterde et al. in 2019 described the disease course of patients without RF or ACPA in an inception cohort of patients with early inflammatory arthritis. This ESPOR cohort included 748 patients and showed that, at a 3-year follow-up, SNRA patients had mean disease activity and quality of life similar to that observed in SPRA patients; additionally, the proportion of patients who achieved disease remission was similar. Despite this, the modified total Sharp score and radiographic progression at 3 years were lower in the SNRA group. These patients also used less conventional and biologic disease-modifying antirheumatic drugs (DMARDs) and glucocorticoids than seropositive patients (2).

It is currently unclear whether SPRA patients have a worse disease course than SNRA patients on measures of disease activity and radiological outcomes. Studies have reported increased disease severity and impaired function in patients with SPRA, both at disease presentation and after DMARD treatment (3). In contrast, other studies reported that SNRA patients had more severe inflammatory activity than SPRA as assessed by ultrasound (US) and plain radiography (4, 5). These discrepancies may be attributed to differences in the patient populations studied, inclusion criteria, and measures of disease activity between different studies. Choi S et al. demonstrated that patients with SNRA manifested more active disease at presentation, with a better response to DMARD treatment than patients with SPRA (6).

Compared to the general population, a considerably higher risk of cardiovascular disease (CVD) is observed in RA (7). Dyslipidemia, diabetes, a family history of CVD, and elevated body mass index are the associated risk factors in RA patients (8). Data suggest that RA-related factors, such as sustained inflammation, are also associated with increased risk in these patients (9). CVD mortality has been associated with the level of inflammation, the HLA-DRB1*0404 allele (10), the use of glucocorticoids (11), and the presence of characteristic RA antibodies (12). High C-reactive protein (CRP) levels among RA patients correlate with lower levels of total cholesterol, LDL-C, and HDL-C; at the same time, elevated CRP is associated with an increased CVD risk (13). Several algorithms that quantify CVD risk are available for use in the general population, which also apply to RA patients. These calculators use traditional parameters such as age, gender, blood pressure, smoking, cholesterol levels, and diabetes to calculate CVD risk (14). Risk prediction models provide a valuable starting point to initiate the primary prevention of CVD risk.

This study aimed to assess whether SNRA patients have a clinical and ultrasonographic less severe disease than SPRA patients.

Materials and methods

Patients

Observational, cross-sectional study that included consecutive outpatients diagnosed with RA according to the 2010 American College of Rheumatology/European League Against Rheumatism (ACR/EULAR) (15) classification criteria who attended the rheumatology clinic of a single tertiary care hospital. Patients were divided into two groups according to their antibody status. Patients with overlap syndrome, malignant neoplasms, hepatitis B or C virus infection, HIV, other active infections, or who had received rituximab in the last year were excluded.

The local ethics committee approved the protocol. The study was performed following the Declaration of Helsinki (16). Patients consented to participate, authorizing the use of clinical, laboratory, and imaging data for research purposes.

Clinical and laboratory assessments

All individuals underwent a detailed evaluation, including medical history, musculoskeletal examination, ultrasound evaluation and laboratory tests. Patients were classified as SPRA if they had positive RF or ACPA and SNRA if both antibodies were negative. In addition, sociodemographic variables, age at onset of joint symptoms, age at diagnosis, smoking habit, and body mass index were recorded. Laboratory data were also collected, including platelets, leukocytes, CRP, and erythrocyte sedimentation rate. Finally, pharmacological therapies at the time of study enrollment were recorded. The extent of disease activity was evaluated using the Disease Activity Score-28 (DAS28-CRP), the Clinical Disease Activity Index (CDAI), and the Simplified Disease Activity Index (SDAI).

We calculated the ten-year cardiovascular risk using the QRISK®3-2018, the Framingham Risk Score, the Reynolds Risk Score, and the 2013 Atherosclerotic Cardiovascular Disease (ASCVD) Risk Estimator in the respective online calculators.

Ultrasound assessment

Musculoskeletal US (MSUS) examinations were performed using the MyLab^{TM}X7 system (Esaote Biomedica, Genoa, Italy) equipped with a 6 to 18 MHz broadband linear transducer. Two rheumatologists (CP and CSF) trained in MSUS, who were blinded to the clinical and laboratory data, scanned all patients. Bilateral MSUS examination was performed of the wrists, 2nd and 3rd metacarpophalangeal (MCP) joints, elbow (anterior and posterior joint recess), knee (suprapatellar and lateral parapatellar joint recess) and ankle (anterior recess of the ankle joint, and peroneal and tibialis posterior tendons) (17).

All US examinations were performed using a multiplanar technique following the EULAR guidelines (18). Assessment of inflammation and neovascularity in joints and tendons was accomplished by Power Doppler (PD) with a pulse repetition frequency of 750 kHz and a Doppler frequency between 6–8 MHz. Special attention was paid to avoiding unnecessary probe pressure and maintaining the relaxation of tendons.

Ultrasound interpretation

We used current OMERACT (Outcome Measures in Rheumatology) definitions for ultrasonographic pathology and elementary lesions for rheumatic disorders (19). In addition, images were scored for synovitis on grayscale (GS) and PD according to the EULAR-OMERACT scoring system, which divides the severity of synovitis and intensity of PD signals from normal (grade 0) to severe (grade 3) (20). An overall GS and PD signal score was calculated as the sum of GS synovitis, PD synovitis and GS tenosynovitis and PD tenosynovitis with the range of scores of 0–36 for GS synovitis, 0–36 for PD synovitis, 0–12 for GS tenosynovitis and 0–12 for PD tenosynovitis.

Finally, in our study, the definition of disease severity is based on the concepts of disease activity using activity indexes (DAS28-CRP, CDAI, SDAI), cardiovascular risk and ultrasonographic evaluation (synovitis in GS and PD, and structural damage/erosions).

Statistical analysis

Discrete variables were described using proportions and percentages, and differences were evaluated using the chi-square test. Means ± standard deviation (SD) or medians with interquartile range (IQR) were used to describe continuous variables, and differences were evaluated using the Student's *t*-test or the Mann–Whitney *U*-test, respectively.

To assess the association between the status of seropositivity and joint damage (bone erosions), linear regression was performed with the total of bone erosions as the dependent variable and the status of seropositivity as the independent variable. Similarly, to assess the association between the status of seropositivity and synovitis in GS and PD, linear regression was performed with the synovitis in the 2nd MCP joint as the dependent variable and the status of seropositivity as the independent variable.

Analyzes were two-tailed, and a $p < 0.05$ value was set for significance. The Graph Pad Prism version 9.3.1 software (Graph Pad Inc, La Jolla, CA, USA) was used for the calculations.

Results

Between July 1, 2019, and May 28, 2022, 114 patients with RA were enrolled (Table 1, Supplementary Table 1). Eighty-five patients were SPRA (76% female), and 29 were SNRA (93% female). SNRA patients had an older age at the onset of the disease (54 ± 11 years vs. 43 ± 14 years; $p < 0.001$), although a similar duration of the disease, so the average age at recruitment was also significantly older (63 ± 9 years vs. 54 ± 13 years; $p < 0.001$). In contrast, the frequency of diabetes, overweight and obesity, hypertension, and history of coronary artery disease was similar. We also found no differences in the degree of disease activity or DMARDs use, except for greater use of sulfasalazine in SPRA patients (47% vs. 17; $p = 0.004$). Regarding the doses of DMARDs, SPRA patients used higher doses of methotrexate, both in the total population and in the subgroup of patients with US [17.5 (IQR 15–23.12) vs 13.75 (IQR 7.5–17.5), $p = 0.003$ and 17.5 (IQR 15–25) vs 15 (IQR 7.5–17.5), $p = 0.006$]. The frequency of use (36 vs. 10%; $p = 0.007$) and the average prednisone dose (7.5 mg/day vs. 2.5 mg/day; $p = 0.033$) was higher in SPRA patients.

TABLE 1 Clinical and laboratory features of patients with rheumatoid arthritis.

	Seropositive patients ($n = 85$)	Seronegative patients ($n = 29$)	p
Age, years	54 ± 13	63 ± 9	**<0.001**
Female, *n* (%)	65 (76)	27 (93)	0.050
Age of disease onset, years	43 ± 14	54 ± 11	**<0.001**
Disease duration, years	3.7 ± 5.0	3.1 ± 3.6	0.550
BMI, kg/m^2	26.8 ± 4.7	26.3 ± 4.4	0.631
Smoking, *n* (%)	8 (9)	1 (3)	0.303
Diabetes, *n* (%)	23 (27)	9 (31)	0.680
Hypertension, *n* (%)	24 (28)	13 (44)	0.099
CAD, *n* (%)	9 (10)	2 (6)	0.561
Disease activity			
• DAS28-CRP, median (IQR)	2.9 (2.1–3.7)	2.5 (1.7–3.5)	0.199
• SDAI, median (IQR)	12.6 (6.7–22.8)	10.6 (3.5–20.0)	0.363
• CDAI, median (IQR)	9 (4–17)	8 (3–18)	0.383
• Extra-articular manifestations, n (%)	9 (10)	2 (6)	0.561
Drug therapies, n (%)			
• Methotrexate	66 (77)	26 (89)	0.157
• Sulfasalazine	40 (47)	5 (17)	**0.004**
• Leflunomide	15 (17)	4 (13)	0.630
• Hydroxychloroquine	47 (55)	14 (48)	0.512
• Statins	12 (14)	7 (24)	0.211
• PDN	31 (36)	3 (10)	**0.007**
• PDN dose, mg/day, median (IQR)	7.5 (5–10)	2.5 (2.5–3.75)	**0.033**
Laboratory studies			
• WBC, 1x10^3 per mm^3	6.9 ± 2.0	5.8 ± 1.5	**0.009**
• Neutrophils, 1x10^3 per mm^3	4.4 ± 1.8	3.5 ± 1.2	**0.011**
• Lymphocytes, 1x10^3 per mm^3	1.6 ± 0.5	1.6 ± 0.4	0.994
• NLR	2.9 ± 1.7	2.1 ± 0.8	**0.036**
• Hemoglobin, g/dl	13.8 ± 1.6	13.4 ± 1.7	0.348
• Platelets, 1x10^3 per mm^3	277 ± 81	279 ± 116	0.923
• Glucose, mg/dl	98.7 ± 28.9	98.8 ± 17.3	0.981
• Creatinine, mg/dl	0.74 ± 0.23	0.75 ± 0.19	0.791
• Albumin, g/dl	4.1 ± 0.2	4.1 ± 0.2	0.967
• Cholesterol, mg/dl	168 ± 34	177 ± 34	0.232
• HDL-C, mg/dl	49 ± 13	53 ± 12	0.160
• Triglycerides, mg/dl	137 ± 74	129 ± 48	0.304
• ESR, mm/h	20.7 ± 17.9	19.6 ± 16.5	0.790
• hs-CRP, mg/L	11.4 ± 15.1	6.7 ± 9.1	0.118

Data are presented as mean ± standard deviation unless otherwise specified. Significant p-values are in bold.
BMI, body mass index; CAD, coronary artery disease; CDAI, Clinical Disease Activity Index; DAS28-CRP, Disease Activity Score 28-joint counts; ESR; erythrocyte sedimentation rate; HDL-C, high-density lipoprotein cholesterol; hs-CRP, high-sensitivity C-reactive protein; NLR; neutrophil-to-lymphocyte ratio; PDN, prednisone; SDAI; Simple Disease Activity Index; WBC, white blood cells.

Clinical assessment

The extent of disease activity and extra-articular manifestations were similar in both study groups (Table 1). Laboratory studies showed that SPRA patients had higher leukocyte (6.9 ± 2.0 x10^3 vs. 5.8 ± 1.5 x10^3; $p = 0.009$) and neutrophil (4.4 ± 1.8 x10^3 vs. 3.5 ± 1.2 x10^3; $p = 0.011$) counts, resulting in a higher neutrophil/lymphocyte ratio (2.9 ± 1.7 vs. 2.1 ± 0.8; $p = 0.036$). Meanwhile, blood cells other than leukocytes, glucose, creatinine, albumin, and lipids were

similar between patients. No differences were observed in acute-phase proteins.

Cardiovascular risk scores

Table 2 summarizes the risk of coronary artery disease or stroke at 10 years. There is a notable trend for SNRA patients to be at higher risk than SPRA patients, although none of these differences reached statistical significance. Cardiovascular risk measured by the different scales was only correlated with CRP values (Spearman's rho: QRISK®3-2018, 0.53, $p < 0.001$; Framingham Risk Score, 0.4, $p = 0.001$; Reynolds Risk Score, 0.53, $p < 0.001$; and ASCVD Risk Estimator, 0.52, $p < 0.001$), while the rest of the variables, including synovitis in GS and PD, ACPA and RF, among others, did not correlate with cardiovascular risk.

US assessment

Musculoskeletal US was performed in 49 SPRA patients and 21 with SNRA. A total of 12 joints per patient were evaluated, namely elbows, wrists, 2nd and 3rd MCP joints, knees, and ankles, in addition to peroneal and tibialis posterior tendons. Table 3, Supplementary Table 2 summarizes the main joint findings. US joint inflammation was found more frequently in SPRA patients in the 2nd MCP joint, both in GS (71 vs. 38%; $p = 0.008$) and PD (53 vs. 9%; $p < 0.001$) assessments; structural joint damage manifested as bone erosions (36 vs. 9%; $p = 0.020$) were also more frequent. In contrast, no significant differences were observed in the frequency of pathologic findings in any of the other joint areas, despite a persistent trend toward greater damage in SPRA patients. We found no differences in the involvement of the posterior tibial and peroneal tendons between groups.

Subsequently, we analyzed the US findings according to the severity of the elementary lesions in the small joints of the hands (Table 4). We found greater severity in the PD signals in the 2nd MCP (median 0, IQR 0–0.25 vs. 0, 0–0; $p < 0.001$) and 3rd MCP (0, 0–0 vs. 0, 0–0; $p = 0.011$) joints of the SPRA patients, while the GS was higher only in the 2nd MCP joint (0, 0–2 vs. 0, 0–0; $p < 0.001$). There were no differences in the wrists. The percentage of total joints displaying evidence of structural damage (erosive disease) (9 vs. 1%; $p < 0.001$) and 2nd MCP joints with erosions (25 vs. 7%; $p < 0.001$) was significantly higher in SPRA patients (Figure 1).

In multivariate analysis, only seropositivity status and disease of duration were associated with bone erosions (damage) (Table 5). For synovitis, differences were only found in the 2nd MCP, while seropositivity status and DAS-28 CRP score were associated with synovitis in this joint, both in GS and PD (Supplementary Table 3). In the multivariate analysis for erosions and synovitis, we included other variables such as gender, drugs used, and HAQ, but they were not significant.

Discussion

SNRA is considered a less severe disease than SPRA, although, controversy still exists (2, 4, 5). In this study, we aimed to analyze the differences in SNRA as a less severe disease compared to SPRA.

We found significant differences in the age of onset of the disease since seronegative patients were older (54 ± 11 years), compared to seropositive patients (43 ± 14 years). No differences in extra-articular manifestations and the clinical activity scales were observed.

There are some similarities and some discrepancies in the literature with our findings. Mouterde et al. aimed to describe the disease course of patients without RF and ACPA in an inception cohort of early inflammatory arthritis patients and to determine baseline predictors of fulfilling 2010 ACR/EULAR criteria for RA within 3 years. They used a large, prospective, early-arthritis cohort from the community. The disease was less active based on DAS28-ESR and also less severe in terms of the functional index and radiographic score at baseline in the seronegative patients than in the seropositive patients (21). These results agree with those of the Norfolk Arthritis Register (NOAR) (3), but not with the Canadian early-arthritis cohort (CATCH), showing seronegative patients with higher mean swollen joint count, DAS28, and erosive disease, which suggests that these patients are more frequently referred to rheumatology if they have more active and severe disease. The disease progression was less severe and DMARD or glucocorticoid use less frequent in the seronegative vs. the seropositive group during follow-up in the ESPOIR cohort, which agrees with other early-arthritis cohorts (22).

Choi et al. found that SNRA patients manifested more active disease at baseline compared than SPRA patients (6). This could be partly explained by the fact that 99.5% of SPRA patients met the 2010 ACR/EULAR criteria, while only 27.5% of SNRA patients did. The 2010 ACR/EULAR criteria give much weight to serology markers to detect patients with RA early in the disease course. Therefore, seropositive patients with only one or two involved joints could be diagnosed with RA (22). This could explain the older mean age reported in our study in the SNRA group.

There were also differences in the pharmacological treatment. SNRA group needed fewer DMARDs combinations than the SPRA group, being more evident with sulfasalazine since only five of the seronegative patients was taking this drug, compared to the 47% of the SPRA group; additionally, the dose of methotrexate was higher for the SPRA group. Glucocorticoid requirement was less in the seronegative group, only three patients (10%) needed prednisone, with mean doses of 2.5

TABLE 2 Risk of coronary heart disease or stroke at 10 years.

	Seropositive patients ($n = 85$)	Seronegative patients ($n = 29$)	p
QRISK® 3–2018	8.0 (1.8–20.5)	9.6 (5.5–20.1)	0.122
Framingham risk score	4 (2–10)	4 (3–6)	0.468
Reynolds risk score	1.7 (0.6–4.5)	2.5 (1.1–4.6)	0.303
ASCVD risk estimator	2.7 (0.6–10.1)	4.6 (2.0–9.7)	0.124

Data are presented as median (interquartile range).
ASCVD, Atherosclerotic Cardiovascular Disease.

TABLE 3 Pathological findings observed on ultrasound in 12 main joint areas.

	Seropositive patients ($n = 49$)	Seronegative patients ($n = 21$)	p
2nd MCP joint			
· Grayscale	35 (71)	8 (38)	**0.008**
· Power Doppler	26 (53)	2 (9)	**<0.001**
· Erosions	18 (36)	2 (9)	**0.020**
3rd MCP joint			
· Grayscale	30 (61)	10 (47)	0.291
· Power Doppler	21 (42)	4 (19)	0.056
· Erosions	4 (8)	0	0.138
Wrist			
· Grayscale	36 (73)	14 (66)	0.563
· Power Doppler	29 (59)	9 (42)	0.208
· Erosions	10 (20)	1 (4)	0.099
Elbow			
· Grayscale	25 (51)	10 (47)	0.794
· Power Doppler	5 (10)	1 (4)	0.456
· Erosions	5 (10)	0	0.128
Knee			
· Grayscale	28 (57)	16 (76)	0.130
· Power Doppler	9 (18)	8 (38)	0.077
· Erosions	1 (2)	0	0.509
Ankle			
· Grayscale	23 (46)	10 (47)	0.958
· Power Doppler	10 (20)	2 (9)	0.268
· Erosions	3 (6)	0	0.246

MCP, metacarpophalangeal joint. Significant p-values are in bold.

(2.5–3.75 IQR) mg per day, compared to the seropositive group with 31 patients (36%) taking prednisone with mean doses of 7.5 (5–10 IQR) mg per day ($p = 0.007$). SNRA has been considered to represent a less severe disease subset than SPRA, with less radiographic damage (23). It has been suggested that seronegative patients should be treated less aggressively than seropositive patients, which is also reflected in the 2016 EULAR treatment recommendations (24). Nordberg et al. found that in RA patients classified according to the new criteria, SNRA is not a mild form of the disease and requires intensive treat-to-target therapy similar to treatment of SPRA. In their study, there was a trend toward more radiographic damage in seronegative compared with seropositive patients, both at baseline and after 24 months. The treatment response at 3 months was better in seropositive than seronegative patients, whereas the number of patients in remission at the end of the study was similar across groups. This observation may indicate that seronegative patients might respond well to treat-to-target strategies, even

TABLE 4 Ultrasonographic findings, according to the severity of the lesions, in hand joints.

	Seropositive patients ($n = 49$)	Seronegative patients ($n = 21$)	p
2nd MCP joints			
· Grayscale	0 (0–2)	0 (0–0)	**<0.001**
· Power Doppler	0 (0–0.25)	0 (0–0)	**<0.001**
3rd MCP joints			
· Grayscale	0 (0–1)	0 (0–0.25)	0.058
· Power Doppler	0 (0–0)	0 (0–0)	**0.011**
Wrists			
· Grayscale	1 (0–2)	1 (0–1)	0.116
· Power Doppler	0 (0–1)	0 (0–1)	0.142

Data are presented as median (interquartile range). Significant p-values are in bold.

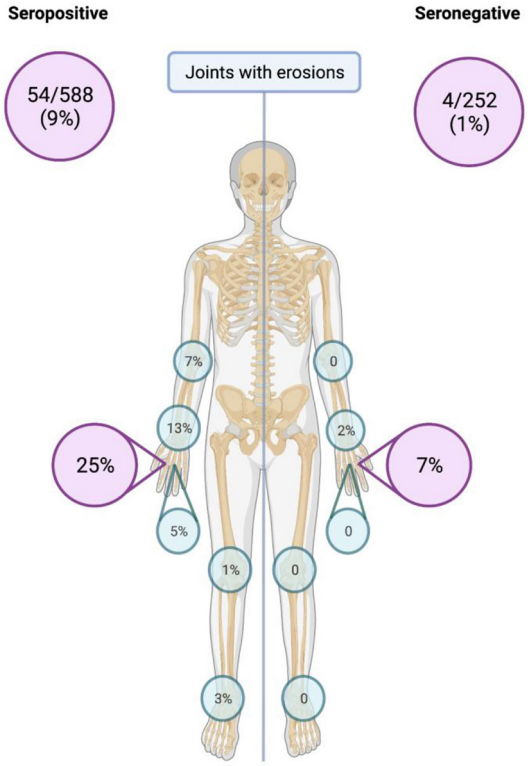

FIGURE 1
Total number and percentage of joints with structural joint damage (erosions) detected by ultrasound.

TABLE 5 Results of linear regression analyses of seropositivity status in relation to the joint damage (bone erosions).

Independent variable	Beta (95% CI)	p-value
Univariable analysis		
Constant	0.2 (−0.35 to 0.75)	0.4
Status of seropositivity	0.29 (0.16 to 1.47)	0.015
Multivariable analysis		
Constant	−0.10 (−0.7 to 0.5)	0.7
Status of seropositivity	0.28 (0.14 to 1.42)	0.016
Disease duration	0.24 (0.003–0.082)	0.03

CI, Confidence Interval.

if the initial treatment response is delayed compared with seropositive patients (25).

Our results differ from results presented by Choi et al. and Nordberg et al. (4, 6); however, both studies included DMARD-naive patients, and in the study by Choi et al. when following the patients they observed that those with SNRA had a better response to treatment. With these results, we could conclude that patients with SNRA during their follow-up had a lower frequency and degree of synovitis involvement.

We evaluated cardiovascular risk using scoring systems to analyze the risk of coronary heart disease or stroke at 10 years. ACPAs have been associated with coronary artery disease in a previous report (26). Some other studies have also shown that seropositive patients have more severe inflammatory activity than patients with SNRA (27). CVD mortality has been associated with sustained inflammation, the level of inflammation (9), and with the presence of characteristic RA antibodies (12). Moreover, increased risk of coronary heart disease in RA is associated with elevated CRP and erythrocyte sedimentation rate, the presence of RF and/or ACPA, as well as with highly active or severe RA (28). Rheumatoid factor and antinuclear antibodies have been associated with heart disease and overall mortality, even in patients without rheumatic diseases (29). Considering all these findings, we were expecting to find some differences between SNRA and SPRA, however, we did not find statistically significant differences in 10-year cardiovascular risk scores.

In general, MSUS results showed a higher percentage of damage and a greater degree of involvement in the right 2nd MCP joint in both GS and PD in SPRA patients. Of the rest of the joints, we found some other differences in both scales, with a greater degree of involvement in the left ankle and left 2nd MCP joint in GS and with greater frequency of PD presence in the left 2nd MCP joint and right 3rd MCP joint in the group of patients with SPRA. Only at the level of the knees did patients with SNRA have a greater degree of involvement in GS and a higher frequency of PD. With these findings, we can conclude that patients with SPRA show a tendency to have more synovitis in both GS and DP. These findings are consistent with the recently published article by Ramirez et al. in which patients with ACPA had a greater presence of proliferative synovitis (30).

Regarding erosions, recently, in the study by Grose et al. in which patients were compared according to ACPA status, they found that patients with positive ACPA had a higher proportion of erosions by US (31). Our results agree with those described in this study, in which we found a higher frequency of erosions in the SPRA group, mainly due to the higher proportion of erosions in the 2nd MCP joint, without differences in the rest of the joints; however, we believe that this is because we used a simplified score, which has the disadvantage that it does not include the joints with the highest frequency of erosions (5th MCP joint and 2nd, 3rd, and 5th metatarsophalangeal joints).

The main strength of our study is that it's one of the few studies that compare clinical, ultrasonographic, laboratory variables and cardiovascular risk between both study subgroups (SPRA vs SNRA), which allows for a better definition of the phenotype presented by patients with SNRA.

Finally, our study has several limitations. One of the main limitations is the sample size and that not all patients included in the study could undergo MSUS mainly due to complications associated with the pandemic. Another important limitation of our study is that we used a simplified score to evaluate the joints, which, although it has a very good sensitivity to evaluate synovitis in GS and PD, does not evaluate all the joints in which erosions occur more frequently. A third limitation is that we did not include the evaluation of erosions by radiographs. A final limitation is that we didn't evaluate the presence of anti-carbamylated proteins antibody.

Conclusions

RA patients show a differentiated phenotype according to their ACPA and RF status. In seronegative patients, RA begins later in life and has a lower requirement for antirheumatic therapies. On US evaluation, seropositive patients show more joint damage, especially in MCP joints. Despite this, long-term cardiovascular risk is similar among RA patients, regardless of their RF and ACPA status.

Data availability statement

The datasets obtained and/or analyzed during the current study will be available from the corresponding author on reasonable request.

Ethics statement

The studies involving human participants were reviewed and approved by Ethical and Research Committee Instituto Nacional de Rehabilitation. The patients/participants provided their written informed consent to participate in this study.

Author contributions

NC-B, CS-F, and LA-G: acquisition of data, analysis and interpretation of data, drafting of the article, critical revision of the intellectual content, and final approval of the version to be published. AB-M, TV, AH-D, VJ-R, and AM-G: acquisition of data. CP: substantial contributions to the design, acquisition of data, critical revision of the intellectual content, and final approval of the version to be published. LS: ideation of the study, substantial contributions to the design, critical revision of the intellectual content, and final approval of the version to be published. All authors contributed to the article and approved the submitted version.

Conflict of interest

The authors declare that the research was conducted in the absence of any commercial or financial relationships that could be construed as a potential conflict of interest.

Publisher's note

All claims expressed in this article are solely those of the authors and do not necessarily represent those of their affiliated organizations, or those of the publisher, the editors and the reviewers. Any product that may be evaluated in this article, or claim that may be made by its manufacturer, is not guaranteed or endorsed by the publisher.

Supplementary material

The Supplementary Material for this article can be found online at: https://www.frontiersin.org/articles/10.3389/fmed.2022.978351/full#supplementary-material

References

1. Peláez-Ballestas I, Sanin L, Moreno-Montoya J, Alvarez-Nemegyei J, Burgos-Vargas R, Garza-Elizondo M, et al. Epidemiology of the rheumatic diseases in Mexico. A study of 5 regions based on the COPCORD methodology. *J Rheumatol Suppl.* (2011) 86(Suppl 86):3–8. doi: 10.3899/jrheum.100951

2. Avouac J, Gossec L, Dougados M. Diagnostic and predictive value of anti-cyclic citrullinated protein antibodies in rheumatoid arthritis: a systematic literature review. *Ann Rheum Dis.* (2005) 65:845–51. doi: 10.1136/ard.2006.051391

3. Farragher TM, Lunt M, Plant D, Bunn DK, Barton A, Symmons DPM. Benefit of early treatment in inflammatory polyarthritis patients with anti-cyclic citrullinated peptide antibodies versus those without antibodies. *Arthritis Care Res.* (2010) 62:664–75. doi: 10.1002/acr.20207

4. Nordberg LB, Lillegraven S, Lie E, Aga A-B, Olsen IC, Hammer HB, et al. Patients with seronegative RA have more inflammatory activity compared with patients with seropositive RA in an inception cohort of DMARD-naïve patients classified according to the 2010 ACR/EULAR criteria. *Ann Rheum Dis.* (2017) 76:341–5. doi: 10.1136/annrheumdis-2015-208873

5. Geng Y, Zhou W, Zhang Z-L, A comparative study on the diversity of clinical features between the sero-negative and sero-positive rheumatoid arthritis patients. *Rheumatol Int.* (2012) 32:3897–901. doi: 10.1007/s00296-011-2329-5

6. Choi S-T, Lee K-H. Clinical management of seronegative and seropositive rheumatoid arthritis: a comparative study. *PLoS ONE.* (2018) 13:1–10. doi: 10.1371/journal.pone.0199468

7. Radner H, Lesperance T, Accortt NA, Solomon DH. Incidence and prevalence of cardiovascular risk factors among patients with rheumatoid arthritis, psoriasis, or psoriatic arthritis. *Arthritis Care Res.* (2017) 69:1510–8. doi: 10.1002/acr.23171

8. Gonzalez A, Kremers HM, Crowson CS, Ballman K V, Roger VL, Jacobsen SJ, et al. Do cardiovascular risk factors confer the same risk for cardiovascular outcomes in rheumatoid arthritis patients as in non-rheumatoid arthritis patients? *Ann Rheum Dis.* (2008) 67:64–9. doi: 10.1136/ard.2006.059980

9. Zhang J, Chen L, Delzell E, Muntner P, Hillegass WB, Safford MM, et al. The association between inflammatory markers, serum lipids and the risk of cardiovascular events in patients with rheumatoid arthritis. *Ann Rheum Dis.* (2014) 73:1301–8. doi: 10.1136/annrheumdis-2013-204715

10. Gonzalez-Gay MA, Gonzalez-Juanatey C, Lopez-Diaz MJ, Piñeiro A, Garcia-Porrua C, Miranda-Filloy JA, et al. HLA–DRB1 and persistent chronic inflammation contribute to cardiovascular events and cardiovascular mortality in patients with rheumatoid arthritis. *Arthritis Rheum.* (2007) 57:125–32. doi: 10.1002/art.22482

11. Battafarano DF, Restrepo JF. Erikson JM, Escalante A. Glucocorticoid dose thresholds associated with all-cause and cardiovascular mortality in rheumatoid arthritis. *Arthritis Rheum.* (2014) 66:264–72. doi: 10.1002/art.38210

12. Humphreys JH, Warner A, Chipping J, Marshall T, Lunt M, Symmons DPM, et al. Mortality trends in patients with early rheumatoid arthritis over 20 years: results from the norfolk arthritis register. *Arthritis Care Res.* (2014) 66:1296–301. doi: 10.1002/acr.22296

13. Toms TE, Panoulas VF, Douglas KMJ, Nightingale P, Smith JP, Griffiths H, et al. Are lipid ratios less susceptible to change with systemic inflammation than individual lipid components in patients with rheumatoid arthritis? *Angiology.* (2011) 62:167–75. doi: 10.1177/0003319710373749

14. Goff DC, Lloyd-Jones DM, Bennett G, Coady S, D'Agostino RB, Gibbons R, et al. 2013 ACC/AHA guideline on the assessment of cardiovascular risk. *J Am Coll Cardiol.* (2014) 63:2935–59. doi: 10.1016/j.jacc.2013.11.005

15. Aletaha D, Neogi T, Silman AJ, Funovits J, Felson DT, Bingham CO, et al. 2010 Rheumatoid arthritis classification criteria: an American College of Rheumatology/European League against rheumatism collaborative initiative. *Arthritis Rheum.* (2010) 62:2569–81. doi: 10.1002/art.27584

16. World Medical Association. World medical association declaration of Helsinki. *JAMA.* (2013) 310:2191. doi: 10.1001/jama.2013.281053

17. Naredo E, Rodríguez M, Campos C. Rodríguez-heredia JM, Medina JA, Giner E, et al. Validity, reproducibility, and responsiveness of a twelve-joint simplified power doppler ultrasonographic assessment of joint inflammation in rheumatoid arthritis. *Arthritis Rheum.* (2008) 59:515–22. doi: 10.1002/art.23529

18. Möller I, Janta I, Backhaus M, Ohrndorf S, Bong DA, Martinoli C, et al. The 2017 EULAR standardised procedures for ultrasound imaging in rheumatology. *Ann Rheum Dis.* (2017) 76:1974–9. doi: 10.1136/annrheumdis-2017-211585

19. Bruyn GA, Iagnocco A, Naredo E, Balint P V, Gutierrez M, Hammer HB, et al. OMERACT definitions for ultrasonographic pathologies and elementary lesions of rheumatic disorders 15 years on. *J Rheumatol.* (2019) 46:1388–93. doi: 10.3899/jrheum.181095

20. D'Agostino M-A, Terslev L, Aegerter P, Backhaus M, Balint P, Bruyn GA, et al. Scoring ultrasound synovitis in rheumatoid arthritis: a EULAR-OMERACT ultrasound taskforce — Part 1: definition and development of a standardised, consensus-based scoring system. *RMD Open.* (2017) 3:e000428. doi: 10.1136/rmdopen-2016-000428

21. Mouterde G, Rincheval N, Lukas C, Daien C, Saraux A, Dieudé P, et al. Outcome of patients with early arthritis without rheumatoid factor and ACPA and predictors of rheumatoid arthritis in the ESPOIR cohort. *Arthritis Res Ther.* (2019) 21:140. doi: 10.1186/s13075-019-1909-8

22. Barra L, Pope JE, Orav JE, Boire G, Haraoui B, Hitchon C, et al. Prognosis of seronegative patients in a large prospective cohort of patients with early inflammatory arthritis. *J Rheumatol.* (2014) 41:2361–9. doi: 10.3899/jrheum.140082

23. Syversen SW, Goll GL, Van Der Heijde D, Landewé R, Lie BA, Ødegård S, et al. Prediction of radiographic progression in rheumatoid arthritis and the role of antibodies against mutated citrullinated vimentin: results from a 10-year prospective study. *Ann Rheum Dis.* (2010) 69:345–51. doi: 10.1136/ard.2009.113092

24. De Punder YMR, Hendrikx J, Den Broeder AA, Pascual EV, Van Riel PL, Fransen J. Should we redefine treatment targets in rheumatoid arthritis? Low disease activity is sufficiently strict for patients who are anticitrullinated protein antibody-negative. *J Rheumatol.* (2013) 40:1268–74. doi: 10.3899/jrheum.121438

25. Nordberg LB, Lillegraven S, Aga AB, Sexton J, Olsen IC, Lie E, et al. Comparing the disease course of patients with seronegative and seropositive rheumatoid arthritis fulfilling the 2010 ACR/EULAR classification criteria in a treat-to-target setting: 2-year data from the ARCTIC trial. *RMD Open.* (2018) 4:11–7. doi: 10.1136/rmdopen-2018-000752

26. Cambridge G, Acharya J, Cooper JA, Edwards JC, Humphries SE. Antibodies to citrullinated peptides and risk of coronary heart disease. *Atherosclerosis.* (2013) 228:243–6. doi: 10.1016/j.atherosclerosis.2013.02.009

27. Arnab B, Biswadip G, Arindam P, Shyamash M, Anirban G, Rajan P. Anti-CCP antibody in patients with established rheumatoid arthritis: does it predict adverse cardiovascular profile? *J Cardiovasc Dis Res.* (2013) 4:102–6. doi: 10.1016/j.jcdr.2012.09.003

28. Maradit-Kremers H, Nicola PJ, Crowson CS, Ballman K V, Gabriel SE. Cardiovascular death in rheumatoid arthritis: a population-based study. *Arthritis Rheum.* (2005) 52:722–32. doi: 10.1002/art.20878

29. Liang KP, Maradit-Kremers H, Crowson CS, Snyder MR, Therneau TM, Roger VL, et al. Autoantibodies and the risk of cardiovascular events. *J Rheumatol.* (2009) 36:2462–9. doi: 10.3899/jrheum.090188

30. Ramírez J, Azuaga-Piñango AB, Frade-Sosa B, Gumucio-Sanguino R, Cajiao-Sánchez K, Cuervo AM, et al. Proliferative synovitis, an ultrasound pattern associated with ACPA-positive patients and erosive disease in rheumatoid arthritis. *Clin Exp Rheumatol.* (2022) 40:960–66. doi: 10.55563/clinexprheumatol/so5skx

31. Grosse J, Allado E, Roux C, Pierreisnard A, Couderc M, Clerc-Urmes I, et al. ACPA-positive versus ACPA-negative rheumatoid arthritis: two distinct erosive disease entities on radiography and ultrasonography. *Rheumatol Int.* (2020) 40:615–24. doi: 10.1007/s00296-019-04492-5

frontiers | Frontiers in Medicine

TYPE Original Research
PUBLISHED 26 August 2022
DOI 10.3389/fmed.2022.981804

OPEN ACCESS

EDITED BY
Andrea Di Matteo,
Marche Polytechnic University, Italy

REVIEWED BY
Diogo Jesus,
Universidade da Beira Interior, Portugal
Zunaid Karim,
Mid Yorkshire Hospitals NHS Trust, United Kingdom
Kate Smith,
Leeds Biomedical Research Centre (NIHR), United Kingdom

*CORRESPONDENCE
Juan Molina-Collada
molinacolladajuan@gmail.com

SPECIALTY SECTION
This article was submitted to Rheumatology, a section of the journal Frontiers in Medicine

RECEIVED 29 June 2022
ACCEPTED 11 August 2022
PUBLISHED 26 August 2022

Ultrasound intima media thickness cut-off values for cranial and extracranial arteries in patients with suspected giant cell arteritis

Katerine López-Gloria [1,2], Isabel Castrejón [1,2], Juan Carlos Nieto-González [1,2], Pablo Rodríguez-Merlos [1,2], Belén Serrano-Benavente [1,2], Carlos Manuel González [1,2], Indalecio Monteagudo Sáez[1,2], Teresa González [1,2], José María Álvaro-Gracia [1,2] and Juan Molina-Collada [1,2*]

[1]Department of Rheumatology, Hospital General Universitario Gregorio Marañón, Madrid, Spain, [2]Instituto de Investigación Sanitaria Gregorio Marañón (IiSGM), Madrid, Spain

Objective: To determine the optimal ultrasound (US) cut-off values for cranial and extracranial arteries intima media thickness (IMT) to discriminate between patients with and without giant cell arteritis (GCA).

Methods: Retrospective observational study including patients referred to an US fast-track clinic. All patients underwent bilateral US examination of the cranial and extracranial arteries including the IMT measurement. Clinical confirmation of GCA after 6 months was considered the gold standard for diagnosis. A receiver operating characteristic (ROC) analysis was performed to select the cut-off values on the basis of the best tradeoff values between sensitivity and specificity.

Results: A total of 157 patients were included, 47 (29.9%) with clinical confirmation of GCA after 6 months. 41 (87.2%) of patients with GCA had positive US findings (61.7% had cranial and 44.7% extracranial involvement). The best threshold IMT values were 0.44 mm for the common temporal artery; 0.34 mm for the frontal branch; 0.36 mm for the parietal branch; 1.1 mm for the carotid artery and 1 mm for the subclavian and axillary arteries. The areas under the ROC curves were greater for axillary arteries 0.996 (95% CI 0.991–1), for parietal branch 0.991 (95% CI 0.980–1), for subclavian 0.990 (95% CI 0.979–1), for frontal branch 0.989 (95% CI 0.976–1), for common temporal artery 0.984 (95% CI 0.959–1) and for common carotid arteries 0.977 (95% CI 0.961–0.993).

Conclusion: IMT cut-off values have been identified for each artery. These proposed IMT cut-off values may help to improve the diagnostic accuracy of US in clinical practice.

KEYWORDS

ultrasound, giant cell (temporal) arteritis, vasculitis, imaging, arteries

Introduction

Giant cell arteritis (GCA) is the most frequent systemic vasculitis in elderly patients. An early diagnosis and prompt treatment is crucial to prevent serious complications (1–3). Ultrasound (US) is a valid and reliable tool to detect inflammation in patients with GCA, the non-compressible halo sign being the most relevant US finding. It has been defined by the US Outcome Measures in Rheumatology (OMERACT) large vessel vasculitis working group as a "homogenous, hypoechoic wall thickening that is well delineated toward the luminal side that is visible both in longitudinal and transverse planes, most commonly concentric in transverse scans" (4). According to recent EULAR recommendations, patients with high clinical suspicion of GCA and a positive imaging test do not need additional tests, such as biopsy or other imaging methods, for GCA diagnosis (5). However, false-positive halos may be present in other forms of vasculitis (e.g., in ANCA-associated vasculitis), amyloidosis (6), infectious diseases or even in patients with atherosclerosis (7, 8). Thus, a positive halo needs to be interpreted in the clinical context with an evaluation of the pretest probability (9).

Although the halo sign has been considered the most useful sign to support GCA diagnosis, it can be highly influenced by the sonographer skills and the quality of the US equipment for Doppler settings and artifacts. Sensitivity is highly variable between studies, showing a pooled sensitivity of 77% and a pooled specificity of 96% compared to the clinical diagnosis of GCA (10). Nowadays, thanks to the availability of high resolution transducers, intima media thickness (IMT) of cranial and extracranial arteries can be accurately measured as homogeneous, hypoechoic or anechoic structure delineated by two parallel hyperechoic margins (11). An increased IMT suggestive of GCA may be easily assessed by US, giving the classical appearance of a halo sign using color Doppler mode. However, few data are published regarding the optimal cut-off values for IMT to differentiate patients and controls in clinical practice (12, 13), and only one group studied the subclavian and common carotid arteries, which should require replication.

Our primary objective is to define cut-off values for cranial and extracranial arteries to discriminate patients with and without GCA.

Materials and methods

Patients

This is a retrospective observational study including patients referred to a US fast-track pathway (14) for screening of possible GCA from 2019 to 2021. In our academic center, patients with suspected GCA are referred for US examination within 24 h per protocol. A bilateral US exam of the cranial (superficial temporal arteries and its frontal and parietal branches) and extracranial (carotid, subclavian, and axillary arteries) arteries is performed as part of the diagnostic work-up. The following inclusion criteria were applied: patients age > 18 years with GCA suspicion according to clinician criteria (history of ESR > 20 mm/h or CRP > 5 mg/l, or cranial/extracranial symptoms of GCA or PMR symptoms). Patients with a previous diagnosis or clinical history of GCA were excluded. All exams were performed in routine daily practice conditions including consecutive patients.

Data collection

The following variables were collected: demographics, presenting symptoms, previous use of glucocorticoids or polymyalgia diagnosis, and laboratory variables as C-reactive protein (CRP), erythrocyte sedimentation rate (ESR), hemoglobin and platelets. GCA clinical diagnosis after 6 months follow-up by the referring rheumatologist was the gold standard for diagnosis.

Ultrasound assessment

All patients underwent bilateral US examination of the three temporal artery (TA) segments (common superficial TA, it parietal and frontal branches) and extracranial (common carotid, subclavian and axillary) arteries within 24 h per protocol (excluding weekends with delays up to 48 h). The exam was performed in a supine position, by the same evaluator (JMC) using an EsaoteMyLab8 (Esaote, Genoa). For superficial TA at it parietal and frontal branches we used a 12–18 MHz

frequency transducer [B-mode frequency, 18 MHz; depth, 15 mm; focus point at approximately 3–5 mm below the skin surface, depending on the depth of the segment; color Doppler frequency, 11 MHz, pulse repetition frequency (PRF), 2.0 KHz]. An 8–14 frequency transducer was used for extracranial arteries (B-mode frequency, 14 MHz; depth, 3 cm; focus at 2 cm below the skin surface depending on the depth of the segment; color Doppler frequency, 9 MHz; PRF, 3.0 kHz). The subclavian arteries were scanned at the infraclavicular fossa and axillary arteries at the axillary fossa. The IMT was measured in gray scale mode and the presence of a non-compressible halo sign was checked in all arteries. We checked the presence of a halo defined according to the recent OMERACT Large Vessel Vasculitis Ultrasound Working Group definition (4). The measurement of the IMT of each artery was made from the luminal–intimal interface to the medial–adventitial interfaces on the arterial wall distal to the probe on longitudinal planes. The measurement of the IMT was obtained on B mode in all arteries (not only those showing a halo). For the frontal and parietal branches, the IMT was measured approximately 1 cm distal to the bifurcation of the superficial TA, and for axillary arteries at the level of the humeral head. Color Doppler signal was used to confirm the correct measurement of the IMT in doubtful cases. The presence of a halo and/or compression sign in temporal arteries and the presence of a halo in extracranial arteries was considered a positive US finding for GCA.

Statistical analysis

Quantitative data were described as mean (S.D.) and qualitative variables as absolute frequency and/or corresponding percentages. Mean IMT values of each artery were compared between patients according to GCA clinical diagnosis by independent samples *T*-test. Receiver operating characteristics (ROC) analysis was performed and the Youden index was used to determine the optimal cut-off value for IMT of each artery. SPSS software (version 23.0; IBM, Armonk, NY, United States) was used for statistical analysis.

Ethical approval

This study was performed in accordance with the ethical standards of the responsible committee on human experimentation and the Helsinki Declaration of 1975, as revised in 1983. Research ethics committee approval for the protocol was obtained prior to commencing the study (RHEUM0322) and written informed consent was determined to be not mandatory.

Results

Patients' characteristics

A total of 157 patients evaluated in the US fast-track pathway were included for analysis, of whom 67.5% were female and mean (*SD*) age was 73.7 (10.8) years, median (interquartile range 25th–75th) 74 (66–82). Polymyalgia rheumatica diagnosis before US examination was present in 43 (27.4%) patients and 78 (50%) patients were on steroids before US examination, mean (*SD*) corticosteroid dose was 48.4 (146.5) mg/day (min 2.5, max 1,000). After 6-months of follow-up, 47 (29.9%) patients had GCA clinical confirmation according to clinician diagnosis. TA biopsy was performed per clinician criteria in 31 patients, 10 (43.5%) with positive results. Clinical, laboratory and main US findings of patients with and without GCA are shown in **Table 1**. GCA patients had higher acute phase reactants: CRP [mg/dL) 10.7 (18.2) vs. 3.8 (5), $p = 0.001$ and ESR (mm/h) (68.2 (34) vs. 45 (31.8), $p = 0.001$].

Ultrasound findings

US findings are presented in detail in **Tables 1**, **2**. In total, 41 (87.2%) patients with GCA and only 5 (4.5%) patients without GCA had positive US findings (overall sensitivity 87.2%, specificity 95.5%, positive predictive value 89.1%, negative predictive value 94.6%). Among patients with GCA, the most frequent finding was temporal artery involvement in 29 (61.7%) patients, followed by extracranial involvement in 21 (44.7%) patients and 9 (19.1%) patients with a mixed pattern of cranial and extracranial arteries involvement (**Figure 1**).

Intima media thickness cut-off values

Values of IMT of cranial and extracranial arteries in patients with and without GCA are shown in **Table 2**. The IMT cut-off values showing the highest diagnostic accuracy to discriminate between patients with and without GCA were for the cranial arteries (0.44 mm for the common superficial temporal artery; 0.34 mm for the frontal branch and 0.36 mm for the parietal branch) and for the extracranial arteries (1.1 mm for the carotid artery and 1 mm for the subclavian and axillary arteries) (**Table 2**). The area under the ROC curve of the IMT for a clinical diagnosis of GCA was 0.984 (95% CI 0.959–1) for common superficial temporal artery, 0.989 (95% CI 0.976–1) for frontal branch, 0.991 (95% CI 0.980–1) for parietal branch, 0.977 (95% CI 0.961–0.993) for carotid, 0.99 (95% CI 0.979–1) for subclavian and 0.996 (95% CI 0.991–1) for axillary arteries. Sensitivities and specificities of each IMT cut-off value are shown in **Table 2**.

TABLE 1 Clinical, laboratory and US findings of patients with and without GCA.

	Total $n = 157$	Patients with GCA $n = 47$ (29.9)	Patients without GCA $n = 110$ (70.1)	*P*
Demographics				
Age, mean (*SD*)	73.7 (10.8)	75.3 (11.3)	73 (10.6)	0.245
Female, *n* (%)	106 (67.5)	31 (66)	75 (68.2)	0.785
Arterial hypertension, *n* (%)	96 (61.5)	30 (65.2)	66 (60)	0.541
Mellitus diabetes, *n* (%)	37 (23.7)	13 (28.3)	24 (21.8)	0.388
Smoker, *n* (%)	16 (10.3)	6 (13)	10 (9.1)	0.458
Former smoker, *n* (%)	26 (16.7)	10 (21.7)	16 (14.5)	0.272
Clinical variables				
Baseline use of steroids, *n* (%)	78 (50)	21 (45.7)	57 (51.8)	0.482
PMR diagnosis before US examination, *n* (%)	43 (27.4)	8 (17)	35 (31,8)	0.121
Laboratory findings				
CRP (mg/dL), mean (*SD*)	5.9 (11.3)	10.7 (18.2)	3.8 (5)	0.001
ESR (mm/h), mean (*SD*)	52.8 (34.2)	68.2 (34)	45 (31.8)	0.001
Hemoglobin (g/dL), mean (*SD*)	13.7 (17.6)	11.7 (1.6)	14.5 (21)	0.185
Platelets 10^9/L, mean (*SD*)	293 (124.7)	335.4 (143.3)	274.7 (111.6)	0.014
US variables				
Positive US findings*, *n* (%)	46 (29.3)	41 (87.2)	5 (4.5)	<0.001
Temporal artery positive US findings, *n* (%)	32 (20.4)	29 (61.7)	3 (2.7)	<0.001
Extracranial arteries positive US findings, *n* (%)	23 (14.6)	21 (44.7)	2 (1.8)	<0.001
Temporal + extracranial arteries positive US findings, *n* (%)	9 (5.7)	9 (19.1)	0 (0)	<0.001

PMR, polymyalgia rheumatica; CRP, C-reactive protein; ESR, erythrocyte sedimentation rate; US, ultrasound; SD, standard deviation; *Presence of a halo and/or compression sign in temporal arteries and/or presence of a halo in extracranial arteries.

Discussion

Few studies have defined IMT cut-off values for GCA diagnosis after adequate evaluation. In this observational cross-sectional study, we provide the optimal cut-off values for IMT of cranial and extracranial arteries.

Several studies have shown the usefulness and good performance of US for the diagnosis of GCA (15–19) and this has led to the recent EULAR recommendations (5) identifying US as the test of initial imaging in patients with suspected GCA presenting with predominantly cranial symptoms. Although the halo sign is considered the most characteristic US finding of GCA, the measurement of IMT provides a more accurate diagnosis, probably because it is not influenced by potential Doppler artifacts. However, when analyzing a quantitative measure as a diagnostic test it is important to provide the optimal cut-off values to differentiate between patients and controls.

In our sample, 87.2% of patients with GCA had positive US results with a positive predictive value of 89.1%. The most frequent finding was the involvement of the temporal arteries (61.7% of patients), followed by extracranial involvement (44.7%). The area under the ROC curve of each explored artery were high with excellent sensitivities and specificities and proposed IMT cut-off values showed the highest diagnostic accuracy to discriminate between patients and controls. These values are high enough to justify the use of these cut-off values with high diagnostic precision. Previous studies have suggested variables cut-off values for temporal arteries: 0.3 mm (20), 0.4 mm (21), 0.5 mm (22), 0.7 mm (23), and 1 mm (24). Moreover, cut-off values for extracranial arteries of 1.3 mm (25) and 2 mm (26), and 1.5 mm (27) for the axillary artery exclusively, have been suggested. All of them based on the criteria and clinical experience of each author, respectively. Our results are in line with a recent study by Ješe et al. (12), in which they determined potential cut-off values for IMT in seven preselected arteries (temporal, facial, occipital, carotid, vertebral, subclavian, and axillary) comparing them between patients with and without GCA. They found positive US findings in 98.4% of patients with GCA with involvement of the temporal artery in 77.4%, and involvement of extracranial arteries in 35.1%. In relation to the cut-off values, they reached high levels of diagnostic precision with an IMT of 0.4 mm for the temporal arteries and an IMT of 1 mm for the carotid, subclavian and axillary arteries. Our findings were also compared with a recent study investigating IMT cut-off values by Schäfer et al. (13) who compared the IMT of 40 newly diagnosed GCA patients and 40 healthy controls. In this study the control group consisted in patients with other rheumatic and non-rheumatic diseases, but not suspected GCA. They established cut-off values of 0.42 mm for the common superficial temporal artery, 0.34 mm for the frontal branch, 0.29 mm for the parietal branch, and 1 mm for the axillary artery. Our cut-off values for IMT of 0.44 mm for the common superficial temporal artery and 0.36 mm for the parietal branch differ from those proposed by Schäfer et al. (0.42 for the common superficial temporal artery and 0.29 for the parietal branch). Although we used a 18 MHz probe, these

10.3389/fmed.2022.981804

TABLE 2 Optimal IMT cut-off values for cranial and extracranial arteries.

Artery	Side	Patients without GCA	Patients with GCA	Cut-off (mm)	AUC (CI 95%)	Sensitivity (%)	Specificity (%)	Geometric mean
Common superficial temporal artery mm, mean (*SD*)	Right	0.33 (0.06)	0.68 (0.28)	0.43	0.997 (0.988–1)	100	97.1	0.985
	Left	0.35 (0.11)	0.57 (0.21)	0.45	0.966 (0.905–1)	100	92.3	0.961
	Both	0.34 (0.08)	0.63 (0.25)	0.44	0.984 (0.959–1)	94.7	95.1	0.949
Frontal branch mm, mean (*SD*)	Right	0.26 (0.05)	0.4 (0.18)	0.34	0.994 (0.983–1)	100	97.1	0.985
	Left	0.27 (0.05)	0.4 (0.18)	0.34	0.985 (0.962–1)	100	96.1	0.980
	Both	0.26 (0.05)	0.4 (0.18)	0.34	0.989 (0.976–1)	100	96.6	0.983
Parietal branch mm, mean (*SD*)	Right	0.27 (0.05)	0.43 (0.18)	0.36	0.994 (0.981–1)	100	98.9	0.994
	Left	0.27 (0.05)	0.41 (0.16)	0.36	0.987 (0.967–1)	100	97.6	0.988
	Both	0.27 (0.05)	0.42 (0.17)	0.36	0.991 (0.980–1)	100	98.3	0.991
Carotid mm, mean (*SD*)	Right	0.8 (0.17)	0.88 (0.29)	1	0.974 (0.949–0.999)	100	92.6	0.962
	Left	0.82 (0.15)	1 (0.42)	1.2	0.982 (0.961–1)	90.9	96.2	0.935
	Both	0.81 (0.16)	0.96 (0.36)	1.1	0.977 (0.961–0.993)	90	94	0.920
Subclavian mm, mean (*SD*)	Right	0.74 (0.18)	0.99 (0.44)	1	0.987 (0.97–1)	100	93.4	0.966
	Left	0.67 (0.17)	0.9 (0.35)	1.1	0.991 (0.975–1)	100	98.3	0.991
	Both	0.7 (0.18)	0.94 (0.4)	1	0.99 (0.979–1)	100	96	0.980
Axillary mm, mean (*SD*)	Right	0.69 (0.16)	0.99 (0.5)	1	0.992 (0.982–1)	100	96	0.980
	Left	0.67 (0.17)	0.99 (0.49)	1	0.998 (0.995–1)	100	98.3	0.991
	Both	0.68 (0.17)	0.99 (0.49)	1	0.996 (0.991–1)	100	97.1	0.985

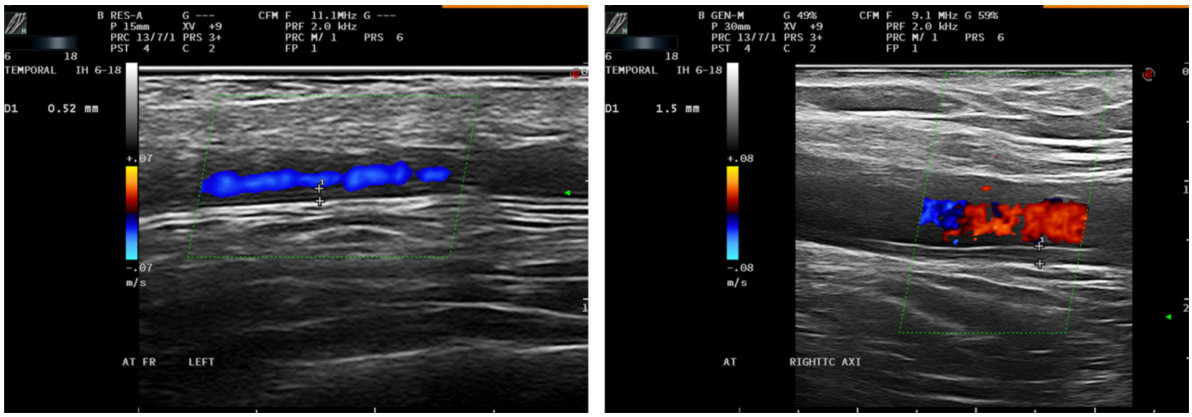

FIGURE 1
Longitudinal US scan (left) of the frontal branch of the left temporal artery in a patient with newly GCA diagnosis. Longitudinal US scan (right) of the right axillary artery in patient with large vessel GCA. Both arteries show increase IMT above the proposed cut-off values.

slight differences should be addressed in further studies. The proposed IMT cut-off of 1 mm for the axillary artery coincides with previous studies (13, 28). Our group previously presented preliminary data on the diagnostic value of IMT cut-off values studying the same population included in this work, with similar results (29).

Examination of the axillary arteries in patients with suspected GCA is most useful when US of the temporal arteries is negative or inconclusive and there is a high clinical suspicion of large vessel GCA (5). Although in this scenario it is not clear which extracranial arteries should be examined (30). Skoog et al. (31) recently evaluated the diagnostic performance of an extended US protocol (which in addition to temporal and axillary arteries, also includes subclavian, brachiocephalic, and carotid arteries) in patients with suspected GCA. According to their results, they found that 86% had involvement of the temporal arteries and 28% of patients showed inflammatory changes in both the temporal and extracranial arteries with a sensitivity of 95% and specificity of 98%. In our population, the sensitivity and specificity were slightly lower with values of 87.2 and 95.5%, respectively.

In 2018, De Miguel et al. (8) evaluated 40 patients with high cardiovascular risk and found an association between atherosclerotic disease and an increase of IMT values of the temporal arteries. Taking into account that atherosclerosis is prevalent in this group of patients presenting with clinical symptoms of GCA, they proposed a cut-off value for IMT of 0.34 mm in at least two temporal artery branches. In our study, the cut-off value for IMT of the temporal artery and its branches are in accordance with that proposed by De Miguel although the cardiovascular risk in our population was not specifically investigated. Despite the availability of excellent IMT cut-off values for the cranial and extracranial arteries, it is always important to take into account the clinical context of the patient, since findings above the proposed IMT cut-off values may be present in patients with atherosclerosis.

The main strength of our study is the systematically assessment of IMT in patients with suspected GCA in a well-established fast-track clinic. Our study has limitations including the retrospective design and being conducted in a single center. The initial use of steroids was relatively high, in almost half of the patients, that may affect the sensitivity of the US examination. However, polymyalgia rheumatica before US was present in 27.4% of the study population, finding comparable to previous studies (1, 32, 33). Ultrasonographer was not blinded to clinical data and clinician's making the diagnosis were not blinded to US findings, that may lead to bias in the diagnostic accuracy of US, although this bias is common in all studies aiming at validate a diagnostic tool in GCA. On the other hand, since no gold standard is valid for GCA diagnosis, we selected the clinical diagnosis at 6-month as the reference standard. However, as the majority of patients may continue with corticosteroid treatment at this time, other potential diseases may be masked. In addition, inter-observer reliability was not be investigated.

In summary, US of cranial and extracranial arteries has shown great diagnostic performance as an initial diagnostic test in patients with suspected GCA. These proposed cut-off values for IMT may help to improve the diagnostic accuracy of US in clinical practice. Finally, further validation of the cut-off values in different cohorts will be needed.

Data availability statement

The original contributions presented in this study are included in the article/supplementary material, further inquiries can be directed to the corresponding author.

Ethics statement

The studies involving human participants were reviewed and approved by Research Ethical Committee of Hospital General Universitario Gregorio Marañón (RHEUM0322). Written informed consent for participation was not required for this study in accordance with the national legislation and the institutional requirements.

Author contributions

KL-G and JM-C performed the study design, statistical analysis, subject recruitment, US examinations, and collection of the epidemiological and clinical data. KL-G, IC, JN-G, PR-M, BS-B, CG, IM, TG, JÁ-G, and JM-C drafted the manuscript. All authors revised the final manuscript and made substantial contributions to the conception and design of this study.

Acknowledgments

We thank all the patients who participated in this study.

Conflict of interest

The authors declare that the research was conducted in the absence of any commercial or financial relationships that could be construed as a potential conflict of interest.

Publisher's note

References

1. Buttgereit F, Dejaco C, Matteson EL, Dasgupta B. Polymyalgia rheumatica and giant cell arteritis: A systematic review. *JAMA*. (2016) 315:2442–58. doi: 10.1001/jama.2016.5444

2. Soriano A, Muratore F, Pipitone N, Boiardi L, Cimino L, Salvarani C. Visual loss and other cranial ischaemic complications in giant cell arteritis. *Nat Rev Rheumatol.* (2017) 13:476–84. doi: 10.1038/nrrheum.2017.98

3. Koster MJ, Matteson EL, Warrington KJ. Large-vessel giant cell arteritis: Diagnosis, monitoring and management. *Rheumatology.* (2018) 57:ii32–42. doi: 10.1093/rheumatology/kex424

4. Chrysidis S, Duftner C, Dejaco C, Schäfer VS, Ramiro S, Carrara G, et al. Definitions and reliability assessment of elementary ultrasound lesions in giant cell arteritis: A study from the OMERACT large vessel vasculitis ultrasound working group. *RMD Open.* (2018) 4:e000598. doi: 10.1136/rmdopen-2017-000598

5. Dejaco C, Ramiro S, Duftner C, Besson FL, Bley TA, Blockmans D, et al. EULAR recommendations for the use of imaging in large vessel vasculitis in clinical practice. *Ann Rheum Dis.* (2018) 77:636–43. doi: 10.1136/annrheumdis-2017-212649

6. Molina Collada J, Ruíz Bravo-Burguillos E, Monjo I, Bonilla G, Fernández E, Balsa A, et al. Positive ultrasound halo sign of temporal arteries due to amyloidosis. *Rheumatology.* (2019) 58:2067–9. doi: 10.1093/rheumatology/kez182

7. Fernández-Fernández E, Monjo-Henry I, Bonilla G, Plasencia C, Miranda-Carús ME, Balsa A, et al. False positives in the ultrasound diagnosis of giant cell arteritis: Some diseases can also show the halo sign. *Rheumatology.* (2020) 59:2443–7. doi: 10.1093/rheumatology/kez641

8. De Miguel E, Beltran LM, Monjo I, Deodati F, Schmidt WA, Garcia-Puig J. Atherosclerosis as a potential pitfall in the diagnosis of giant cell arteritis. *Rheumatology.* (2018) 57:318–21. doi: 10.1093/rheumatology/kex381

9. Thalhammer C, Husmann M, Glanzmann C, Studer G, Amann-Vesti BR. Carotid artery disease after head and neck radiotherapy. *Vasa.* (2015) 44:23–30. doi: 10.1024/0301-1526/a000403

10. Duftner C, Dejaco C, Sepriano A, Falzon L, Schmidt WA, Ramiro S. Imaging in diagnosis, outcome prediction and monitoring of large vessel vasculitis: A systematic literature review and meta-analysis informing the EULAR recommendations. *RMD Open.* (2018) 4:e000612. doi: 10.1136/rmdopen-2017-000612

11. Schmidt WA. Ultrasound in the diagnosis and management of giant cell arteritis. *Rheumatology.* (2018) 57:ii22–31. doi: 10.1093/rheumatology/kex461

12. Ješe R, Rotar Ž, Tomšiè M, Hoèevar A. The cut-off values for the intima-media complex thickness assessed by colour Doppler sonography in seven cranial and aortic arch arteries. *Rheumatology.* (2021) 60:1346–52. doi: 10.1093/rheumatology/keaa578

13. Schäfer VS, Juche A, Ramiro S, Krause A, Schmidt WA. Ultrasound cut-off values for intima-media thickness of temporal, facial and axillary arteries in giant cell arteritis. *Rheumatology.* (2017) 56:1479–83. doi: 10.1093/rheumatology/kex143

14. Diamantopoulos AP, Haugeberg G, Lindland A, Myklebust G. The fast-track ultrasound clinic for early diagnosis of giant cell arteritis significantly reduces permanent visual impairment: Towards a more effective strategy to improve clinical outcome in giant cell arteritis? *Rheumatology.* (2016) 55:66–70. doi: 10.1093/rheumatology/kev289

15. Schmidt WA, Kraft HE, Vorpahl K, Völker L, Gromnica-Ihle EJ. Color duplex ultrasonography in the diagnosis of temporal arteritis. *N Engl J Med.* (1997) 337:1336–42. doi: 10.1056/NEJM199711063371902

16. Ball EL, Walsh SR, Tang TY, Gohil R, Clarke JMF. Role of ultrasonography in the diagnosis of temporal arteritis. *Br J Surg.* (2010) 97:1765–71. doi: 10.1002/bjs.7252

17. Arida A, Kyprianou M, Kanakis M, Sfikakis PP. The diagnostic value of ultrasonography-derived edema of the temporal artery wall in giant cell arteritis: A second meta-analysis. *BMC Musculoskelet Disord.* (2010) 11:44. doi: 10.1186/1471-2474-11-44

18. Karassa FB, Matsagas MI, Schmidt WA, Ioannidis JPA. Meta-analysis: Test performance of ultrasonography for giant-cell arteritis. *Ann Intern Med.* (2005) 142:359–69. doi: 10.7326/0003-4819-142-5-200503010-00011

19. Rinagel M, Chatelus E, Jousse-Joulin S, Sibilia J, Gottenberg JE, Chasset F, et al. Diagnostic performance of temporal artery ultrasound for the diagnosis of giant cell arteritis: A systematic review and meta-analysis of the literature. *Autoimmun Rev.* (2019) 18:56–61. doi: 10.1016/j.autrev.2018.07.012

20. De Miguel E, Roxo A, Castillo C, Peiteado D, Villalba A, Martín-Mola E. The utility and sensitivity of colour Doppler ultrasound in monitoring changes in giant cell arteritis. *Clin Exp Rheumatol.* (2012) 30:S34–8.

21. Muratore F, Boiardi L, Restuccia G, Macchioni P, Pazzola G, Nicolini A, et al. Comparison between colour duplex sonography findings and different histological patterns of temporal artery. *Rheumatology.* (2013) 52:2268–74. doi: 10.1093/rheumatology/ket258

22. Habib HM, Essa AA, Hassan AA. Color duplex ultrasonography of temporal arteries: Role in diagnosis and follow-up of suspected cases of temporal arteritis. *Clin Rheumatol.* (2012) 31:231–7. doi: 10.1007/s10067-011-1808-0

23. Karahaliou M, Vaiopoulos G, Papaspyrou S, Kanakis MA, Revenas K, Sfikakis PP. Colour duplex sonography of temporal arteries before decision for biopsy: A prospective study in 55 patients with suspected giant cell arteritis. *Arthritis Res Ther.* (2006) 8:R116. doi: 10.1186/ar2003

24. Salvarani C, Silingardi M, Ghirarduzzi A, Lo Scocco G, Macchioni P, Bajocchi G, et al. Is duplex ultrasonography useful for the diagnosis of giant-cell arteritis? *Ann Intern Med.* (2002) 137:232–8. doi: 10.7326/0003-4819-137-4-200208200-00006

25. Ghinoi A, Pipitone N, Nicolini A, Boiardi L, Silingardi M, Germanò G, et al. Large-vessel involvement in recent-onset giant cell arteritis: A case-control colour-Doppler sonography study. *Rheumatology.* (2012) 51:730–4. doi: 10.1093/rheumatology/ker329

26. Förster S, Tato F, Weiss M, Czihal M, Rominger A, Bartenstein P, et al. Patterns of extracranial involvement in newly diagnosed giant cell arteritis assessed by physical examination, colour coded duplex sonography and FDG-PET. *Vasa.* (2011) 40:219–27. doi: 10.1024/0301-1526/a000096

27. Schmidt WA, Seifert A, Gromnica-Ihle E, Krause A, Natusch A. Ultrasound of proximal upper extremity arteries to increase the diagnostic yield in large-vessel giant cell arteritis. *Rheumatology.* (2008) 47:96–101. doi: 10.1093/rheumatology/kem322

28. Lensen KDF, Voskuyl AE, Comans EFI, van der Laken CJ, Smulders YM. Extracranial giant cell arteritis: A narrative review. *Neth J Med.* (2016) 74:182–92.

29. Gloria KL, Rodríguez-Merlos P, Serrano-Benavente B, González JCN, Gonzalez C, Sáez IM, et al. Ab0594 ultrasound intima media thickness cut-off values for cranial and extracranial arteries in patients with giant cell arteritis. *Ann Rheum Dis.* (2022) 81:1423–4. doi: 10.1136/annrheumdis-2022-eular.3353

30. Molina Collada J, Martínez-Barrio J, Serrano-Benavente B, Castrejón I, Nieto-González JC, Caballero Motta LR, et al. Subclavian artery involvement in patients with giant cell arteritis: Do we need a modified Halo Score? *Clin Rheumatol.* (2021) 40:2821–7. doi: 10.1007/s10067-020-05577-4

31. Skoog J, Svensson C, Eriksson P, Sjöwall C, Zachrisson H. The diagnostic performance of an extended ultrasound protocol in patients with clinically suspected giant cell arteritis. *Front Med.* (2022) 8:807996. doi: 10.3389/fmed.2021.807996

32. Gonzalez-Gay MA. Giant cell arteritis and polymyalgia rheumatica: Two different but often overlapping conditions. *Semin Arthritis Rheum.* (2004) 33:289–93. doi: 10.1016/j.semarthrit.2003.09.007

33. González-Gay MA, Matteson EL, Castañeda S. Polymyalgia rheumatica. *Lancet.* (2017) 390:1700–12. doi: 10.1016/S0140-6736(17)31825-1

CITATION

López-Gloria K, Castrejón I, Nieto-González JC, Rodríguez-Merlos P, Serrano-Benavente B, González CM, Monteagudo Sáez I, González T, Álvaro-Gracia JM and Molina-Collada J (2022) Ultrasound intima media thickness cut-off values for cranial and extracranial arteries in patients with suspected giant cell arteritis. *Front. Med.* 9:981804. doi: 10.3389/fmed.2022.981804

frontiers | Frontiers in Medicine

TYPE Review
PUBLISHED 03 October 2022
DOI 10.3389/fmed.2022.981659

OPEN ACCESS

EDITED BY
Andrea Di Matteo,
Marche Polytechnic University, Italy

REVIEWED BY
Juan Molina Collada,
Gregorio Marañón Hospital, Spain
Hector Corominas,
Hospital de la Santa Creu i Sant Pau, Spain

*CORRESPONDENCE
Colm Kirby
colmkirby11@gmail.com

SPECIALTY SECTION
This article was submitted to Rheumatology, a section of the journal Frontiers in Medicine

RECEIVED 29 June 2022
ACCEPTED 26 August 2022
PUBLISHED 03 October 2022

CITATION
Kirby C, Flood R, Mullan R, Murphy G and Kane D (2022) Evolution of ultrasound in giant cell arteritis. *Front. Med.* 9:981659. doi: 10.3389/fmed.2022.981659

Evolution of ultrasound in giant cell arteritis

Colm Kirby[1,2]*, Rachael Flood[1], Ronan Mullan[1], Grainne Murphy[2] and David Kane[1]

[1]Department of Rheumatology, Tallaght University Hospital and Trinity College Dublin, Dublin, Ireland, [2]Department of Rheumatology, Cork University Hospital and University College Cork, Cork, Ireland

Ultrasound (US) is being increasingly used to diagnose Giant Cell Arteritis (GCA). The traditional diagnostic Gold Standard has been temporal artery biopsy (TAB), but this is expensive, invasive, has a false-negative rate as high as 60% and has little impact on clinical decision-making. A non-compressible halo with a thickened intima-media complex (IMC) is the sonographic hallmark of GCA. The superficial temporal arteries (STA) and axillary arteries (AA) are the most consistently inflamed arteries sonographically and imaging protocols for evaluating suspected GCA should include at least these two arterial territories. Studies evaluating temporal artery ultrasound (TAUS) have varied considerably in size and methodology with results showing wide discrepancies in sensitivity (9–100%), specificity (66–100%), positive predictive value (36–100%) and negative predictive value (33–100%). Bilateral halos increase sensitivity as does the incorporation of pre-test probability, while prior corticosteroid use decreases sensitivity. Quantifying sonographic vasculitis using Halo Counts and Halo Scores can predict disease extent/severity, risk of specific complications and likelihood of treatment response. Regression of the Halo sign has been observed from as little as 2 days to as late as 7 months after initiation of immunosuppressive treatment and occurs at different rates in STAs than AAs. US is more sensitive than TAB and has comparable sensitivity to MRI and PET/CT. It is time-efficient, cost-effective and allows for the implementation of fast-track GCA clinics which substantially mitigate the risk of irreversible blindness. Algorithms incorporating combinations of imaging modalities can achieve a 100% sensitivity and specificity for a diagnosis of GCA. US should be a standard first line investigation in routine clinical care of patients with suspected GCA with TAB reserved only for those having had a normal US in the context of a high pre-test probability.

KEYWORDS

giant cell (temporal) arteritis, ultrasound, large vessel vasculitis, biomarkers, temporal artery biopsy

Introduction

Giant Cell Arteritis (GCA) is a vasculitis of large- and medium-sized vessels. It is the commonest idiopathic systemic vasculitis and incidence increases with age, predominantly affecting those aged > 70 years (1). Typical symptoms include headache, visual disturbance, jaw claudication and polymyalgia rheumatica (PMR). Prompt

diagnosis and initiation of corticosteroids is key to prevent the most severe complications of stroke and/or irreversible blindness (2). The traditional gold standard for diagnosis involves performing a temporal artery biopsy (TAB) (3).

TAB has many shortcomings when assessing suspected cases of GCA. Not only is it costly and invasive, but it has repeatedly been shown to have a false negative rate as high as 60%, most likely due to inadequate sampling, skip lesions and pre-operative steroid use (4). Additionally, its impact on clinical decision-making is questionable. In recent years, the use of temporal artery ultrasound (TAUS) in assessing suspected GCA has increased considerably.

The definitions of what constitutes vasculitis on US are still evolving, as is our understanding of its true place not only in the diagnosis, but also in the long-term monitoring of GCA. Advances in technology have undoubtedly contributed hugely to this growing body of knowledge and we suggest where future innovations might lead to. We also compare TAUS to other imaging modalities in GCA and discuss how TAUS is currently utilized in routine clinical care with reference to current international guidelines. Lastly we describe our current understanding of the reliability and applicability of TAUS and suggest where US may ultimately be incorporated into a diagnostic algorithm for GCA.

Impact of TAB on clinical decisions

TAB still has high value as a diagnostic test due to specificity of 100% for a diagnosis of GCA. However, given the high false-negative rate it is clear that many, if not the majority, of GCA patients are diagnosed based on clinical criteria despite the presence of a negative TAB result. A number of studies have examined the impact of TAB results on clinical decisions within this context. In one retrospective cohort of 290 patients in whom GCA was suspected with a subsequent negative diagnostic test (147 of whom had a negative bilateral TAUS and 143 of whom had a negative unilateral TAB), there was no between-group difference in the number of patients who had steroids discontinued, despite further stratification accounting for pre-test probability of having GCA. Additionally, there was no between-group differences noted in adverse outcomes (including blindness) or number of alternative diagnoses considered. These findings suggest that TAUS serves the same purpose as TAB but without the associated procedural risks while other large retrospective cohorts have shown that 41–87% of those with negative biopsies have corticosteroid therapy continued anyway (5–7). Thus, while most TABs that are performed are negative, in most cases negative TABs have no impact on clinical decision-making. Importantly, data suggests that incorporating TAUS into the workup for suspected GCA increases the positive yield of TABs from 8.5 to 24% with an associated 38% reduction in the number of TABs being performed overall and with a substantial cost-saving (8, 9).

Defining the presence of vasculitis on ultrasound

In 1995 *Schmidt* first described, what still remains to this day, the cardinal sonographic hallmark of vasculitis- "The Halo Sign" (Figure 1) (10). It describes a sonographically hypoechoic ring of inflamed, oedematous vessel wall, surrounding the lumen of an artery. In a prospective study of 30 patients with clinically diagnosed GCA, confirmed by two independent rheumatologists, 22/30 had a Halo Sign identified in their superficial temporal arteries (STA), bilaterally in 17, and the rate of agreement between the two sonographers was 100%. No Halo Sign was identified in the 82 patients who had GCA excluded on clinical grounds (11).

In 2012, a new sonographic hallmark of vasculitis was reported: "The Compression Sign" (Figure 2). In a prospective study of 80 suspected cases of GCA (43 ultimately diagnosed as GCA based an ACR criteria), all participants had bilateral TAUS performed, examining for the presence of Halo Sign and/or Compression Sign. The Compression Sign was defined as persistent visibility of the STA despite transducer-imposed arterial compression (i.e., persistent contrasting echogenicity between vessel wall and surrounding tissue). Three physician-sonographers were involved in scanning and were blinded to the clinical details of the case. Interestingly, the Halo Sign and Compression Sign were both observed in 34/43 GCA patients and both signs were absent in all patients in the non-GCA group, showing a sensitivity and specificity of 79 and 100% respectively, for both signs in diagnosing GCA (12, 13). In 2018, the OMERACT LVV US working group defined the Halo and Compression Signs as the most significant sonographic abnormalities of GCA with inter-rater agreements of 91–99% and mean kappa values of 0.83–0.98 for both inter-rater and intra-rater reliabilities. The group defined the Halo Sign as "homogenous, hypoechoic wall thickening, well delineated toward the luminal side, visible both in longitudinal and transverse planes, most commonly concentric in transverse scans." The Compression Sign was defined as being assessed "by applying pressure *via* the transducer until the lumen of the temporal artery occludes and no arterial pulsation remains visible" (14).

More recently, the "Slope Sign" of axillary artery (AA) vasculitis has been described. This sign describes a long, thickened segment of inflamed arterial wall that slides down to a normal intima-media structure (double line) (Figure 3). In 214 patients referred to a fast-track GCA clinic, 81 were diagnosed with GCA, 23 of whom had axillary vasculitis. The slope sign was observed in all patients with AA vasculitis (15, 16).

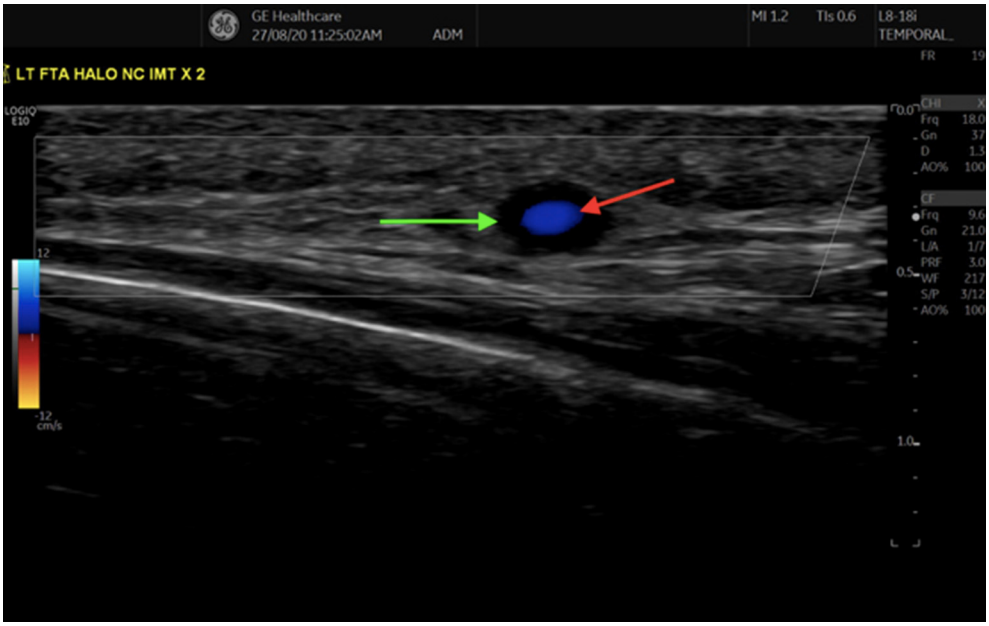

FIGURE 1
Transverse view of the frontal branch of the Superficial Temporal Artery, demonstrating a halo sign, as indicated by the anechoic region (green arrow) surrounding the inner Doppler (red arrow) signal.

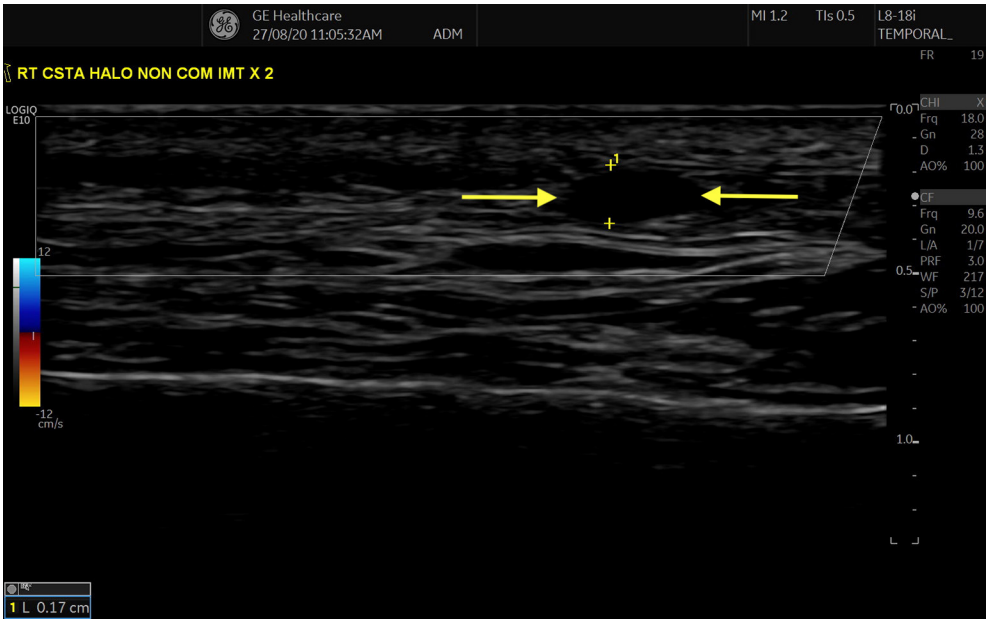

FIGURE 2
"Compression" sign in STA, transverse view. Hypoechoic/ anechoic region between two parallel hyperechoic lines (adventitia) represents an oedematous Intima-Media Complex (region between two yellow arrows).

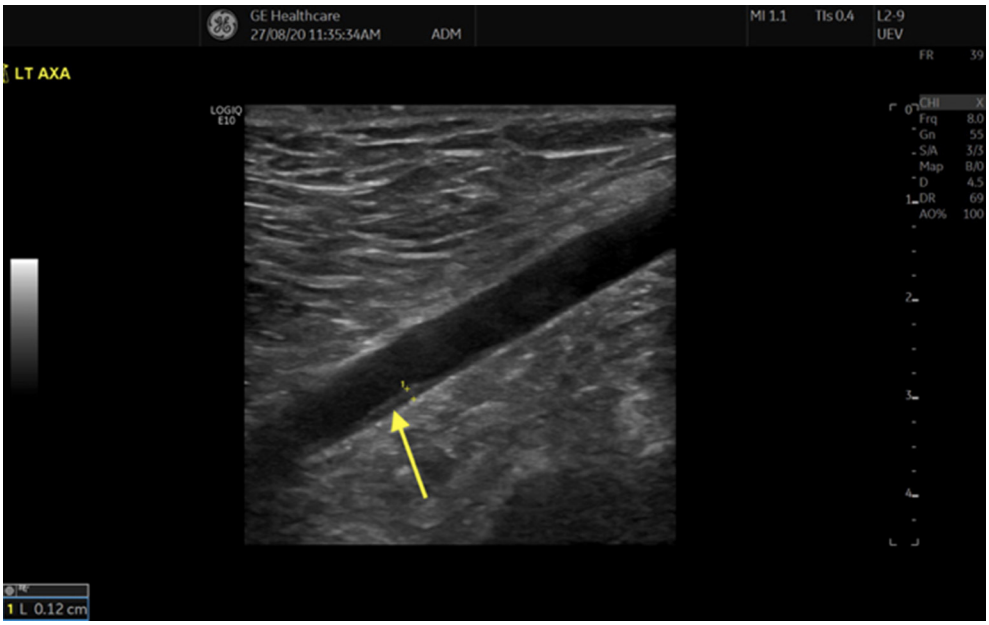

FIGURE 3
"Slope" sign in axillary artery vasculitis (yellow arrow).

Normal vs. abnormal intima-media thickness

In 2017, normal cut-off values for intima-media thickness (IMT) of arteries involved in GCA were first published. IMT measurements of the STAs, facial arteries and AAs in 40 new GCA cases and 40 controls were obtained, with the gold standard being a clinical diagnosis of GCA. The cut-off values with sensitivities and specificities of the various arterial segments for a diagnosis of GCA are outlined in Table 1 (17). A recent study looked at 101 patients aged > 50 years, without a diagnosis of GCA or PMR, but with varying degrees of perceived cardiovascular (CV) risk. US of STAs and AAs were performed on all and notably, in those deemed to have high/very high CV risk, mean IMT was greater than in those with moderate/low risk both in STAs and AAs. IMT was greater than standard normal cut-off values in at least one artery in 10.1% of patients, 80% of whom had very high/ high CV risk (18).

Thus, while early sonographic definitions of vasculitis included the presence of vessel stenosis and occlusions, the current standard is to diagnose vasculitis based on the presence of a Halo Sign, a non-compressible artery (Compression Sign) and a thickened intima-media complex (IMC). The precision of these definitions remains a constant process of refinement and further research is needed in this field to further specify normal/abnormal IMT values. Additionally, false-positive ultrasounds can occur, as demonstrated in a cohort of 305 patients in whom TAUS confirmed the presence of a Halo Sign, but 14 of whom ultimately had a variety of diagnoses other than GCA (19).

TABLE 1 Cut-off values for distinguishing vasculitic artery from normal artery in suspected cases of GCA with sensitivities and specificities for a clinical diagnosis of GCA (17).

Artery	IMT cut-off (mm)	Sensitivity	Specificity
Common Superficial Temporal Artery (STA)	0.42	100%	100%
Frontal branch of STA	0.34	100%	100%
Parietal branch of STA	0.29	97.2%	98.7%
Facial artery	0.37	87.5%	98.8%
Axillary artery	1.0	100%	100%

Distribution of pathology in GCA on US

Up to 2002, the frequency and location of peripheral arterial sonographic changes in GCA was unknown. In 10/33 GCA patients in one study, a Halo Sign could be demonstrated in peripheral arteries but importantly, sonographic vasculitis was consistently present in STAs and/or AAs if also present elsewhere (21). Additionally, it has been demonstrated that performing AAUS increases the diagnostic yield for large-vessel GCA with a detection-rate of 98 vs. 62% for TAUS

TABLE 2 Meta-analyses and systematic reviews relating to TAUS.

Author	Year	Sample size-total (GCA)	Reference standard	US definition of vasculitis	Sensitivity	Specificity
Karassa	2005	2,036	Clinical	Halo	55%	94%
			Biopsy	Halo	69%	82%
Arida	2010	575 (204)	Clinical	U/L Halo	68%	91%
Ball	2010	998	Biopsy	Halo / stenosis /occlusion	75%	83%
Duftner	2018	605 (605)	Clinical	Halo	77%	96%
			Clinical	MRI Cranial Arteries	73%	88%
			Clinical/ Biopsy	PET-CT	67–77%	66–100%
Rinagel	2019	20 studies	Biopsy	Halo	68%	81%

alone, while asymptomatic abdominal aortic aneurysms may be detected in 33% of biopsy-proven GCA cases on US despite no clinical evidence of same (22–25). Other studies have consistently shown varying degrees of involvement of occipital, vertebral, carotid and femero-popliteal arteries (26–30). However, STA and AA are the most consistently inflamed arteries sonographically and imaging protocols for evaluating suspected GCA should include at least these two arterial territories.

Temporal artery ultrasound in diagnosing GCA

Over the past 25 years, many studies have examined the diagnostic performance of TAUS against that of biopsy and clinical criteria (Table 2). In 2005, Karassa et al. undertook the first meta-analysis including all studies of >4 patients, which investigated the sensitivity and specificity of TAUS in GCA, using TAB or ACR classification criteria as the gold standard. Twenty-three studies of 2,036 patients demonstrated a weighted sensitivity and specificity of the Halo sign of 69 and 82%, respectively, compared with biopsy, and 55 and 94%, respectively, compared with ACR criteria. The studies included were mostly small with heterogenous methodology but they did show that in the presence of a low pre-test probability of GCA, a negative ultrasound can help out-rule the disease (31). A second meta-analysis was published in 2010 specifically examining the Halo sign and included eight studies of 575 patients (204 with GCA). Unilateral Halo sign achieved an overall sensitivity and specificity of 68 and 91%, respectively for GCA. The odds of having GCA in patients with a Halo Sign vs. in those without (pooled diagnostic odds ratio) was 34 (32). A systematic review by *Ball* looked at trials comparing TAUS and TAB and included 17 homogenous studies of 998 patients. When the sonographic halo was compared with TAB, the sensitivity was 75% and the specificity was 83%, leading the authors to conclude that TAUS was relatively accurate for diagnosing GCA and had promise as a first-line investigation, perhaps with TAB being reserved only for those with a normal US (33).

The seminal TABUL study was published in 2016 and showed that US was more sensitive and cost effective than TAB in investigating suspected GCA and importantly, the sensitivity of TAB was only 39% vs. previously published figures of >80%. In this prospective, multicentre study of 381 patients (257 with a reference standard clinical diagnosis of GCA, 124 without), all patients underwent US followed by TAB within 7 days of commencing treatment for GCA. 101 patients and 162 patients had positive TAB and US, respectively, with concordant results in 70% (kappa value 0.35). The sensitivities and specificities of biopsy and ultrasound were 39 and 100%, and 54 and 81%, respectively. Positive biopsy rate fell after 3 days of high-dose glucocorticoids whereas US abnormalities regressed within 4 days [a finding which concurred with those of a number of other studies highlighting the prompt regression of Halo Sign in those on corticosteroids (11, 34, 35)]. Of note, the authors demonstrated that a strategy of combining clinical assessment with US results was substantially cheaper (£485 per patient) than combining clinical assessment with biopsy (4).

Many studies therefore, have interrogated US as a diagnostic tool in GCA over the past two decades but have varied considerably in size and methodology with results showing wide discrepancies in sensitivity (9–100%), specificity (66–100%), positive predictive value (36–100%) and negative predictive value (33–100%) of US for a clinical or histological diagnosis of GCA. Most of the conflicting results are likely related to heterogenous methodologies, variances in sonographer technique and advances in ultrasound technology. The ever-expanding literature in this field has also shown us that the presence of bilateral halos increases sensitivity of US as does the incorporation of pre-test probability, while duration of prior corticosteroid use correlates inversely with likelihood of having a positive scan. A prospective study at Southend University Hospital assessing the validity of their pre-test probability score will be published in late 2022 (36).

TAUS in monitoring GCA

Early studies evaluating the role of US in GCA disease-monitoring seemed to agree that Halo regression occurred within 3–4 weeks of initiating treatment (11, 21, 37–40). Later studies however, presumably due to improvements in US technology, identified halo persistence as late as 6 months after commencing immunosuppressive treatment for GCA (41–43). It is also notable that halo regression appears to occur more quickly in STA than AA, in those with relapsing vs. new-onset disease, in those who achieve clinical remission earlier, and in those with fewer STA branches affected at baseline (44–46). By contrast however, it has been demonstrated that there is no difference in relapse rate/steroid consumption between those with and without wall-thickening regression (47). In 2021, a prospective study evaluated the role of US in monitoring GCA in a cohort of 49 patients. The number of arterial segments with halo and the maximal IMT were measured at weeks 1, 3, 6, 12 and 24 and showed significant differences at all time points in STAs and after 6 weeks in AAs. Higher halo numbers/thickness correlated with inflammatory markers, cumulative steroid dose and lower likelihood of achieving remission with no such associations seen for AA halo. In cases of relapse, 16/17 cases had increased halo IMT compared to last measured value (48). However, no reliable conclusions can be drawn regarding the use of US in monitoring GCA based on available data.

Development of an US score in GCA

A sub-study of the TABUL cohort demonstrated that an US score incorporating maximal IMT and bilaterality of STA/AA halos was useful for predicting likelihood for positive TAB but not for predicting clinical outcome at 6 months (49). More recently, Halo Counts (HC, number STA/AA branches with Halo) and Halo Scores (HS, composite of number and size of halos, Table 3) have been described. Both have shown a high degree of sensitivity for a clinical diagnosis of GCA (area under ROC curve 0.892 and 0.921) and strong associations with degrees of systemic inflammation and likelihood of ocular complications. In addition, the scores correlate positively with likelihood of having a subsequent positive TAB and they appear to be unaffected by cumulative steroid dose over the first week of treatment (50). These scores have so far been validated in one inception cohort for diagnosis but research is ongoing to assess their utility in monitoring disease activity long-term (20).

TABLE 3 Each branch is assigned a score based on the maximal intima-media thickness (IMT) identified in that branch.

Halo score	Common STA	Frontal STA	Parietal STA	Axillary Artery
0	0–0.3	0–0.1	0–0.2	0–0.5
1	0.31–0.4	0.11–0.2	0.21–0.3	0.51–0.6
2	0.41–0.5	0.21–0.3	0.31–0.4	0.61–0.89
3	0.51–0.79	0.31–0.49	0.41–0.59	0.9–1.5
4	≥ 0.8	≥ 0.5	≥ 0.6	≥ 1.6

IMT ranges (in millimeters) and their corresponding scores are outlined. Values for axillary arteries are multiplied by three to account for it having fewer branches. The scores are added to give a Total Halo Score, with a maximum value of 48. Halo scores are evaluated on serial scans to assess for wall-thickness regression. STA, Superficial Temporal Artery (50).

TAUS in predicting GCA phenotype and prognosis

In a number of studies, STA involvement without AA involvement is predictive of ocular disease with a stronger association being seen for those with bilateral halos (50–54). Involvement of both STAs and AAs infers a significantly higher risk of relapse and a more frequent requirement for steroid-sparing agents relative to those patients with either isolated cranial or isolated upper limb GCA with a similar association being seen for higher baseline HC and HS (48, 55).

Comparison of ultrasound with other imaging modalities in GCA

MRI has the resolution to accurately depict vessel wall thickening and oedema using contrast agents. While primarily used for large vessels, recent protocols specifically for STAs have shown promise but sensitivities for a diagnosis of GCA vary widely (33.3–69% sensitivity, 87.5–91% specificity) and a combination of clinical examination and US have shown higher sensitivities (66.7 and 77.7%) and specificities (100%) relative to MRI (56, 57). Additionally, the sensitivity of baseline US and MRI of STAs for diagnosing GCA reduce rapidly with corticosteroid treatment. With TAB as the reference gold-standard, the respective sensitivities of MRI and US in a cohort of 59 suspected cases of GCA were as follows: 90 and 92% (when scanned within 1st day after steroid initiation), 77.8 and 80% (when scanned within 2–4 days after steroid initiation) and 80 and 50% (when scanned more than 4 days after steroid initiation) (58). Notably, other data have shown no statistical difference between US and MRI for detecting

superficial cranial vessel vasculitis while US appears to detect vasculitic change more frequently than MRI both in those with new-onset disease and in those with chronic disease in the axillary, subclavian and carotid arteries (59). Multiple studies have also evaluated PET/CT relative to US in diagnosing GCA. PET/CT has shown greater sensitivity than US for identifying vertebral artery lesions but comparable sensitivity for diagnosing large-vessel disease, although abnormalities are often incongruous within single vascular regions (60–62).

TAUS in routine clinical practice

While US is clearly a very useful clinical tool in rheumatology, as recently as 2014 only 1% of its use among rheumatologists was for the purpose of diagnosing vasculitis while 74–94% of rheumatologists prefer TAB over TAUS as a confirmatory test for GCA (63–65). However, since the publication of updated EULAR guidelines on imaging in LVV in 2018, its use has increased considerably, as reported by De Miguel et al., citing data from the Spanish ARTESER registry.

A number of European rheumatology centers have equipped themselves with the technology and expertise to operate Fast-track GCA clinics, which consist of same-day TAUS and initiation of treatment. The relative risk of permanent blindness in the GCA patients diagnosed through the Fast-track clinic is 88% lower compared with those diagnosed by the conventional route with a shorter mean duration of inpatient care by 3 days (66). The effectiveness of standardized training programmes for TAUS has shown excellent inter-reader reliability. In a study of 112 GCA patients who has vascular US (VUS) performed by five sonographers who underwent standardized training, an interobserver agreement of 95–96% with mean kappa values of 0.88–0.92 (95% CI 0.78 to 0.99) were achieved (67).

Past and present innovations in US technology

Recently, very-high resolution ultrasound (VHRU, 55 MHz) has been shown to non-invasively and reliably, define the thickness of the arterial intima layer. In 37 patients who had negative TAB, intimal thickening (IT >0.06 mm on histology) could be identified as a "four-line pattern" in VHRU with a sensitivity and specificity of 96.3 and 100% respectively and excellent agreement between histologic and VHRU IT measurement (68). Recently, in a proof-of-concept study in 24 GCA patients, contrast-enhanced US (CEUS) of large vessels had a sensitivity and specificity of 91.7 and 100% for detecting active LVV (69). It provides detailed images of lumen-to-vessel wall border and abnormalities correlate well with those seen on FDG-PET (70, 71). Most significantly however, Roncato et al. have described an automated image analysis tool for diagnosis of GCA using artificial intelligence (AI) algorithms. They reported on a retrospective cohort of 137 patients with suspected GCA who had VUS performed and labelled with VIA software. They obtained a sensitivity of 60% and specificity of 95% for their test set (72). Yet, while inter-rater agreements for US are high, it is an inherently subjective test with interpretation relying upon sonographer expertise/ experience. Incorporation of AI algorithms will provide more objectivity and standardization of US between individuals/centers and, we expect, eliminate the disparities between study results that we have observed to date.

Current recommendations for the use of US in GCA

In 2018, EULAR issued its first guidance document on the use of imaging in LVV, including ultrasound, with a new taskforce expected to update these recommendations in 2023 (73). In addition to some technical specifications, they state the following:

1. In patients with suspected GCA, an early imaging test is recommended to complement the clinical criteria for diagnosing GCA, assuming high expertise and prompt availability of the imaging technique.
2. In patients in whom there is a high clinical suspicion of GCA and a positive imaging test, the diagnosis of GCA may be made without an additional test (biopsy or further imaging). In patients with a low clinical probability and a negative imaging result, the diagnosis of GCA can be considered unlikely.
3. Ultrasound of temporal ± axillary arteries is recommended as the first imaging modality in patients with suspected predominantly cranial GCA. A non-compressible "Halo" sign is the ultrasound finding most suggestive of GCA.

The BSR has also issued recommendations for evaluating and managing GCA (74). They strongly recommended using a confirmatory diagnostic test, either TAUS, TAB, or both and they stress the importance of considering the pre-test probability prior to initiating investigations.

US should be a standard first line investigation in routine clinical care of patients with suspected GCA with TAB perhaps reserved for those only having had a normal US in the context of a high pre-test probability. It is more sensitive and cost-effective than TAB with an estimated saving of approximately €500 per

patient and performs as well as MRI and PET/CT with the added benefit of easier access and lower relative cost when compared to those two investigations. Importantly however, it has been shown that algorithms incorporating combinations of imaging modalities can achieve a 100% sensitivity and specificity (62, 75). Moving forward, it is likely that such algorithms will become the Gold Standard in diagnosing GCA, rather than clinicians having to rely upon one specific test.

Author contributions

All authors listed have made a substantial, direct, and intellectual contribution to the work and approved it for publication.

Conflict of interest

The authors declare that the research was conducted in the absence of any commercial or financial relationships that could be construed as a potential conflict of interest.

Publisher's note

All claims expressed in this article are solely those of the authors and do not necessarily represent those of their affiliated organizations, or those of the publisher, the editors and the reviewers. Any product that may be evaluated in this article, or claim that may be made by its manufacturer, is not guaranteed or endorsed by the publisher.

References

1. Duftner C, Dejaco C, Sepriano A, Falzon L, Schmidt WA, Ramiro S. Imaging in diagnosis, outcome prediction and monitoring of large vessel vasculitis: a systematic literature review and meta-analysis informing the EULAR recommendations. *RMD open.* (2018) 4:e000612. doi: 10.1136/rmdopen-2017-000612

2. Salvarani C, Pipitone N, Versari A, Hunder GG. Clinical features of polymyalgia rheumatica and giant cell arteritis. *Nat Rev Rheumatol.* (2012) 8:509–21. doi: 10.1038/nrrheum.2012.97

3. Hall S, Persellin S, Lie JT, O'Brien PC, Kurland LT, Hunder GG. The therapeutic impact of temporal artery biopsy. *Lancet.* (1983) 2:1217–20. doi: 10.1016/S0140-6736(83)91269-2

4. Luqmani R, Lee E, Singh S, Gillett M, Schmidt WA, Bradburn M, et al. The role of ultrasound compared to biopsy of temporal arteries in the diagnosis and treatment of giant cell arteritis (TABUL): a diagnostic accuracy and cost-effectiveness study. *Health Technol Assess.* (2016) 20:1–238. doi: 10.3310/hta20900

5. Alberts MS, Mosen DM. Diagnosing temporal arteritis: duplex vs. biopsy. *QJM: Monthly Journal of the Association of Physicians.* (2007) 100:785–9. doi: 10.1093/qjmed/hcm103

6. Deyholos C, Sytek MC, Smith S, Cardella J, Orion KC. Impact of temporal artery biopsy on clinical management of suspected giant cell arteritis. *Ann Vasc Surg.* (2020) 69:254–60. doi: 10.1016/j.avsg.2020.06.012

7. Bowling K, Rait J, Atkinson J, Srinivas G. Temporal artery biopsy in the diagnosis of giant cell arteritis: Does the end justify the means? *Ann Med Surg.* (2012). 20:1–5. doi: 10.1016/j.amsu.2017.06.020

8. Cristaudo AT, Mizumoto R, Hendahewa R. The impact of temporal artery biopsy on surgical practice. *Ann Med Surg.* (2012) 11:47–51. doi: 10.1016/j.amsu.2016.09.004

9. Alberts M. Temporal arteritis: improving patient evaluation with a new protocol. *Perm J.* (2013) 17:56–62. doi: 10.7812/TPP/12-067

10. Schmidt WA, Kraft HE, Völker L, Vorpahl K, Gromnica-Ihle EJ. Colour Doppler sonography to diagnose temporal arteritis. *Lancet.* (1995) 345:866. doi: 10.1016/S0140-6736(95)93005-1

11. Schmidt WA, Kraft HE, Vorpahl K, Völker L, Gromnica-Ihle EJ. Color duplex ultrasonography in the diagnosis of temporal arteritis. *N Engl J Med.* (1997) 337:1336–42. doi: 10.1056/NEJM199711063371902

12. Aschwanden M, Daikeler T, Kesten F, Baldi T, Benz D, Tyndall A, et al. Temporal artery compression sign–a novel ultrasound finding for the diagnosis of giant cell arteritis. *Ultraschall in der Medizin.* (2013) 34:47–50. doi: 10.1055/s-0032-1312821

13. Aschwanden M, Imfeld S, Staub D, Baldi T, Walker UA, Berger CT, et al. The ultrasound compression sign to diagnose temporal giant cell arteritis shows an excellent interobserver agreement. *Clin Exp Rheumatol.* (2015) 33(2 Suppl 89):S-113-5.

14. Chrysidis S, Duftner C, Dejaco C, Schäfer VS, Ramiro S, Carrara G, et al. Definitions and reliability assessment of elementary ultrasound lesions in giant cell arteritis: a study from the OMERACT Large Vessel Vasculitis Ultrasound Working Group. *RMD Open.* (2018) 4:e000598. doi: 10.1136/rmdopen-2017-000598

15. Milchert M, Brzosko M, Bull Haaversen A, Diamantopoulos AP. Correspondence to 'Slope sign': a feature of large vessel vasculitis? *Ann Rheum Dis.* (2019) 80:e198. doi: 10.1136/annrheumdis-2019-216601

16. Dasgupta B, Smith K, Khan AAS, Coath F, Wakefield RJ. 'Slope sign': a feature of large vessel vasculitis? *Ann Rheum Dis.* (2019) 78:1738. doi: 10.1136/annrheumdis-2019-216213

17. Schäfer VS, Juche A, Ramiro S, Krause A, Schmidt WA. Ultrasound cut-off values for intima-media thickness of temporal, facial and axillary arteries in giant cell arteritis. *Rheumatology.* (2017) 56:1479–83. doi: 10.1093/rheumatology/kex143

18. Martire MV, Cipolletta E, Di Matteo A, Di Carlo M, Jesus D, Grassi W, et al. Is the intima-media thickness of temporal and axillary arteries influenced by cardiovascular risk? *Rheumatology.* (2021) 60:5362–8. doi: 10.1093/rheumatology/keab117

19. Fernández-Fernández E, Monjo-Henry I, Bonilla G, Plasencia C, Miranda-Carús ME, Balsa A, et al. False positives in the ultrasound diagnosis of giant cell arteritis: some diseases can also show the halo sign. *Rheumatology.* (2020) 59:2443–7. doi: 10.1136/annrheumdis-2019-eular.4008

20. Molina Collada J, Martínez-Barrio J, Serrano-Benavente B, Castrejón I, Caballero Motta LR, Trives Folguera L, et al. Diagnostic value of ultrasound halo count and Halo Score in giant cell arteritis: a retrospective study from routine care. *Ann Rheum Dis.* (2020) 81:e175. doi: 10.1136/annrheumdis-2020-218631

21. Schmidt WA, Natusch A, Möller DE, Vorpahl K, Gromnica-Ihle E. Involvement of peripheral arteries in giant cell arteritis: a color Doppler sonography study. *Clin Exp Rheumatol.* (2002) 20:309–18.

22. Schmidt WA, Seifert A, Gromnica-Ihle E, Krause A, Natusch A. Ultrasound of proximal upper extremity arteries to increase the diagnostic yield in large-vessel giant cell arteritis. *Rheumatology.* (2008) 47:96–101. doi: 10.1093/rheumatology/kem322

23. Agard C, Hamidou MA, Said L, Ponge T, Connault J, Chevalet P, et al. [Screening of abdominal aortic involvement using Doppler sonography in active giant cell (temporal) arteritis at the time of diagnosis. A prospective study of 30 patients]. *La Revue de Medecine Interne.* (2007) 28:363–70. doi: 10.1016/j.revmed.2006.12.018

24. Hop H, Mulder DJ, Sandovici M, Glaudemans A, van Roon AM, Slart R, et al. Diagnostic value of axillary artery ultrasound in patients with suspected giant cell arteritis. *Rheumatology.* (2020) 59:3676–84. doi: 10.1093/rheumatology/keaa102

25. Nielsen BD, Hansen IT, Keller KK, Therkildsen P, Gormsen LC, Hauge EM. Diagnostic accuracy of ultrasound for detecting large-vessel giant cell arteritis using FDG PET/CT as the reference. *Rheumatology.* (2020) 59:2062–73. doi: 10.1093/rheumatology/kez568

26. Gehlen M, Schaefer N, Schwarz-Eywill M, Maier A. Ultrasound to detect involvement of vertebral artery in giant cell arteritis. *Clin Exp Rheumatol.* (2018) 36(Suppl 111):169–70.

27. Czihal M, Zanker S, Rademacher A, Tatò F, Kuhlencordt PJ, Schulze-Koops H, et al. Sonographic and clinical pattern of extracranial and cranial giant cell arteritis. *Scand J Rheumatol.* (2012) 41:231–6. doi: 10.3109/03009742.2011.641581

28. Ješe R, Rotar Ž, Tomšič M, Hočevar A. The role of colour doppler ultrasonography of facial and occipital arteries in patients with giant cell arteritis: a prospective study. *Eur J Radiol.* (2017) 95:9–12. doi: 10.1016/j.ejrad.2017.07.007

29. Diamantopoulos AP, Haugeberg G, Hetland H, Soldal DM, Bie R, Myklebust G. Diagnostic value of color Doppler ultrasonography of temporal arteries and large vessels in giant cell arteritis: a consecutive case series. *Arthritis Care Res.* (2014) 66:113–9. doi: 10.1002/acr.22178

30. Zachrisson H, Svensson C, Dremetsika A, Eriksson P. An extended high-frequency ultrasound protocol for detection of vessel wall inflammation. *Clin Physiol Funct Imaging.* (2018) 38:586–94. doi: 10.1111/cpf.12450

31. Karassa FB, Matsagas MI, Schmidt WA, Ioannidis JP. Meta-analysis: test performance of ultrasonography for giant-cell arteritis. *Ann Intern Med.* (2005) 142:359–69. doi: 10.7326/0003-4819-142-5-200503010-00011

32. Arida A, Kyprianou M, Kanakis M, Sfikakis PP. The diagnostic value of ultrasonography-derived edema of the temporal artery wall in giant cell arteritis: a second meta-analysis. *BMC Musculoskelet Dis.* (2010) 11:44. doi: 10.1186/1471-2474-11-44

33. Ball EL, Walsh SR, Tang TY, Gohil R, Clarke JM. Role of ultrasonography in the diagnosis of temporal arteritis. *Br J Surg.* (2010) 97:1765–71. doi: 10.1002/bjs.7252

34. Seitz L, Christ L, Lötscher F, Scholz G, Sarbu AC, Bütikofer L, et al. Quantitative ultrasound to monitor the vascular response to tocilizumab in giant cell arteritis. *Rheumatology.* (2021) 60:5052–9. doi: 10.1093/rheumatology/keab484

35. Soares C, Costa A, Santos R, Abreu P, Castro P, Azevedo E. Clinical, laboratory and ultrasonographic interrelations in giant cell arteritis. *J Stroke Cerebrovasc Dis.* (2021) 30:105601. doi: 10.1016/j.jstrokecerebrovasdis.2021.105601

36. Sebastian A, Tomelleri A, Kayani A, Prieto-Pena D, Ranasinghe C, Dasgupta B. Probability-based algorithm using ultrasound and additional tests for suspected GCA in a fast-track clinic. *RMD Open.* (2020) 6:e001297. doi: 10.1136/rmdopen-2020-001297

37. Lauwerys BR, Puttemans T, Houssiau FA, Devogelaer JP. Color Doppler sonography of the temporal arteries in giant cell arteritis and polymyalgia rheumatica. *J Rheumatol.* (1997) 24:1570–4.

38. Schmid R, Hermann M, Yannar A, Baumgartner RW. [Color duplex ultrasound of the temporal artery: replacement for biopsy in temporal arteritis]. *Ophthalmologica.* (2002) 216:16–21. doi: 10.1159/000048291

39. Karahaliou M, Vaiopoulos G, Papaspyrou S, Kanakis MA, Revenas K, Sfikakis PP. Colour duplex sonography of temporal arteries before decision for biopsy: a prospective study in 55 patients with suspected giant cell arteritis. *Arthritis Res Ther.* (2006) 8:R116. doi: 10.1186/ar2003

40. Santoro L, D'Onofrio F, Bernardi S, Gremese E, Ferraccioli G, Santoliquido A. Temporal ultrasonography findings in temporal arteritis: early disappearance of halo sign after only 2 days of steroid treatment. *Rheumatology.* (2013) 52:622. doi: 10.1093/rheumatology/kes387

41. Pérez López J, Solans Laqué R, Bosch Gil JA, Molina Cateriano C, Huguet Redecilla P, Vilardell Tarrés M. Colour-duplex ultrasonography of the temporal and ophthalmic arteries in the diagnosis and follow-up of giant cell arteritis. *Clin Exp Rheumatol.* (2009) 27(1 Suppl 52):S77–82.

42. Aschwanden M, Kesten F, Stern M, Thalhammer C, Walker UA, Tyndall A, et al. Vascular involvement in patients with giant cell arteritis determined by duplex sonography of 2x11 arterial regions. *Ann Rheum Dis.* (2010) 69:1356–9. doi: 10.1136/ard.2009.122135

43. Diamantopoulos AP, Myklebust G. Long-term inflammation in the temporal artery of a giant cell arteritis patient as detected by ultrasound. *Ther Adv Musculoskelet Dis.* (2014) 6:102–3. doi: 10.1177/1759720X14521109

44. Ford JA, DiIorio MA, Huang W, Sobiesczcyk P, Docken WP, Tedeschi SK. Follow-up vascular ultrasounds in patients with giant cell arteritis. *Clin Exp Rheumatol.* (2020) 38(Suppl 124):107–11.

45. De Miguel E, Roxo A, Castillo C, Peiteado D, Villalba A, Martín-Mola E. The utility and sensitivity of colour Doppler ultrasound in monitoring changes in giant cell arteritis. *Clin Exp Rheumatol.* (2012) 30(1 Suppl 70):S34–8.

46. Monti S, Floris A, Ponte CB, Schmidt WA, Diamantopoulos AP, Pereira C, et al. The proposed role of ultrasound in the management of giant cell arteritis in routine clinical practice. *Rheumatology.* (2018) 57:112–9. doi: 10.1093/rheumatology/kex341

47. Aschwanden M, Schegk E, Imfeld S, Staub D, Rottenburger C, Berger CT, et al. Vessel wall plasticity in large vessel giant cell arteritis: an ultrasound follow-up study. *Rheumatology.* (2019) 58:792–7. doi: 10.1093/rheumatology/key383

48. Ponte C, Monti S, Scirè CA, Delvino P, Khmelinskii N, Milanesi A, et al. Ultrasound halo sign as a potential monitoring tool for patients with giant cell arteritis: a prospective analysis. *Ann Rheum Dis.* (2021) 80:1475–82. doi: 10.1136/annrheumdis-2021-220306

49. Monti S, Ponte C, Pereira C, Manzoni F, Klersy C, Rumi F, et al. The impact of disease extent and severity detected by quantitative ultrasound analysis in the diagnosis and outcome of giant cell arteritis. *Rheumatology (Oxford).* (2020) 59:2299–307. doi: 10.1093/rheumatology/kez554

50. van der Geest KSM, Borg F, Kayani A, Paap D, Gondo P, Schmidt W, et al. Novel ultrasonographic Halo Score for giant cell arteritis: assessment of diagnostic accuracy and association with ocular ischaemia. *Ann Rheum Dis.* (2020) 79:393–9. doi: 10.1136/annrheumdis-2019-216343

51. Schmidt WA, Krause A, Schicke B, Kuchenbecker J, Gromnica-Ihle E. Do temporal artery duplex ultrasound findings correlate with ophthalmic complications in giant cell arteritis? *Rheumatology.* (2009) 48:383–5. doi: 10.1093/rheumatology/ken515

52. Gribbons KB, Ponte C, Craven A, Robson JC, Suppiah R, Luqmani R, et al. Diagnostic assessment strategies and disease subsets in giant cell arteritis: data from an international observational cohort. *Arthritis Rheumatol.* (2020) 72:667–76. doi: 10.1002/art.41165

53. Ponte C, Serafim AS, Monti S, Fernandes E, Lee E, Singh S, et al. Early variation of ultrasound halo sign with treatment and relation with clinical features in patients with giant cell arteritis. *Rheumatology.* (2020) 59:3717–26. doi: 10.1093/rheumatology/keaa196

54. Schmidt D, Hetzel A, Reinhard M, Auw-Haedrich C. Comparison between color duplex ultrasonography and histology of the temporal artery in cranial arteritis (giant cell arteritis). *Eur J Med Res.* (2003) 8:1–7.

55. Czihal M, Piller A, Schroettle A, Kuhlencordt P, Bernau C, Schulze-Koops H, et al. Impact of cranial and axillary/subclavian artery involvement by color duplex sonography on response to treatment in giant cell arteritis. *J Vasc Surg.* (2015) 61:1285–91. doi: 10.1016/j.jvs.2014.12.045

56. Bley TA, Reinhard M, Hauenstein C, Markl M, Warnatz K, Hetzel A, et al. Comparison of duplex sonography and high-resolution magnetic resonance imaging in the diagnosis of giant cell (temporal) arteritis. *Arthritis Rheum.* (2008) 58:2574–8. doi: 10.1002/art.23699

57. Ghinoi A, Zuccoli G, Nicolini A, Pipitone N, Macchioni L, Bajocchi GL, et al. 1T magnetic resonance imaging in the diagnosis of giant cell arteritis: comparison with ultrasonography and physical examination of temporal arteries. *Clin Exp Rheumatol.* (2008) 26(3 Suppl 49):S76–80.

58. Hauenstein C, Reinhard M, Geiger J, Markl M, Hetzel A, Treszl A, et al. Effects of early corticosteroid treatment on magnetic resonance imaging and ultrasonography findings in giant cell arteritis. *Rheumatology.* (2012) 51:1999–2003. doi: 10.1093/rheumatology/kes153

59. Yip A, Jernberg ET, Bardi M, Geiger J, Lohne F, Schmidt WA, et al. Magnetic resonance imaging compared to ultrasonography in giant cell arteritis: a cross-sectional study. *Arthritis Res Ther.* (2020) 22:247. doi: 10.1186/s13075-020-02335-4

60. Czihal M, Tatò F, Förster S, Rademacher A, Schulze-Koops H, Hoffmann U. Fever of unknown origin as initial manifestation of large vessel giant cell arteritis: diagnosis by colour-coded sonography and 18-FDG-PET. *Clin Exp Rheumatol.* (2010) 28:549–52.

61. Förster S, Tato F, Weiss M, Czihal M, Rominger A, Bartenstein P, et al. Patterns of extracranial involvement in newly diagnosed giant cell arteritis assessed by physical examination, colour coded duplex sonography and FDG-PET. *VASA Zeitschrift fur Gefasskrankheiten.* (2011) 40:219–27. doi: 10.1024/0301-1526/a000096

62. Imfeld S, Aschwanden M, Rottenburger C, Schegk E, Berger CT, Staub D, et al. [18F]FDG positron emission tomography and ultrasound in the diagnosis of giant cell arteritis: congruent or complementary imaging methods? *Rheumatology.* (2020) 59:772–8. doi: 10.1093/rheumatology/kez362

63. de Miguel E, Andreu JL, Naredo E, Möller I. Ultrasound in rheumatology: where are we and where are we going? *Reumatol Clin.* (2014) 10:6–9. doi: 10.1016/j.reuma.2013.04.005

64. Mahr A, Belhassen M, Paccalin M, Devauchelle-Pensec V, Nolin M, Gandon S, et al. Characteristics and management of giant cell arteritis in France: a study based on national health insurance claims data. *Rheumatology.* (2020) 59:120–8. doi: 10.1093/rheumatology/kez251

65. Ing E, Xu QA, Chuo J, Kherani F, Landau K. Practice preferences: temporal artery biopsy versus doppler ultrasound in the work-up of giant cell arteritis. *Neuro-ophthalmology.* (2020) 44:174–81. doi: 10.1080/01658107.2019.1656752

66. Diamantopoulos AP, Haugeberg G, Lindland A, Myklebust G. The fast-track ultrasound clinic for early diagnosis of giant cell arteritis significantly reduces permanent visual impairment: towards a more effective strategy to

improve clinical outcome in giant cell arteritis? *Rheumatology.* (2016) 55:66–70. doi: 10.1093/rheumatology/kev289

67. Chrysidis S, Terslev L, Christensen R, Fredberg U, Larsen K, Lorenzen T, et al. Vascular ultrasound for the diagnosis of giant cell arteritis: a reliability and agreement study based on a standardised training programme. *RMD Open.* (2020) 6:e001337. doi: 10.1136/rmdopen-2020-001337

68. Sundholm JKM, Paetau A, Albäck A, Pettersson T, Sarkola T. Non-invasive vascular very-high resolution ultrasound to quantify artery intima layer thickness: validation of the four-line pattern. *Ultrasound Med Biol.* (2019) 45:2010–8. doi: 10.1016/j.ultrasmedbio.2019.04.017

69. Bergner R, Splitthoff J, Wadsack D. Use of contrast-enhanced ultrasound sonography in giant cell arteritis: a proof-of-concept study. *Ultrasound Med Biol.* (2022) 48:143–8. doi: 10.1016/j.ultrasmedbio.2021.09.019

70. Schinkel AF, van den Oord SC, van der Steen AF, van Laar JA, Sijbrands EJ. Utility of contrast-enhanced ultrasound for the assessment of the carotid artery wall in patients with Takayasu or giant cell arteritis. *Eur Heart J Cardiovasc Imaging.* (2014) 15:541–6. doi: 10.1093/ehjci/jet243

71. Germanò G, Macchioni P, Possemato N, Boiardi L, Nicolini A, Casali M, et al. Contrast-enhanced ultrasound of the carotid artery in patients with large vessel vasculitis: correlation with positron emission tomography findings. *Arthritis Care Res.* (2017) 69:143–9. doi: 10.1002/acr.22906

72. Roncato C, Perez L, Brochet-Guégan A, Allix-Béguec C, Raimbeau A, Gautier G, et al. Colour doppler ultrasound of temporal arteries for the diagnosis of giant cell arteritis: a multicentre deep learning study. *Clin Exp Rheumatol.* (2020) 38(Suppl 124):120–5.

73. Dejaco C, Ramiro S, Duftner C, Besson FL, Bley TA, Blockmans D, et al. EULAR recommendations for the use of imaging in large vessel vasculitis in clinical practice. *Ann Rheum Dis.* (2018) 77:636–43. doi: 10.1136/annrheumdis-2017-212649

74. Mackie SL, Dejaco C, Appenzeller S, Camellino D, Duftner C, Gonzalez-Chiappe S, et al. British Society for Rheumatology guideline on diagnosis and treatment of giant cell arteritis: executive summary. *Rheumatology.* (2020) 59:487–94. doi: 10.1093/rheumatology/kez664

75. Pfadenhauer K, Weinerth J, Hrdina C. Vertebral arteries: a target for FDG-PET imaging in giant cell arteritis? Clinical, ultrasonographic and PET study in 46 patients. *Nuklearmedizin.* (2011) 50:28–32. doi: 10.3413/nukmed-0335-10-07

frontiers | Frontiers in Immunology

TYPE Original Research
PUBLISHED 10 October 2022
DOI 10.3389/fimmu.2022.935132

OPEN ACCESS

EDITED BY
Andrea Di Matteo,
Marche Polytechnic University, Italy

REVIEWED BY
Javier Eduardo Rosa,
Italian Hospital of Buenos Aires, Argentina
Jagdish Nair,
Liverpool University Hospitals NHS Foundation Trust, United Kingdom
Florentin Ananu Vreju,
University of Medicine and Pharmacy of Craiova, Romania

*CORRESPONDENCE
Zhuoli Zhang
zhuoli.zhang@126.com

SPECIALTY SECTION
This article was submitted to Autoimmune and Autoinflammatory Disorders, a section of the journal Frontiers in Immunology

RECEIVED 03 May 2022
ACCEPTED 26 September 2022
PUBLISHED 10 October 2022

CITATION
Geng Y, Song Z, Zhang X, Deng X, Wang Y and Zhang Z (2022) Improved diagnostic performance of CASPAR criteria with integration of ultrasound. *Front. Immunol.* 13:935132. doi: 10.3389/fimmu.2022.935132

Improved diagnostic performance of CASPAR criteria with integration of ultrasound

Yan Geng, Zhibo Song, Xiaohui Zhang, Xuerong Deng, Yu Wang and Zhuoli Zhang*

Department of Rheumatology and Clinical Immunology, Peking University First Hospital, Beijing, China

Background: The difficulty in determining synovitis, tenosynovitis, or enthesitis by physical examination (PE) has limited the diagnostic capability of CASPAR for psoriatic arthritis (PsA). Therefore, we aimed to evaluate the diagnostic utility of CASPAR with the integration of ultrasound (US).

Methods: Patients with a hint of PsA were enrolled. Besides routine PE for tender or swollen joints, enthesitis, and dactylitis, US was performed to evaluate peripheral joints, entheses, and tendons. The additional value of the US to the CASPAR criteria was analyzed.

Results: A total of 326 consecutive patients with 164 PsA and 162 non-PsA were enrolled. A total of 162 non-PsA patients consisted of 58 cases of psoriasis (PsO), 27 osteoarthritis with PsO/family history of PsO, five fibromyalgia with PsO, 69 sero-negative rheumatoid arthritis, and three undifferentiated arthritis. Significantly higher frequencies of tenosynovitis and enthesitis on US and new bone formation on X-rays were found in PsA vs. non-PsA patients (59.1% *vs*. 13.0%; 63.4% *vs*. 14.2%; 62.2% *vs*. 8.0%, p <0.01 for all). Logistic regression analysis showed that dactylitis (OR = 12.0, p <0.01), family history of PsO/PsA (OR = 3.1, p <0.05), nail involvement (OR = 3.5, p = 0.01), new bone formation on X-ray (OR = 14.8, p <0.01), tenosynovitis on US (OR = 21.3, p <0.01), and enthesitis on US (OR = 21.7, p <0.01) were independent risk factors for PsA. By combining US tenosynovitis and/or enthesitis, the diagnostic utility of CASPAR criteria was improved, with superior specificity (91.4% *vs*. 84.0%) and similar sensitivity (95.7% *vs*. 94.5%). Replacing X-ray by US or adding US, the CASPAR criteria showed comparable sensitivity and specificity for PsA diagnosis. The diagnostic accuracy was 89.3% for CASPAR criteria based on PE, 93.6% for CASPAR added with US, and 93.3% for CASPAR with US replacing X-ray.

Conclusion: The diagnostic utility of the CASPAR was improved by integrating tenosynovitis and/or enthesitis when using US. US provides additional value for PsA recognition.

KEYWORDS

psoriatic arthritis, diagnostic utility, CASPAR criteria, ultrasound, integration

Introduction

Psoriatic arthritis (PsA) is a chronic inflammatory disease, manifesting as peripheral arthritis, enthesitis, dactylitis, or spondylitis besides skin and nail psoriasis (1). Peripheral joints and entheses are the most commonly involved domains. Moreover, inflammatory articular disease is the prerequisite for CASPAR (ClASsification criteria for Psoriatic Arthritis), the most widely used criteria in the diagnosis of PsA (2). Nevertheless, it is often difficult to determine the cause of synovitis, tenosynovitis, enthesitis, or dactylitis by physical examination (PE) alone.

In recent years, ultrasound (US) has been recognized as a feasible, reliable, and non-radiative tool, and it has been widely used in assessing inflammatory arthritis. Some previous studies have also demonstrated that subclinical synovitis and enthesitis identified by US are common in PsA and even in some psoriasis (PsO) patients. On the other hand, overestimation of inflammatory articular disease also happens in practice due to osteoarthritis or fibromyalgia (3). Therefore, the European League Against Rheumatism (EULAR) recommended detecting arthritis, tenosynovitis, and enthesitis in peripheral spondyloarthritis by application of US instead of clinical examination only to improve the diagnostic accuracy (4).

Although the CASPAR criteria have been validated, CASPAR based on PE is not the "gold standard." The final diagnosis of PsA is usually made by experienced rheumatologists after considering all the available evidence. In this study, we tried to explore the contribution of US on the basis of CASPAR criteria to the diagnosis of PsA.

Materials and methods

Study population and participants

We conducted a cross-sectional study on patients with suspected PsA at Peking University First Hospital. The patients were enrolled from June 2019 to May 2021. In detail, patients with the following clinical features were included: 1. Presence of PsO/family history of PsO plus at least one of the following: (1) presence of tender and/or swollen joint on physical examination; (2) tender entheses on physical examination; (3) swollen digits with/without tender on physical examination and 2. The absence of PsO/family history of PsO, being seronegative, but physical examination revealed tender and/or swollen joints, or tender entheses, or swollen digits with/without tender. Those suspected PsA patients with axial involvement were excluded. The exclusion criteria were as follows: 1. use of disease-modifying antirheumatic drugs within 3 months before enrollment; and 2. steroid therapy (oral and intra-articular) or non-steroidal anti-inflammatory drugs within 2 weeks before enrollment. The research protocol was approved by the Peking University First Hospital Institutional Review Board for clinical research and consent forms were obtained from all participants in compliance with the Helsinki Declaration.

Clinical and laboratory assessment

The demographics, including age, sex, family history of PsO, and body mass index (BMI), were recorded. The duration of arthralgia and/or enthesis pain was recorded. The following variables were collected and further calculated: swollen joint counts (SJC), tender joint counts (TJC) of 46 joints [bilateral elbows, wrists, metacarpophalangeal joints, proximal interphalangeal joints, distal interphalangeal joints, knee, ankle, and metatarsophalangeal joints], global assessment of patients (0–10), and global assessment of physicians (0–10). Tenderness of 16 entheses (bilateral proximal patellar tendon, distal patellar tendon, quadriceps tendon, Achilles' tendon, plantar aponeurosis, common extensor tendon, common flexor tendon, and triceps tendon) and dactylitis on 20 digits (bilateral hands and feet) were examined. Psoriasis was scored using the psoriasis area and severity index (PASI). Nail involvement was recorded. The following laboratory tests were recorded: erythrocyte sedimentation rate, C-reactive protein, rheumatoid factor (RF), and anti-cyclic citrullinated peptide (anti-CCP).

Ultrasound and X-ray assessment

US examination was performed by a rheumatologist (XRD) who was the ultrasound trainer endorsed by EULAR with over 10 years of experience in maneuvering US and was blinded to all clinical and laboratory findings. A total of 46 joints (same to TJC and SJC), 16 entheses (same to tenderness count), and 36 tendons (flexor and extensor tendon of digit, compartments of extensor tendons of wrist, posterior tibialis tendon, and anterior tibialis tendon) were scanned. The US protocol included transverse and longitudinal scans of the joints and enthesis. Each scan took at least 20 min, and the representative images were archived. The GE LOGIQ E9 US machine with linear ML 15–6 MHz or small-footprint linear array 18–8 MHz transducers was used in our study. The gray-scale and Doppler settings were as below: wall filter low, pulse repetition frequency (PRF) 1.0 kHz, and gain was adjusted to just below the level at which Doppler artifacts appeared beneath bone. The severity of synovitis was measured and graded using the 2001 Szkudlarek semi-quantitative method (5). Gray Scale (GS) and Power Doppler (PD) synovitis scores in each joint were respectively graded on a scale of 0–3. GS ≥2 or PD ≥1 for a joint was defined as synovitis (6). Enthesitis was defined as

hypoechoic and/or thickened insertion of the tendon close to the bone (within 2 mm from the bony cortex), which exhibits Doppler signal if active, and which may show erosions and enthesophytes/calcifications as a sign of structural damage (7) (Figures 1A, B).

Tenosynovitis was defined as abnormal anechoic and/or hypoechoic tendon sheath widening with or without PD signals (Figures 1C, D). Erosion was defined as intra-articular discontinuity of the bone surface observed in two perpendicular planes (8). The effects of synovitis, enthesitis, tendon involvement, and erosion on the US were analyzed in a dichotomous way.

A posterior–anterior X-ray of the hands and feet was taken for all the patients. New bone formation was evaluated by a radiologist who was blinded to all clinical data (9).

Diagnostic criteria

For analyzing the diagnostic accuracy of US features and the additional value of US to CASPAR, the clinical diagnosis of PsA made by experienced rheumatologists was taken as the standard. All controversial cases were reviewed by a panel of three experts (ZZ, YG, and ZS) who were blinded to the US findings.

Statistical analysis

All statistical analyses were performed using Statistical Package of Social Science (SPSS Inc., Chicago, IL, USA) software v. 22.0. A T-test or Mann–Whitney U-test was used for measurement data, and χ^2 test was used for categorical data in the comparative analysis between groups. The analysis based on the receiver operating characteristic (ROC) curve was performed to determine the optimal cut-off value for the best combination of sensitivity and specificity. Logistic regression was used to predict the independent risk factors for the diagnosis of PsA. P-values <0.05 were considered as being significant. P-values <0.01 were considered as highly significant.

Results

Comparisons of demographics and clinical features between PsA and non-PsA groups

Three hundred and twenty-six patients were enrolled in the study. Clinically, 164 were diagnosed as PsA. A total of 162 non-PsA consisted of 58 PsO, 27 osteoarthritis with PsO/

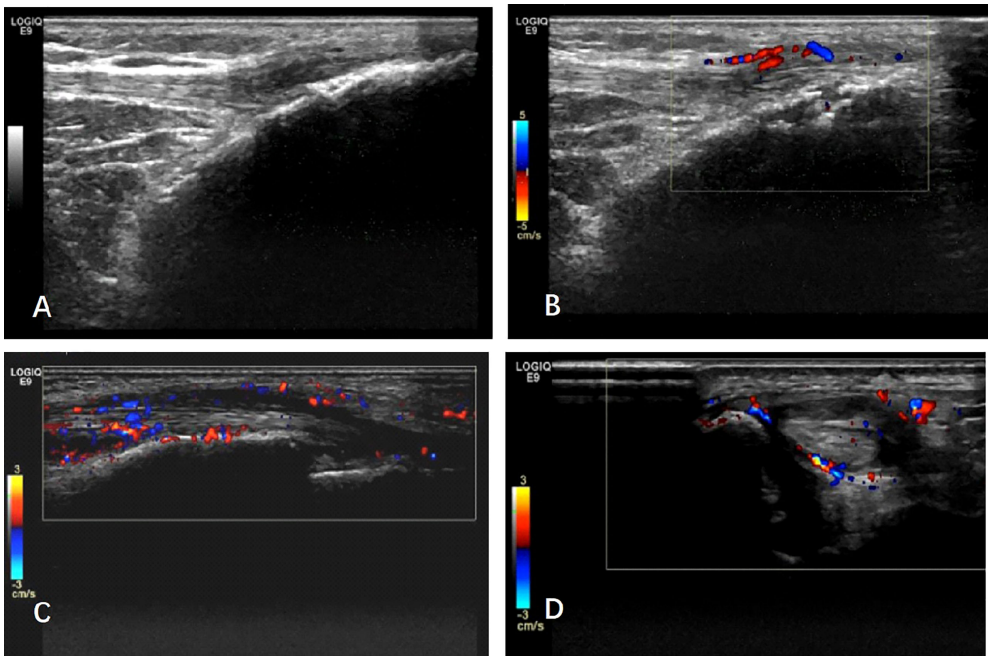

FIGURE 1
The typical ultrasound image of psoriatic arthritis: **(A, B)** Enthesitis: **(A)** longitudinal scan of patellar tendon at its distal insertion into the anterior tibial tuberosity. Note the presence of hypoechoic areas, entheseal thickening together with an enthesophyte. **(B)** B-mode signs of enthesitis are detectable. The image shows evidence of power Doppler signal at the entheseal area, together with erosion. **(C, D)** Tenosynovitis: longitudinal and transverse scan of anterior tibialis tendon. Note abnormal anechoic and hypoechoic tendon sheath widening with intense power Doppler signals.

family history of PsO, five fibromyalgia with concomitant PsO, 69 sero-negative rheumatoid arthritis, and three undifferentiated arthritis.

The demographics and clinical characteristics of patients with PsA and non-PsA are shown in Table 1. Their average age was 48.3 years. More patients reported a family history of PsO/PsA in the PsA group than in the non-PsA group (43.9% *vs.* 25.9%, p <0.01). The PASI score was higher in the PsA group than in the non-PsA group (6.6 ± 9.6 *vs.* 3.0 ± 8.0, p <0.01). More patients had clinical enthesitis, dactylitis, and nail involvement in the PsA group than in the non-PsA group (20.1% *vs.* 9.9%, p <0.05; 35.4% *vs.* 2.5%, p <0.01; 58.3% *vs.* 24.7%, p <0.01, respectively). The presence of RF or anti-CCP was very low, with no statistical significance between the two groups.

Among US characteristics, synovitis was found in 59.8% of PsA patients and 46.3% of non-PsA patients (p <0.05). The presence of tenosynovitis, enthesitis and bone erosion was significantly more in the PsA group than in the non-PsA group (59.1% *vs.* 13.0%; 63.4% *vs.* 14.2%; 51.2% *vs.* 23.5%; p <0.01 for all). Compared to the non-PsA group, a significantly higher proportion of patients in the PsA group had new bone formation on X-ray (62.2% *vs.* 8.0%, p <0.01).

Independent risk factors for predicting the diagnosis of PsA

Age, sex, family history of PsO/PsA, PASI score, nail involvement, dactylitis, new bone formation on X-ray, and various US features were included in the multivariate analysis to identify the possible predicting factors. We found that dactylitis (OR = 12.0, 95% CI 2.7–53.5, p <0.01), nail involvement (OR = 3.5, 95% CI 1.4–9.3, p = 0.01), family history of PsO/PsA (OR = 3.1, 95% CI 1.2–8.4, p <0.05), new bone formation on X -ray (OR = 14.8, 95% CI 5.3–41.4, p <0.01) and tenosynovitis on US (OR = 21.3, 95% CI 6.8–66.9, p <0.01),

TABLE 1 Comparisons of the demographics and clinical features between PsA and non-PsA groups.

	PsA group(n = 164)	Non-PsA group (n = 162)	P
Demographic characteristics			
Female, n (%)	65 (39.6%)	105 (64.8%)	<0.01
Age (years)	46.2 ± 13.5	48.3 ± 16.0	0.102
BMI (kg/m^2)	25.1 ± 4.1	25.4 ± 6.3	0.947
Family history of PsO/PsA, n (%)	72 (43.9%)	42 (25.9%)	<0.01
Clinical characteristics			
Joint symptom duration (years)	4.7 ± 6.3	3.9 ± 5.4	0.113
Tender joint count, n	5.8 ± 6.2	3.7 ± 5.4	<0.01
Swollen joint count, n	4.0 ± 4.5	2.0 ± 4.1	<0.01
Enthesitis, n (%)	33 (20.1%)	16 (9.9%)	0.015
Dactylitis, n (%)	58 (35.4%)	4 (2.5%)	<0.01
PGA (0–10), mm	3.6 ± 2.2	3.0 ± 2.8	0.067
PhGA (0–10), mm	3.5 ± 2.1	2.8 ± 2.6	0.017
Nail involvement, n (%)	95 (58.3%)	40 (24.7%)	<0.01
PASI score	6.6 ± 9.6	3.0 ± 8.0	<0.01
Laboratory parameters			
ESR (mm/h)	21.4 ± 24.0	21.2 ± 21.6	0.121
CRP (mg/L)	12.6 ± 21.2	11.4 ± 17.5	0.365
RF positive, n (%)	2 (1.2%)	5 (3.7%)	0.275
Anti-CCP positive, n (%)	2 (1.2%)	2 (1.2%)	1.000
US characteristics			
Synovitis, n (%)	98 (59.8%)	75 (46.3%)	0.015
Tenosynovitis, n (%)	97 (59.1%)	21 (13.0%)	<0.01
Enthesitis, n (%)	104 (63.4%)	23 (14.2%)	<0.01
Erosion, n (%)	84 (51.2%)	38 (23.5%)	<0.01
Osteophyte, n (%)	89 (54.3%)	88 (54.3%)	0.992
X-ray characteristics			
New bone formation	102 (62.2%)	13 (8.0%)	<0.01

The measurement data were presented as mean ± SD unless it was indicated specifically. BMI, body mass index; PsA, psoriatic arthritis; PsO, psoriasis; PGA, patient global assessment; PhGA, physician global assessment; PASI, Psoriasis Area and Severity Index; ESR, erythrocyte sedimentation rate; CRP, C-reactive protein; RF, rheumatoid factor; anti-CCP, anti-cyclic citrullinated peptide; US, ultrasound.

enthesitis on US (OR = 21.7, 95% CI 7.7–61.4, p <0.01) were independent risk factors for predicting the diagnosis of PsA (Table 2).

Diagnostic values of US features for PsA

Among US characteristics, tenosynovitis and enthesitis were significantly more commonly observed in the PsA group and were identified as independent risk factors for predicting PsA. In this study, tenosynovitis in the US showed 59.1% sensitivity and 87.0% specificity for the diagnosis of PsA. Enthesitis in the US showed 63.4% sensitivity and 85.8% specificity in diagnosing PsA. In contrast, the CASPAR criteria based on physical examination had a high sensitivity of 94.5% but a relatively low specificity of 84.0%.

The added value of US to the CASPAR criteria

Since US features, including tenosynovitis and enthesitis, were risk factors for predicting PsA, we subsequently added US tenosynovitis and/or enthesitis to the CASPAR scoring system. The presence of US tenosynovitis and/or enthesitis was given the same weight as nail involvement (1 point), and the cut-off total score of ≥4 was used to classify a patient as having PsA.

Compared to the original CASPAR criteria based on PE, the modified CASPAR criteria integrated with US findings showed better performance, with improved specificity (91.4% *vs.* 84.0%) and similar sensitivity (95.7% *vs.* 94.5%) (Figure 2). Diagnostic accuracy was improved from 89.3% to 93.6% ($p = 0.052$), with better positive predictive value (91.8% *vs.* 85.6%) and comparable negative predictive value (95.5% *vs.* 93.8%).

An X-ray is an invasive procedure and is incapable of disclosing inflammation. It is always ideal if an X-ray can be substituted by US. Therefore, we tried replacing X-rays in the CASPAR criteria with US. Unexpectedly, we found both the sensitivity and specificity were noninferior to CASPAR criteria with combined US (96.3% *vs.* 95.7% and 90.1% *vs.* 91.4%) (Figure 2). The diagnostic accuracy was also comparable (93.3% *vs.* 93.6%, $p = 0.250$), with a positive predictive value of 90.8% and a negative predictive value of 96.1%.

The ROC curve illustrated the diagnostic performance of two modified CASPAR criteria added with US, and substituting X-ray by US, as well as the original CASPAR criteria. The corresponding areas under the ROC curves (AUC) were 0.954 (95% CI 0.928, 0.979; <0.01), 0.944 (95% CI 0.916, 0.972; p <0.01), and 0.933 (95% CI 0.903, 0.962; p <0.01).

Discussion

CASPAR is most widely used in the diagnosis of PsA in practice. Its utility has been assessed by a series of studies, showing relatively high specificity and sensitivity. The better performance of CASPAR than the Moll and Wright criteria as well as the European Spondyloarthropathy Study Group criteria has also been demonstrated (10).

Early identification of PsA is crucial for a better long-term outcome. A previous study showed that even a 6-month delay of PsA diagnosis in a rheumatology clinic resulted in worse outcomes, including more peripheral joint erosion and functional impairment (11). Thus, close attention to the joint symptoms and a comprehensive physical examination are needed to identify the inflammatory articular disease. Nevertheless, it is always difficult to precisely identify synovitis and enthesitis by swelling and/or tenderness of the joint or entheseal *via* physical examination (12). Moreover, PsO patients with concomitant osteoarthritis or fibromyalgia often easily satisfy the CASPAR criteria, leading to over-diagnosis of PsA. This may explain the result of good sensitivity but poor specificity of CASPAR in our study.

US has been validated as a useful tool in evaluating joint, tendon, and entheseal lesions in PsA (13–15). But few studies evaluated the overall value of US in addition to clinical findings in

TABLE 2 The risk factors for predicting PsA by multivariate logistic regression analysis.

Parameters	OR (95% CI)	P
Dactylitis	12.0 (2.7,53.5)	0.001
Family history of PsO/PsA	3.1 (1.2–8.4)	0.022
Nail involvement	3.5 (1.4–9.3)	0.010
PASI score	1.0 (0.9–1.1)	0.343
New bone formation on X-ray	14.8 (5.3–41.4)	<0.01
Synovitis on US	0.9 (0.4–2.5)	0.943
Tenosynovitis on US	21.3 (6.8–66.9)	<0.01
Enthesitis on US	21.7 (7.7–61.4)	<0.01
Erosion on US	2.7 (0.9–7.5)	0.055

PsA, psoriatic arthritis; PsO, psoriasis; PASI, Psoriasis Area and Severity Index; US, ultrasound.

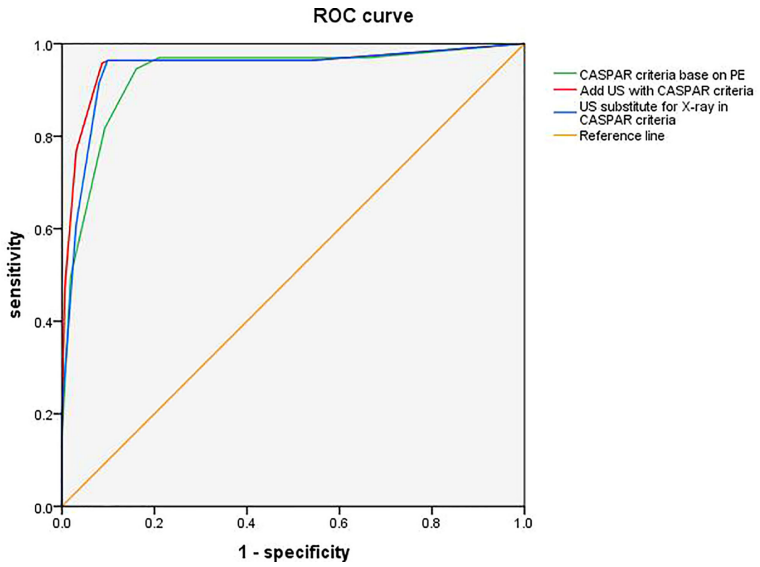

FIGURE 2
Receiver operating characteristic (ROC) curves for adding US or substituting X-ray by US in CASPAR. ROC curve illustrates the diagnosis performance of CASPAR with US added, CASPAR with replacing X-ray by US, and CASPAR based on physical examination only. The corresponding areas under the ROC curves (AUC) were 0.954 (95% CI 0.928, 0.979; p <0.01), 0.944 (95% CI 0.916, 0.972; p <0.01), and 0.933 (95% CI 0.903, 0.962; p <0.01). CASPAR, ClASsification criteria for Psoriatic Arthritis; US, ultrasound.

the diagnosis of PsA (16). In this study, 326 patients with suspected PsA were included and detected for various pathological changes, including inflammatory and chronic lesions on US. We found higher frequencies of synovitis, tenosynovitis, enthesitis, and bone erosion in PsA patients compared with the non-PsA group. Among these lesions, tenosynovitis and enthesitis were identified as independent risk factors for PsA. Further analysis revealed significantly improved specificity and fair sensitivity of CASPAR for the diagnosis of PsA when US tenosynovitis (87.0% and 59.1%) or US enthesitis (85.8% and 63.4%) were incorporated. In line with our study, Zabotti et al. reported that the presence of at least one extra-synovial feature in hands on US was significantly associated with early PsA, with specificity of 88.1% and sensitivity of 68.0% (17). Qiu et al. found that joint synovitis, bone erosions, tenosynovitis, and enthesitis on US were more frequently observed in PsA patients than in non-PsA patients. Tendon sheath synovial thickening showed the highest sensitivity (78.5%), while PD signal and bone erosion of enthesis showed high specificities (94.6% and 96.9% respectively) for PsA (18). A systemic review of 20 studies indicated that US tenosynovitis was highly specific (95%–100%) but entheseal lesions showed considerable variation in specificity (33%–99%) (19). There were several possible reasons to explain these discrepancies, for instance, different lesions and sites assessed, diverse enrolled patients, and study designs. In the study, we used a similar US protocol to the UPSTREAM study, but we additionally scanned four joints (bilateral elbow and ankle) and four entheses (bilateral common flexor tendon and triceps tendon). The US protocol in revealing typical changes in PsA has been validated by a few studies (20, 21).

The recognition of PsA by either the US alone or CASPAR based on physical examination alone was unsatisfactory. But when US was used with CASPAR, the specificity was increased from 84.0% to 91.4% while keeping the sensitivity for PsA diagnosis. Although based on limited evidence (22), US assessment integrated with clinical assessment has been proposed to improve the early identification of PsA. Our study confirmed the diagnostic value of the US evaluation for CASPAR. An X-ray is an invasive procedure and is incapable of disclosing inflammation. Although new bone formation on an X-ray is a characteristic feature of PsA, standing for long-term structural damage secondary to inflammation, and it is therefore unhelpful for early diagnosis. US, in contrast, is a sensitive, reliable, and non-radiative tool. Therefore, it would be beneficial if the X-ray could be substituted with US. In our study, when we modified the CASPAR by substituting the X-ray with US, both the sensitivity and specificity were as good as the modified CASPAR with US added. The area under the ROC curve was also similar between *the* modified CASPAR criteria. For the same diagnostic performance, the use of a radiation-free imaging modality is preferable. Therefore, US should be recommended as a substitute for X-rays in CASPAR.

The advantages of this study are the comprehensive evaluation of US in addition to clinical assessment and the large number of patients enrolled in a single center study. We are aware of some limitations. First, the PsA and non-PsA patients in our study were not sex-matched, but this bias was corrected

by the multivariate statistical analysis. Second, US features were not evaluated quantitively and did not distinguish between inflammatory or structural damage components. The US scan protocol is complicated and time-consuming. Future studies on establishing a simplified US score system that encompasses both joint and extra-articular structures are warranted. Third, using only one US examiner for all patients in our study reduced the inter-observer bias by its maximum but could not guarantee intra-observer reliability. Fourth, the conclusions from this single-center study still require external validation.

Conclusion

The modified CASPAR (the integration of US) improves the diagnosis utility. Moreover, X-rays can be substituted with US, which is a valuable tool in assisting the diagnosis of PsA in clinical practice.

Data availability statement

The raw data supporting the conclusions of this article will be made available by the authors, without undue reservation.

Ethics statement

This study was reviewed and approved by the Ethics Committee of Peking University First Hospital. The patients/participants provided their written informed consent to participate in this study.

Author contributions

ZZ conceived of the study and critically revised the manuscript. YG had full access to all the data collection, analysis, interpretation, and drafted the manuscript. ZS, XZ, XD, and YW contributed to the data collection. All authors contributed to the article and approved the submitted version.

Funding

This work was supported by the Interdisciplinary Clinical Research Project of the Peking University First Hospital (2021CR30), the Youth Clinical Research Project of the Peking University First Hospital (2019CR28), and the National Natural Science Foundation of China (grant nos. 81901646, 81801611, 81971524 and 81771740).

Acknowledgments

The authors would like to thank all the patients and rheumatology nurses who contributed to our study. Patients or the public were not involved in the design, conduct, reporting, or dissemination plans of our research.

Conflict of interest

The authors declare that the research was conducted in the absence of any commercial or financial relationships that could be construed as a potential conflict of interest.

Publisher's note

References

1. Ritchlin CT, Colbert RA, Gladman DD. Psoriatic arthritis. *N Engl J Med* (2017) 376(10):957–70. doi: 10.1056/NEJMra1505557

2. Taylor W, Gladman D, Helliwell P, Marchesoni A, Mease P, Mielants H, et al. Classification criteria for psoriatic arthritis: Development of new criteria from a Large international study. *Arthritis Rheumatism* (2006) 54(8):2665–73. doi: 10.1002/art.21972

3. Freeston JE, Coates LC, Nam JL, Moverley AR, Hensor EM, Wakefield RJ, et al. Is there subclinical synovitis in early psoriatic arthritis? a clinical comparison with Gray-scale and power Doppler ultrasound. *Arthritis Care Res* (2014) 66 (3):432–9. doi: 10.1002/acr.22158

4. Mandl P, Navarro-Compan V, Terslev L, Aegerter P, van der Heijde D, D'Agostino MA, et al. Eular recommendations for the use of imaging in the diagnosis and management of spondyloarthritis in clinical practice. *Ann Rheumatic Dis* (2015) 74(7):1327–39. doi: 10.1136/annrheumdis-2014-206971

5. Szkudlarek M, Court-Payen M, Strandberg C, Klarlund M, Klausen T, Ostergaard M. Power Doppler ultrasonography for assessment of synovitis in the metacarpophalangeal joints of patients with rheumatoid arthritis: A comparison with dynamic magnetic resonance imaging. *Arthritis Rheumatism* (2001) 44 (9):2018–23. doi: 10.1002/1529-0131(200109)44:9<2018::AID-ART350>3.0.CO;2-C

6. D'Agostino MA, Terslev L, Aegerter P, Backhaus M, Balint P, Bruyn GA, et al. Scoring ultrasound synovitis in rheumatoid arthritis: A eular-omeract ultrasound taskforce-part 1: Definition and development of a standardised, consensus-based scoring system. *RMD Open* (2017) 3(1):e000428. doi: 10.1136/rmdopen-2016-000428

7. Balint PV, Terslev L, Aegerter P, Bruyn GAW, Chary-Valckenaere I, Gandjbakhch F, et al. Reliability of a consensus-based ultrasound definition and scoring for enthesitis in spondyloarthritis and psoriatic arthritis: An omeract us

initiative. *Ann Rheumatic Dis* (2018) 77(12):1730–5. doi: 10.1136/annrheumdis-2018-213609

8. Wakefield RJ, Balint PV, Szkudlarek M, Filippucci E, Backhaus M, D'Agostino MA, et al. Musculoskeletal ultrasound including definitions for ultrasonographic pathology. *J Rheumatol* (2005) 32(12):2485–7.

9. van der Heijde D. How to read radiographs according to the Sharp/Van der heijde method. *J Rheumatol* (1999) 26(3):743–5.

10. Zlatkovic-Svenda M, Kerimovic-Morina D, Stojanovic RM. Psoriatic arthritis classification criteria: Moll and Wright, essg and Caspar – a comparative study. *Acta Reumatol Port* (2013) 38(3):172–8.

11. Haroon M, Gallagher P, FitzGerald O. Diagnostic delay of more than 6 months contributes to poor radiographic and functional outcome in psoriatic arthritis. *Ann Rheumatic Dis* (2015) 74(6):1045–50. doi: 10.1136/annrheumdis-2013-204858

12. Fiorenza A, Bonitta G, Gerratana E, Marino F, Sarzi-Puttini P, Salaffi F, et al. Assessment of enthesis in patients with psoriatic arthritis and fibromyalgia using clinical examination and ultrasound. *Clin Exp Rheumatol* (2020) 38 Suppl 123(1):31–9.

13. Acquacalda E, Albert C, Montaudie H, Fontas E, Danre A, Roux CH, et al. Ultrasound study of entheses in psoriasis patients with or without musculoskeletal symptoms: A prospective study. *Joint bone Spine Rev du Rhumatisme* (2015) 82 (4):267–71. doi: 10.1016/j.jbspin.2015.01.016

14. Bandinelli F, Prignano F, Bonciani D, Bartoli F, Collaku L, Candelieri A, et al. Ultrasound detects occult entheseal involvement in early psoriatic arthritis independently of clinical features and psoriasis severity. *Clin Exp Rheumatol* (2013) 31(2):219–24.

15. De Simone C, Caldarola G, D'Agostino M, Carbone A, Guerriero C, Bonomo L, et al. Usefulness of ultrasound imaging in detecting psoriatic arthritis of fingers and toes in patients with psoriasis. *Clin Dev Immunol* (2011) 2011:390726. doi: 10.1155/2011/390726

16. Zabotti A, Bandinelli F, Batticciotto A, Scire CA, Iagnocco A, Sakellariou G, et al. Musculoskeletal ultrasonography for psoriatic arthritis and psoriasis patients: A systematic literature review. *Rheumatol (Oxford)* (2017) 56(9):1518–32. doi: 10.1093/rheumatology/kex179

17. Zabotti A, Errichetti E, Zuliani F, Quartuccio L, Sacco S, Stinco G, et al. Early psoriatic arthritis versus early seronegative rheumatoid arthritis: Role of dermoscopy combined with ultrasonography for differential diagnosis. *J Rheumatol* (2018) 45(5):648–54. doi: 10.3899/jrheum.170962

18. Tang Y, Cheng S, Yang Y, Xiang X, Wang L, Zhang L, et al. Ultrasound assessment in psoriatic arthritis (Psa) and psoriasis vulgaris (Non-psa): Which sites are most commonly involved and what features are more important in psa? *Quant Imaging Med Surg* (2020) 10(1):86–95. doi: 10.21037/qims.2019.08.09

19. Sakellariou G, Scire CA, Adinolfi A, Batticciotto A, Bortoluzzi A, Delle Sedie A, et al. Differential diagnosis of inflammatory arthropathies by musculoskeletal ultrasonography: A systematic literature review. *Front Med (Lausanne)* (2020) 7:141. doi: 10.3389/fmed.2020.00141

20. Zabotti A, Piga M, Canzoni M, Sakellariou G, Iagnocco A, Scire CA. Ultrasonography in psoriatic arthritis: Which sites should we scan? *Ann Rheumatic Dis* (2018) 77(10):1537–8. doi: 10.1136/annrheumdis-2018-213025

21. Canzoni M, Piga M, Zabotti A, Scire CA, Carrara G, Olivieri I, et al. Clinical and ultrasonographic predictors for achieving minimal disease activity in patients with psoriatic arthritis: The upstream (Ultrasound in psoriatic arthritis treatment) prospective observational study protocol. *BMJ Open* (2018) 8(7):e021942. doi: 10.1136/bmjopen-2018-021942

22. Gutierrez M, Draghessi A, Bertolazzi C, Erre GL, Saldarriaga-Rivera LM, Lopez-Reyes A, et al. Ultrasound in psoriatic arthritis. can it facilitate a best routine practice in the diagnosis and management of psoriatic arthritis? *Clin Rheumatol* (2015) 34(11):1847–55. doi: 10.1007/s10067-015-3053-4

frontiers | Frontiers in Medicine

TYPE Original Research
PUBLISHED 20 October 2022
DOI 10.3389/fmed.2022.1015895

OPEN ACCESS

EDITED BY
Andrea Di Matteo,
Marche Polytechnic University, Italy

REVIEWED BY
Edoardo Cipolletta,
Marche Polytechnic University, Italy
Andrea Becciolini,
University Hospital of Parma, Italy
Juan Jose De Agustin,
Vall d'Hebron University Hospital, Spain

*CORRESPONDENCE
Gabor Baksa
gabor.baksa.md@gmail.com

SPECIALTY SECTION
This article was submitted to Rheumatology, a section of the journal Frontiers in Medicine

RECEIVED 10 August 2022
ACCEPTED 03 October 2022
PUBLISHED 20 October 2022

CITATION
Baksa G, Czeibert K, Sharp V, Handschuh S, Gyebnar J, Barany L, Benis S, Nyiri G, Mandl P, Petnehazy O and Balint PV (2022) Vascular supply of the metacarpophalangeal joint. *Front. Med.* 9:1015895. doi: 10.3389/fmed.2022.1015895

Vascular supply of the metacarpophalangeal joint

Gabor Baksa[1]*, Kalman Czeibert[2], Veronika Sharp[3], Stephan Handschuh[4], Janos Gyebnar[5], Laszlo Barany[1,6], Szabolcs Benis[7], Gabor Nyiri[8], Peter Mandl[9], Ors Petnehazy[10,11] and Peter Vince Balint[12,13]

[1]Laboratory for Applied and Clinical Anatomy, Department of Anatomy, Histology and Embryology, Semmelweis University, Budapest, Hungary, [2]Department of Ethology, Institute of Biology, Eötvös Loránd University, Budapest, Hungary, [3]Division of Rheumatology, Department of Medicine, Santa Clara Valley Medical Center, San Jose, CA, United States, [4]VetCore Facility for Research, University of Veterinary Medicine Vienna, Vienna, Austria, [5]Medical Imaging Centre, Faculty of Medicine, Semmelweis University, Budapest, Hungary, [6]Department of Neurosurgery, University of Erlangen-Nürnberg, Erlangen, Germany, [7]Department of Orthopedic Surgery and Traumatology, Ghent University Hospital, Ghent, Belgium, [8]Laboratory of Cerebral Cortex Research, Institute of Experimental Medicine, Budapest, Hungary, [9]Division of Rheumatology, Department of Internal Medicine III, Medical University Vienna, Vienna, Austria, [10]Medicopus Non-profit Ltd, Kaposvar, Hungary, [11]Justanatomy Ltd, Kaposvar, Hungary, [12]Károly Rácz Doctoral School of Clinical Medicine, Semmelweis University, Budapest, Hungary, [13]3rd Department of Rheumatology, National Institute of Rheumatology and Physiotherapy, Budapest, Hungary

Objective: To describe in detail the arterial vasculature of metacarpophalangeal joints 2–5 on cadaver specimens and to compare it to ultrasound imaging of healthy subjects.

Methods: Eighteen hands of donated human cadavers were arterially injected and investigated with either corrosion casting or cryosectioning. Each layer of cryosectioned specimens was photographed in high-resolution. Images were then segmented for arterial vessels of the metacarpophalangeal (MCP) joints 2–5. The arterial pattern of the joints was reconstructed from the segmented images and from the corrosion cast specimens. Both hands of ten adult healthy volunteers were scanned focusing on the vasculature of the same joints with high-end ultrasound imaging, including color Doppler. Measurements were made on both cryosectioned arteries and Doppler images.

Results: The arterial supply of MCP joints 2–5 divides into a metacarpal and a phalangeal territory, respectively. The metacarpal half receives arteries from the palmar metacarpal arteries or proper palmar digital arteries, while the phalangeal half is supplied by both proper and common palmar digital arteries. Comparing anatomical and ultrasonographic results, we determined the exact anatomic location of normal vessels using Doppler images acquired of healthy joints. All, except three branches, were found with less than 50% frequency using ultrasound. Doppler signals were identified significantly more frequently in MCP joints 2–3 than on 4–5 ($p < 0.0001$). Similarly, Doppler signals differed in the number of detectable small, intraarticular vessels ($p < 0.009$), but not that of the large extraarticular ones ($p < 0.1373$). When comparing

measurements acquired by ultrasound and on cadaver vessels, measurements using the former technique were found to be larger in all joints ($p < 0.0001$).

Conclusion: Using morphological and ultrasonographic techniques, our study provides a high-resolution anatomical maps and an essential reference data set on the entire arterial vasculature of healthy human MCP 2–5 joints. We found that Doppler signal could be detected in less than 50% of the vessels of healthy volunteers except three locations. Intraarticular branches were detected with ultrasound imaging significantly more frequently on healthy MCP 2–3 joints, which should be taken into account when inflammatory and normal Doppler signals are evaluated. Our study also provides reference data for future, higher-resolution imaging techniques.

KEYWORDS

arterial supply, articular, Doppler, metacarpophalangeal joint, rheumatoid arthritis, ultrasound

Introduction

Inflammation of tissues and/or vessels of different location and size is a major component of common rheumatological pathologies such as synovitis, enthesitis and vasculitis (1–4). Metacarpophalangeal (MCP) joints are frequently involved in inflammatory arthritides especially in rheumatoid arthritis (RA), psoriatic arthritis (PsA), and juvenile idiopathic arthritis (5–7). Additionally, finger arteries are often affected in various types of vasculitides (3). Color-, power Doppler, and B (brightness)-flow ultrasonography can visualize the blood flow inside vessels of different sizes (8). Spectral Doppler can depict this same blood flow in a graph (9). Advanced imaging applications targeting microvascular imaging are evolving techniques (10, 11), which can detect velocity of blood cells in real-time, while contrast-enhanced ultrasound is based on detecting intravenous microbubbles (12). Ultrasound is capable of recording both still images or videos of musculoskeletal tissue in various regions during static or dynamic examination (13). However, ultrasound has its own limitations. Without an acoustic window or without adequate sensitivity for small vessels or for slow flow, ultrasound is not capable of detecting flow signal (8). All limitations and advantages considered, ultrasound has a better resolution but is much less sensitive for detecting color than the human eye. Most humans are trichromats and are able to distinguish 10 million shades of color while a typical high-end ultrasound unit can display only around 256 shades (14–16).

Ultrasonography is commonly used by rheumatologists to detect pathological blood flow in a plethora of subclinical or clinical rheumatic and musculoskeletal disease (RMD) or to document diminished flow in cases of Raynaud phenomenon (5, 17, 18). However, one needs to be cognizant that nowadays high-end ultrasound equipment is also capable of detecting normal blood flow (with some limitations) in healthy or asymptomatic joints (19, 20).

Operator dependency has been an obstacle to rheumatological ultrasonography. For proficiency in ultrasonography not only proper image acquisition but correct interpretation is paramount. Besides a deep understanding of ultrasound physics and equipment operation techniques, a high level of anatomical and pathological knowledge is crucial to perform musculoskeletal ultrasonography appropriately. While large vessel anatomy of the hand is routinely taught at medical courses, small vessel anatomy is usually only included in teaching material for hand surgical specialties (21).

The aim of this study was to map the arterial vasculature of MCP joints 2–5 using hand corrosion casts and cryosectioning from injected cadaver specimens, two validated anatomical techniques (22). In addition, we used musculoskeletal ultrasound investigation of healthy individuals, a readily accessible, patient-friendly imaging technique, in order to provide an atlas, which would facilitate distinguishing Doppler flow in healthy vessels from pathological signal seen in RMDs.

Materials and methods

Source and preparation of cadaveric specimens

Cadaveric specimens with post mortem time 1–4 days were harvested from donated bodies at the Department of Anatomy, Histology and Embryology, Semmelweis University, Budapest, Hungary. Body donation is permitted and controlled by Section 222 of Chapter 12 of Act CLIV on Health 1997 and by Senate's decree Act 110/2020. (VII.07.) "Handling procedures of donated

human material (body/organ/tissue)." Hands of female and male cadavers were separated 7–10 cm above the wrist. Both the radial and the ulnar arteries were identified, cannulated and irrigated with saline. At this step both hands of one male and one female cadaver were further prepared for cryosectioning, while the remaining hands underwent corrosion casting.

Cryosectioning

The arteries were injected with Vytaflex 20® (Smooth-On Inc., Macungie, PA, USA) polyurethane colored with So Strong® (Smooth-On Inc., Macungie, PA, USA) red tint. Following a 24-h hardening time at 4°C the hands were placed on −30°C. After the hands were frozen, four blocks each containing one region-of-interest (MCP 2–5) were cut out using a band saw. The blocks extended from the middle of the proximal phalanx of the 3rd finger distally to the middle of the metacarpal bone of the thumb proximally in the axial plane. All four metacarpal blocks per cadaver were positioned in one plastic container facing palmar side down, then embedded in porcine gelatin (G2500-500G, gel strength 300, Type A) (SIGMA-ALDRICH Chemie GmbH, Steinheim, Germany) and were kept on −80°C after the gelatin hardened. Cryosectioning was carried out with the plastic container attached to a CNC milling machine (NCT Kondia 640B, NCT, Budapest, Hungary; rotational speed 3,000 rpm, cutter diameter 200 mm, feed rate 800 mm per revolution). The layer thickness of milling was 50 μm. At every milling step the fresh surface was photographed with a Canon EOS 5DS camera at 8,688 × 5,792 pixels resolution per image. Images were then processed using Adobe Photoshop CS3[1] and Thermo Fisher Scientific Amira for Life Sciences 6.1 software.[2] Since the subsequent image segmentation step in Amira required a 8-bit grayscale volume, we used a Photoshop algorithm to convert the RGB (Red Green Blue) volume to a grayscale image stack, while maintaining the high contrast of the arteries using a selective red color channel subtraction. The grayscale images were then imported into Amira. Possible minor image dislocations were corrected with the "Align Slices" module. Subsequently, using the "Segment Editor" panel of the "Edit New Label Field" module, semi-automatic segmentation was performed to model the arteries. Measurements were taken at predefined locations detailed by the results (section "Measurements on cryosectioned specimens"). The applied technique of cryosectioning, including the steps of image processing and segmentation of the vessels is described in an earlier publication by our group (22).

Corrosion casting

The remaining hands were injected with ACRIFIX 190 (2 R 0190) (Evonik Industries AG., Germany) colored with red Akemi Akepox coloring paste (AKEMI GmbH., Nurnberg, Germany) and catalyzed with Betox 50-PC hardener (Oxytop Sp. z o.o., Stęszew, Poland). Following a 24-h hardening time, the hands were put separately in 2 L plastic containers filled with tap water and adjusted with two Somat Gold 12 Actions (Henkel AG., Germany) dishwasher tablets. The specimens were kept in this solution at +36°C for 6–10 weeks. The solution was changed every 2–3 weeks, while the specimens were handled with great care to avoid fracture of the intermediate corrosion casts due to potential tearing caused by movement of the soft tissue mass. After all soft tissue was digested, the specimens were carefully washed and left in cold water for 3 days to eliminate the remaining chemicals and odor. The vascular pattern of each MCP joint 2–5 were investigated visually and if needed with a Wild Heerbrugg M5A stereomicroscope (Wild Heerbrugg Switzerland Microscope, Switzerland) using 12–50× magnification. All findings were documented using a Canon EOS 5D digital camera, Macro Ring Lite MR-14EX flash and 50, 100, and 65 mm macro lenses (CANON Inc., Tokyo, Japan), respectively.

Ultrasound examination

Study participants

All examined persons were asymptomatic without current diagnosis of rheumatic and musculoskeletal hand disease. MCP joints 2–5 of both hands were scanned for vascular signals using an ultrasonography machine (GE Logiq E9, General Electric Company, Boston, MA, USA) equipped with a small-footprint high-frequency ultrasound transducer (GE L8-18i).

Scanning method

Before scanning a joint, patients were asked to place their examined hand in a tap water bath measuring 38°C as confirmed by a thermometer for 4 min to eliminate confounding of outdoor temperature and of individual temperature variance of the hands. No other vasodilating method or agent was used. For scanning, hands were first positioned palm down, fingers extended and slightly abducted, after which hands were placed palm up, with the fingers kept in the same position. Scanning was carried out on both the palmar and dorsal side of each examined joint, and additionally on the radial side of the 2nd and on the ulnar side of the 5th MCP joints, respectively. The ultrasound machine was used in color Doppler mode. The parameters for color Doppler were 11.9 MHz, PRF 0.6, WF 54, and the Doppler box was set to maximal size in both the horizontal and vertical planes and gain was reduced until artifacts disappeared. The settings were kept unchanged for each ultrasound examination except for the value of the color gain which was adjusted if needed within a very narrow range (15.5–19). The ultrasound transducer was held parallel to the force bearing axis of the metacarpal bone on every side of the examined joint. Each joint was scanned from the radial to the ulnar margin. Additionally, the radial side of the 2nd and the

1 www.adobe.com

2 www.fei.com

ulnar side of the 5th metacarpal joints were scanned from the dorsal to the palmar surface. Special care was taken to use abundant gel and to avoid compression to prevent temporary closure of smaller blood vessels.

Image interpretation and measurement

Doppler signals were interpreted as valid if both of the following criteria were met: (1) the localization of the Doppler signal had to match a vessel on both cryosectioned and corrosion cast anatomical specimens; (2) reverberating Doppler signals were excluded. The strength and extension of the Doppler signal had no influence on the decision of validity. Measurements were taken on the shortest diameter of the vascular signals.

Statistical analysis

The statistical analysis was performed using the R Software (version 4.0.3). The level of the statistical significance was set at $p = 0.05$. Fisher's exact test was used for comparing categorical variables. Continuous variables were compared using two-sampled t-test after confirming their normal distribution using Shapiro–Wilk test.

Results

Cadaveric specimens

Eight right and six left hands of 8 female cadavers (ages 55–84 years, mean 69.5 ± 14.5 years) and three right and two left hands of 4 male cadavers (ages 48–94 years, mean 71 ± 23 years) were used for anatomical preparation. The arteries of both hands of a 48-year-old male and a 55-year-old female cadaver were used for cryosectioning while the remaining hands were used for corrosion casting. The number of joints used for each technique are shown in Table 1. Seven joints (1 MCP1, 1 MCP2, 2 MCP4, and 3 MCP5 joint) were excluded from the anatomical techniques either due to damage during the preparation procedure (corrosion casting, n:3) or due to failed injection (cryosectioning, n:4). Based on the corrosion casting and cryosectioning results we divided the arterial supply into metacarpal (proximal half) and phalangeal (distal half) territories, respectively. As many corrosion cast specimens suffered partial injuries of the phalangeal territory despite careful handling, the blood supply of the distal half of the metacarpal joints was investigated only on cryosectioned specimens. However, the total number of investigated joint specimens was large enough in both territories to determine their general arterial pattern, and to compare it with ultrasound imaging results.

TABLE 1 Number of metacarpophalangeal joints 2–5 by method of investigation.

Investigation method	MCP2	MCP3	MCP4	MCP5
Corrosion casting[a]	15	15	14	13
Cryosectioning	3	3	3	3
Ultrasound	20	20	19	18
Total number of joints	38	38	36	34

MCP, metacarpophalangeal joint.
[a]Investigated only for the blood supply of the metacarpal territory.

Arterial supply of the metacarpal territory on cadaveric specimens

In general, for each metacarpal joint we found two main supplying arteries arising from the palmar side, each giving off further articular branches. One vessel ran toward the radial and the other vessel toward the ulnar side. Therefore, we labeled these "R-branch" and "U-branch," respectively. Both the R- and U-branch were present as single vessels in 69/69 (100%) joints investigated with corrosion casting or cryosectioning. Usually they originated from the palmar metacarpal arteries (PMA) of the deep palmar arch (DPA), except for the MCP5 joint, where the proper palmar digital artery (PPDA) was the most frequent source. Representative images of the anatomical variants are shown on Figure 1, their distribution in Table 2.

In numerous cases, the R- and U-branches formed connections to the DMA or its collateral branch parallel to the metacarpal shaft. Specific examples are connections at the MCP5 joint to the carpal rete and simultaneous anastomoses with the vessels listed above. In total, single or multiple anastomoses were seen depending on joint location radially in 60–88.89% of cases, ulnar in 61.11–82.35% of cases (these ranges represent the different probabilities of localizations on MCP2-MCP5, Figures 1D, 2A). Coursing further on the lateral surface of metacarpal heads, both the R- and U-branches gave off a single and strong forward running artery in 88.41% of the joints. In the remaining 11.59% of the joints the same was found, only either radially or ulnar, except one case of bilateral absence. Parallel to this vessel, which we labeled the "main lateral artery" (MLA), a shorter "accessory lateral artery" (ALA) was detected radially in 12 joints (17.39%) and ulnar in 12 joints (17.39%). These originated either from the MLA, or directly from the R- and U-branches below or above the origin of the MLA. A last segment of the R- and U-branches curving on to the dorsal surface of the metacarpal head was recognized radially in 81.25–94.44%, on the ulnar side in 72.22–94.44% of joints, respectively. In 49.28% they formed an anastomosis immediately according to the dorsal depression, which we labeled the "dorsal arcade" (DA) (Figures 2, 3B, 4A–C). Simultaneously, in five specimens (7.25%) an anastomosis was detected between the R- and U-branches. In these cases, a complete arterial ring was present around the metacarpal head. The frequency of these findings is summarized in Table 3.

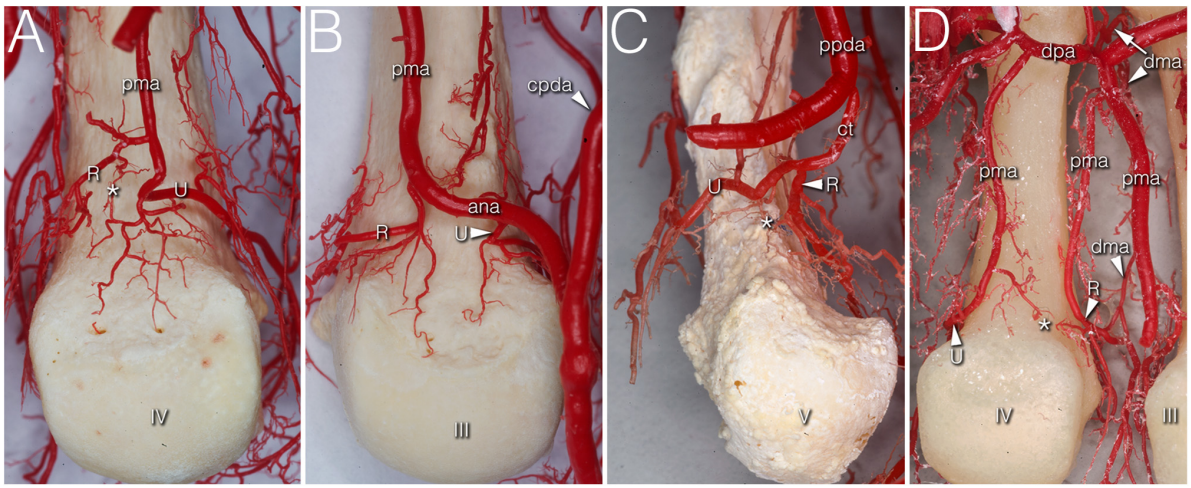

FIGURE 1
Variations of R- and U- branches on corrosion cast specimens (palmar view). **(A)** Dominant U-branch as a continuation of the palmar metacarpal artery. Note the two palmar enosseal vessels originating as a common trunk from the U-branch. **(B)** The U-branch originates from the anastomosis between the palmar metacarpal artery and the common palmar digital artery. **(C)** The R- and U-branches originate as a common trunk from the 10th proper palmar digital artery. **(D)** The R-branch originates from the early dividing neighboring palmar metacarpal artery. The U-branch is the continuation of a separately originating palmar metacarpal artery. Note the dorsal metacarpal artery anastomosing with the R-branch. ana, anastomosis between the palmar metacarpal artery and the common palmar digital artery; *, anastomosis between R and U branch; cpda, common palmar digital artery; ct, common trunk; dma, dorsal metacarpal artery; dpa, deep palmar arch; pma, palmar metacarpal artery; ppda, proper palmar digital artery; R, R-branch; U, U-branch; III, IV, V: 3rd, 4th, and 5th metacarpal heads.

TABLE 2 Varying origins of the radial and ulnar branches based on localization.

		MCP2 *n* = 18 (%)	MCP3 *n* = 18 (%)	MCP4 *n* = 17 (%)	MCP5 *n* = 16 (%)
R-branch	PMA (%)	**13** (72.2)	**5** + **13**[c] (100)	**13** + **1**[c] (82.4)	**5** (31.25)
	PPDA (%)	**5**[a] (27.8)	0	0	**10** (62.5)
	DMA (%)	0	0	**3**[d] (17.6)	**1**[d] (6.25)
U-branch	PMA (%)	**11** (61.1)	**5** + **13**[c] (100)	**16** + **1**[c] (100)	**4** (25.0)
	PPDA (%)	0	0	0	**12** (75.0)
	PMA/CPDA anastomosis (%)	**7**[b] (38.9)	0	0	0

CPDA, common palmar digital artery; DMA, dorsal metacarpal artery; PMA, palmar metacarpal artery; PPDA, proper palmar digital artery; R, radial; U, ulnar.
[a]If no princeps pollicis artery is present, then this shows the origin from the 3rd proper palmar digital artery.
[b]Common palmar digital artery supplied partially or completely by the palmar metacarpal artery.
[c]Early division or separate ('doubled') origin of palmar metacarpal artery.
[d]Main supply from the dorsal metacarpal artery or its collateral branch, both of them derived from the deep palmar arch. Proximally thin origin from the palmar metacarpal artery.

During their course, the R- and the U-branches, the MLA and the ALA, respectively, give off radially (64.29–94.12%), or on the ulnar side (70.59–100.00%) 1–4 small branches to the hollow lateral surface of the metacarpal head, which we labeled the "lateral depression" (Figure 2). We investigated the MLA and ALA in the coronal plane of the cryosectioned specimens. In all cases these ran on the outer surface of a triangular shaped enthesis over the metacarpal head and the base of the proximal phalanx. The small branches to the lateral depression penetrated this enthesis. Therefore, we labeled them "enthesial branches" (Figures 4A–C).

The MLA then curved radially (50.00–62.50%) or ulnar (38.89–76.47%) into the space in the dorsal compartment between the articulating bones and terminated there with or without anastomosing with the contralateral MLA (Figures 2A,B). These terminal segments of the MLA were consequently found to supply the dorsal triangle on the cryosectioned specimens (Figures 4A,D). Independent from the presence or absence of an anastomosis, we labeled these "triangular arcades." In two isolated cases several small perpendicular branches were detected along this arcade showing a pectinate character in the axial plane (Figure 3B).

The most terminal arteries supplied the metacarpal heads. These appeared most frequently at the dorsal depression (1–7 vessels, 58.82–73.33%) coming from the dorsal arcade or, in case no anastomosis was present, from the terminal

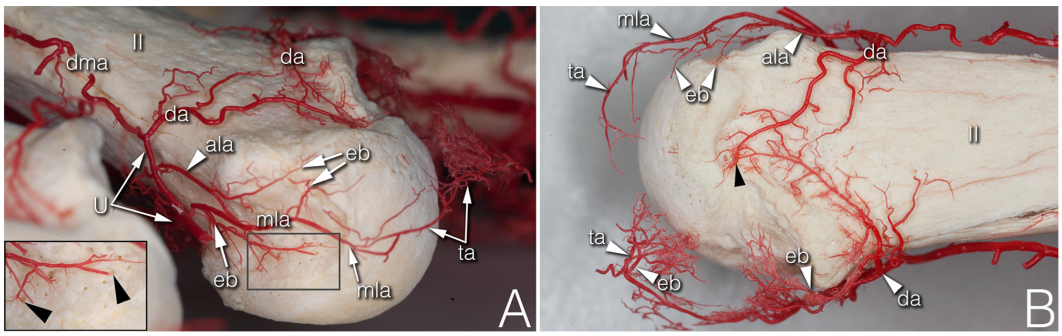

FIGURE 2
Supplying branches to the metacarpal territory on corrosion cast specimens. **(A)** (right hand anterolateral view) A strong enthesial branch arises directly from the first part of the main lateral artery and gives off branches running toward the nutrient foramina of the lateral depression (see insert). Both the upper accessory lateral artery and the main lateral artery give off one further enthesial branch to the upper part of the lateral depression. The main lateral artery curves to and terminates at the projection of the triangular arcade. **(B)** (upper view of the same specimen) Note the spiky character of the ulnar sided enthesial branches (top of image), while radially (bottom of image) both the enthesial branch and the triangular arcade artery demonstrate a bushy appearance. ala, accessory lateral artery; da, dorsal arcade; dma, dorsal metacarpal artery; eb, enthesial branch; mla, main lateral artery; ta, triangular arcade; U, U-branch; black arrowheads, entry point of enosseal arteries; II, 2nd metacarpal head.

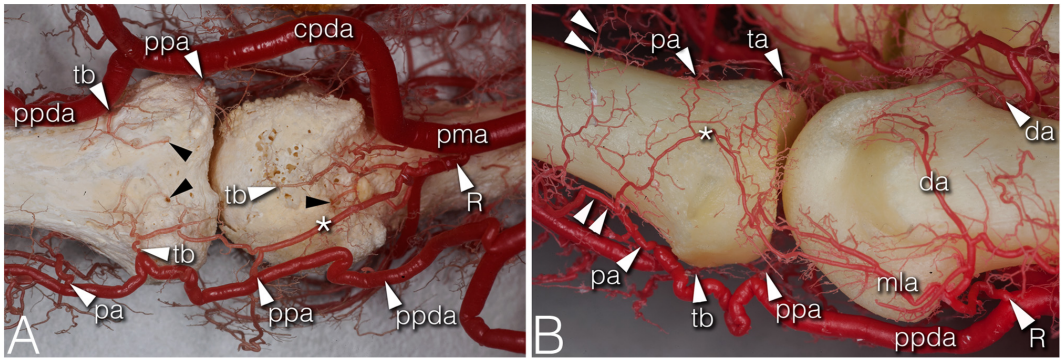

FIGURE 3
Arteries of the phalangeal territory on corrosion cast specimens. **(A)** (4th finger, palmar view) Note the long anastomosis between the R-branch and the palmar plate artery. Proximal from the anastomosis a short trunk arises acting as a tenosynovial vessel, with one branch reaching to the metacarpal head and another branch extending to the projection of the flexor tendon. **(B)** (2nd finger, dorsolateral view) The phalangeal arcade originates as one common trunk, with one branch supplying the arcade on the dorsal surface of the phalanx, and another branch forming a more superficial arcade according to the projection of the extensor hood. The triangular and phalangeal arcade are in connection through a short anastomosis. Note the small branches from the triangular arcade showing a pectinate character in the axial plane. *, anastomosis; cpda, common palmar digital artery; da, dorsal arcade; mla, main lateral artery; pa, phalangeal arcade; pma, palmar metacarpal artery; ppa, palmar plate artery; ppda, proper palmar digital artery; R, R-branch; ta, triangular arcade; tb, tenosynovial branch; black arrowheads, entry point of enosseal arteries; doubled arrowheads, supplying arch for the extensor tendon.

part of the R- and U-branches, respectively (Figure 2B). The second most frequent occurrence was found on the ulnar aspect (1–7 vessels, 26.67–66.67%) (Figure 2A). The third most common occurrence was on the palmar surface (1–5 vessels, 26.67–55.56%) (Figures 1A, 3A). The radial side showed the lowest occurrence (1–3 vessels, 17.65–27.78%). Both the radial and ulnar arteries originated from enthesial branches (Figures 4A–C), while the palmar ones originated directly from the R- and U-branches (Figures 1A, 4F). In cryosectioned specimens enosseal anastomoses of these arteries were also detected (Figures 4B,E,F).

Arterial supply of the phalangeal territory on cadaveric specimens

The main supplying vessels were the PPDAs and the CPDAs of each finger, respectively. In general, a short trunk was observed radially (66.67%) or ulnar (58.33% of all cases) either separate from the PPDAs or originating from the bifurcation point of CPDAs supplying the palmar plate. Therefore, we labeled these the "palmar plate arteries" (PPA) (Figure 4D).

Distally, the PPDAs gave off a second artery radially (83.33%) or ulnar (100%), which then branched into a long and thin, forward running vessel penetrating the flexor tendon

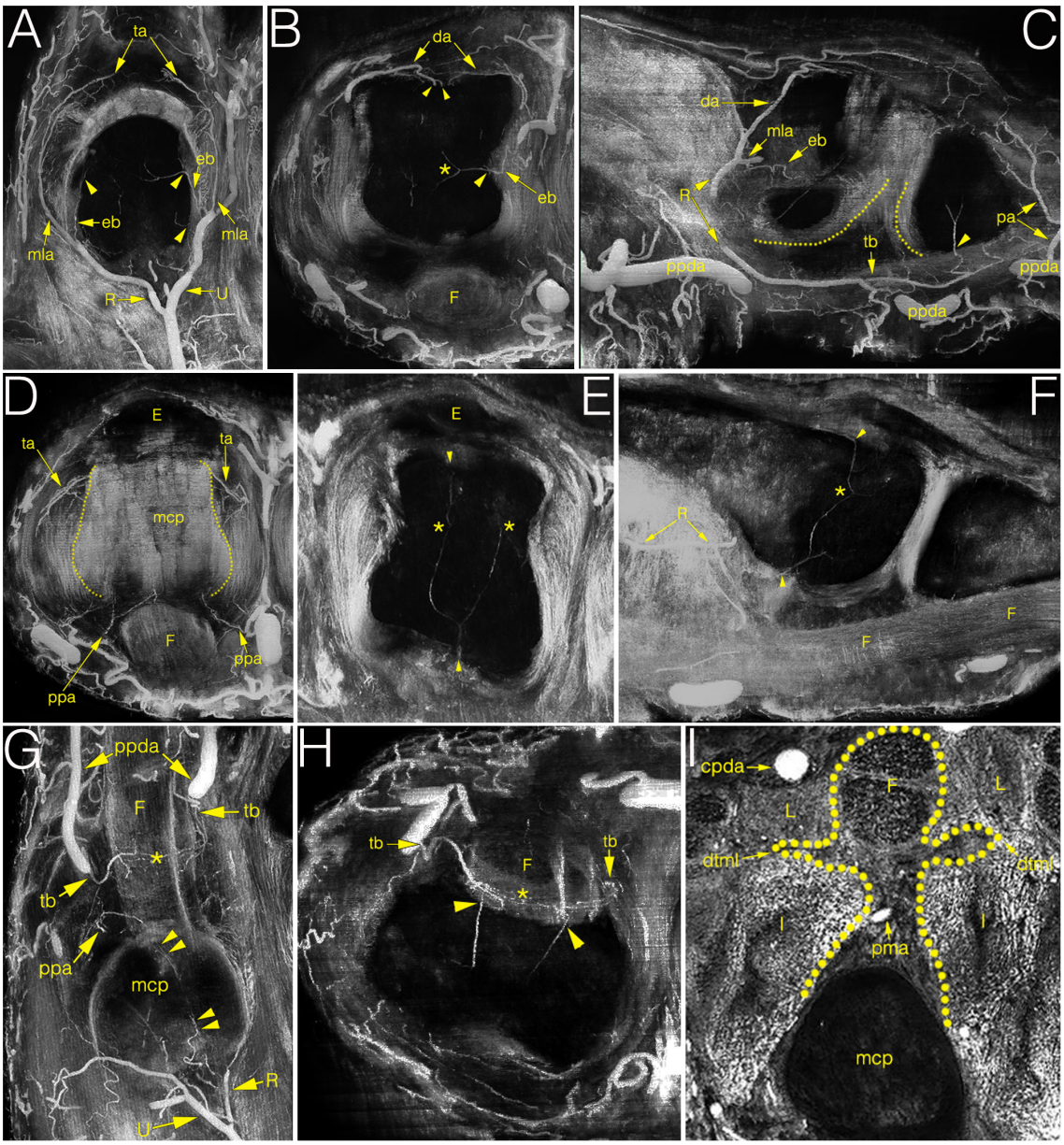

FIGURE 4
Multiplanar (MIP) image reconstructions on cryosectioned specimens demonstrating the relationship between arteries and joint structures. **(A–C)** main supplying branches on coronal, axial and sagittal plane, respectively. Note on C the elongated anastomosis between the R-branch and the tenosynovial branch. Dotted lines indicate the palmar articular surfaces of bones; **(D)** palmar plate artery and the triangular arcade on the axial plane. Dotted lines indicate the lateral borders of metacarpal head; **(E,F)** blood supply of the metacarpal head on the axial and sagittal plane. Note the anastomosis between the dorsal, palmar and lateral enosseal arteries, respectively. Compare with panel **(B)**. **(G,H)** origin and course of the tenosynovial trunk on the coronal and axial plane. Note the anastomosis between the two sides within the flexor tendon. **(I)** homuncule shaped (dotted line) soft tissue complex in the center with the palmar metacarpal artery on the axial plane. *, anastomosis; cpda, common palmar digital artery; da, dorsal arcade; dtml, deep transverse metacarpal ligament; eb, enthesial branch; E, extensor tendon; F, flexor tendon; I, interosseous muscle; L, lumbrical muscle; mcp, metacarpal; mla, main lateral artery; pa, phalangeal arcade; pma, palmar metacarpal artery; ppa, palmar plate artery; ppda, proper palmar digital artery; R, R-branch; ta, triangular arcade; tb, tenosynovial trunk; U, U-branch; arrowheads, entry point of enosseal arteries; doubled arrowheads, supplying artery from the R-branch to the flexor tendons.

sheaths, while its other branch coursed medially and backward to supply the palmar surface of the proximal phalanx's base. We labeled this artery "tenosynovial branch" (Figures 4G,H). In one case, the radial tenosynovial branch of the index finger originated directly from the R-branch and served small branches also to the palmar plate (Figure 4C). A third relevant branch was detected radially (50.00%) directly from the PPDA, but ulnar (41.67%) from the tenosynovial branch. These ran to

TABLE 3 Occurrence of the main lateral arteries, accessory lateral arteries and dorsal arcade at metacarpophalangeal joints 2–5.

$\Sigma_n = 69$		MCP2 $n = 18$ (%)	MCP3 $n = 18$ (%)	MCP4 $n = 17$ (%)	MCP5 $n = 16$ (%)
MLA	Bilateral(%)	**17** (94.4)	**16** (88.9)	**15** (88.2)	**13** (81.25)
	Radial (%)	–	**2** (11.1)	–	–
	Ulnar (%)	**1** (5.6)	–	**2** (11.8)[a]	**2** (12.5)
	Absent (%)	–	–	–	**1** (6.25)
ALA	Radial (%)	**3** (16.7)	**2** (11.1)	**3** (17.7)	**4** (25.00)
	Ulnar (%)	**1** (5.6)	**1** (5.6)	**3** (17.7)	**7** (43.8)
DA	Present (%)	**10** (55.6)	**8** (44.4)	**8** (47.1)	**8** (50.0)
	Absent (%)	**8** (44.4)	**10** (55.6)	**9** (52.9)	**8** (50.0)
	Multiple (%)	**4** (22.2)	–	**2** (12.5)	**4** (28.6)

[a]In one case the radial main lateral artery was absent, but the territory of it was from a deep seated dorsal metacarpal artery supplied.
ALA, accessory lateral artery; DA, dorsal arcade; MCP, metacarpophalangeal joint; MLA, main lateral artery.
The bold values describe the number of joints based on vascular findings and localization.

the dorsal side of the base of the proximal phalanx, where—independently from their origin - these branches anastomosed with the contralateral ones creating an arterial arch in 75.00% of the cases. The latter was labeled "phalangeal arcade" (Figures 3, 4C). In the remaining cases, where present, we observed the phalangeal arcade originating bilaterally from the MLA (16.67%).

Arteries with detectable size supplying the base of the proximal phalanx were detected only on the palmar and dorsal surfaces of the bone. On the palmar surface, symmetrically (both on the radial and ulnar side) one artery penetrated the bony cortex (83.33%). In one case, two arteries were observed radially. In one additional joint no supplying branch was found. The palmar vessels originated from the tenosynovial branch (Figures 3A, 4C,H). Dorsal phalangeal arteries were identified only in 50.00% of the joints branching directly from the phalangeal arcade. In 41.67% we found these only radially, in one case bilaterally. A schematic drawing about the general arterial pattern of metacarpophalangeal joints 2–5 is shown in Figure 5.

Measurements on cryosectioned specimens

The arterial diameters were measured in both the metacarpal (Figure 6) and the phalangeal territories. Attention was paid proximally to the R- and U-branches and their primary branches as the MLAs, DA and the arcade of the dorsal triangle, respectively. The R- and U-branches and the MLAs were measured next to their origin. The diameter of both arcades—also in cases when no anastomosis present—was recorded on both the radial and ulnar sides next to the midline of the metacarpal. Finally, the enthesial and bone supplying arteries were also measured. Distally, measurements were undertaken on the palmar plate artery, tenosynovial branch, phalangeal arcade and the supplying branches of the base of the proximal phalanx. The arcade was measured on both the radial and ulnar side of the midline of the phalanx. All the other vessels were measured at their origins. Data are summarized in Supplementary Table 1.

Ultrasonographic mapping on healthy volunteers

The MCP joints 2–5 of both hands of two males (ages 31 and 59 years, mean 45 years) and eight females (ages 21–76 years, mean 48.25 years) were scanned as described above (section "Scanning method"). Three joints (1 MCP4 and 2 MCP5) were excluded due to technical problems leaving a total of 77 joints examined using color Doppler mode (Table 1 and Figure 7). The number of recorded images of the left hand ranged between 56–238 (average: 146.6) and 78–266 (average: 139.7) on the right hand, respectively. Supplementary Table 2 summarizes the number of joint specimens with Doppler-signal and their diameters. Due to the lack of proper acoustic window

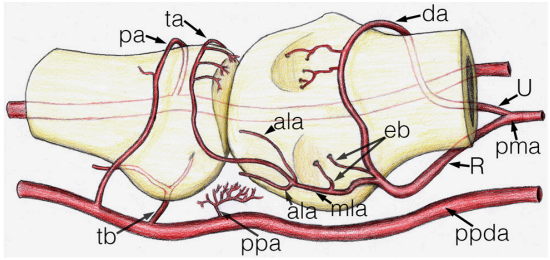

FIGURE 5
Schematic drawing of the main arterial vessels of the metacarpophalangeal joint. The proximal (metacarpal) half and distal (phalangeal) half are shown on the right and left side of the image respectively. ala, accessory lateral artery; da, dorsal arcade; eb, enthesial branch; mla, main lateral artery; pa, phalangeal arcade; pma, palmar metacarpal artery; ppa, palmar plate artery; ppda, proper palmar digital artery; R, R-branch; ta, triangular arcade; tb, tenosynovial branch; U, U-branch.

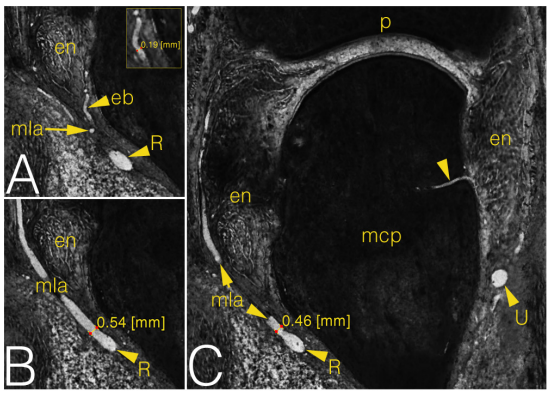

FIGURE 6
Grayscale images of a cryosectioned right MCP2 joint demonstrating joint anatomy and measurement on the arteries in coronal plane. **(A)** Corresponds to the left inferior quadrant of panel **(C)**, level of cryosectioning 13 layers (0.65 mm) palmar. Insert shows diameter measurement on enthesial branch. **(B)** Corresponds to the left inferior quadrant of panel **(C)**, level of cryosectioning 9 layers (0.45 mm) dorsal. **(C)** Metacarpal part of the joint with an ulnar enosseal branch. Note the difference between the diameter values of the same radial main lateral artery depending on measurement's localization. arrowhead, enosseal branch; eb, enthesial branch; en, enthesis; mcp, metacarpal; mla, main lateral artery; p, phalanx; R, R-branch; U, U-branch.

no data were registered on the interdigital surfaces of the joints. The most frequent location with detected Doppler signal was the dorsal depression of the metacarpal head (64.94%) (**Figure 7D**) and the location of the main lateral arteries (68.42%) (**Figure 7A**). The distal PMA was identified in 53.25% of the joints, typically embedded in a homunculus-shaped connective tissue mass on axial plane images (**Figures 4I, 7I**). In all other locations, Doppler signal was captured in less than 50% of cases (**Supplementary Table 2**).

Difference in Doppler signal among metacarpophalangeal joints

Doppler signal (any) could be identified more frequently in MCP joints 2–3 (MCP2: 136/320, MCP3: 68/260), as compared MCP joints 4–5 (MCP4: 51/247, MCP5: 64/288) ($p < 0.0001$). Comparing the numbers of the intraarticular vessels (enosseal, enthesial and palmar plate) successfully identified with ultrasound, this difference was also observable between MCP joints 2–3 (MCP2: 54/160, MCP3: 29/120) and 4–5 (MCP4: 23/114, MCP5: 24/144) ($p = 0.009$). However, such difference was not present ($p = 0.1373$) between these joints when comparing the great, extraarticular vessels (R-branch, U-branch, main lateral artery). Difference between the vessel diameters measured with ultrasound and on the cryosectioned specimens was significant in all joints getting higher values when measured with ultrasound ($p < 0.0001$) (**Supplementary Table 2** and **Figure 8**).

Discussion

This study describes the arterial supply of MCP joints and compares anatomic data to *in vivo* Doppler imaging on healthy volunteers. Although various imaging techniques are capable of depicting inflammation within and surrounding the metacarpophalangeal joints and fingers (21, 23), none of them can detect inflammatory mediators, inflammatory cells or the normal synovial lining. However, they can capture and visualize synovial hyperplasia, normal and abnormal vessels to a certain extent (24). One study showed synovial vascularization with Doppler ultrasound corresponding to normal vessels in healthy wrists, first carpometacarpal joints and less frequently in MCP joints (20). Another study raised attention to possible misinterpretation of Doppler-artifacts outside of healthy tendon sheaths on the wrist, 2nd and 3rd fingers, respectively (25). Further studies emphasized that synovial hyperplasia and locally altered vascularization are both important parameters to define and score synovitis (13). On the other hand, the threshold between normal detectable Doppler signal (which represents normal vessels, or normal variants) and pathologic Doppler signal (representing abnormal vessels and flows) remains unknown (20). Padovano et al. described the presence of effusion, synovial hyperplasia or low-grade power Doppler signal in some MCP joints in a large cohort of healthy subjects, emphasizing the need to distinguish between physiologic and pathologic ultrasound findings at the level of the hand joints (19). High-end ultrasonographic equipment is also a validated tool when distinguishing between vascular channels, bony erosions and pseudoerosions in many cases of RA patients and healthy subjects, respectively (26, 27). However, the reliability of ultrasonographic differential diagnostic depends on a lot of factors (e.g., site, size, shape, and scenery as the "four S") making the decision difficult especially in early RA and young people (27). Considering our results, how to interpret based on the site and size any cortical interruption remains already a question. As it is highlighted in our study, in case of metacarpal heads the vessels enter typically on all four sides the bone, what can be in overlap with erosions site. Finzel et al. described with ultrasonography more false positive results of bony erosions on the palmar aspect of metacarpal heads when comparing them with micro CT images, which was explained with the presence of vascular channels misinterpreted with ultrasound (28). However, we detected anatomically a generally higher number of entering vessels on the dorsal side, which we also confirmed with the much higher number of detected Doppler signals in the same location compared to the palmar side. Despite performance of nowadays ultrasound machines, there is no definite cut-off level for secure differentiation between a lesion and a physiologic vascular channel. As both our anatomical and ultrasonographic measurements confirmed, the size of bone entering vessels remains consequently under

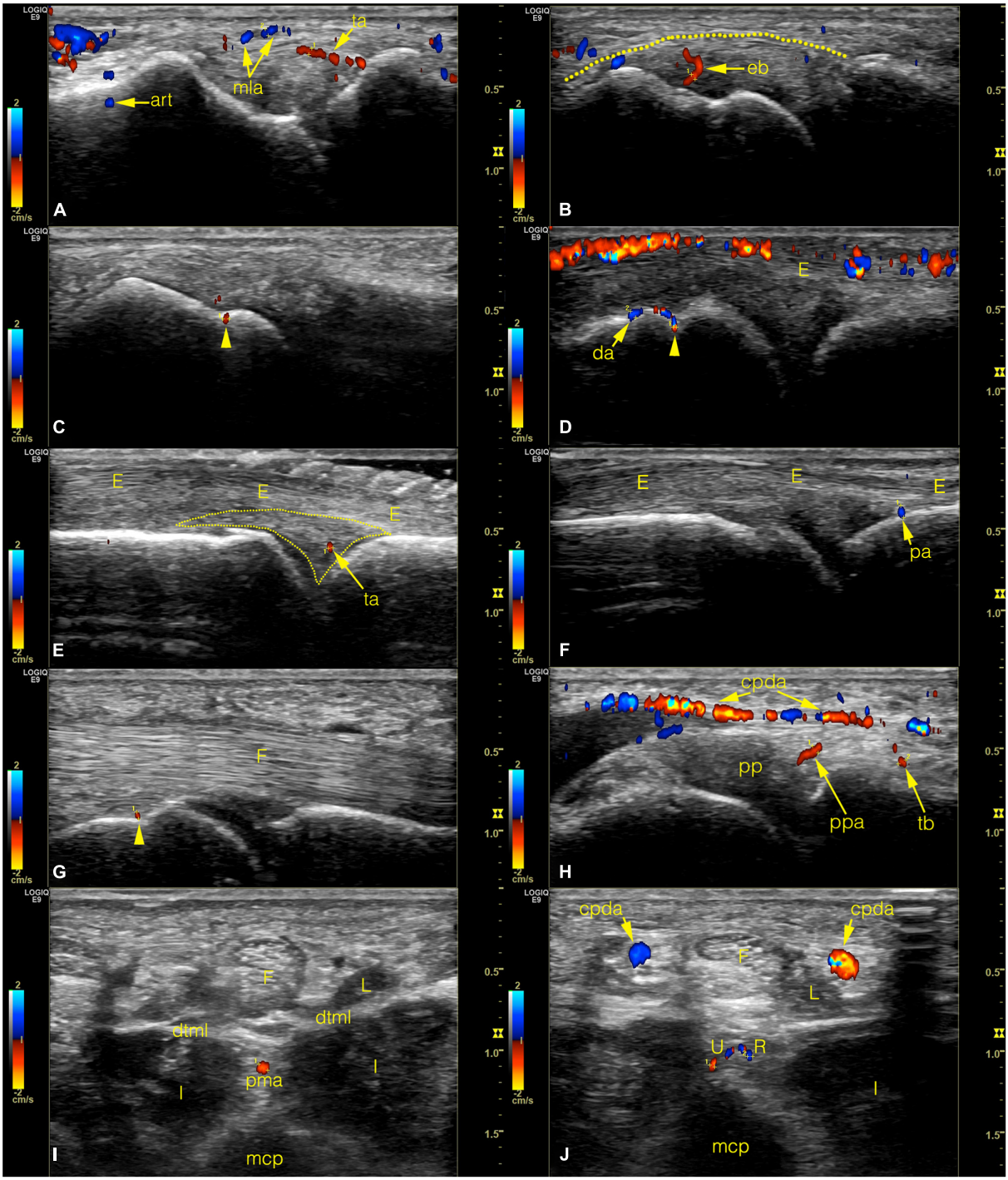

FIGURE 7
Color Doppler ultrasonographic images of normal joint vessels on healthy volunteers. (Left side of the images refers to the metacarpal half.) **(A–C)** radial side of the 2nd joint on coronal plane. On panel **(B)** the dotted line indicates the outer border of the enthesis. **(D–F)** dorsal side of the joint on sagittal plane images. Note the superficial cutaneous vein along the top of panel **(D)**. On panel **(E)** the dotted line indicates the dorsal triangle. **(G,H)** palmar side on sagittal plane. **(I,J)** axial plane images with the homuncule shaped soft tissue complex in the center with palmar metacarpal artery and it's bifurcation into R- and U-branches, respectively. arrowhead, entry point of a bone supplying vessel; art, Doppler mirror artifact; cpda, common palmar digital artery; da, dorsal arcade; dtml, deep transverse metacarpal ligament; eb, enthesial branch; E, extensor tendon; F, flexor tendon; I, interosseous muscle; L, lumbrical muscle; mcp, metacarpal; mla, main lateral artery; pa, phalangeal arcade; pma, palmar metacarpal artery; pp, palmar plate; ppa, palmar plate artery; ppda, proper palmar digital artery; R, R-branch; ta, triangular arcade; tb, tenosynovial trunk; U, U-branch.

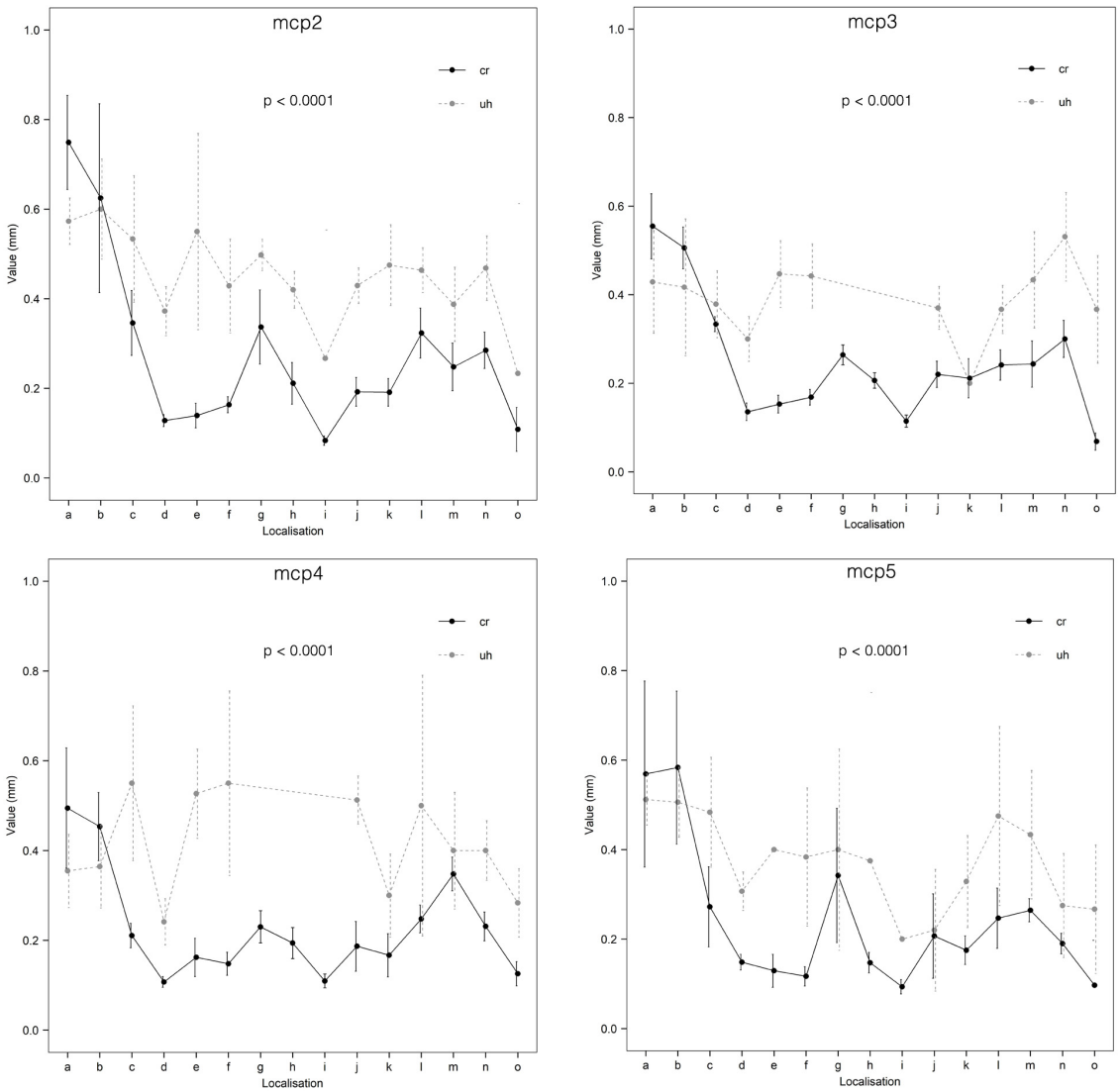

FIGURE 8
Comparison of ultrasonographic and cryosectioned diameter measurements (CI = 95%). cr, cryosectioning; uh, ultrasonography; a, R-branch; b, U-branch; c, dorsal arcade; d, dorsal enosseal; e, palmar enosseal; f, dorsal triangle arcade; g, main lateral artery; h, enthesial; i, enosseal lateral; j, palmar plate radial; k, palmar plate ulnar; l, tenosynovial branch radial; m, tenosynovial branch ulnar; n, phalanx arcade; o, phalanx dorsal enosseal.

0.7 mm. This fact should be taken into account when examining cortical brakes based on their diameter.

In the past, several anatomical and surgical studies investigated the vascular supply of MCP joints (29, 30). None of these methods provided true *in situ*, high resolution layer-by-layer investigation of the entire joint vasculature. To this date there are no published studies that describe the periarticular, articular arteries (intraenthesial, tenosynovial branches, the dorsal triangle arcade and the phalangeal arcade). There are also no studies that match vascular sonographic findings with the exact anatomy of these articular and periarticular vessels. The cryosectioning method for *in situ* visualization of different human and veterinary tissues has been available for a long time (31–34). We have improved several phases of this method, resulting in a higher resolution (22), which is comparable to histological examination (35). The ultrathin layer technique utilized in our study allowed the precise mapping of very small branches independent of their original three-dimensional course, and enabled computer-aided reconstruction and measurements of them.

The ultrasonographic measurements were carried out on healthy volunteers by the same investigator under standardized circumstances (constant room temperature, warm bath to heat the joints before examination) (36, 37). We chose color

Doppler rather than power Doppler because this has been shown to be more sensitive on our ultrasound machine (8). The ultrasonographic settings were based on the guidelines described by Torp-Pedersen et al. (36). In their recent publication, they highlighted that manual settings improved the Doppler sensitivity by an average of 78% and a maximum of 273% over factory settings. Therefore, our machine was calibrated by a professional GE technician with special emphasis on small vessel detection. The timing of ultrasonographic investigations depended on availability of the volunteers, thus the scans were carried out between 7 am and 10 pm. Although Semerano et al. reported higher Doppler signals in MCP circulation of rheumatoid arthritis patients in the morning, this circadian change is likely due to periodic changes in inflammation, because it correlated well with the patient's symptoms (38). Therefore, it is highly unlikely that the timing of our ultrasonographic investigations had any effect on the variability of our results because our healthy volunteers had no rheumatological complaints on their hands.

Our study revealed that in healthy volunteers, small intraarticular vessels adjacent to the bony cortex or joint space can be detected by ultrasound significantly more frequently in the MCP 2–3 joints as compared to MCP 4–5 joints. This finding is in line with the increased frequency of the involvement of MCP 2–3 in inflammation compared to MCP 4–5 joints seen in RA patients (39).

Our study has also some limitations. Both the comparison of inevitably different joint specimens using post mortem cryosectioning and *in vivo* ultrasonography and the consideration of possible anatomical variations could necessitate a higher number of cadaver specimens and healthy controls, respectively. However, our detailed anatomical mapping on the joint arteries reviled a rather constant pattern of vascularity, and the ultrasonographic examinations were all carried out based on these morphological results. Furthermore, only one ultrasound machine was used by only one examiner. The choice of the applied high-end machine based on the fact, that both the Doppler modality and the calibration data for flow investigation in joints were tested and published in detail previously (8, 36). As the localization of possible vascular signals was clearly determined by the anatomical part of this study, and the investigations were carried out under predefined criteria with no limit on scanning time, no second examiner was invited to the ultrasonographic part. In a future investigation a large pathological group consisting of different inflammatory diseases compared to a higher number of healthy volunteers using different ultrasound machines by more examiners could serve valuable data on (mis)interpretation possibilities of joint blood flow under different clinical conditions.

In summary, we described the entire arterial vasculature of MCP 2–5 joints on anatomical specimens divided it in metacarpal and phalangeal territories, peri- and intraarticular branches. We found that Doppler signal could be detected in only less than 50% of the vessels of healthy volunteers, however the detection probability of the dorsal enosseal branches and the main lateral arteries were much higher. Intraarticular branches were detected with ultrasound imaging significantly more frequently on MCP 2–3 joints. Our findings using ultrasound imaging provide the first reference data for MCP joints Doppler signal appearance and measurements on morphological bases. Our study also provides reference data for future, higher resolution imaging techniques.

Data availability statement

The original contributions presented in this study are included in the article/**Supplementary material**, further inquiries can be directed to the corresponding author.

Ethics statement

Ethical review and approval was not required for the study on human participants in accordance with the local legislation and institutional requirements. Written informed consent for the use of donated human cadaver tissue was not required in accordance with the national legislation and the institutional requirements. All volunteers provided written informed consent to participate in this study.

Author contributions

GB contributed to the study design. GB, KC, OP, and SB prepared the anatomical specimens. GB, KC, OP, JG, SH, and GN collected the data. GB, VS, PM, PB, and KC wrote the first draft of the manuscript. GB and LB made all the statistical examinations and designed the figures and tables. All authors revised the manuscript critically and approved the final version of the manuscript.

Funding

This work was supported by the Pfizer Aegrotus Foundation, the Istvan Apathy Foundation, and the Janos Bolyai Research Scholarship of the Hungarian Academy of Sciences (BO/00921/19).

Acknowledgments

We kindly thank to Viktor Pankovics for preparing the colored drawing summarizing the arterial supply of metacarpophalangeal joints. Special thanks to Ferenc Szabo,

who supported with technical assistance preparing the cadavers, to Lajos Patonay for providing professional instrumentation for photo documentation of corrosion cast specimens, and to Peter Szabo for the professional photographing of each cryosectioned layer. We also thank to Attila Csapo sr. for providing the CNC milling possibility for cryosectioning.

Conflict of interest

OP was employed by Medicopus Non-profit Ltd and Justanatomy Ltd.

The remaining authors declare that the research was conducted in the absence of any commercial or financial relationships that could be construed as a potential conflict of interest.

Publisher's note

Supplementary material

The Supplementary Material for this article can be found online at: https://www.frontiersin.org/articles/10.3389/fmed.2022.1015895/full#supplementary-material

References

1. Veale DJ. Synovial tissue biopsy research. *Front Med.* (2019) 6:72. doi: 10.3389/fmed.2019.00072

2. Balint PV, Terslev L, Aegerter P, Bruyn GAW, Chary-Valckenaere I, Gandjbakhch F, et al. Reliability of a consensus-based ultrasound definition and scoring for enthesitis in spondyloarthritis and psoriatic arthritis: an OMERACT US initiative. *Ann Rheum Dis.* (2018) 77:1730–5. doi: 10.1136/annrheumdis-2018-213609

3. Kazandjieva J, Antonov D, Kamarashev J, Tsankov N. Acrally distributed dermatoses: vascular dermatoses (purpura and vasculitis). *Clin Dermatol.* (2017) 35:68–80. doi: 10.1016/j.clindermatol.2016.09.013

4. Guggenberger KV, Bley TA. Imaging in vasculitis. *Curr Rheumatol Rep.* (2020) 22:34. doi: 10.1007/s11926-020-00915-6

5. Filippou G, Sakellariou G, Scirè CA, Carrara G, Rumi F, Bellis E, et al. The predictive role of ultrasound-detected tenosynovitis and joint synovitis for flare in patients with rheumatoid arthritis in stable remission. Results of an Italian multicentre study of the Italian society for rheumatology group for ultrasound: the STARTER study. *Ann Rheum Dis.* (2018) 77:1283–9. doi: 10.1136/annrheumdis-2018-213217

6. Macía-Villa C, Falcao S, Gutierrez M, Medina J, Hammer HB, De Miguel E. What is metacarpophalangeal joint swelling in psoriatic arthritis? Ultrasound findings and reliability assessment. *Clin Exp Rheumatol.* (2018) 36:896–9.

7. Rossi-Semerano L, Breton S, Semerano L, Boubaya M, Ohanyan H, Bossert M, et al. Application of the OMERACT synovitis ultrasound scoring system in juvenile idiopathic arthritis: a multicenter reliability exercise. *Rheumatology.* (2020) 2020:804. doi: 10.1093/rheumatology/keaa804

8. Torp-Pedersen S, Christensen R, Szkudlarek M, Ellegaard K, D'Agostino MA, Iagnocco A, et al. Power and color doppler ultrasound settings for inflammatory flow: impact on scoring of disease activity in patients with rheumatoid arthritis. *Arth Rheumatol.* (2015) 67:386–95. doi: 10.1002/art.38940

9. Yadav A, Mehra N, Pal S, Hlawndo J, Sachdev N, Yadav TP. Evaluation of enthesitis in patients with juvenile idiopathic arthritis by power color and spectral doppler ultrasonography. *Eur J Rheumatol.* (2021) 8:2–6. doi: 10.5152/eurjrheum.2020.20056

10. Lee GY, Kim S, Choi ST, Song JS. The superb microvascular imaging is more sensitive than conventional power doppler imaging in detection of active synovitis in patients with rheumatoid arthritis. *Clin Rheumatol.* (2019) 38:2613–20. doi: 10.1007/s10067-019-04550-0

11. Lim AKP, Satchithananda K, Dick EA, Abraham S, Cosgrove DO. Microflow imaging: new doppler technology to detect low-grade inflammation in patients with arthritis. *Eur Radiol.* (2018) 28:1046–53. doi: 10.1007/s00330-017-5016-4

12. Ohrndorf S, Hensch A, Naumann L, Hermann KGA, Scheurig-Münkler C, Meier S, et al. Contrast-enhanced ultrasonography is more sensitive than grayscale and power doppler ultrasonography compared to MRI in therapy monitoring of rheumatoid arthritis patients. *Ultraschall Med.* (2011) 32:38–44. doi: 10.1055/s-0031-1281770

13. D'Agostino MA, Terslev L, Aegerter P, Backhaus M, Balint PV, Bruyn GA, et al. Scoring ultrasound synovitis in rheumatoid arthritis: a EULAR-OMERACT ultrasound taskforce-part 1: definition and development of a standardised, consensus-based scoring system. *RMD Open.* (2017) 3:1. doi: 10.1136/rmdopen-2016-000428

14. van Holsbeeck M, Soliman S, Van Kerkhove F, Craig J. Advanced musculoskeletal ultrasound techniques: what are the applications? *Am J Roentgenol.* (2020) 216:436–45. doi: 10.2214/AJR.20.22840

15. Rostgaard J, Qvortrup K. A note about retinal structure and visual acuity. A light microscopic study of the cones in fovea centralis. *Acta Ophthalmol Scand.* (1999) 77:45–9. doi: 10.1034/j.1600-0420.1999.770111.x

16. McCrone J. Tetrachromats. *Lancet Neurol.* (2002) 1:136. doi: 10.1016/S1474-4422(02)00051-0

17. Gul HL, Eugenio G, Rabin T, Burska A, Parmar R, Wu J, et al. Defining remission in rheumatoid arthritis: does it matter to the patient? A comparison of multi-dimensional remission criteria and patient reported outcomes. *Rheumatology.* (2020) 59:613–21. doi: 10.1093/rheumatology/kez330

18. Schioppo T, Orenti A, Boracchi P, De Lucia O, Murgo A, Ingegnoli F. Evidence of macro- and micro-angiopathy in scleroderma: an integrated approach combining 22-MHz power doppler ultrasonography and video-capillaroscopy. *Microvasc Res.* (2019) 122:125–30. doi: 10.1016/j.mvr.2018.07.001

19. Padovano I, Costantino F, Breban M, D'Agostino MA. Prevalence of ultrasound synovial inflammatory findings in healthy subjects. *Ann Rheum Dis.* (2016) 75:1819–23. doi: 10.1136/annrheumdis-2015-208103

20. Terslev L, Torp-Pedersen S, Qvistgaard E, von der Recke P, Bliddal H. Doppler ultrasound findings in healthy wrists and finger joints. *Ann Rheum Dis.* (2004) 63:644–8. doi: 10.1136/ard.2003.009548

21. Carstensen SMD, Terslev L, Jensen MP, Østergaard M. Future use of musculoskeletal ultrasonography and magnetic resonance imaging in rheumatoid arthritis. *Curr Opin Rheumatol.* (2020) 32:264–72. doi: 10.1097/BOR.0000000000000709

22. Czeibert K, Baksa G, Grimm A, Nagy SA, Kubinyi E, Petnehazy O. MRI, CT and high resolution macro-anatomical images with cryosectioning of a beagle brain: creating the base of a multimodal imaging atlas. *PLoS One.* (2019) 14:13458. doi: 10.1371/journal.pone.0213458

23. Balint PV, Mandl P. *Ultrasonography of the hand in rheumatology*. Cham, Switzerland: Springer (2018). doi: 10.1007/978-3-319-74207-6

24. Burke CJ, Alizai H, Beltran LS, Regatte RR. MRI of synovitis and joint fluid. *J Magn Reson Imaging.* (2019) 49:1512–27. doi: 10.1002/jmri.26618

25. Ammitzbøll-Danielsen M, Janta I, Torp-Pedersen S, Naredo E, Østergaard M, Terslev L. Three-dimensional doppler ultrasound findings in healthy wrist and

finger tendon sheaths - can feeding vessels lead to misinterpretation in doppler-detected tenosynovitis? *Arthr Res Ther.* (2016) 18:70. doi: 10.1186/s13075-016-0968-3

26. Finzel S, Ohrndorf S, Englbrecht M, Stach C, Messerchmidt J, Schett G, et al. A detailed comparative study of high-resolution ultrasound and micro-computed tomography for detection of arthritic bone erosions. *Arthr Rheum.* (2011) 63:1231–6. doi: 10.1002/art.30285

27. Cipolletta E, Smerilli G, Di Matteo A, Di Battista J, Di Carlo M, Grassi W, et al. The sonographic identification of cortical bone interruptions in rheumatoid arthritis: a morphological approach. *Ther Adv Musculoskelet Dis.* (2021) 13:1759720X211004326. doi: 10.1177/1759720X211004326

28. Finzel S, Aegerter P, Schett G, D'Agostino MA. Identification, localization and differentiation of erosions and physiological bone channels by ultrasound in rheumatoid arthritis patients. *Rheumatology.* (2020) 59:3784–92. doi: 10.1093/rheumatology/keaa183

29. Tan RES, Lahiri A. Vascular anatomy of the hand in relation to flaps. *Hand Clin.* (2020) 36:1–8. doi: 10.1016/j.hcl.2019.08.001

30. Bonnel F, Teissier J, Allieu Y, Rabischong P, Mansat M. Arterial supply of ligaments of the metacarpophalangeal joints. *J Hand Surg Am.* (1982) 7:445–9. doi: 10.1016/s0363-5023(82)80037-3

31. Park JS, Chung MS, Hwang SB, Lee YS, Har DH, Park HS. Visible Korean human: improved serially sectioned images of the entire body. *IEEE Trans Med Imaging.* (2005) 24:352–60. doi: 10.1109/tmi.2004.842454

32. Park HS, Shin DS, Cho DH, Jung YW, Park JS. Improved sectioned images and surface models of the whole dog body. *Ann Anat.* (2014) 196:352–9.

33. Dogdas B, Stout D, Chatziioannou AF, Leahy RM. Digimouse: a 3D whole body mouse atlas from CT and cryosection data. *Phys Med Biol.* (2007) 52:577–87. doi: 10.1088/0031-9155/52/3/003

34. Zhang SX, Heng PA, Liu ZJ, Tan LW, Qiu MG, Li QY, et al. Creation of the Chinese visible human data set. *Anat Rec B New Anat.* (2003) 275:190–5. doi: 10.1002/ar.b.10035

35. Davies DV, Edwards DAW. The blood supply of the synovial membrane and intra-articular structures. *Ann R Coll Surg Engl.* (1948) 2:142–6.

36. Torp-Pedersen ST, Terslev L. Settings and artefacts relevant in colour/power doppler ultrasound in rheumatology. *Ann Rheum Dis.* (2008) 67:143–9. doi: 10.1136/ard.2007.078451

37. Ellegaard K, Torp-Pedersen S, Henriksen M, Lund H, Danneskiold-Samsøe B, Bliddal H. Influence of recent exercise and skin temperature on ultrasound doppler measurements in patients with rheumatoid arthritis–an intervention study. *Rheumatology.* (2009) 48:1520–3. doi: 10.1093/rheumatology/kep294

38. Semerano L, Gutierrez M, Falgarone G, Filippucci E, Guillot X, Boissier MC, et al. Diurnal variation of power doppler in metacarpophalangeal joints of patients with rheumatoid arthritis: a preliminary study. *Ann Rheum Dis.* (2011) 70:1699–700. doi: 10.1136/ard.2010.146761

39. Hurnakova J, Filippucci E, Cipolletta E, Di Matteo A, Salaffi F, Carotti M, et al. Prevalence and distribution of cartilage damage at the metacarpal head level in rheumatoid arthritis and osteoarthritis: an ultrasound study. *Rheumatology.* (2019) 58:1206–13. doi: 10.1093/rheumatology/key443

frontiers | Frontiers in Medicine

TYPE Review
PUBLISHED 31 October 2022
DOI 10.3389/fmed.2022.984379

OPEN ACCESS

EDITED BY
Andrea Di Matteo,
Marche Polytechnic University, Italy

REVIEWED BY
Georgios Filippou,
IRCCS Istituto Ortopedico Galeazzi, Italy
Riccardo Mashadi Mirza,
Ospedale Cervesi di Cattolica, Italy

*CORRESPONDENCE
Riccardo Picasso
riccardo.picasso@gmail.com

SPECIALTY SECTION
This article was submitted to Rheumatology, a section of the journal Frontiers in Medicine

RECEIVED 01 July 2022
ACCEPTED 12 September 2022
PUBLISHED 31 October 2022

CITATION
Zaottini F, Picasso R, Pistoia F, Sanguinetti S, Pansecchi M, Tovt L, Viglino U, Cabona C, Garnero M, Benedetti L and Martinoli C (2022) High-resolution ultrasound of peripheral neuropathies in rheumatological patients: An overview of clinical applications and imaging findings.
Front. Med. 9:984379.
doi: 10.3389/fmed.2022.984379

High-resolution ultrasound of peripheral neuropathies in rheumatological patients: An overview of clinical applications and imaging findings

Federico Zaottini[1], Riccardo Picasso[1]*, Federico Pistoia[2], Sara Sanguinetti[2], Michelle Pansecchi[3], Luca Tovt[3], Umberto Viglino[3], Corrado Cabona[1,4], Martina Garnero[1,4], Luana Benedetti[1,4] and Carlo Martinoli[1,3]

[1]San Martino Hospital, Istituto di Ricovero e Cura a Carattere Scientifico, Genoa, Italy, [2]Dipartimento di Medicina Sperimentale, Scuola di Scienze Mediche e Farmaceutiche, Università di Genova, Genoa, Italy, [3]Dipartimento di Scienze della Salute, Scuola di Scienze Mediche e Farmaceutiche, Università di Genova, Genoa, Italy, [4]Eye Clinic, Department of Neuroscience, Rehabilitation, Ophthalmology, Genetics, Maternal and Child Science, School of Medical and Pharmaceutical Sciences, University of Genoa, Genoa, Italy

Peripheral neuropathies are surprisingly common and can be associated with a number of conditions, including rheumatological diseases. Whether the co-existence of peripheral neuropathies with rheumatological disorders is coincidental or related to a common pathogenic mechanism, these disabling conditions can affect the outcome of rheumatological patients and should be targeted with specific treatment. The clinical presentation of peripheral neuropathy can be multifaceted and difficult to recognize in polysymptomatic patients. However, physicians adopting state-of-art diagnostic strategies, including nerve imaging, may improve the detection rate and management of neuropathies. In particular, a diagnostic approach relying exclusively on clinical history and nerve conduction studies may not be sufficient to disclose the etiology of the nerve damage and its anatomical location and thus requires integration with morphological studies. High-Resolution Ultrasound (HRUS) is increasingly adopted to support the diagnosis and follow-up of both joint disorders in rheumatology and peripheral neuropathies of different etiologies. In this review, the different types of nerve disorders associated with the most common syndromes of rheumatological interest are discussed, focusing on the distinctive sonographic features

KEYWORDS

ultrasound, nerve imaging, polyneuropathy etiology, rheumatologic conditions, magnetic resonance imaging

Introduction

Peripheral neuropathies (PNs) are frequently encountered in the context of rheumatic disease (1). However, the pathogenic mechanisms determining this association are multiple and partially still unrevealed. Indeed, PN in musculoskeletal inflammatory disorders can be directly caused by a wide variety of mechanisms, such as compression, vasa nervorum inflammation, or drug toxicity. In other circumstances, rheumatic disease and coexisting neuropathy share an immune-mediated mechanism. Finally, in some instances, the link between the two conditions cannot be firmly proven, as is the case of small-fiber neuropathies.

In the last years, we have witnessed an increasing use of ultrasound (US) for assessing patients with inflammatory arthritis. In addition to being an inexpensive, safe and widely available tool, the use of US allows a more accurate assessment of the soft tissue inflammation compared to clinical examination also providing the same sensitivity as magnetic resonance imaging (MRI) (2, 3).

Furthermore, the recent advances in electronics and signal filtering algorithms, together with the innovation of high-frequency broadband linear transducers (>18 MHz), have all contributed to increasing the spatial resolution of US and its diagnostic performance. This technology known as High-Resolution Ultrasound (HRUS) is excellent for rapidly assessing long nerve tracts in the extremities (4). Moreover, this technical upgrade has allowed US to become an increasingly useful diagnostic tool for the differentiation of the pathogenetic mechanisms underlying a particular neuropathy, such as entrapment neuropathy, traumatic neuropathy, or inflammatory polyneuropathies (5–9). In addition, HRUS is non-invasive and is an easily available diagnostic instrument that can provide promising imaging biomarkers (10) for a neuropathy follow-up either after treatment and/or during rehabilitation protocol.

Since rheumatic patients frequently seek medical advice for symptoms that are not always attributable to joint involvement or to extra-articular causes, a thorough knowledge of US findings, characterizing the different subtypes of neuropathies, may well help in promptly recognizing the subgroup of rheumatic patients affected by neuropathies, thus improving the appropriate clinical management of their conditions. The purpose of this narrative review is to provide an overview of the clinical and HRUS features of the neuropathies associated with rheumatic diseases, summarizing the literature evidences regarding these conditions.

Classification of neuropathies and clinical diagnosis

Peripheral neuropathies can be categorized in different types according to specific criteria (11). The most commonly applied criterion used today by neuropathologists is based on the anatomical structure involved. Therefore, these conditions are classified as Axonopathy, Myelinopathy, Ganglionopathy, or Neuronopathy each according to the neural structure involved. Considering the number of nerves affected, it is said to be mono-neuropathy if a single nerve is damaged, multifocal neuropathy if at least two separate nerve areas are asymmetrically and asynchronously involved, or polyneuropathy when multiple nerves are affected symmetrically. In addition, according to the type of function, neuropathies can also be divided into sensory, motor, autonomic, or mixed neuropathies, while based on the subtypes of fibers affected, they can be classified as large fiber or small fiber neuropathies. Finally, these conditions can be further divided into acute or chronic neuropathies depending on their onset and progression. The whole spectrum of these neuropathies can be found in rheumatological patients.

In a clinical setting, the different subtypes of neuropathies are defined according to the nerve conduction studies (NCS), which typically correspond to specific symptoms.

Single mono-neuropathies are characterized by sensory disturbances and a loss of muscle strength in the innervation territory of the affected nerve, as commonly found in the case of compression neuropathies. In compression neuropathies, symptoms can range from sensory abnormalities, paresthesia, and pain in the initial stages to motor deficit and permanent sensory impairment as the injury progresses. Demyelination accounts for the slowing of the nerve conduction in the initial phase of the alteration with the prevalent involvement of sensitive fibers; as the damage progresses, motor fibers are deranged and the alteration reaches the axons (12).

Occasionally, compression neuropathies may initiate with prevalent motor or sensory symptoms according to which group of fascicles is pre-eminently affected (13). Auto-immune demyelinating polyneuropathies are characterized by the symmetric or asymmetric slowing of conduction, more or less associated with conduction blocks that involve both motor and sensory fibers. This group of neuropathies, also include the Motor Multifocal Neuropathy (MMN), a purely motor neuropathy characterized by asymmetrical involvement, conduction blocks, and intact sensory nerve action potential. Axonal sensory polyneuropathy can be characterized by paresthesia and a sensory loss (including mild touch, proprioception, and vibration sensations) in the distal part of the limbs, mainly the lower limbs, and the affected patients may also complain of a burning, painful sensation in the feet. In addition to the sensory manifestations, motor weakness may be found in sensorimotor axonal polyneuropathy, usually affecting the extensor muscles of the toes or feet (11) (**Figure 1**). Selective motor neuropathies are characterized by paresis, atrophy and fasciculations, mainly in the distal limbs (11). Small-fiber neuropathy (SFN) results from selective damage to small myelinated and unmyelinated nerve fibers. SFN is usually found in the early stages of several systemic diseases, such as diabetes, amyloidosis and rheumatic conditions (14).

The main clinical manifestations are numbness, a burning sensation, electric pain, a pricking sensation, and pruritus involving the limbs, trunk or face (11). SFN consists of two different types, the "length-dependent" SFN and the "non-length-dependent" SFN. The first one is related to the most distal axon degenerations causing neuropathic pain arising in a distal "stocking-and-glove" distribution; in the second type, the neuronal degeneration involves the proximal region of the peripheral nervous system and dorsal root ganglia; these patients suffer from neuropathic pain in the face, truncus, and proximal arms and legs (15). However, it is worth noting that NCS cannot distinguish between small fibers or amyelinic fibers pathology and a conventional electromyogram or NCS are non-contributory to the diagnosis of a small fiber neuropathy (16).

High-resolution ultrasound findings

As a consequence of the variable clinical manifestations, the diagnosis of PN is a challenging clinical issue, moreover in polysymptomatic disorders such as rheumatic diseases. HRUS may represent the first screening instrument to discriminate nerve damage from joint and soft tissue involvement. In addition, the morphological information provided by HRUS complements the NCS and clinical information to unveil the etiology of PN, the potential site of injury and the extent of nerve alterations (17). The different types of PNs found in rheumatological conditions may occur by way of several mechanisms, including the direct effects of compression or the invasion of neural tissues by hypertrophic synovium, vasculitic involvement of the vasa nervorum, auto-immune mechanisms directed against the myelin antigens, occasionally triggered by biological drugs, or the direct neurotoxic effect of drugs or deposited material (e.g., amyloids).

Scanning technique and normal nerve appearance

Ultrasound study of the nerves should be conducted according the so called "elevator technique" (18). It consists in using anatomic landmarks to find the target nerve in its short axis and scanning it cranially and caudally along the entire course. In short axis, normal peripheral nerves demonstrates a characteristic honeycomb-like appearance, related to the presence of hypoechoic axons arranged in fascicles and multiple layers of hyperechoic connective tissue surrounding the axons bundles. In the long axis, the nerve appears as elongated structures with alternating hypo-and hyperechoic bands. The ultrahigh frequency probes (up to 30 MHz) allow visualization of sub-millimetric terminal nerve branches, which are visualized like a single or few hypoechoic dots within a hyperechoic frame lacking the classical expected "honeycomb-like" structure (18). Pathological changes may be focal or diffuse, and are typically recognized at ultrasound as nerve enlargement respect to normal ones and/or changes in the fascicular echotexture. In order to avoid misdiagnosis, the probe should be kept exactly perpendicular to the nerve long axis, otherwise size measurements and echogenicity evaluation may be altered respectively by the obliquity of nerve cross section and the anisotropy. Anisotropy is an artifact typically encountered during scanning of fibrillar structures as muscles and tendons, but also nerves. In fact, when the ultrasound beam is incident on organized fibrils or fascicles, may be reflected in a direction away from the transducer: in those cases, the transducer does not receive the returning echo and the insonated area is displayed hypoechoic. Restoration of the beam perpendicular angle of incidence by tilting the probe, promptly resolve the false image (19). Keeping into consideration the potentials diagnosis pitfalls ensuing an inadequate scanning technique, in the next subparagraphs the sonographic findings of neuropathies are described in relation to the pathogenesis.

Compression neuropathies

Compression mono-neuropathies are relatively frequent conditions in rheumatological diseases with synovial hypertrophy or with structural changes in the connective tissue [i.e., rheumatoid arthritis (RA) or systemic sclerosis] which may, directly or indirectly, create a mass effect on the nerve, especially within the osteofibrous tunnels (**Figure 2**). Regardless of the entrapment site, HRUS signs of compressive neuropathies are stereotypical and consist of nerve flattening at the compression point and nerve swelling proximally or (less commonly) distally to it. In case the transition between swollen and flattened segments is abruct, it represents the patognomonic "notch sign." In order to have the quantification of findings, the nerve cross-sectional area (CSA) or the maximum nerve diameter should be sampled at the site where the nerve is maximally enlarged proximally or distally the compression site, and this value can be used to differentiate normal from compressed nerve (20). In particular, the measured CSA can be compared to a validated cut-off, to the contralateral nerve or to a normal tract from the examined nerve. According the EFSUMB (European Federation of Societies for Ultrasound in Medicine and Biology) guidelines, for the Ultrasound diagnosis of carpal tunnel syndrome (CTS), the CSA threshold value of 10 mm^2 obtained proximal to the flexor retinaculum should be used to differentiate a normal from compressed median nerve. Similarly, an ulnar nerve CSA cut-off value of 10 mm^2 obtained proximal or within retrocondylar groove at the elbow, should be considered for the diagnosis of cubital tunnel syndrome (21).

Nerve CSA is seen to correlate with NCS severity grading, since nerve enlargement corresponds to pathologic changes

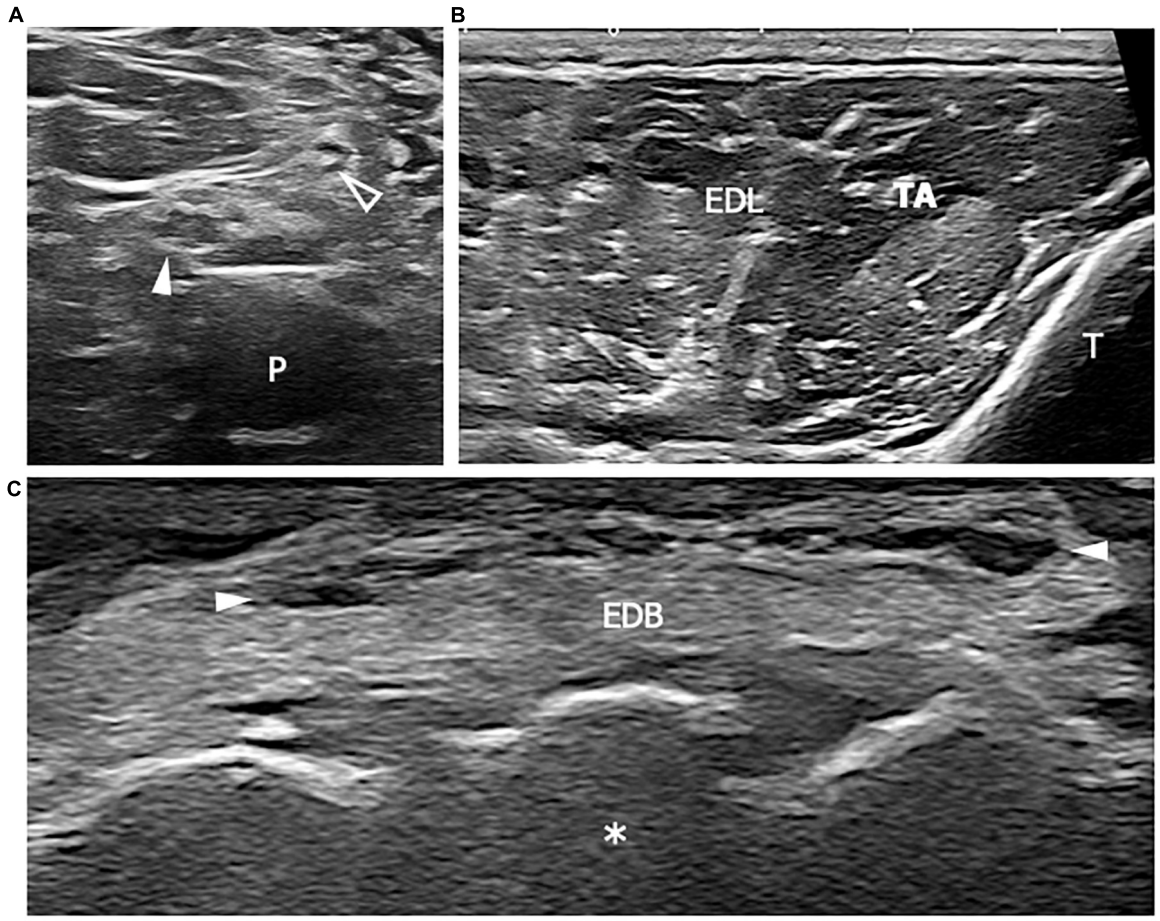

FIGURE 1
This figure shows three 18 MHz HRUS images **(A–C)** of a 44 years old male affected by a mixed connective tissue disease with a lower limb sensory-motor axonal neuropathy. As frequently seen in the axonal neuropathies, in **(A)** no significant morphological changes of the tibial (white arrowhead) and fibular (empty arrowhead) nerves in the popliteal fossa are seen. At the proximal third of the leg, the axial scan in **(B)** does not reveal any sign of denervation in the anterior compartment of the leg muscles (tibialis anterior, TA and extensor digitorum longus, EDL). However, the extensor digitorum brevis muscle (EDM) in **(C)** exhibits signs of advanced atrophy with fat replacement of the muscle fibers. The isolated atrophy of EDM has been described as being associated with axonal neuropathies of different etiologies and it could represent the only HRUS finding under these conditions. White arrowheads in **(C)** represents EDL tendons. P, popliteal vein; T, tibia; white asterisk, tarsal bones.

that directly hamper the nerve functions. In the early phases of compression, intraneural edema and venous congestion are the main factors leading to an enlargement of the nerve and consequent myelin sheets alterations. In severe/long-standing compressions, the nerve loses the fascicular echotexture as a consequence of the swelling of the fascicles and progressive intraneural fibrosis. Differently from the early stages of the disease, nerves with fibrotic changes remain enlarged after decompressive surgery and have poor functional improvement (22, 23).

Dysimmune neuropathies

In regards to auto-immunity, a link has been established between Chronic Inflammatory Demyelinating Polyneuropathy (CIDP) and other auto-immune diseases (24). In fact, certain HLA loci are associated with a greater risk of CIDP and other conditions, such as RA, systemic lupus erythematosus (SLE), and Sjögren's syndrome (SS) (25, 26).

Furthermore, the introduction of immuno-modulating drugs, for example the tumor necrosis factor-α (TNF-α) inhibitors, has been associated with the development of auto-antibodies and immunity activation against peripheral nerve structures. The diagnostic value of HRUS has already been proven in acquired immune-mediated demyelinating neuropathies, either acute or chronic forms (27). Diffusely increased CSAs of the affected nerves, especially in the proximal extremities, and the focal fascicular enlargement at the site of conduction blocks are the sonographic hallmarks in demyelinating neuropathies. Fascicles may alternate in thickened and thinned segments and frequently results

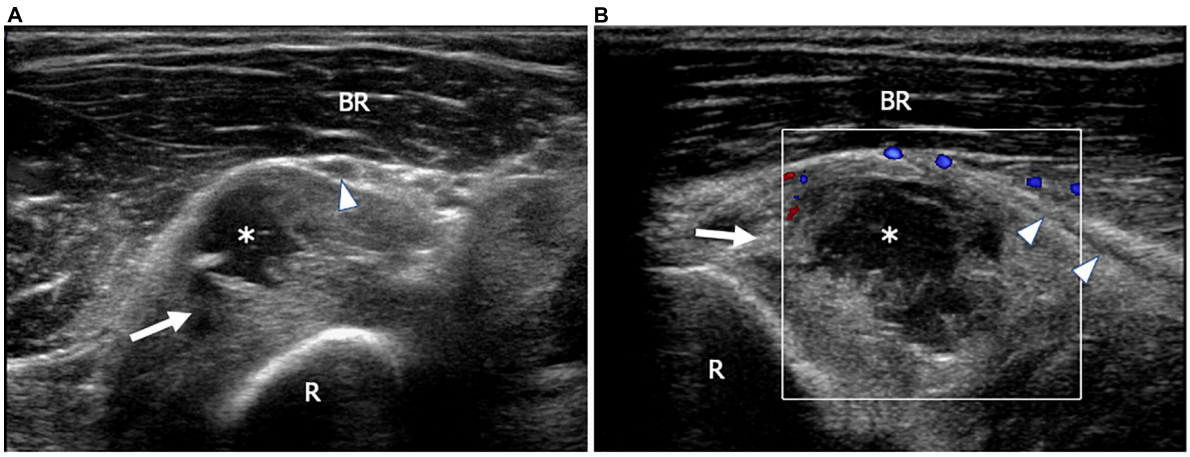

FIGURE 2
This figure shows two 18 MHz HRUS images **(A,B)** of a 53 years old male patient affected by rheumatoid arthritis with a progressive decrease of fingers extension strength. **(A)** An axial view, immediately distal to the humeral-radial joint line, shows the annular recess (white arrow) distended by synovium and fluid (white asterisk); the recess dislocates superficially the posterior interosseus nerve (white arrowhead) immediately proximal to the supinator tunnel. After switching on the Eco-Color Doppler, a slight peripheral vascularization of the synovial wall of the annular recess (white arrow) is shown **(B)**. **(B)** The longitudinal scan also depicts the long axis of the posterior interosseous nerve (white arrowheads) dislocated superficially by the distended recess. BR, brachioradialis muscle; R, radius.

iso-hyperechogenic in comparison to the normal nerves as consequence of intraneural edema. The distribution pattern of nerve alterations can be diffuse, generalized, or focal according to the subtypes of demyelinating neuropathies (28). Nerve enlargement in dysimmune neuropathies in some cases is readly identifiable with a standard visual approach, mostly in the phase of active disease and in multifocal forms; in other cases, mainly in long standings, diffuse disease, nerve and fascicle swelling are mild, and a comparison of CSA measures with a matched control group or literature data is necessary to identify the pathological changes. In case of symmetric polyneuropathies as CIDP, the contralateral side comparison should not be used as diagnostic criteria for detecting nerve alterations. Recently introduced parameters as intranerve-, internerve-, and intra-plexus CSA variabilities and "side to side difference ratio of the intranerve CSA variability" can help into recognizing a diffuse, symmetric nerve involvement respect to multifocal or focal pattern (28, 29). In order to calculate these ratios, a multilevel symmetric CSA sampling should be obtained: in diffuse nerve involvement the variability in multilevel cross sectional area is reduced respect to multifocal or focal nerve alterations. Unfortunately, cut-off values for these parameters has been defined only for the ulnar nerve and there is low agreement between different studies, thus encouraging each ultrasound lab to define its own reference values. Differently from demyelinating neuropathies, nerve morphology is rarely abnormal in axonal polyneuropathies (30, 31). Vasculitic neuropathies may be an exception in the context of these findings. In fact, according to Leupold et al. (32), pronounced changes in different nerves may be detected in vasculitis using HRUS even if it shows the electro-diagnostic features of axonal neuropathy. Differently from demyelinating neuropathies, in vasculitic neuropathy, the mean CSA value sampled at different nerve levels bilaterally are normal or just slightly increased but focal nerve swelling, with impressively enlarged fascicles in the affected nerves, may be visualized (33). The enlarged fascicles are the results of ischemic axonal damage with Wallerian degeneration and the pattern of nerve involvement is typically multifocal (also known as "mononeuritis multiplex"). Other minor findings of vasculitic neuropathies include a decreased echogenicity of the fascicles with a hyperechogenic, thickened epineurium, which can persist after immunosuppression as described in a case report (34) (**Figures 3**, **4**). Since the axonal neuropathies do not generally show a significant nerve enlargement at HRUS, nerve morphological alterations in the case of asymmetric axonal damage of unknown origin may suggest the diagnosis of nerve vasculitis.

Morphological and echotextural nerve alterations are detectable also in the acute form of autoimmune polyneuropathy, namely the Guillain-Barrè syndrome (GBS) and its variants (e.g., Miller Fisher syndrome). Among GBS subtypes, acute inflammatory demyelinating polyradiculoneuropathy and acute motor axonal neuropathy are the most common (35). According to HRUS findings in GBS, in the first three days of symptom onset, a diffuse nerve swelling involving the proximal segments (e.g., cervical roots) has been reported, although the frequency and extent of the morphological changes vary both inter- and intra-individually (35). The morphology of the purely sensory sural nerve was not significantly altered, which corresponds to the electrophysiological findings of "sural sparing" (36). The degree of cervical spinal nerve enlargement was found to be

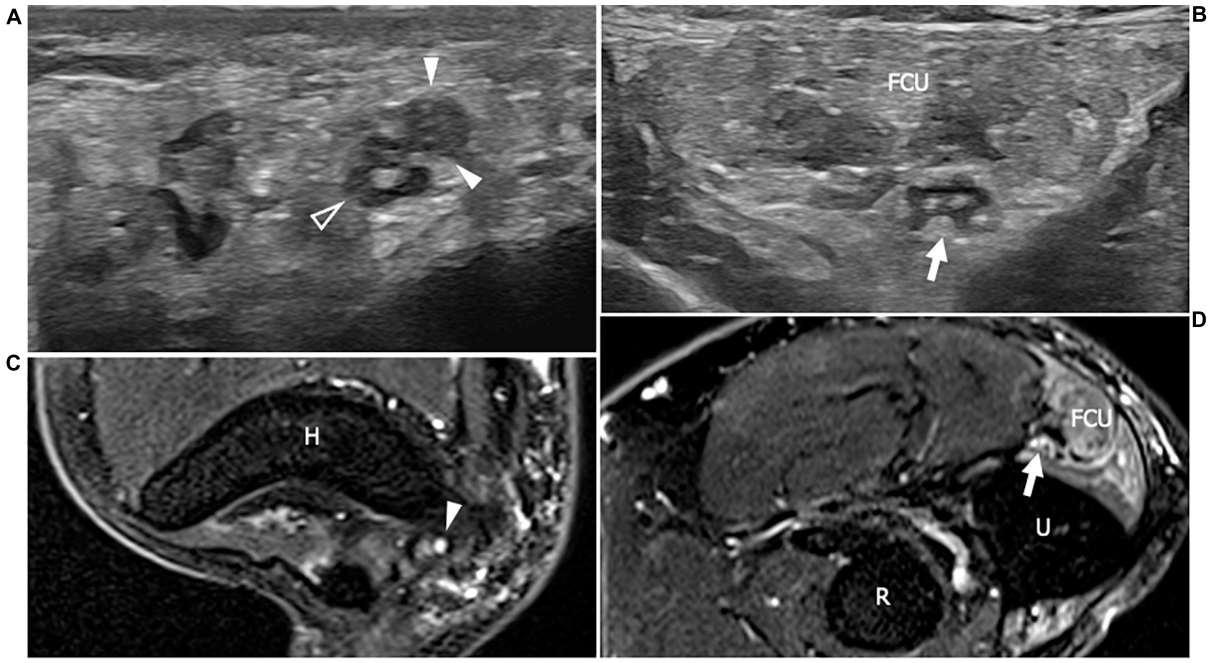

FIGURE 3
This figure shows two 18 MHz HRUS axial images **(A,B)** and two T2-weighted with fat suppression axial magnetic resonance (MR) images **(C,D)** in a 48 years old female patients with ANCA-associate vasculitis and a multifocal mononeuropathy of the ulnar nerve. **(A)** The axial view of the ulnar nerve (empty arrowhead) just cranial to the epitrochlear groove can be observed: the nerve is characterized by a single fascicle enlargement (white arrowheads) to which a focal T2-signal hyperintensity in the correlative MR image corresponds (white arrowhead in **C**). More distally, within the cubital tunnel, the ulnare nerve fascicles (white arrow) appear slightly enlarged and hypoechoic **(B)** with a s increase of T2-signal intensity in the matching axial MR image (white arrow in **D**). The flexor carpi ulnaris muscle (FCU) appears diffusely hyperechogenic in **(B)** as a consequence of denervation; in **(D)**, the denervation process provokes an intramuscular edema seen to have increased the T2-signal within the muscular tissue. H, humerus; R, radius; U, ulna.

correlated significantly with the CSF protein and may represent the ultrasonic correlation of focal inflammatory demyelination with the swelling of the nerve sheaths, as reported in the histopathology (35). Nevertheless, the nerve's echogenicity seems not to be altered in contrast to the descriptions in CIDP (35). The vagus nerve may also result morphologically altered and might well serve as an early risk marker of autonomic dysregulation. The proximal cervical nerve enlargement is reported to go back to normal 6 months after the beginning of symptoms and the start of therapy. However, the alterations in the distal nerve segments may last more than 6 months, possibly as a consequence of remyelination processes and/or Wallerian degeneration (36).

Within the setting of dysimmune neuropathies, HRUS is also able to demonstrate the response to systemic immunosuppressive treatment by showing a decrease in the nerve or in the fascicle cross-section area (**Figure 5**). Several study groups have found a correspondence between symptom variation and nerve morphological changes after therapy; in particular in chronic inflammatory demyelinating neuropathies. In addition, after immunoglobulin therapy a correlation between muscle strength and CSA of the affected nerves was demonstrated (37). Also in GBS, a regression of nerve enlargements might represent a good parameter for clinical recovery during follow-up (37, 38). Therefore, even though further studies are needed in order to prove the accuracy in demonstrating early signs of response to therapy or disease activity, nerve US might be a promising monitoring method.

Muscle denervation

In the case of motor neuropathies, using HRUS, it is possible to identify and grade the ensuing muscle atrophy. A denervated muscle presents a variable appearance depending on the severity of axonal loss, durations of nerve damage and its evolution, the presence of reinnervation process. The muscle echogenicity is usually compared to subcutaneous tissue or the unaffected muscle, while the muscle volume is compared to the contralateral side. In literature are reported three pattern of echotextural alterations: no echo-intensity changes in case of monophasic, slight, axonal neuropathy; diffuse or patchy increased echogenicity in longer standing denervation without reinnervation; "moth eaten" pattern as consequence of chronic denervation and reinnervation processes. In this latter

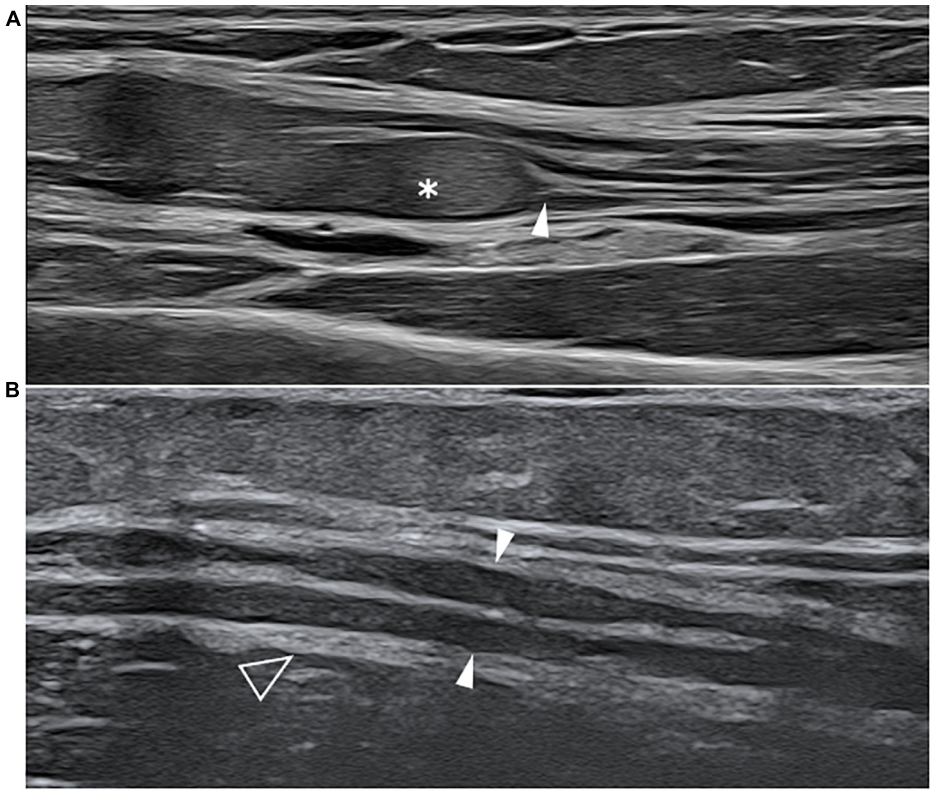

FIGURE 4
This figure shows two 22 MHz HRUS images, longitudinal view, one from a 45 years old female patient affected by systemic lupus erythematosus (SLE) who developed a chronic demyelinating polyneuropathy **(A)** and one from a 53 years old female patient affected by polyarteritis nodosa with a mononeuritis multiplex. The comparison of the two HRUS images point out the main distinguishing features of the two neuropathies: in **(A)**, there is a marked, iso-hyperechoic, irregular median nerve enlargement (white asterisk) with an abrupt change in caliber (white arrowhead) at the passage between the pathological and unaffected fascicles while in **(B)**, the ulnar nerve (white arrowheads) presents a slight, diffuse, irregular and hypoechogenic enlargement of the fascicle with a tick epineurium (empty arrowhead). Panel **(A)** was obtained at the mid-portion of the forearm while panel **(B)** was obtained at the distal third of the arm.

pattern, the hypoechoic areas correspond to viable, reinnervated motor units, that are interspersed in a hyperechoic background related to the fibrotic substitution of chronically denervated muscle bundles (39). Alterations in muscle echogenicity are indeed complex and may reflect denervation edema in the initial weeks after nerve injury followed by fat and fibrous tissue replacement of the muscle fibers with ongoing denervation (40).

Current literature is slightly contradicting on the ultrasound appearance of the muscle edema: according to some studies the edema determines muscle hyperechogenicity due to an increased number of reflecting interfaces (41). On the contrary, other studies state that edematous muscles appear swollen and hypoechogenic because of loosely packed peri and endomysial connective tissue (42). For this reason, in the acute phase (within the first 2-weeks) MRI is more sensitive and specific than ultrasound in detecting muscle denervation. As the fat replacement progresses, the muscle decrease in size and definitely increase in echogenicity (43).

In the recent years, software to quantify muscle thickness and echogenicity are more extensively adopted in clinical practice, in order to make a reproducible analysis of muscle denervation. By using quantification of muscle parameters, the severity of the ultrasound changes correlated with the severity of denervation on EMG. Furthermore, there is also potential for ultrasound measurements recorded from muscles to be included in disease assessment protocols (44).

In conclusion, HRUS may play a relevant role in the diagnosis and follow-up of neuropathies thanks to the number of anatomical details it can provide relating to the nerves and to the muscle, as well as its non-invasiveness and its availability for any care-setting environment. In the face of a spatial and contrast resolution not inferior to magnetic resonance neurography at least for the superficial nerves, further HRUS advantages include cost benefits, portability, dynamic imaging, and contra-lateral side comparisons. In addition, HRUS can also be performed on patients who are unable to tolerate MRI or patients carrying metallic hardware (45).

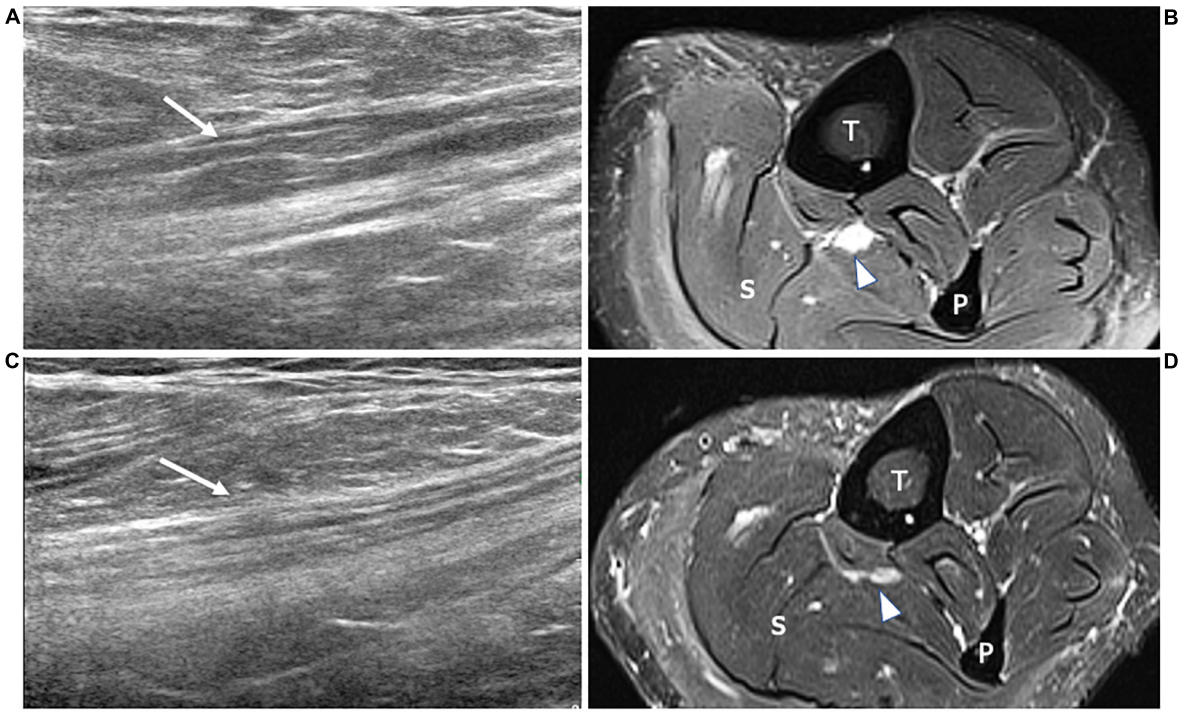

FIGURE 5
This figure includes two 18 MHz HRUS images **(A,C)** and two T2-weighted with fat suppression axial MR images **(B,D)** in a 45 years old female patient affected by rheumatoid arthritis who developed a motor multifocal neuropathy of the tibial nerve after starting a treatment with the anti-TNF-α drug Etanercept. **(A)** The longitudinal scan of the tibial nerve at the proximal leg shows the focal enlargement of the nerve fascicles (white arrow) to which corresponds the T2-signal hyperintensity (white arrowhead) of the MR image in **(B)**. Both the nerve size and the T2-signal alteration, compatible with intraneural edema ensuing an inflammatory process, result markedly reduced in **(B,D)**. These latter were acquired after 6 months of therapy with immunoglobulin. The findings of this figure highlight the role of HRUS in monitoring the disease activity of dysimmune demyelinating neuropathies. T, tibia; F, fibula; S, soleus muscle.

However, among its limitations, we should mention the lack of a standardized methodology for US measurements, as well as the influence of the equipment, patients habitus and the nerve anatomy (whether superficial or deep, the presence of fibrosis in the overlying tissue, etc.) on US diagnostic performance. In fact, these factors, taken altogether, limit the repeatability and reproducibility of the studies. Recently, the operator dependency of US findings has been disproved by a study from Telleman et al. (46). However, for HRUS to be effective, a long learning curve of the operator is required (46).

Neuropathies in the most common acquired rheumatological conditions and systemic conditions of rheumatological interest

In this paragraph, the epidemiology, clinical features, patho-mechanism and sonographic features of PNs in acquired rheumatologic conditions most commonly encountered in clinical practice are discussed (Table 1).

Systemic lupus erythematosus

Patients affected by Systemic Lupus Erytehamatosus (SLE) may suffer from PN in a percentage ranging from 1.5 to 36% (47–53). However, studies that considered only NCS parameter and not the clinical symptoms reported a prevalence of 21–42%, suggesting that some patients may present asymptomatic neuropathy (51). While NCS is a marker of peripheral nerve function, the significance of asymptomatic electrophysiological neuropathy is unclear. NCS parameters of SLE may deteriorate over time and the worsening seems related only to the age (48). According to some authors (54–56), SLE may cause an early damage to the peripheral nerve function before it can be detected by NCS or the patient experiences the initial symptoms: the clinical manifestations of PN are indeed the result of a slowly cumulative damage, as can be inferred by their correlation with age. Concerning the type of neuropathies, a

TABLE 1 This table shows the different types of neuropathies (first row) that may be found in each Rheumatological disease (first column).

	Acute demyelinating neuropathy (GBS-like)	Chronic demyelinating polyneuropathy (CIDPS-like)	Multifocal mononeuropathy	Compressive neuropathy	Sensory-motor axonal neuropathy	Small-fibers neuropathy
Systemic Lupus Erythematosus	+	-	-	-	+++	-
Sjogren's Syndrome	-	++	+++	+	++	-
Systemic Sclerosis	-	-	-	++	++	+
Rheumatoid Arthritis	-	-	+	++	+++	-
Polyarteritis Nodosa	-	-	+++	-	-	-
ANCA-Associated Vasculitis	+	-	+++	-	++	-
Giant Cell Arteritis	-	-	+	++	+	-
Takayasu Arteritis	-	-	-	+	+	-
Behcet Syndrome	-	-	-	-	++	-
Psoriatic Arthritis	-	-	-	+	+	+
Mixed Connective Tissue Disease	-	-	-	++	++	-
Sarcoydosis	-	+	+	+	++	+
Gout and Pseudogout	-	-	-	+++	+	+
Dermato-Polymyositis	-	-	-	-	++	-
Drug-related neuropathies	++	++	+	-	-	++
Covid-related neuropathies	++	++	+	+	+	-
Amyloidosis	-	-	+	+++	-	+

The relative frequency of a neuropathy in respect to the other types is indicated by the number of + (+++, frequently present; ++, present; +, rarely present).

higher prevalence of sensory-motor involvement with axonal patterns is reported (49). The most commonly affected nerves are in decreasing order the peroneal nerve, the tibial, and sural nerves, while the ulnar and median nerves involvement is uncommon (54). Although GBS is a rare type of PN in SLE patients, it represent one of the main causes of morbidity and mortality (57, 58).

The pathogenetic mechanisms of PN directly attributable to SLE neuropathy are not completely understood, but may include auto-antibody-mediated nerve damage and nerve vasculitis. And interestingly, the 30–40% of PN occurring in SLE are coincidental, related, for example, to diabetes mellitus, chronic renal failure, drug toxicity, or compressive neuropathy (59). The relation between PN occurrence and SLE disease activity or systemic involvement is not univocal: in some studies the symptomatic polyneuropathy was independently associated only with age while other case series have found associations with age onset and SLE disease activity scores (51, 59). Regarding nerve imaging, only one study has investigated the morphological features of PN related to SLE (60): in a cohort of 37 patients, the mean CSA of the ulnar nerve at the Guyon's canal and mid-humerus, of the tibial nerve at the distal leg and proximal to the tarsal tunnel and of the peroneal nerve at the popliteal fossa resulted significantly increased in respect to gender and age-matched healthy control group. As already reported, HRUS is less informative in axonal neuropathies since the findings are less remarkable. Although the axonal polyneuropathies are the more represented subtypes among SLE-neuropathies, further data is needed in order to increase our knowledge about morphological HRUS findings in SLE, in particular in regards to nerve echotexture and fascicular size in the early asymptomatic phase when NCS and clinical examinations are normal.

Sjögren's syndrome

Sjögren's syndrome (SS) is the second most common chronic auto-immune rheumatic disease, considering both primary Sjögren's syndrome (pSS) and secondary Sjögren's syndrome (sSS). The frequency, prevalence, and diagnostic criteria for peripheral nervous system involvement in SS have been the object of several studies as well as the underlying pathogenetic mechanisms. The reported prevalence of PN varies from 19 to 72% and may represent the first clinical manifestation (61–65). A cross-sectional study from China in 2018 reported a higher prevalence of PN in sSS than in pSS patients (31.1 vs. 19%) (61). Concerning the types of PN in SS, several studies found a higher prevalence of symmetric sensorimotor polyneuropathy (axonal and demyelinating type) and symmetric sensory polyneuropathy (66, 67); however, mononeuropathy (as entrapment neuropathy) or mononeuritis multiplex is also frequently encountered (61). Atypical presentations consist of pure motor neuropathies, hypertrophic neuropathies, and ganglionopathies (61, 68, 69). Regarding pathogenetic mechanisms, vasculitis seems to be strongly related to nerve damage, while the role of T-cell infiltrates and their cytotoxic effect is still unknown. Auto-antibodies, in particular the anti-muscarinic receptor 3 Ab, are implicated in the development of autonomic neuropathies (70).

Evidence about the imaging features of neurological involvement in SS is mainly focused on the central nervous system (CNS). The only ultrasound study found nerve morphological alterations in 72% of patients with suspected neuropathy related to SS. According to this study, nerve thickening is detected more frequently than fascicle thickening (90 vs. 52%, respectively), while in 40% of those patients combined nerve and fascicle thickening can be found (71). As observed in other autoimmune neuropathies, US abnormalities in the SS-associated neuropathy may occur in a single nerve site, as well as multifocally (71, 72). The morphological alterations reported in the study are consistent with the NCS diagnosis of demyelinating neuropathies, thus suggesting that this subtype of polyneuropathies is the most represented at least in the cohort examined by the authors (**Figure 6**). Further imaging studies based on HRUS are warranted on a larger cohort of subjects to disclose any nerve alterations in asymptomatic patients and to verify the utility of US nerve measurements as biomarkers of disease activity.

Systemic sclerosis or scleroderma

Systemic sclerosis (SSc) is an autoimmune disease characterized by vasculopathy, fibrosis, and immune abnormalities affecting the muscles, joints, skin, lungs, heart, digestive system, kidneys, and nervous system. Both central and peripheral nervous systems may be involved. In regard to PNs, in a cross-sectional study by Raja et al. (73) and Paik et al. (74), the prevalence of PN in SSc varied from 28 to 36.6%. In a recent systematic review from AlMehmadi et al. (75), compression neuropathies were reported in 26.5% of the studies, and according to Yagci et al. (76) and Sriwong et al. (77), the prevalence of median neuropathy in SSc is estimated to be 35%. Most CTS in patients with SSc were asymptomatic. Among non-compressive neuropathies, sensorimotor neuropathies (usually presenting as mononeuropathies) are the most frequent, whilst small-fiber neuropathies are detected more frequently than large-fiber neuropathies. Several etiologies were proposed, including intra-nerve fibrosis secondary to tissue edema. Calcinosis cutis and, less commonly, soft tissue thickening, resulted in the main risk factor for compression neuropathies in SSc (**Figure 7**). Risk factors for non-compression neuropathies include advanced diffuse diseases, anti-centromere antibodies, presence of vasculitis, iron deficiency with anemia, drugs such as metoclopramide and pembrolizumab, silicosis, and uremia (77). Autonomic nervous systems, especially cardiac autonomic functions, may also be altered in SSc (78). Literature evidence on nerve sonography in SSc patients is limited to the compression neuropathies. Tagliafico et al. systematically studied the median and ulnar nerves along their entire course in the upper limbs to find, as pathological alterations, nerve enlargement just proximal to the osteofibrous tunnel (the carpal tunnel and cubital tunnel), compatible with compression neuropathies. Occasionally, calcific deposits were found around the nerve (79). However, no sign of dysimmune neuropathies or vasculitis neuropathies were detected. Interestingly, Yagci et al. performed an elastography study on the median nerve revealing that the nerve loses its elasticity while the CSA's is in the normal range in patients with SSC. The increased intraneural stiffness is likely to be related to the intraneural fibrosis, a finding which is also supported by the decreased "nerve density" evaluated using HRUS reported by Bignotti et al. (80). In fact, the computer-aided sonographic quantitative assessment of intraneural hyperechoic pixel/hypoechoic pixel ratio, demonstrated an increase of hyperechoic tissue in the nerves of patients affected by cutaneous Scleroderma, possibly related to an increased fibrotic tissue and/or decrease of fascicular size. The nerve density also resulted in being inferior in symptomatic patients with respect to the asymptomatic ones.

Rheumatoid arthritis

The prevalence of PN in RA ranges from 10.81% (81) to 75.28% (82) according to the method of diagnosis, length of illness, and variability in selection criteria; the prevalence estimation is further complicated by the large fraction of asymptomatic patients. The chance of being affected by PN seems to vary according to the subtypes of RA considered. Kumar et al. (83) reported that the prevalence of PN in seropositive RA patients and seronegative RA patients was 34.4 vs. 15.4, respectively. However, the relationship between the presence of anti-cyclic citrullinated antibodies and the higher risk of developing PN needs further investigation. Among RA patients with the long-standing disease, sensory neuropathy is the most common form of PN (84), followed in order by distal sensorimotor polyneuropathy, mononeuritis multiplex, entrapment neuropathy, and neuropathy related to drug toxicity (84). Neuropathic abnormalities detected by NCS are most often axonal, although demyelinating features are sometimes present (85). Kaeley et al. (82) found that pure motor neuropathy was not a rare entity. The patient's age, disease duration, use of disease-modifying anti-rheumatoid drugs, disease severity (disease activity score-28) and presence of subcutaneous nodules were found to correlate with the incidence of PN. Autonomic dysfunction also occurred in RA, characterized by heart rate responses to a deep breath, heart rate response to standing, blood pressure response to hand grip and sudomotor function impairment (86). Uncommon but severe peripheral nerve alterations included ischemic neuropathies caused by necrotizing arteritis of the vasa vasorum (87), presenting as multifocal nerve involvement. Entrapment neuropathy in RA is frequently related to synovial proliferation and joint deformation thus leading to nerve compression in proximity to the osteofibrous tunnel (88). No correlation was found between

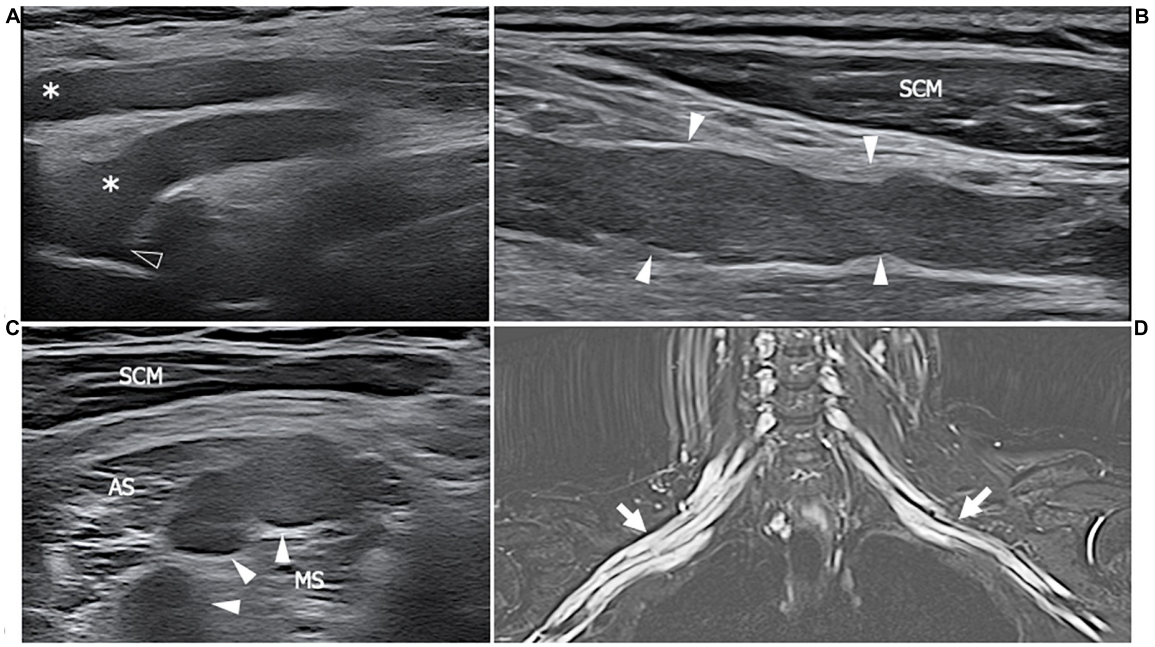

FIGURE 6
This figure shows three 18 MHz HRUS images **(A–C)** and a T2-weighted with fat-suppression magnetic resonance image **(D)** of a 50 years old female affected by SS who developed a predominant-upper limb sensory-motor demyelinating neuropathy. **(A)** A long-axis view of brachial plexus roots (white asterisk) at the exit from the intervertebral foramens (empty arrowhead) is obtained: the massive hypoechoic enlargement of the nerves with the complete loss of the typical fascicular echotexture is observed; these findings extend also more distally at the level brachial plexus trunks and divisions as seen in **(B)**. Also in the latter, the long axis view depicts the irregular profile of the nerves (white arrowheads), with areas of thinning and area of nerve enlargement, findings which are typical of a CIDP neuropathy. **(C)** A short axis view of the pathological nerve trunks (white arrows) in the interscalenic space is shown. **(D)** The MR coronal view of the neck and upper thorax demonstrates a massive, irregular enlargement of the brachial plexus bilaterally (white arrows); the increased T2-signal of the brachial plexus roots, trunks, divisions and cords is due to an intraneural edema consequential to the nerve inflammation. SCM, sternocleidomastoid muscle; AS, anterior scalene muscle; MS, middle scalene muscle.

compression neuropathies and sex, duration of RA, functional class, the occurrence of other extra-articular manifestations, seropositivity, or the level of the acute phase plasma proteins. CTS is the most frequent compressive neuropathy in RA, but other entrapment neuropathies are reported, such as anterior and posterior tarsal tunnel syndrome (involving respectively a branch of deep peroneal nerve and the tibial nerve), the posterior interosseous nerve entrapment within the supinator tunnel, the cubital tunnel sydrome (involving the ulnar nerve at the elbow) and the common peroneal nerve compression at the fibular neck (88–90). The posterior tarsal tunnel syndrome is due to the compression of the tibial nerve as it enters in the tarsal tunnel, an osteo-fibrous canal delimited by the flexor retinaculum and medial malleolus and containing the tibialis posterior, flexor digitorum longus, and flexor hallucis longus tendons (89). The compression may results from tenosynovitis, the inflammation of the flexor retinaculum, or the pes valgus deformity. Symptoms include paresthesia and pain on the plantar aspect of the foot and the first through to the third toes. If the nerve compression persists, in the later stages atrophy and weakness of the intrinsic foot muscles occur as consequence of motor denervation. Prior to the availability of biological medications, from 5 to 25% of RA patients had electrophysiological abnormalities which are characteristic of tarsal tunnel syndrome, although not all of these patients were symptomatic (89). Median nerve entrapment commonly occurs at the wrist, within the carpal tunnel, as consequence of flexor tendons tenosynovitis or distension of radiocarpal and midcarpal volar recesses. Rarely, the compression can be identified in a more cranial position, at the level of the pronator muscle (pronator teres syndrome). Similarly to the median, ulnar nerve entrapment may be found at the elbow, within the cubital tunnel determined by distension of ulno-humeral joint recesses or at the wrist, within the Guyon canal; in this latter osteo-fibrous space, the ulnar nerve run in close proximity to the piso-triquetral joint, whilst, more distally, outside the tunnel, the motor branch may be compressed by a ganglion cyst from the metacarpophalangeal joint. The hip joint recesses and psoas bursa may determine femoral nerve palsy leading to sensory and motor defects (90). The tibial nerve may be compressed by a popliteal cyst, while ganglion cyst from the proximal tibio-peroneal joint may involve the peroneal nerve and its division branches. In the case of peripheral nerve entrapment and a concurrent cervical roots compression, the resulting syndrome

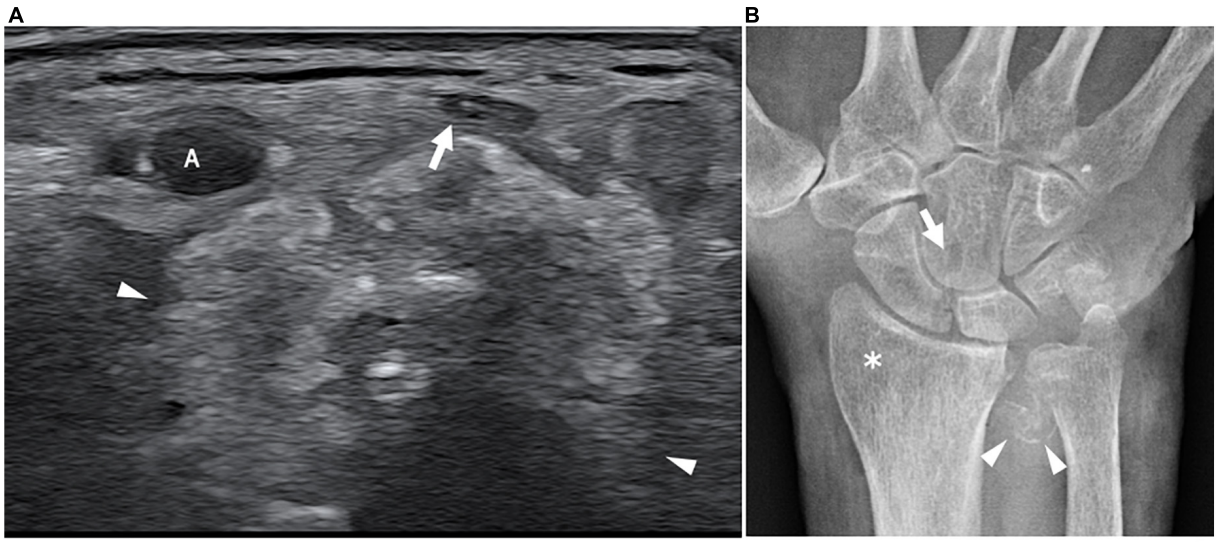

FIGURE 7
This figure shows an axial 18 MHz HRUS image of the wrist **(A)** and an antero-posterior X-ray image of the wrist in a 68 years old female affected by systemic sclerosis and monolateral carpal tunnel syndrome. **(A)** The distal radio-ulnar joint recess is distended by hyperechoic amorphous material partially calcified (white arrowheads) which compresses and superficially dislocates the median nerve (white arrow). **(B)** The X-ray confirms the presence of calcification (white arrowheads) in correspondence to the soft tissue in proximity to the distal radio-ulnar joint. Para-articular osteoporosis (white asterisk) and erosions (white arrow) at the level of the carpal bones are also observed. A, radial artery.

has been termed "double crush" syndrome; the exact prevalence of this syndrome is not reported, however, considering the frequency of cervical spine involvement, it should always considered among differentials diagnosis of PN in RA.

Sonographic imaging research mainly considered CTS in patients affected by RA, even if the whole spectrum of compression and part of non-compression neuropathies are amenable to HRUS.

The sonographic features of CTS in RA patients are defined by the presence of finger flexor tendons tenosynovitis and/or radio-carpal joint synovitis which lead to median nerve compression. Conversely, a marked median nerve swelling in absence of the "inflammatory pattern" above described is the dominant feature in idiopathic CTS (91), in which other factors such as the flexor retinaculum thickness play a more relevant role in the pathogenesis of nerve compression.

Polyarteritis nodosa

Polyarteritis nodosa (PAN) is a systemic necrotizing vasculitis of the medium and small sized muscular arteries. Among vasculites, PAN presents one of the highest PN prevalence. In a study on 27 patients from India, the prevalence reported is 88.9% (22 of 27 cases) (92). According to de Boysson et al. (93) and Imboden et al. (94), between 65 and 85% of PAN patients suffer from peripheral nerve disorders. Mononeuritis multiplex with axonal-type alteration affecting the major nerve trunks is the main form of PN manifestation, probably because PAN mainly affects the medium-size vessels, which supply slightly larger nerves. However, polyneuropathies, radiculopathies, lumbar or brachial plexopathies have all been reported. The chronic forms are predominant, even if rare cases of acute neuropathy related to necrotizing vasculitis may occur (95). As above described in the dysimmune neuropathies section and also reported by Kara et al., multifocal, hypoechoic nerve enlargements are the main sonographic features of mononeuritis multiplex related to vasculitis (96). The pathophysiology of nerve enlargement and fascicular swelling in vasculitic neuropathies remains unclear. The inflammation of the vasa nervorum, mainly affecting the epineural arteries may represent the first step leading to ischemic damage of the axon and consequent focal edema (96).

Anti-neutrophil cytoplasmic antibody-associated vasculitis

Anti-neutrophil cytoplasmic antibody (ANCA)-associated vasculitis is a systemic disorder that encompasses three distinct conditions: microscopic polyangiitis (MPA), granulomatosis with polyangiitis (GPA, previously Wegener's granulomatosis), and eosinophilic granulomatosis with polyangiitis (EGPA, previously Churg-Strauss syndrome). In order to clarify the pathogenetic mechanism, Nishi et al. (97) compared sural nerve biopsy specimens of 27 EGPA patients with anti-myeloperoxidase-ANCA and 55 EGPA patients specimens without anti-myeloperoxidase-ANCA. They found that the

positive anti-myeloperoxidase-ANCA group was mainly characterized by vasculitis in epineural vessels, while the negative anti-myeloperoxidase MPO-ANCA group was mainly characterized by eosinophil infiltration, suggesting the existence of at least two distinct mechanisms. In a large cross-sectional study from Bischof et al. (98), the prevalence of peripheral nerve involvement was 65% in EGPA, 23% in MPA, and 19% in GPA. The characteristics of neuropathies caused by small vessel vasculitis, as the ANCA-associated vasculitis, are similar (99). The symptoms develop acutely in a single nerve territory followed by the gradual involvement of other nerves. At the beginning of the disease, the sensory symptoms are limited to one or few body areas, reproducing the typical pattern of mononeuritis multiplex; as the damage progressively involves multiple nerves, the clinical manifestations may reproduce the pattern observed in polyneuropathies (100). Often sensory disturbances are associated with muscle weakness and atrophy, whereas pure motor neuropathy is an exclusion criterion for vasculitic neuropathy (101). Mononeuritis multiplex is reported in approximately 70–90% of patients, probably due to the immunosuppressive treatment which limits the nerve damage thus avoiding the progression to symmetric or asymmetric polyneuropathy. In EGPA, the nerves in the lower extremities are primarily affected, with the peroneal nerve being the most frequently and severely involved. Patients affected by ANCA- vasculitis may also have symptoms of autonomic dysfunction which is independent of the disease duration and its severity (102). Atypical manifestations include acute sciatic nerve neuropathy (103) and GBS-like syndrome (104).

Excluding the typical ultrasound findings of mononeuritis multiplex, enlargement of the peroneal nerve and sural nerves have been described in small vessel vasculitis, in particular, the peroneal nerve CSA came-back larger in the vasculitis patient group than in the non-immuno-mediated, idiopathic neuropathy group (105).

Giant cell arteritis and Takayasu arteritis

Reported evidence regarding PN in the large vessels vasculitis such as giant cell arteritis (GCA) and Takayasu arteritis (TAK) are scant. A literature review by Bougea et al. (106) found that PN affected 15% of GCA patients. CTS is the most common neuropathic complication of GCA, while mononeuritis multiplex and distal symmetrical sensorimotor polyneuropathies result uncommon. A rare neurological complication is the bilateral acute brachial radiculo-plexopathy, presenting as diplegia of the upper extremities with intact mobility of the head and lower limbs (107, 108). Also some cases with atypical symptoms, such as compressive common peroneal neuropathy (109) have been reported. PNs in TAK are rarer (110), usually presenting as a subacute sensorimotor deficit in a cervicobrachial plexus distribution. Even if uncommon, compression neuropathies should be considered as possible causes of PN. In this regard, a case report by Kim et al. (111) described a brachial plexus compression injury caused by a right axillary artery aneurysm in a young female patient affected by TAK.

Psoriatic arthritis

Peripheral nerve involvement in psoriatic arthritis (PA) has not been extensively indagated. However, according to the data from the DANBIO register (112), the presence of neuropathic pain is reported by 28% of Psoriatic patients assessed through the PainDETECT Questionnaire (PDQ), turning out to be more frequent respect to RA and seronegative Spondylarthritis. It is unclear whether the PDQ actually brings up the presence of peripheral neuropathic pain, or the central sensitization typical of fibromyalgia. In fact, PA neuropathy and fibromyalgia share a similar profile of sensory alterations, including pathological changes in small nerve fibers (113). Narayanaswami et al. (114) reported three cases of polyneuropathy associated with PA. The clinical and electrophysiologic features were consistent with a chronic, distal, symmetric sensorimotor axonal neuropathy. CTS is also frequently encountered: a clinical and sonographic study from Kaya Subaşı et al. (115) found CTS in 30% of RA patients and 41% in PA patients. In both conditions the frequency of CTS was higher with respect to the control group. The CTS in PSA is often associated with flexor tenosynovitis and radio-carpal joint synovitis. Summarizing, length-dependent SFN, symmetric axonal neuropathies, and CTS are the main causes of neuropathic pain in PA. However, further studies on a larger cohort of patients are needed to better characterize with NCS and HRUS the features and etiopathogenesis of PN in the autoimmune dermatoses.

Behcet syndrome

Peripheral neuropathies involvement in Behcet syndrome (BD) is extremely rare. Few cases of distal symmetrical polyneuropathy and mononeuritis multiplex have been reported (116), whilst the overall prevalence of CTS reached 0.8% in a retrospective study. According to the functional and electrophysiological classification, the nerve alterations in BD are axonal and predominantly involve the lower extremities (116).

Mixed connective tissue disease

The prevalence of PN is mixed connective tissue disease (MCTD) varies between 10 and 17% (117), including a relatively high percentage of trigeminal and bilateral facial nerve palsy

(118). Vasculitic and compressive neuropathies such as CTS can also be observed (119), presenting the typical HRUS features described above.

Dermatomyositis and polymyositis

According to previous studies, 7.5% of dermatomyositis (DM)/polymyositis (PM) patients suffer from polyneuropathy (120), mainly of the axonal type. Consequently, no specific HRUS pathological nerve findings have been reported and sonographic imaging should be used as a tool to rule out coincidental compressive or inflammatory neuropathies as the cause of muscle weakness and atrophy. Ultrasound may also help into differentiating a "myogenic pattern" of muscle alteration from a "neurogenic pattern" (121). IN DM and PM usually muscle alterations start with focal hyperechogenic areas which progressively extend to the entire muscle belly; furthermore, subcutaneous edema and calcifications or increased muscle vascularity at Eco-Color Doppler evaluation can be found. Conversely, in muscle denervation, a patchy to diffuse increase in muscle echogenicity with a myotomal pattern of involvement are observed (see section "Muscle denervation").

Sarcoidosis

In a recent narrative review from Tavee (122), peripheral nerve involvement in sarcoidosis (SA) is distinguished in granulomatous neuropathy (GN) and the more recently described non-granulomatous small fibers neuropathy (NGSFN). The two clinical entities differ for anatomo-pathologic features and clinical presentation. The GN occurs in 1% of SA patients and usually manifest as distal, symmetric or asymmetric axonal sensory motor polyneuropathy (123). Less commonly, CIDP pattern or motor multifocal pattern with electromyographic findings of demyelination or conduction blocks are reported (124). Neuropathic symptoms may present as the only clinical manifestation of SA, even if a subclinical systemic involvement commonly coexist. Differently, NGSFN is reported in the 32–44% of patients (125). Typically it starts after 2 years of SA systemic involvement as intermittent sensory disturbances in the distal extremities to become a continuous pain and paresthesia. The pathognomonic pathologic findings in GN are non-caseating granulomas in the perineurium, epineurium or endoneurium of the affected nerves. Rarely, soft tissue granulomas may infiltrates nerves causing acute or subacute mononeuropathies (126). However, granulomatous involvement cannot explain the generalized nerve damage of polyneuropathies: microvasculitis with or without vessels wall necrosis indeed may lead to ischemia and following axonal degeneration in the large myelinated fibers. The demyelination reported in some cases may represent the result of immune damage or be secondary to axonal atrophy. In NGSFN, the damage to the small myelinated A fibers and unmyelinated C-fibers, seems to be mediated by inflammatory cytokines.

Only one ultrasonographic study about nerve involvement in sarcoidosis has hitherto been reported (127). The authors found and increased cross sectional area of the ulnar, fibular, tibial, and sural nerve, associated with loss of fascicular echotexture or with preserved fascicular echotexture but increased size of nerve fascicles. The two types of findings are related to intraneural edema and axonal loss with Wallerian degeneration as consequence of ischemia (loss of fascicular echotexture) or to remodeling following demyelination/remyelination processes (increased size of the fascicles). Further studies are needed to confirm these findings, considering the small sample size (13 patients).

Gout and pseudogout

Gout is one of the most prevalent inflammatory arthritis in the world. In a recent study on a large population (442 patients), prevalence of symptomatic PN was 11% (128); in another study on 162 patients, the prevalence of PN at the NCS was 65% (129). The main risk factor for PN in gout are disease duration, blood level of uric acid and the presence of tophi. The pathogenesis is mainly compressive, related to the presence of thophi along the nerve course, while the toxic effect of urate on axons is a hypothesis that still need to be confirmed with neuropathologic findings. The PNs most commonly encountered are compression mononeuropathies or sensorimotor axonal polyneuropathies. Literature evidences about nerve ultrasound in gout are mainly reports of compression neuropathies by urate crystals deposits in soft tissue, in proximity of osteo-fibrous tunnel. Median nerve compression due to gout tophi within the flexor tendon is described (130) as well as a case of foot drop caused by deposition of urate crystals along the course of fibular nerve at the knee (131).

Similarly to Gout, Calcium Pyrophosphate Dihydrate (CPPD) crystal deposition (pseudogout) may lead to compression neuropathies in the limbs. Several reports of median nerve neuropathy at the carpal tunnel or ulnar nerve disorders at the cubital tunnel studied with HRUS, described hyperechoic crystal deposition in the flexor tendons or in the posterior band of ulnar collateral ligament of the elbow, causing nerve compression (132–135). In conclusion, patients with gout or pseudogout and mononeuropathy symptoms, should be screened with HRUS for the presence of amorphous or punctate hyperechogenic material compressing or dislocating a nerve in proximity of a potential entrapment site.

Drug-induced peripheral neuropathies

Drugs-related neuropathies should be considered among the differentials in rheumatological patients with peripheral nerve alterations, even though the link between PN and drug exposure is often limited to the temporal proximity without any other evidence. In recent years, the treatment of rheumatic conditions has seen a dramatic increase of new drugs which target specific molecules involved in immunity response. Biological immunomodulators, like adalimumab, infliximab, and etanercept, act as inhibitors of the TNF-α and are reported to cause different types of PNs with an incidence of 0.3–0.4 per 1,000 person-years (136, 137). This class of drugs can induce acute demyelinating neuropathy also known as GBS, the GBS variant Miller Fisher syndrome, chronic inflammatory demyelinating polyneuropathy, motor multifocal neuropathy, and axonal neuropathy (138). Nerve damage was attributed to the T-cell and humoral immune attack on the peripheral myelin, vasculitis-induced ischemia, and the inhibition of axon signaling (139). Janus kinase (JAK) inhibitors are included among the therapeutic options for RA, connective tissue diseases (140) and for hemato-oncological conditions. In a study of JAK1 and JAK2 inhibitor treatment of myelofibrosis, a new onset of PN was observed in 22% of patients who complained mainly of sensory symptoms (140). As most medication-induced neuropathies, this class of drugs affects the peripheral nerve axons and causes distal, symmetric, sensory-predominant axonal neuropathy with a progressive proximal extension. In fact, sensory myelinated (Aβ) fibers (i.e., those responsible for proprioception) or Dorsal Root Ganglia are the most sensitive to the toxins, whereas motor fibers, as well as thinly myelinated (Aδ) and unmyelinated ones (which convey temperature/pain and autonomic afferent fibers) seem more resistant to drug-induced damage (141). The immunosuppressive prodrug leflunomide is currently used as a disease-modifying treatment for RA. Also in association with this drug, axonal sensorimotor polyneuropathies are reported (142–145). The pathological analysis reported by Bharadwaj and Haroon based on three nerve biopsies from affected patients, demonstrated epineural perivascular inflammation altering the large and small myelinated nerve fibers, suggesting an axonopathy with features of vasculitis. However, other studies have reported non-specific axonal loss. The electrophysiological demonstration of neuropathy is delayed respect to the symptoms onset and is usually possible from 3 to 6 months after drug use.

Regarding ultrasound imaging of drug-induced neuropathies, to the best of our knowledge, no evidence exists regarding specific HRUS findings. Generally speaking, it is reasonable to expect that the demyelinating form of drug-related neuropathies shows the HRUS features already described in CIDP, whereas for axonal forms, US may result poorly informative. However, further imaging studies with electrodiagnostic and clinical correlation are needed to better characterize these conditions.

COVID-19-related neuropathies

The progressively increasing number of COVID-19 patients and survivors worldwide is accompanied by a rising of neuromuscular and rheumatologic complications reports, likely related to both the virus itself but also to the treatment and hospitalization (146, 147). Arthralgia and myalgia are the most common musculoskeletal symptoms of COVID-19 that can be caused by acute arthritis or myositis of various etiology (viral, reactive, and crystal-arthritis) (148). Regarding peripheral nerves, one of the largest observational studies (214 patients) on the topic reported a peripheral nervous system involvement in up to 9% of COVID-19 patients (149). Different mechanisms have been suggested to cause nerve injury. The hypothetical ability of SARS-CoV-2 to invade peripheral nerves *via* the ACE2 receptor warrants further investigation (150, 151). Alternatively, the similarities between SARS-CoV-2 surface glycoproteins and glycoconjugates in human nervous tissue support the theory of "molecular mimicry" as the mechanism of injury. The COVID-19 vaccination too has been related to many cases of PN. In these cases, the immune-mediated activation against nerve antigens is likely caused by molecular mimicry mechanism and bystander activation, both of which may be triggered by the vaccination (152). The hypothesis of direct nerve insult from the vaccination is unlikely since neuropathies after the vaccination are often reported contra-lateral to the injection site (152).

The spectrum of neuropathies described following the COVID-19 infection or the COVID-19 vaccination include Parsonage-Turner syndrome, GBS, distal symmetric polyneuropathies, entrapment, and position-related neuropathies. High resolution US may help in differentiating the conditions since each of them is characterized by a specific pattern of nerve involvement, as described above. In particular the Parsonage-Turner syndrome may present distinguishing clinical and US findings. Parsonage-Turner syndrome or neuralgic amyotrophy, is an acute inflammatory-dysimmune mononeuropathy or multifocal mononeuropathy with a monophasic course, affecting mainly the brachial plexus and its branches (153). Four types of HRUS nerve abnormalities have been described: swelling, incomplete or complete focal constriction, and fascicular entwinement (154) (**Figure 8**). Although in specific conditions such as Parsonage-Turner syndrome, HRUS may be extremely informative and able to identify patognomomic findings, also for COVID-related musculoskeletal syndromes integration with MRI, clinical and electrodiagnostic studies is mandatory in order to reach the final diagnosis, and guide the therapeutic/rehabilitation plan.

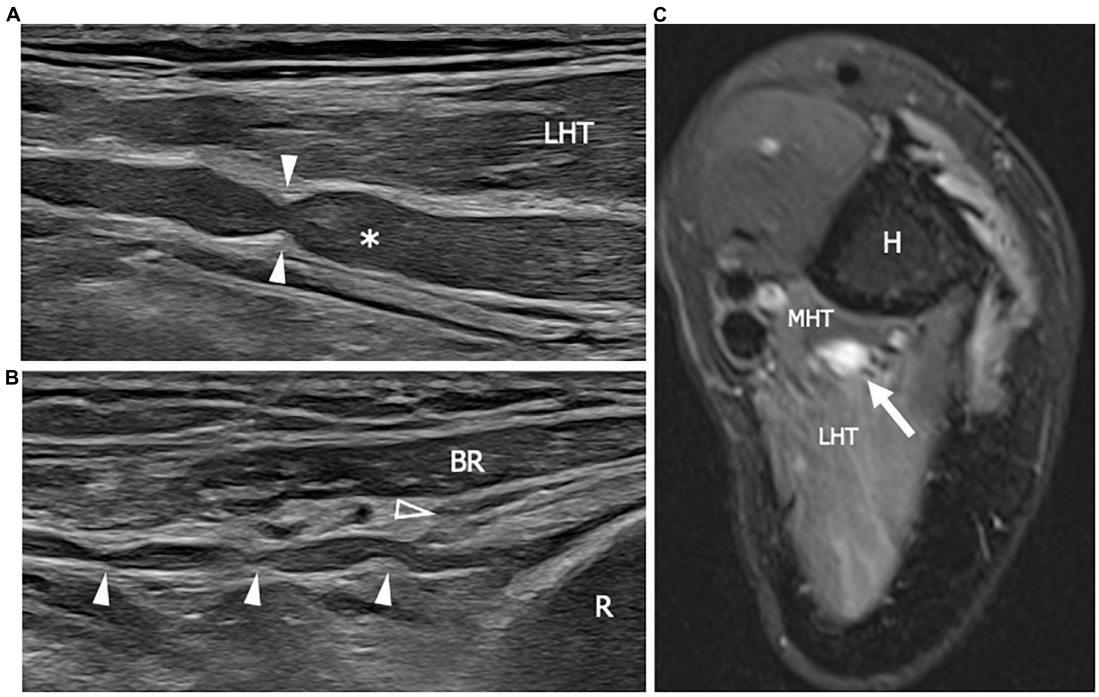

FIGURE 8
This figure shows two 22 MHz HRUS images **(A,B)** and one T2-weighted with fat saturation axial magnetic resonance image **(C)** in a 41 years old patient who developed a Parsonage-Turner syndrome following the vaccination against COVID-19. **(A)** The radial nerve (white asterisk) is seen in its long axis. The nerve results enlarged with a focal stricture (white arrowheads) along its course, deep to the lateral head of the triceps, proximal to the humerus spiral groove. The stricture is a sign of a torsion neuropathy, typically described in association with Parsonage-Turner syndrome. Multiple narrowing points (white arrowheads) can be observed also along the posterior interosseous nerve (PIN) course in **(B)**. The long axis view of the PIN shows the pathological alterations in the nerve tract proximal to the Frohse arcade or the supinator arch (empty arrowhead) which represents the likely fixation point predisposing to PIN torsion. **(C)** The radial nerve appears enlarged with an increase T2-signal as a consequence of intraneural edema. Notice the slight T2-signal hyperintensity of the lateral head and medial head of the triceps (LHT and MHT, respectively) related to muscle denervation. H, humerus; R, radius; BR, brachioradialis muscle.

Amyloidosis

Amyloidosis includes a group of conditions with a common pathomechanism, consisting in extracellular deposition of insoluble, fibrillar proteinaceous material. In the affected patients, amyloid can be demonstrated in the joint and periarticular tissue, although the tissue distribution may vary considerably (155). The protein composition of the amyloid differentiates the amyloidosis types: serum A protein in the case of amyloidosis associated with chronic inflammatory diseases (aa amyloidosis), immunoglobulin light chain in AL amyloidosis, dialysis-associated β2-microglobulin in aβ2m amyloidosis, transthyretin (TTR) or other plasma protein in hereditary systemic amyloidosis.

Peripheral neuropathy is described in association with both hereditary and acquired amyloidosis. Sensorimotor axonal polyneuropathy, compression mononeuropathies such as CTS, or autonomic neuropathy (156) are the main PN in amyloidosis. Ultrasound findings in hereditary amyloid neuropathy have been the subject of several studies. Granata et al. found different morphological alterations associated with TTR-amyloidosis neuropathy which encompassed multiple areas of nerve enlargement as in multifocal neuropathy, bilateral enlargement in proximity of the osteofibrous tunnel (ulnar nerve at the cubital tunnel and median nerve at the carpal tunnel), bilateral nerve enlargement not related to the osteofibrous tunnel. However, the authors concluded that constant HRUS abnormalities were not present but findings differed on a case-by-case basis (156).

One of the most challenging differential diagnosis for amyloid polyneuropathy is CIDP. CIDP and amyloids may show significant overlap in NCS and clinical manifestation. HRUS may help to distinguish the two conditions by showing nerve fascicles uniformly enlarged in amyloidosis in contrast to CIDP, characterized by heterogeneous and irregular nerve swelling (157). Furthermore, TTR-patients have milder nerve enlargement with less variability in CSAs of median nerves than those with CIDP (158).

Finally, nerve HRUS may help in the early diagnosis and monitoring of pre-symptomatic TTR carriers. In fact, while in idiopathic CTS there is a direct correlation between clinical severity and median nerve CSA, in the

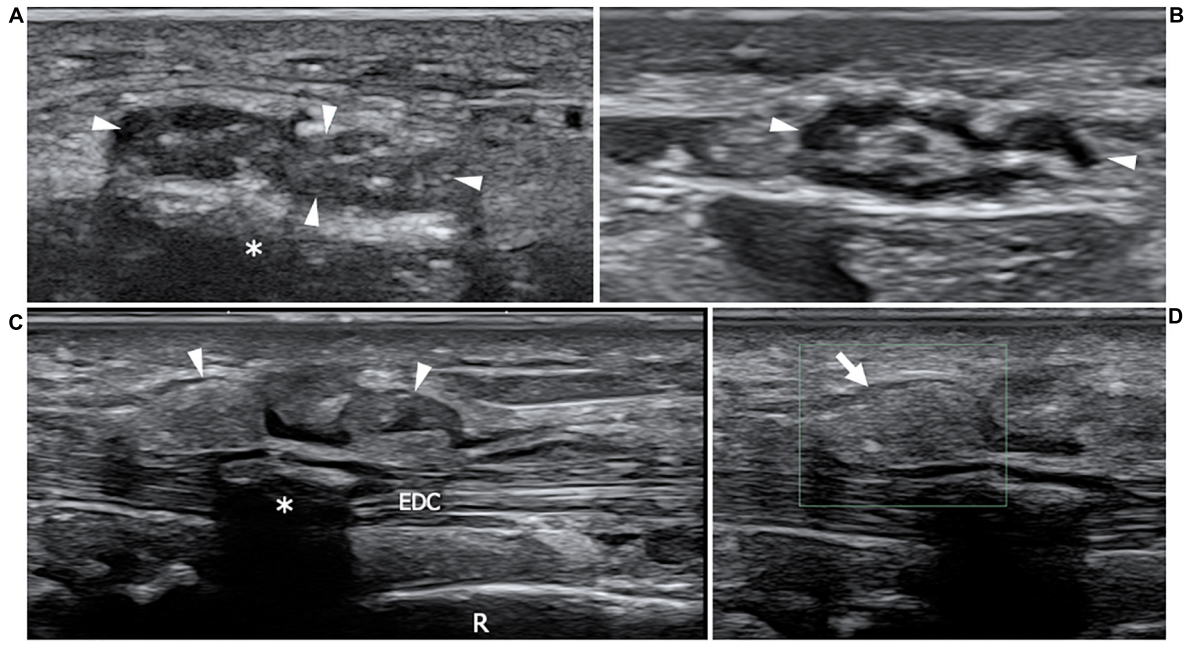

FIGURE 9
This figure shows two 22 MHz HRUS images **(A,B)** and two 18 MHz HRUS images **(C,D)** of a 62 years old male affected by multiple myeloma who developed an AL amyloid arthropathy. **(A)** An axial view of the median nerve (white arrowheads), situated in the proximity of the flexor retinaculum is presented. The nerve appears enlarged, with clumped hypoechoic fascicles, a finding which is related to the compression due to the underlying amorphous, hyperechoic material (white asterisk); the nerve echotextural alterations become even more evident if the image is compared to the image in **(B)** where the median nerve (white arrowheads) is visualized in the short axis at a more cranial level in the forearm. **(C)** On the dorsal aspect of the same wrist, a huge distension of the extensor digitorum communis tendons (EDC) synovial sheath (white arrowheads) can be observed. At the Eco-Color Doppler evaluation showed in **(D)**, the inhomogeneous, hyperechoic material distending the tenosynovial sheath (white arrow) results avascular, a finding which is compatible with an intrasynovial amyloid deposition. White asterisk, intra-tendon calcification; R, radius.

subgroup of TTR subjects a dissociation between nerve morphology and electrodiagnostic findings is found. The morpho-functional dissociation can be considered typical of TTR-amyloidosis neuropathy. Furthermore, patients affected by symptomatic TTR-amyloidosis showed larger nerve CSA than pre-symptomatic carriers in several nerve sites, more pronounced at brachial plexus.

Differently from TTR-amyloidosis, little is known about nerve involvement in acquired amyloidosis. The majority of Ultrasound data about the musculoskeletal acquired amyloids has come from cases with musculoskeletal ß2 amyloidosis due to long-term dialysis (159). In a case report describing a patient affected by light-chain amyloidosis, the authors suggest a correlation between the entity of amyloid deposits and nerve enlargement seen with HRUS (160). The enlarged nerve is commonly accompanied by other sonographic findings in the surrounding soft tissue, notably tendon enlargement, synovial thickening and, synovia-like masses around tendons or within bursas (160). However, the absence of Doppler signal could help to distinguish these hypoechoic para-articular masses in respect to synovitis (**Figure 9**).

Discussion

Although NCS along with clinical history and occasionally nerve biopsy constitute the well established diagnostic approach for the assessment of PNs in rheumatologic conditions, these tools present some shortcomings such as invasiveness and discomfort. In addition, clinical and electrodiagnostic approaches may produce false-negatives, show low positive predictive value and be non-localizing in patients with mild lesions or cases of severe axonal injury. By contrast, HRUS provides unparalleled complementary information which strengthens and accelerates PN diagnosis. Furthermore, HRUS is useful for the assessment of the response to treatment in inflammatory PNs. Even if the availability of 3T MRI with morphological and functional sequences is an appealing diagnostic tool, it should be considered as a complementary instrument to HRUS because it is costly, requires long scanning times and has lower spatial resolution than HRUS for the superficial nerves. However, PNs in rheumatologic diseases in most of the cases do not present specific sonographic patterns, but the US findings reproduce those reported in an idiopathic counterpart. Furthermore, at now, a significant

percentage of neuropathies, mainly the axonal ones, are difficult to detect with HRUS. In view of the above, ultrasound is still extremely useful in differentiating a compressive neuropathies from a demyelinating autoimmune neuropathy or an amyloid neuropathy, all them potentially affecting the same rheumatologic patient but requires diverse therapeutic approaches. Our narrative review points out many potential triggers for further research regarding ultrasound applications in the diagnostic workup of the different neuropathies in rheumatology. In fact, in many conditions as LES, SS, the acquired forms of systemic amyloidosis, drug-related neuropathies etc., the scant imaging research focused mainly on entrapment neuropathies. However, the dysimmune polyneuropathies coexisting with autoimmune musculoskeletal disorders may be amenable to HRUS evaluation. In particular, it could be interesting to carry out morphological studies in those patients showing a mismatch between clinical neuropathic symptoms and NCS, frequently reported in many rheumatologic conditions: HRUS may result a useful, non-invasive screening tool for early recognition of nerve damage. Even those neuropathies which may result underdiagnosed with HRUS by applying a standard pattern recognition approach, could be better characterized by using quantitative parameters as nerve CSA, maximum and minimum fascicle diameter, intra-nerve and internerve CSA variability. Furthermore, the recent development of a radiomic type analysis seems to further increase the information that HRUS may yield. Radiomics is a relatively new approach for converting information and features present in medical images into quantifiable data. Moreover, machine learning algorithms have used these quantifiable data to enhance the diagnostic models. Ultrasound-based radiomics is a rapidly growing approach in imaging research that has already been applied to various organ (161). We expect in the next future the Ultrasound-based radiomics will be applied to nerves for a more precise identification of PNs.

Author contributions

FZ and RP conceived and designed the review. FZ wrote the manuscript. FP, SS, MP, LT, UV, MG, CC, and LB collected the pathological cases and contributed to the literature search. CM supervised the study and contributed to the review design. All authors contributed to the article and approved the submitted version.

Funding

This work has been partially supported by the "Ricerca Corrente" funding provided by the Italian Ministry of Health to the IRCCS Ospedale Policlinico San Martino.

Conflict of interest

The authors declare that the research was conducted in the absence of any commercial or financial relationships that could be construed as a potential conflict of interest.

Publisher's note

All claims expressed in this article are solely those of the authors and do not necessarily represent those of their affiliated organizations, or those of the publisher, the editors and the reviewers. Any product that may be evaluated in this article, or claim that may be made by its manufacturer, is not guaranteed or endorsed by the publisher.

References

1. Agarwal V, Singh R, Wiclaf, Chauhan S, Tahlan A, Ahuja CK, et al. A clinical, electrophysiological, and pathological study of neuropathy in rheumatoid arthritis. *Clin Rheumatol.* (2008) 27:841–4. doi: 10.1007/s10067-007-0804-x

2. Colebatch AN, Edwards CJ, Østergaard M, van der Heijde D, Balint PV, D'Agostino MA, et al. EULAR recommendations for the use of imaging of the joints in the clinical management of rheumatoid arthritis. *Ann Rheum Dis.* (2013) 72:804–14. doi: 10.1136/annrheumdis-2012-203158

3. D'Agostino MA, Terslev L, Aegerter P, Backhaus M, Balint P, Bruyn GA, et al. Scoring ultrasound synovitis in rheumatoid arthritis: a EULAR-OMERACT ultrasound taskforce-Part 1: definition and development of a standardised, consensus-based scoring system. *RMD Open.* (2017) 3:e000428. doi: 10.1136/rmdopen-2016-000428

4. Padua L, Liotta G, Di Pasquale A, Granata G, Pazzaglia C, Caliandro P, et al. Contribution of ultrasound in the assessment of nerve diseases. *Eur J Neurol.* (2012) 19:47–54. doi: 10.1111/j.1468-1331.2011.03421.x

5. Goedee HS, van der Pol WL, van Asseldonk JH, Franssen H, Notermans NC, Vrancken AJ, et al. Diagnostic value of sonography in treatment-naive chronic inflammatory neuropathies. *Neurology.* (2017) 88:143–51. doi: 10.1212/WNL.0000000000003483

6. Telleman JA, Grimm A, Goedee S, Visser LH, Zaidman CM. Nerve ultrasound in polyneuropathies. *Muscle Nerve.* (2018) 57:716–28. doi: 10.1002/mus.26029

7. Torres-Costoso A, Martínez-Vizcaíno V, Álvarez-Bueno C, Ferri-Morales A, Cavero-Redondo I. Accuracy of ultrasonography for the diagnosis of carpal tunnel syndrome: a systematic review and meta-analysis. *Arch Phys Med Rehabil.* (2018) 99:758–65.e10. doi: 10.1016/j.apmr.2017.08.489

8. Visser LH, Hens V, Soethout M, De Deugd-Maria V, Pijnenburg J, Brekelmans GJ. Diagnostic value of high-resolution sonography in common fibular neuropathy at the fibular head. *Muscle Nerve.* (2013) 48:171–8. doi: 10.1002/mus.23729

9. Zaidman CM, Al-Lozi M, Pestronk A. Peripheral nerve size in normals and patients with polyneuropathy: an ultrasound study. *Muscle Nerve.* (2009) 40:960–6. doi: 10.1002/mus.21431

10. Di Pasquale A, Morino S, Loreti S, Bucci E, Vanacore N, Antonini G. Peripheral nerve ultrasound changes in CIDP and correlations with

nerve conduction velocity. *Neurology.* (2015) 84:803–9. doi: 10.1212/WNL.0000000000001291

11. Casteleyn V, Hahn K, Stenzel W, Siegert E. Periphere Nervenbeteiligung bei rheumatischen Erkrankungen [Peripheral nerve involvement in rheumatic diseases]. *Z Rheumatol.* (2019) 78:339–51. German. doi: 10.1007/s00393-019-0621-z

12. Tapadia M, Mozaffar T, Gupta R. Compressive neuropathies of the upper extremity: update on pathophysiology, classification, and electrodiagnostic findings. *J Hand Surg Am.* (2010) 35:668–77. doi: 10.1016/j.jhsa.2010.01.007

13. Crowley B, Gschwind CR, Storey C. Selective motor neuropathy of the median nerve caused by a ganglion in the carpal tunnel. *J Hand Surg Br.* (1998) 23:611–2. doi: 10.1016/s0266-7681(98)80013-2

14. Birnbaum J, Bingham CO III. Non-length-dependent and length-dependent small-fiber neuropathies associated with tumor necrosis factor (TNF)-inhibitor therapy in patients with rheumatoid arthritis: expanding the spectrum of neurological disease associated with TNF-inhibitors. *Semin Arthritis Rheum.* (2014) 43:638–47. doi: 10.1016/j.semarthrit.2013.10.007

15. Weisman A, Bril V, Ngo M, Lovblom LE, Halpern EM, Orszag A, et al. Identification and prediction of diabetic sensorimotor polyneuropathy using individual and simple combinations of nerve conduction study parameters. *PLoS One.* (2013) 8:e58783. doi: 10.1371/journal.pone.0058783

16. England JD, Gronseth GS, Franklin G, Miller RG, Asbury AK, Carter GT, et al. Distal symmetrical polyneuropathy: definition for clinical research. *Muscle Nerve.* (2005) 31:113–23. doi: 10.1002/mus.20233

17. Hobson-Webb LD, Padua L, Martinoli C. Ultrasonography in the diagnosis of peripheral nerve disease. *Expert Opin Med Diagn.* (2012) 6:457–71. doi: 10.1517/17530059.2012.692904

18. Kowalska B, Sudoł-Szopińska I. Normal and sonographic anatomy of selected peripheral nerves. Part I: sonohistology and general principles of examination, following the example of the median nerve. *J Ultrason.* (2012) 12:120–30. doi: 10.15557/JoU.2012.0001

19. Lin DC, Nazarian LN, O'Kane PL, McShane JM, Parker L, Merritt CR. Advantages of real-time spatial compound sonography of the musculoskeletal system versus conventional sonography. *AJR Am J Roentgenol.* (2002) 179:1629–31. doi: 10.2214/ajr.179.6.1791629

20. Martinoli C, Bianchi S, Gandolfo N, Valle M, Simonetti S, Derchi LE. US of nerve entrapments in osteofibrous tunnels of the upper and lower limbs. *Radiographics.* (2000) 20:S199–213; discussion S213-7. doi: 10.1148/radiographics.20.suppl_1.g00oc08s199

21. Fodor D, Rodriguez-Garcia SC, Cantisani V, Hammer HB, Hartung W, Klauser A, et al. The EFSUMB guidelines and recommendations for musculoskeletal ultrasound - Part I: extraarticular pathologies. *Ultraschall Med.* (2022) 43:34–57. English. doi: 10.1055/a-1562-1455

22. Duncan I, Sullivan P, Lomas F. Sonography in the diagnosis of carpal tunnel syndrome. *AJR Am J Roentgenol.* (1999) 173:681–4. doi: 10.2214/ajr.173.3.10470903

23. Martinoli C, Bianchi S, Pugliese F, Bacigalupo L, Gauglio C, Valle M, et al. Sonography of entrapment neuropathies in the upper limb (wrist excluded). *J Clin Ultrasound.* (2004) 32:438–50. doi: 10.1002/jcu.20067

24. Rodríguez Y, Vatti N, Ramírez-Santana C, Chang C, Mancera-Páez O, Gershwin ME, et al. Chronic inflammatory demyelinating polyneuropathy as an autoimmune disease. *J Autoimmun.* (2019) 102:8–37. doi: 10.1016/j.jaut.2019.04.021

25. Chused TM, Kassan SS, Opelz G, Moutsopoulos HM, Terasaki PI. Sjögren's syndrome association with HLA-Dw3. *N Engl J Med.* (1977) 296:895–7. doi: 10.1056/NEJM197704212961602

26. Scherak O, Kolarz G, Mayr WR. HLA-B8 in caucasian patients with systemic lupus erythematosus. *Scand J Rheumatol.* (1978) 7:3–6.

27. Kerasnoudis A, Pitarokoili K, Behrendt V, Gold R, Yoon MS. Nerve ultrasound score in distinguishing chronic from acute inflammatory demyelinating polyneuropathy. *Clin Neurophysiol.* (2014) 125:635–41. doi: 10.1016/j.clinph.2013.08.014

28. Kerasnoudis A, Klasing A, Behrendt V, Gold R, Yoon MS. Intra- and internerve cross-sectional area variability: new ultrasound measures. *Muscle Nerve.* (2013) 47:146–7. doi: 10.1002/mus.23520

29. Kerasnoudis A, Pitarokoili K. Ulnar nerve reference values for cross-sectional area, intranerve cross sectional area variability and side to side difference ratio. *Rheumatol Int.* (2014) 34:551–2. doi: 10.1007/s00296-013-2708-1

30. Zaidman CM, Harms MB, Pestronk A. Ultrasound of inherited vs. acquired demyelinating polyneuropathies. *J Neurol.* (2013) 260:3115–21. doi: 10.1007/s00415-013-7123-8

31. Grimm A, Heiling B, Schumacher U, Witte OW, Axer H. Ultrasound differentiation of axonal and demyelinating neuropathies. *Muscle Nerve.* (2014) 50:976–83. doi: 10.1002/mus.24238

32. Leupold D, Felbecker A, Tettenborn B, Hundsberger T. Nerve ultrasound as a decisive tool in nonsystemic vasculitic neuropathy: a case report. *Case Rep Neurol.* (2016) 8:108–14. doi: 10.1159/000446314

33. Grimm A, Décard BF, Bischof A, Axer H. Ultrasound of the peripheral nerves in systemic vasculitic neuropathies. *J Neurol Sci.* (2014) 347:44–9. doi: 10.1016/j.jns.2014.09.017

34. Ito T, Kijima M, Watanabe T, Sakuta M, Nishiyama K. Ultrasonography of the tibial nerve in vasculitic neuropathy. *Muscle Nerve.* (2007) 35:379–82. doi: 10.1002/mus.20673

35. Grimm A, Décard BF, Schramm A, Pröbstel AK, Rasenack M, Axer H, et al. Ultrasound and electrophysiologic findings in patients with Guillain-Barré syndrome at disease onset and over a period of six months. *Clin Neurophysiol.* (2016) 127:1657–63. doi: 10.1016/j.clinph.2015.06.032

36. Derksen A, Ritter C, Athar P, Kieseier BC, Mancias P, Hartung HP, et al. Sural sparing pattern discriminates Guillain-Barré syndrome from its mimics. *Muscle Nerve.* (2014) 50:780–4. doi: 10.1002/mus.24226

37. Kerasnoudis A, Pitarokoili K, Behrendt V, Gold R, Yoon MS. Correlation of nerve ultrasound, electrophysiological and clinical findings in chronic inflammatory demyelinating polyneuropathy. *J Neuroimaging.* (2015) 25:207–16. doi: 10.1111/jon.12079

38. Gallardo E, Noto Y, Simon NG. Ultrasound in the diagnosis of peripheral neuropathy: structure meets function in the neuromuscular clinic. *J Neurol Neurosurg Psychiatry.* (2015) 86:1066–74. doi: 10.1136/jnnp-2014-309599

39. Yu JY, Jeong JG, Lee BH. Evaluation of muscle damage using ultrasound imaging. *J Phys Ther Sci.* (2015) 27:531–4. doi: 10.1589/jpts.27.531

40. Küllmer K, Sievers KW, Reimers CD, Rompe JD, Müller-Felber W, Nägele M, et al. Changes of sonographic, magnetic resonance tomographic, electromyographic, and histopathologic findings within a 2-month period of examinations after experimental muscle denervation. *Arch Orthop Trauma Surg.* (1998) 117:228–34. doi: 10.1007/s004020050234

41. Campbell SE, Adler R, Sofka CM. Ultrasound of muscle abnormalities. *Ultrasound Q.* (2005) 21:87–94; quiz 150, 153–4.

42. Weber MA. Ultrasound in the inflammatory myopathies. *Ann N Y Acad Sci.* (2009) 1154:159–70. doi: 10.1111/j.1749-6632.2009.04390.x

43. Albayda J, van Alfen N. Diagnostic value of muscle ultrasound for myopathies and myositis. *Curr Rheumatol Rep.* (2020) 22:82. doi: 10.1007/s11926-020-00947-y

44. Simon NG, Ralph JW, Lomen-Hoerth C, Poncelet AN, Vucic S, Kiernan MC, et al. Quantitative ultrasound of denervated hand muscles. *Muscle Nerve.* (2015) 52:221–30. doi: 10.1002/mus.24519

45. Gutiérrez J, Sandoval H, Pérez-Neri I, Arauz A, López-Hernández JC, Pineda C. Advances in imaging technologies for the assessment of peripheral neuropathies in rheumatoid arthritis. *Rheumatol Int.* (2021) 41:519–28. doi: 10.1007/s00296-020-04780-5

46. Telleman JA, Herraets IJT, Goedee HS, Verhamme C, Nikolakopoulos S, van Asseldonk JH, et al. Nerve ultrasound: a reproducible diagnostic tool in peripheral neuropathy. *Neurology.* (2018):10.1212/WNL.0000000000006856. [Online ahead of print]. doi: 10.1212/WNL.0000000000006856

47. Liang MH, Corzillius M, Bae SC, Lew RA, Fortin PR, Gordon C, et al. The American College of Rheumatology nomenclature and case definitions for neuropsychiatric lupus syndromes. *Arthritis Rheum.* (1999) 42:599–608. doi: 10.1002/1529-0131(199904)42:4<599::AID-ANR2>3.0.CO;2-F

48. Shaban A, Leira EC. Neurological complications in patients with systemic lupus erythematosus. *Curr Neurol Neurosci Rep.* (2019) 19:97. doi: 10.1007/s11910-019-1012-1

49. Xianbin W, Mingyu W, Dong X, Huiying L, Yan X, Fengchun Z, et al. Peripheral neuropathies due to systemic lupus erythematosus in China. *Medicine (Baltimore).* (2015) 94:e625. doi: 10.1097/MD.0000000000000625

50. Toledano P, Orueta R, Rodríguez-Pintó I, Valls-Solé J, Cervera R, Espinosa G. Peripheral nervous system involvement in systemic lupus erythematosus: prevalence, clinical and immunological characteristics, treatment and outcome of a large cohort from a single centre. *Autoimmun Rev.* (2017) 16:750–5. doi: 10.1016/j.autrev.2017.05.011

51. Saigal R, Bhargav R, Goyal L, Agrawal A, Mital P, Wadhwani D. Peripheral neuropathy in systemic lupus erythematosus: clinical and electrophysiological properties and their association with disease activity parameters. *J Assoc Physicians India.* (2015) 63:15–9.

52. Bortoluzzi A, Piga M, Silvagni E, Chessa E, Mathieu A, Govoni M. Peripheral nervous system involvement in systemic lupus erythematosus: a retrospective study on prevalence, associated factors and outcome. *Lupus.* (2019) 28:465–74. doi: 10.1177/0961203319828499

53. Hanly JG, Li Q, Su L, Urowitz MB, Gordon C, Bae SC, et al. Peripheral nervous system disease in systemic lupus erythematosus: results from an international inception cohort study. *Arthritis Rheumatol.* (2020) 72:67–77. doi: 10.1002/art.41070

54. Goh K, Wang C, Leong S, Tan C. Peripheral neuropathy in systemic lupus erythematosus: electrophysiological features in 50 consecutive cases. *Neurol J Southeast Asia.* (1996) 1:47–51.

55. Omdal R, Løseth S, Torbergsen T, Koldingsnes W, Husby G, Mellgren SI. Peripheral neuropathy in systemic lupus erythematosus-a longitudinal study. *Acta Neurol Scand.* (2001) 103:386–91. doi: 10.1034/j.16000404.2001.103006386.x

56. Fong SY, Raja J, Wong KT, Goh KJ. Systemic lupus erythematosus may have an early effect on peripheral nerve function in patients without clinical or electrophysiological neuropathy: comparison with age- and gender-matched controls. *Rheumatol Int.* (2021) 41:355–60. doi: 10.1007/s00296-020-04610-8

57. Fargetti S, Ugolini-Lopes MR, Pasoto SG, Seguro LPC, Shinjo SK, Bonfa E, et al. Short- and long-term outcome of systemic lupus erythematosus peripheral neuropathy: bimodal pattern of onset and treatment response. *J Clin Rheumatol.* (2021) 27:S212–6. doi: 10.1097/RHU.0000000000001201

58. Zhang N, Cao J, Zhao M, Sun L. The introspection on the diagnosis and treatment process of a case of Guillain-Barré syndrome (GBS) attributed to systemic lupus erythematosus (SLE): a case report. *Medicine (Baltimore).* (2017) 96:e9037. doi: 10.1097/MD.0000000000009037

59. Florica B, Aghdassi E, Su J, Gladman DD, Urowitz MB, Fortin PR. Peripheral neuropathy in patients with systemic lupus erythematosus. *Semin Arthritis Rheum.* (2011) 41:203–11. doi: 10.1016/j.semarthrit.2011.04.001

60. Mahran SA, Galluccio F, Khedr TM, Elsonbaty A, Allam AE, Garcia Martos A, et al. Peripheral neuropathy in systemic lupus erythematosus: what can neuromuscular ultrasonography (NMUS) tell us? A cross-sectional study. *Lupus Sci Med.* (2021) 8:e000521. doi: 10.1136/lupus-2021-000521

61. Ye W, Chen S, Huang X, Qin W, Zhang T, Zhu X, et al. Clinical features and risk factors of neurological involvement in Sjögren's syndrome. *BMC Neurosci.* (2018) 19:26. doi: 10.1186/s12868-018-0427-y

62. Seeliger T, Prenzler NK, Gingele S, Seeliger B, Körner S, Thiele T, et al. Neuro-Sjögren: peripheral neuropathy with limb weakness in Sjögren's syndrome. *Front Immunol.* (2019) 10:1600. doi: 10.3389/fimmu.2019.01600

63. Carvajal Alegria G, Guellec D, Mariette X, Gottenberg JE, Dernis E, Dubost JJ, et al. Epidemiology of neurological manifestations in Sjögren's syndrome: data from the French ASSESS Cohort. *RMD Open.* (2016) 2:e000179. doi: 10.1136/rmdopen-2015-000179

64. Perzyńska-Mazan J, Maślińska M, Gasik R. Neurophysiological features of peripheral nervous system involvement and immunological profile of patients with primary Sjögren syndrome. *J Rheumatol.* (2020) 47:1661–7. doi: 10.3899/jrheum.181464

65. Sireesha Y, Kanikannan MA, Pyal A, Sandeep G, Uppin MS, Kandadai RM, et al. Patterns of peripheral neuropathy in Sjogren's syndrome in a tertiary care hospital from South India. *Neurol India.* (2019) 67:S94–9. doi: 10.4103/0028-3886.250714

66. Jaskólska M, Chylińska M, Masiak A, Siemiński M, Ziętkiewicz M, Czuszyńska Z, et al. Neuro-Sjögren: uncommon or underestimated problem? *Brain Behav.* (2020) 10:e01665. doi: 10.1002/brb3.1665

67. Jaskólska M, Chylińska M, Masiak A, Nowicka-Sauer K, Siemiński M, Ziętkiewicz M, et al. Peripheral neuropathy and health-related quality of life in patients with primary Sjögren's syndrome: a preliminary report. *Rheumatol Int.* (2020) 40:1267–74. doi: 10.1007/s00296-020-04543-2

68. Alunno A, Carubbi F, Bartoloni E, Cipriani P, Giacomelli R, Gerli R. The kaleidoscope of neurological manifestations in primary Sjögren's syndrome. *Clin Exp Rheumatol.* (2019) 37(Suppl. 118):192–8.

69. Sivadasan A, Muthusamy K, Patel B, Benjamin RN, Prabhakar AT, Mathew V, et al. Clinical spectrum, therapeutic outcomes, and prognostic predictors in Sjogren's syndrome-associated neuropathy. *Ann Indian Acad Neurol.* (2017) 20:278–83. doi: 10.4103/aian.AIAN_116_17

70. Pavlakis PP, Alexopoulos H, Kosmidis ML, Mamali I, Moutsopoulos HM, Tzioufas AG, et al. Peripheral neuropathies in Sjögren's syndrome: a critical update on clinical features and pathogenetic mechanisms. *J Autoimmun.* (2012) 39:27–33. doi: 10.1016/j.jaut.2012.01.003

71. Seeliger T, Bönig L, Gingele S, Prenzler NK, Thiele T, Ernst D, et al. Nerve ultrasound findings in Sjögren's syndrome-associated neuropathy. *J Neuroimaging.* (2021) 31:1156–65. doi: 10.1111/jon.12907

72. Padua L, Granata G, Sabatelli M, Inghilleri M, Lucchetta M, Luigetti M, et al. Heterogeneity of root and nerve ultrasound pattern in CIDP patients. *Clin Neurophysiol.* (2014) 125:160–5. doi: 10.1016/j.clinph.2013.07.023

73. Raja J, Balaikerisnan T, Ramanaidu LP, Goh KJ. Large fiber peripheral neuropathy in systemic sclerosis: a prospective study using clinical and electrophysiological definition. *Int J Rheum Dis.* (2021) 24:347–54. doi: 10.1111/1756-185X.14042

74. Paik JJ, Mammen AL, Wigley FM, Shah AA, Hummers LK, Polydefkis M. Symptomatic and electrodiagnostic features of peripheral neuropathy in scleroderma. *Arthritis Care Res (Hoboken).* (2016) 68:1150–7.

75. AlMehmadi BA, To FZ, Anderson MA, Johnson SR. Epidemiology and treatment of peripheral neuropathy in systemic sclerosis. *J Rheumatol.* (2021) 48:1839–49. doi: 10.3899/jrheum.201299

76. Yagci I, Kenis-Coskun O, Ozsoy T, Ozen G, Direskeneli H. Increased stiffness of median nerve in systemic sclerosis. *BMC Musculoskelet Disord.* (2017) 18:434. doi: 10.1186/s12891-017-1793-9

77. Sriwong PT, Sirasaporn P, Foochareon C, Srichompoo K. Median neuropathy at the wrist in patients with systemic sclerosis: two-year follow-up study. *Reumatologia.* (2018) 56:294–300. doi: 10.5114/reum.2018.79500

78. Tadic M, Zlatanovic M, Cuspidi C, Stevanovic A, Celic V, Damjanov N, et al. Systemic sclerosis impacts right heart and cardiac autonomic nervous system. *J Clin Ultrasound.* (2018) 46:188–94. doi: 10.1002/jcu.22552

79. Tagliafico A, Panico N, Resmini E, Derchi LE, Ghio M, Martinoli C. The role of ultrasound imaging in the evaluation of peripheral nerve in systemic sclerosis (scleroderma). *Eur J Radiol.* (2011) 77:377–82. doi: 10.1016/j.ejrad.2009.08.010

80. Bignotti B, Ghio M, Panico N, Tagliafico G, Martinoli C, Tagliafico A. High-resolution ultrasound of peripheral nerves in systemic sclerosis: a pilot study of computer-aided quantitative assessment of nerve density. *Skeletal Radiol.* (2015) 44:1761–7. doi: 10.1007/s00256-015-2230-5

81. Biswas M, Chatterjee A, Ghosh SK, Dasgupta S, Ghosh K, Ganguly PK. Prevalence, types, clinical associations, and determinants of peripheral neuropathy in rheumatoid patients. *Ann Indian Acad Neurol.* (2011) 14:194–7. doi: 10.4103/0972-2327.85893

82. Kaeley N, Ahmad S, Pathania M, Kakkar R. Prevalence and patterns of peripheral neuropathy in patients of rheumatoid arthritis. *J Family Med Prim Care.* (2019) 8:22–6. doi: 10.4103/jfmpc.jfmpc_260_18

83. Kumar B, Das MP, Misra AK. A cross-sectional study of association of serostatus and extra-articular manifestations in patients with rheumatoid arthritis in a teaching hospital. *J Family Med Prim Care.* (2020) 9:2789–93. doi: 10.4103/jfmpc.jfmpc_99_20

84. Cojocaru IM, Cojocaru M, Silosi I, Vrabie CD. Peripheral nervous system manifestations in systemic autoimmune diseases. *Maedica (Bucur).* (2014) 9:289–94.

85. Bekkelund SI, Torbergsen T, Husby G, Mellgren SI. Myopathy and neuropathy in rheumatoid arthritis. A quantitative controlled electromyographic study. *J Rheumatol.* (1999) 26:2348–51.

86. Syngle V, Syngle A, Garg N, Krishan P, Verma I. Predictors of autonomic neuropathy in rheumatoid arthritis. *Auton Neurosci.* (2016) 201:54–9. doi: 10.1016/j.autneu.2016.07.008

87. Puéchal X, Said G, Hilliquin P, Coste J, Job-Deslandre C, Lacroix C, et al. Peripheral neuropathy with necrotizing vasculitis in rheumatoid arthritis. A clinicopathologic and prognostic study of thirty-two patients. *Arthritis Rheum.* (1995) 38:1618–29. doi: 10.1002/art.1780381114

88. Nakano KK. The entrapment neuropathies of rheumatoid arthritis. *Orthop Clin North Am.* (1975) 6:837–60.

89. Baylan SP, Paik SW, Barnert AL, Ko KH, Yu J, Persellin RH. Prevalence of the tarsal tunnel syndrome in rheumatoid arthritis. *Rheumatol Rehabil.* (1981) 20:148–50. doi: 10.1093/rheumatology/20.3.148

90. Tatsumura M, Mishima H, Shiina I, Hara Y, Nishiura Y, Ishii T, et al. Femoral nerve palsy caused by a huge iliopectineal synovitis extending to the iliac fossa in a rheumatoid arthritis case. *Mod Rheumatol.* (2008) 18:81–5. doi: 10.1007/s10165-007-0009-9

91. Smerilli G, Di Matteo A, Cipolletta E, Carloni S, Incorvaia A, Di Carlo M, et al. Ultrasound assessment of carpal tunnel in rheumatoid arthritis and idiopathic carpal tunnel syndrome. *Clin Rheumatol.* (2021) 40:1085–92. doi: 10.1007/s10067-020-05293-z

92. Sharma A, Pinto B, Dhooria A, Rathi M, Singhal M, Dhir V, et al. Polyarteritis nodosa in north India: clinical manifestations and outcomes. *Int J Rheum Dis.* (2017) 20:390–7. doi: 10.1111/1756-185X.12954

93. de Boysson H, Guillevin L. Polyarteritis nodosa neurologic manifestations. *Neurol Clin.* (2019) 37:345–57. doi: 10.1016/j.ncl.2019.01.007

94. Imboden JB. Involvement of the peripheral nervous system in polyarteritis nodosa and antineutrophil cytoplasmic antibodies-associated vasculitis. *Rheum Dis Clin North Am.* (2017) 43:633–9. doi: 10.1016/j.rdc.2017.06.011

95. James J, Jose J, Thulaseedharan NK. Acute necrotizing vasculitic neuropathy due to polyarteritis nodosa. *Oman Med J.* (2018) 33:253–5. doi: 10.5001/omj.2018.46

96. Kara M, Ozçakar L. Ultrasonographic imaging of the sciatic nerves in a patient with polyarteritis nodosa. *Rheumatol Int.* (2012) 32:3327–8. doi: 10.1007/s00296-011-2138-x

97. Nishi R, Koike H, Ohyama K, Fukami Y, Ikeda S, Kawagashira Y, et al. Differential clinicopathologic features of EGPA-associated neuropathy with and without ANCA. *Neurology.* (2020) 94:e1726–37. doi: 10.1212/WNL.0000000000009309

98. Bischof A, Jaeger VK, Hadden RDM, Luqmani RA, Pröbstel AK, Merkel PA, et al. Peripheral neuropathy in antineutrophil cytoplasmic antibody-associated vasculitides: insights from the DCVAS study. *Neurol Neuroimmunol Neuroinflamm.* (2019) 6:e615. doi: 10.1212/NXI.0000000000000615

99. Said G, Lacroix C. Primary and secondary vasculitic neuropathy. *J Neurol.* (2005) 252:633–41. doi: 10.1007/s00415-005-0833-9

100. Hattori N, Mori K, Misu K, Koike H, Ichimura M, Sobue G, et al. Mortality and morbidity in peripheral neuropathy associated Churg-Strauss syndrome and microscopic polyangiitis. *J Rheumatol.* (2002) 29:1408–14.

101. Collins MP, Dyck PJ, Gronseth GS, Guillevin L, Hadden RD, Heuss D, et al. Peripheral nerve society. peripheral nerve society guideline on the classification, diagnosis, investigation, and immunosuppressive therapy of non-systemic vasculitic neuropathy: executive summary. *J Peripher Nerv Syst.* (2010) 15:176–84. doi: 10.1111/j.1529-8027.2010.00281.x

102. Moog P, Eren O, Witt M, Rauschel V, Kossegg S, Straube A, et al. Assessment of autonomic function in a cohort of patients with ANCA-associated vasculitis. *Clin Auton Res.* (2016) 26:279–85. doi: 10.1007/s10286-016-0364-8

103. Murata K, Endo K, Nishimura H, Tanaka H, Shishido T, Yamamoto K. Eosinophilic granulomatosis with polyangiitis presenting as acute sciatic nerve neuropathy resembling lumbar disease. *J Orthop Sci.* (2015) 20:224–8. doi: 10.1007/s00776-013-0437-7

104. Camara-Lemarroy CR, Infante-Valenzuela A, Villareal-Montemayor HJ, Soto-Rincon CA, Davila-Olalde JA, Villareal-Velazquez HJ. Eosinophilic granulomatosis with polyangiitis presenting as acute polyneuropathy mimicking guillain-barre syndrome. *Case Rep Neurol Med.* (2015) 2015:981439. doi: 10.1155/2015/981439

105. Üçeyler N, Schäfer KA, Mackenrodt D, Sommer C, Müllges W. High-resolution ultrasonography of the superficial peroneal motor and sural sensory nerves may be a non-invasive approach to the diagnosis of vasculitic neuropathy. *Front Neurol.* (2016) 7:48. doi: 10.3389/fneur.2016.00048

106. Bougea A, Anagnostou E, Spandideas N, Triantafyllou N, Kararizou E. An update of neurological manifestations of vasculitides and connective tissue diseases: a literature review. *Einstein (Sao Paulo).* (2015) 13:627–35. doi: 10.1590/S1679-45082015RW3308

107. Duval F, Lacoste I, Galli G, Chaumont H, Solé G, Léger F, et al. Acute brachial radiculoplexopathy and giant cell arteritis. *Neurologist.* (2018) 23:23–8. doi: 10.1097/NRL.0000000000000162

108. Calle-Lopez Y, Fernandez-Ramirez AF, Franco-Dager E, Gomez-Lopera JG, Vanegas-Garcia AL. Sindrome del hombre en el barril: manifestacion atipica de la arteritis de celulas gigantes [«Man-in-the-barrel» syndrome: atypical manifestation of giant cell arteritis]. *Rev Neurol.* (2018) 66:373–6. Spanish.

109. Conway R, Kinsella JA, Molloy ES. Peroneal neuropathy in giant cell arteritis. *Rheumatology (Oxford).* (2017) 56:169–70. doi: 10.1093/rheumatology/kew363

110. Finsterer J. Systemic and non-systemic vasculitis affecting the peripheral nerves. *Acta Neurol Belg.* (2009) 109:100–13.

111. Kim D, Roche-Nagle G. Axillary artery aneurysm combined with brachial plexus palsy due to Takayasu arteritis. *BMJ Case Rep.* (2018) 2018:bcr2017221863. doi: 10.1136/bcr-2017-221863

112. Rifbjerg-Madsen S, Christensen AW, Christensen R, Hetland ML, Bliddal H, Kristensen LE, et al. Pain and pain mechanisms in patients with inflammatory arthritis: a Danish nationwide cross-sectional DANBIO registry survey. *PLoS One.* (2017) 12:e0180014. doi: 10.1371/journal.pone.0180014

113. Koroschetz J, Rehm SE, Gockel U, Brosz M, Freynhagen R, Tölle TR, et al. Fibromyalgia and neuropathic pain–differences and similarities. A comparison of 3057 patients with diabetic painful neuropathy and fibromyalgia. *BMC Neurol.* (2011) 11:55. doi: 10.1186/1471-2377-11-55

114. Narayanaswami P, Chapman KM, Yang ML, Rutkove SB. Psoriatic arthritis-associated polyneuropathy: a report of three cases. *J Clin Neuromuscul Dis.* (2007) 9:248–51. doi: 10.1097/CND.0b013e31814839d6

115. Kaya Subaşı P, Güler T, Yurdakul FG, Ataman S, Bodur H. Carpal tunnel syndrome in patients with rheumatoid arthritis and psoriatic arthritis: an electrophysiological and ultrasonographic study. *Rheumatol Int.* (2021) 41:361–8. doi: 10.1007/s00296-020-04745-8

116. Lee J, Cho S, Kim DY, Zheng Z, Park H, Bang D. Carpal tunnel syndrome in Behçet's disease. *Yonsei Med J.* (2015) 56:1015–20. doi: 10.3349/ymj.2015.56.4.1015

117. Gao XJ, Li YH, Zhang XW, Chen S, Liu YY. [Clinical analysis of 12 cases of mixed connective tissue disease-associated trigeminal neuropathy]. *Zhonghua Yi Xue Za Zhi.* (2020) 100:938–41. Chinese. doi: 10.3760/cma.j.cn112137-20191113-02471

118. Jasinska D, Boczon J. Melkersson-Rosenthal syndrome as an early manifestation of mixed connective tissue disease. *Eur J Med Res.* (2015) 20:100. doi: 10.1186/s40001-015-0192-7

119. Naqvi S, Talib V, Aijaz R, Ali Z, Bashir S, Ahmad SM, et al. Autoamputation and polyneuropathy in mixed connective tissue disorder: a case report. *Cureus.* (2017) 9:e1313. doi: 10.7759/cureus.1313

120. Irie T, Shigeto H, Koge J, Yamaguchi H, Murai H, Kira J-I. Dermatomyositis complicated with asymmetric peripheral neuritis on exacerbation: a case report and literature review. *Clin Exp Neuroimmunol.* (2016) 7:373–80.

121. Wijntjes J, van Alfen N. Muscle ultrasound: present state and future opportunities. *Muscle Nerve.* (2021) 63:455–66. doi: 10.1002/mus.27081

122. Tavee J. Peripheral neuropathy in sarcoidosis. *J Neuroimmunol.* (2022) 368:577864. doi: 10.1016/j.jneuroim.2022.577864

123. Ramos-Casals M, Pérez-Alvarez R, Kostov B, Gómez-de-la-Torre R, Feijoo-Massó C, Chara-Cervantes J, et al. SarcoGEAS-SEMI registry. Clinical characterization and outcomes of 85 patients with neurosarcoidosis. *Sci Rep.* (2021) 11:13735. doi: 10.1038/s41598-021-92967-6

124. Singhal NS, Irodenko VS, Margeta M, Layzer RB. Sarcoid polyneuropathy masquerading as chronic inflammatory demyelinating polyneuropathy. *Muscle Nerve.* (2015) 52:664–8. doi: 10.1002/mus.24652

125. Bakkers M, Merkies IS, Lauria G, Devigili G, Penza P, Lombardi R, et al. Intraepidermal nerve fiber density and its application in sarcoidosis. *Neurology.* (2009) 73:1142–8. doi: 10.1212/WNL.0b013e3181bacf05

126. Mattiassich G, Schubert H, Hutarew G, Wechselberger G. A rare manifestation of sarcoidosis with sensomotoric neuropathy of the ulnar nerve as the only symptom. *BMJ Case Rep.* (2012) 2012:bcr2012007430. doi: 10.1136/bcr-2012-007430

127. Kerasnoudis A, Woitalla D, Gold R, Pitarokoili K, Yoon MS. Sarcoid neuropathy: correlation of nerve ultrasound, electrophysiological and clinical findings. *J Neurol Sci.* (2014) 347:129–36. doi: 10.1016/j.jns.2014.09.033

128. Guo K, Liang N, Wu M, Chen L, Chen H. Prevalence and risk factors for peripheral neuropathy in chinese patients with gout. *Front Neurol.* (2022) 13:789631. doi: 10.3389/fneur.2022.789631

129. Lopez CL, Dominguez EC, Montes-Castillo M, Llinas H, Hernandez EA, Ballestas IP, et al. Thu0417 peripheral neuropathy in patients with gout. Alterations beyond local damage. *Ann Rheum Dis.* (2017) 76:365. doi: 10.1136/annrheumdis-2017-eular.5060

130. Therimadasamy A, Peng YP, Putti TC, Wilder-Smith EP. Carpal tunnel syndrome caused by gouty tophus of the flexor tendons of the fingers: sonographic features. *J Clin Ultrasound.* (2011) 39:463–5. doi: 10.1002/jcu.20799

131. Daoussis D, Karamessini M, Chroni E, Kraniotis P. Gout and foot drop. *Joint Bone Spine.* (2016) 83:229. doi: 10.1016/j.jbspin.2015.03.012

132. Chiu KY, Ng WF, Wong WB, Choi CH, Chow SP. Acute carpal tunnel syndrome caused by pseudogout. *J Hand Surg Am.* (1992) 17:299–302. doi: 10.1016/0363-5023(92)90409-i

133. Rate AJ, Parkinson RW, Meadows TH, Freemont AJ. Acute carpal tunnel syndrome due to pseudogout. *J Hand Surg Br.* (1992) 17:217–8. doi: 10.1016/0266-7681(92)90093-h

134. Spiegel PG, Ginsberg M, Skosey JL, Kwong P. Acute carpal tunnel syndrome secondary to pseudogout: case report. *Clin Orthop Relat Res.* (1976):185–7.

135. Taniguchi Y, Yoshida M, Tamaki T. Cubital tunnel syndrome associated with calcium pyrophosphate dihydrate crystal deposition disease. *J Hand Surg Am.* (1996) 21:870–4. doi: 10.1016/S0363-5023(96)80206-1

136. Léger JM, Guimarães-Costa R, Muntean C. Immunotherapy in peripheral neuropathies. *Neurotherapeutics.* (2016) 13:96–107. doi: 10.1007/s13311-015-0401-7

137. Lin YJ, Anzaghe M, Schülke S. Update on the pathomechanism, diagnosis, and treatment options for rheumatoid arthritis. *Cells.* (2020) 9:880. doi: 10.3390/cells9040880

138. Vilholm OJ, Christensen AA, Zedan AH, Itani M. Drug-induced peripheral neuropathy. *Basic Clin Pharmacol Toxicol.* (2014) 115:185–92. doi: 10.1111/bcpt.12261

139. Jones MR, Urits I, Wolf J, Corrigan D, Colburn L, Peterson E, et al. Drug-induced peripheral neuropathy: a narrative review. *Curr Clin Pharmacol.* (2020) 15:38–48. doi: 10.2174/1574884714666190121154813

140. Pardanani A, Laborde RR, Lasho TL, Finke C, Begna K, Al-Kali A, et al. Safety and efficacy of CYT387, a JAK1 and JAK2 inhibitor, in myelofibrosis. *Leukemia.* (2013) 27:1322–7. doi: 10.1038/leu.2013.71

141. Kandula T, Farrar MA, Kiernan MC, Krishnan AV, Goldstein D, Horvath L, et al. Neurophysiological and clinical outcomes in chemotherapy-induced neuropathy in cancer. *Clin Neurophysiol.* (2017) 128:1166–75. doi: 10.1016/j.clinph.2017.04.009

142. Bharadwaj A, Haroon N. Peripheral neuropathy in patients on leflunomide. *Rheumatology (Oxford).* (2004) 43:934. doi: 10.1093/rheumatology/keh191

143. Martin K, Bentaberry F, Dumoulin C, Longy-Boursier M, Lifermann F, Haramburu F, et al. Neuropathy associated with leflunomide: a case series. *Ann Rheum Dis.* (2005) 64:649–50. doi: 10.1136/ard.2004.027193

144. Kho LK, Kermode AG. Leflunomide-induced peripheral neuropathy. *J Clin Neurosci.* (2007) 14:179–81. doi: 10.1016/j.jocn.2005.08.021

145. Richards BL, Spies J, McGill N, Richards GW, Vaile J, Bleasel JF, et al. Effect of leflunomide on the peripheral nerves in rheumatoid arthritis. *Intern Med J.* (2007) 37:101–7. doi: 10.1111/j.1445-5994.2007.01266.x

146. Ramani SL, Samet J, Franz CK, Hsieh C, Nguyen CV, Horbinski C, et al. Musculoskeletal involvement of COVID-19: review of imaging. *Skeletal Radiol.* (2021) 50:1763–73. doi: 10.1007/s00256-021-03734-7

147. Paliwal VK, Garg RK, Gupta A, Tejan N. Neuromuscular presentations in patients with COVID-19. *Neurol Sci.* (2020) 41:3039–56. doi: 10.1007/s10072-020-04708-8

148. Ciaffi J, Meliconi R, Ruscitti P, Berardicurti O, Giacomelli R, Ursini F. Rheumatic manifestations of COVID-19: a systematic review and meta-analysis. *BMC Rheumatol.* (2020) 4:65. doi: 10.1186/s41927-020-00165-0

149. Xu XW, Wu XX, Jiang XG, Xu KJ, Ying LJ, Ma CL, et al. Clinical findings in a group of patients infected with the 2019 novel coronavirus (SARS-Cov-2) outside of Wuhan, China: retrospective case series. *BMJ.* (2020) 368:m606. [Published correction appears in BMJ 2020;368:m792]. doi: 10.1136/bmj.m606

150. Matschke J, Lütgehetmann M, Hagel C, Sperhake JP, Schröder AS, Edler C, et al. Neuropathology of patients with COVID-19 in Germany: a post-mortem case series. *Lancet Neurol.* (2020) 19:919–29. doi: 10.1016/S1474-4422(20)30308-2

151. Dyer O. COVID-19: regulators warn that rare Guillain-Barré cases may link to J&J and AstraZeneca vaccines. *BMJ.* (2021) 374:n1786. doi: 10.1136/bmj.n1786

152. De Beuckelaer A, Grooten J, De Koker S. Type I interferons modulate CD8+ T cell immunity to mRNA vaccines. *Trends Mol Med.* (2017) 23:216–26. doi: 10.1016/j.molmed.2017.01.006

153. Queler SC, Towbin AJ, Milani C, Whang J, Sneag DB. Parsonage-turner syndrome following COVID-19 vaccination: MR neurography. *Radiology.* (2022) 302:84–7. doi: 10.1148/radiol.2021211374

154. ArÁnyi Z, Csillik A, DéVay K, Rosero M, Barsi P, BÖhm J, et al. Ultrasonography in neuralgic amyotrophy: sensitivity, spectrum of findings, and clinical correlations. *Muscle Nerve.* (2017) 56:1054–62. doi: 10.1002/mus.25708

155. Perfetto F, Moggi-Pignone A, Livi R, Tempestini A, Bergesio F, Matucci-Cerinic M. Systemic amyloidosis: a challenge for the rheumatologist. *Nat Rev Rheumatol.* (2010) 6:417–29. doi: 10.1038/nrrheum.2010.84

156. Granata G, Luigetti M, Coraci D, Del Grande A, Romano A, Bisogni G, et al. Ultrasound evaluation in transthyretin-related amyloid neuropathy. *Muscle Nerve.* (2014) 50:372–6. doi: 10.1002/mus.24168

157. Yamazaki H, Takamatsu N, Nodera H, Kawarai T, Izumi K, Kaji R. Distinguishing features of amyloid polyneuropathy on nerve ultrasound. *J Neurol Sci.* (2017) 381:1099. doi: 10.1016/j.jns.2017.08.3102

158. Du K, Xu K, Cheng S, Lv H, Zhang W, Wang Z, et al. Nerve ultrasound comparison between transthyretin familial amyloid polyneuropathy and chronic inflammatory demyelinating polyneuropathy. *Front Neurol.* (2021) 12:632096. doi: 10.3389/fneur.2021.632096

159. Fukuda K, Yamamoto H. Dialysis-related amyloidosis. *Semin Musculoskelet Radiol.* (2001) 5:113–9. doi: 10.1055/s-2001-15879

160. Rasenack M, Proebstel AK, Athanasopoulou IM, Décard BF, Grimm A. Nerve hypertrophy in primary amyloidosis. *Muscle Nerve.* (2016) 54:510–2. doi: 10.1002/mus.25113

161. Hoshino I, Yokota H. Radiogenomics of gastroenterological cancer: the dawn of personalized medicine with artificial intelligence-based image analysis. *Ann Gastroenterol Surg.* (2021) 5:427–35. doi: 10.1002/ags3.12437

frontiers | Frontiers in Medicine

TYPE Review
PUBLISHED 23 November 2022
DOI 10.3389/fmed.2022.1058510

OPEN ACCESS

EDITED BY
Ashish Jacob Mathew,
Christian Medical College and Hospital, India

REVIEWED BY
Felipe Julio Ramírez,
Hospital Clinic of Barcelona, Spain
Juan Carlos Nieto González,
Gregorio Marañón Hospital, Spain

*CORRESPONDENCE
Kate Harnden
kate.harnden@nhs.net

SPECIALTY SECTION
This article was submitted to Rheumatology, a section of the journal Frontiers in Medicine

RECEIVED 30 September 2022
ACCEPTED 07 November 2022
PUBLISHED 23 November 2022

CITATION
Harnden K, Di Matteo A and Mankia K (2022) When and how should we use imaging in individuals at risk of rheumatoid arthritis? *Front. Med.* 9:1058510. doi: 10.3389/fmed.2022.1058510

When and how should we use imaging in individuals at risk of rheumatoid arthritis?

Kate Harnden*, Andrea Di Matteo and Kulveer Mankia

Leeds Institute of Rheumatic and Musculoskeletal Medicine, University of Leeds, Leeds, United Kingdom

In recent years rheumatologists have begun to shift focus from early rheumatoid arthritis (RA) to studying individuals at risk of developing the disease. It is now possible to use blood, clinical and imaging biomarkers to identify those at risk of progression before the onset of clinical synovitis. The use of imaging, in particular ultrasound (US) and magnetic resonance imaging (MRI), has become much more widespread in individuals at-risk of RA. Numerous studies have demonstrated that imaging can help us understand RA pathogenesis as well as identifying individuals at high risk of progression. In addition, imaging techniques are becoming more sophisticated with newer imaging modalities such as high-resolution peripheral quantitative computed tomography (HR-pQRCT), nuclear imaging and whole body-MRI (WB-MRI) starting to emerge. Imaging studies in at risk individuals are heterogeneous in nature due to the different at-risk populations, imaging modalities and protocols used. This review will explore the available imaging modalities and the rationale for their use in the main populations at risk of RA.

KEYWORDS

ultrasound, rheumatoid arthritis, magnetic resonance imaging, computed tomography, at risk of rheumatoid arthritis, clinically suspect arthralgia, ACPA, palindromic rheumatism

Introduction

Rheumatoid arthritis (RA) is a chronic autoimmune disorder, which is characterized by poly-articular and systemic inflammation. It affects around 1% of the population and if poorly treated can lead to irreversible joint damage and disability (1). It is now widely accepted that early diagnosis and tight control of disease activity is associated with improved long-term outcomes (2). Subsequently the early phase of RA within 3 months of the development of synovitis, has been named the "window of opportunity." Diagnosing and treating RA patients within this window can be difficult due to delays in patient presentation, referral delays and waiting times in secondary care (3). Furthermore, once RA has developed, drug free remission, which is effectively cure of

the disease, remains infrequent (4, 5). This has led to a drive in identifying individuals at-risk of RA to offer the opportunity to treat prior to the onset of synovitis and potentially prevent or delay RA development.

A recent European League Against Rheumatism (EULAR) task force has used clinical features to define three main populations that should be considered when studying individuals at risk of RA (**Table 1**) (5, 6). These groups include asymptomatic predisposed individuals, individuals with positive serum auto-antibodies and early clinical arthritis. One specific group of frequently studied patients are those that have inflammatory MSK symptoms and they can be defined as having clinically suspect arthralgia (CSA) (7). Due to the American College of Rheumatology (ACR)/European League Against Rheumatism (EULAR) RA diagnostic criteria update in 2010, many patients who were previously diagnosed with undifferentiated arthritis (UA) would now be diagnosed with RA. As many of the imaging studies in UA recruited patients based on pre-2010 criteria, this review has not included imaging studies that have solely focused on UA patients.

It is now accepted that many of these at risk individuals may be in a very early phase of what has been defined as the "RA disease continuum." In those that do go on to develop RA, this phase can be retrospectively labeled as "pre-RA." Many at risk individuals have biochemical and imaging abnormalities that can be used to predict progression to arthritis. These biomarkers can also provide a better understanding of the pathogenesis of the disease in the preclinical phase. A key point to note is that not all at risk individuals will progress to RA. It is therefore important to understand which biomarkers are the most useful in predicting progression.

TABLE 1 EULAR defined populations at risk of developing RA.

At-risk group	Subgroups
Asymptomatic individuals	• First degree relatives (FDRs) with RA • ACPA positive • Genetically predisposed indigenous populations
MSK symptoms	• Positive RA-related auto antibodies (Rheumatoid factor (RF), anti-citrullinated protein antibodies (ACPA) or Anti-carbamylated antibodies) • Clinically suspect arthralgia (CSA) Inflammatory clinical features such as difficult making a fist, a positive squeeze test or early morning stiffness (EMS) • Subclinical inflammation on imaging
Early clinical arthritis	• Undifferentiated arthritis (UA) • Palindromic Rheumatism (PR).

First group: Asymptomatic individuals with one of the following risk factors; a first-degree relative (FDR) with RA, positive serum anti-citrullinated protein antibodies (ACPA) or originating from a genetically predisposed indigenous population. Second group: Musculoskeletal (MSK) symptoms without clinical arthritis plus positive serum auto-antibodies (Rheumatoid factor (RF), ACPA or Anti-carbamylated antibodies) and/or have inflammatory clinical features such as difficult making a fist (8) or subclinical inflammation on imaging (CSA) (7). Third group: early clinical arthritis including undifferentiated arthritis (UA) and Palindromic Rheumatism (PR).

The use of imaging in RA and other inflammatory arthritidies has increased dramatically in the past two decades. Previously it was mostly limited to the use of plain radiographs to detect irreversible joint damage in established RA. It has subsequently been shown that both Ultrasound (US) and MRI can be used to detect structural damage that is not visible on plain radiographs (9, 10) and subtle inflammation that is not detectable by clinical examination (11, 12). As well as US and MRI, HR-pQCT and molecular imaging techniques such as Position emission tomography (PET) have also shown promise in early RA (13, 14). This increased understanding and breadth of use of different imaging techniques is now being applied to individuals at risk of RA.

Interventional trials are now starting to focus on treating individuals at risk of RA in the preclinical stage. A recent randomized controlled trial (RCT) demonstrated that intervening with methotrexate and corticosteroids in CSA patients with subclinical inflammation on MRI can delay arthritis development and appears to be associated with a milder arthritis phenotype (15). Other RCTs using rituximab and abatacept have demonstrated that intervening in the preclinical stage could also delay and possibly prevent RA development (16, 17). The results of these studies should further our knowledge on the optimum timing and frequency to image individuals at risk of RA. They also demonstrate that halting the development of RA in the preclinical stage is now a realistic prospect. Imaging is likely to remain a central part of this process with its ability to help identify, stratify and manage individuals at risk of RA. Furthermore, patients anecdotally often relate better to images of their condition, allowing them to visualize the disease process, compared to numerical laboratory data. Patients report that undergoing scans is a positive experience and appreciate having the opportunity to view their images (18). In this review we aim to address how different imaging techniques should be used in individuals at risk of RA.

Which imaging technique?

Multiple different imaging modalities have been used in individuals at risk of RA. There are advantages and disadvantages of each imaging method as discussed below (**Table 2**).

Ultrasound

The use of US in both research and clinical practice is now widespread in rheumatology. The benefits of US include accessibility, low cost, lack of radiation exposure and tolerability for patients. US is more sensitive than clinical examination for detecting synovitis (19) and its ability to differentiate synovitis from other causes of joint pain and swelling, such as

TABLE 2 A summary of the advantages and disadvantages of different imaging modalities and the evidence for the use in individuals at risk of RA.

Summary of imaging modalities

	Advantages	Disadvantages	Use in at risk individuals	Predictive value	HR
Ultrasound	• Accessible • Low cost • No radiation • Easily tolerated • Superior to clinical examination at detecting synovitis (41)	• High operator dependency • Risk of false positives • Time consuming to assess multiple joints	Predicting the development of RA in symptomatic patients with autoantibodies and/or CSA (27, 28, 30)	**NPV 89%** for the development of RA in CSA (31)	**PD, HR 1.88–3.7** in ACPA+ with MSK symptoms (27, 28) **GS, HR 2.3** in ACPA+ with MSK symptoms (28)
MRI	• Multiplanar information on bone and soft tissue • Superior sensitivity to US in detecting synovitis and tenosynovitis (33, 35)	• Time-consuming • Expensive • Tolerability • Risk of false positives (specifically limited)	Predicting the development of RA in symptomatic patients with autoantibodies and CSA (41, 42, 55) MRI tenosynovitis is independently associated with IA progression in CSA and ACPA+ arthralgia (42, 55)	MRI inflammation **PPV 25–31%** and **NPV 93–96%** in CSA (41, 42) MRI Tenosynovitis **PPV 25%** and **NPV 95%** in CSA (41)	MRI synovitis **HR 1.08** in ACPA+ with MSK symptoms (55) MRI tenosynovitis **HR 4.02–8.39** in CSA and ACPA+ with MSK symptoms (42, 55)
PET	• Three dimensional imaging as well as functional imaging • Whole body imaging	• high cost • low availability • Ionizing radiation dose • specialist interpretation required	Potential use in predicting the development of RA in ACPA arthralgia patients (45)	N/A	N/A
CT	• Three dimensional imaging of the bone • Visualize early bone cortical changes including cortical microchannels	• Limited ability to assess soft tissues • Unable to detect inflammation • Ionizing radiation dose • HR-pQCT scans can be prone to motion artifacts	Predictive value for the development of RA with HR-pQCT by the detection of CoMiCs over metacarpal heads (51)	N/A	N/A
CR	• Low cost • Easily reproducible • Accessible	• Limited ability to assess soft tissues • Unable to detect inflammation	No evidence for use	N/A	N/A

ACPA+, anti-citrullinated protein antibodies; CoMiCs, cortical micro-channels; CT, computed tomography; CR, conventional radiography; CSA, clinically suspect arthralgia; GS, gray scale; HR-pQCT, high resolution peripheral quantitative computed tomography; MRI, magnetic resonance imaging; MSK, musculoskeletal; PET, positron emission tomography; PPV, positive predictive value; NPV, negative predictive value; PD, power Doppler; HR, hazard ratio.

tenosynovitis or bursitis, makes it an extremely useful tool in early disease, including individuals at risk of RA (20).

The potential disadvantages of US include the high operator dependency and therefore lower reproducibility. Another concern regarding individuals at risk of RA is that US may detect joint inflammation too late in the disease continuum, when clinical arthritis is imminent, therefore leaving limited opportunity for preventive intervention (21, 22). In line with this, when lower risk individuals have been studied, particularly those who have not developed joint symptoms, US abnormalities have not been found (23). Another concern is that not all patients with US inflammation will go on to develop RA (24). Joint effusions, synovial hypertrophy and even low level power Doppler (PD) signal can be commonly found in healthy populations (25). If a clinician finds US synovitis it may be tempting to start immunosuppressant medications which leads to the possibility of over-treating patients and potentially subjecting them to lifelong medications (26).

Despite these concerns, multiple studies have demonstrated the positive predictive value of US abnormalities in individuals at risk of RA. The initial US analysis from Leeds found that presence of US PD in the hands and wrists of CCP+ individuals with new MSK symptoms was associated with progression to IA (27). In a larger study from the same center, 136 ACPA positive patients with MSK symptoms were followed up over a median of 18.3 months. Fifty-seven (42%) patients developed an IA after a median of 8.6 months; 86% of patients that progressed to IA had one or more US abnormalities at baseline compared to 67% of patients that did not progress. Furthermore, US abnormalities were predictive of IA development at both patient and a joint level. Gray scale (GS), PD and erosions were all associated with progression, with PD conferring the highest risk. At joint level,

the presence of PD at baseline was associated with a 10 fold risk of that joint developing clinical synovitis (28). In contrast, an US study in a Dutch seropositive arthralgia cohort found that GS synovitis was predictive of IA progression but PD was not (29). The contrasting results may be explained by cohort differences. This Dutch study included patients with lone RF positivity as well as ACPA positive patients, thus the overall cohort is lower risk. US was associated with progression to RA in a retrospective analysis of 80 patients with inflammatory arthralgia of < 6 weeks duration but negative rheumatoid autoantibodies. The Swiss Sonography Group in Arthritis and Rheumatism (SONAR) scoring system was used but PD was not included in the predictive analysis (30).

The negative predictive value of US has been specifically demonstrated in patients presenting with CSA with at least two painful joints of the hands, feet or shoulders. In a multicentre cohort study, US data was collected at baseline, 6 and 12 months. Fifty-nine percent of patients in this study who had US synovitis (defined as GS $\geq$ 2 and/or PD $\geq$ 1) at baseline developed IA. Importantly, if no joints showed US synovitis at baseline, the negative predictive value was 89%, suggesting that such individuals could be largely reassured of their risk of developing IA (31).

The ability of US tenosynovitis to predict IA has been less well studied than with MRI and has shown mixed results. Molina Collada et al. found that in a cohort of CSA patients PD tenosynovitis at baseline was the only independent predictor of RA and IA development (32). In contrast van de Stadt et al. did not find that US tenosynovitis was significantly predictive of IA progression at joint or patient level (29). Again these contrasting results may be explained by cohort differences as the CSA patients in Molina Collada et al. paper had relatively high average RF and ACPA antibody titres. In a direct comparison of MRI and US, it was found that US was less sensitive than MRI in the early detection of both synovitis and tenosynovitis in patients with CSA (33). **Figure 1** shows representative US findings of sub-clinical synovitis and tenosynovitis in ACPA+ individuals with MSK symptoms.

In a study that has looked at US detected bone erosions in "pre-RA" it was shown that bone erosions in the feet could be predictive for RA development. This was a large study that followed up 400 RA patients over a median of 41.4 months. Bone erosions in more than one joint and bone erosions in fifth MTP joint with US synovitis were the most predictive for the development of IA (34) (**Figure 2**).

In summary, US is a readily available imaging technique that provides valuable information in individuals at risk of RA. The presence of PD synovitis in symptomatic at risk individuals, is strongly associated with imminent future arthritis development and has been used to produce clinically relevant risk stratification models. Conversely, the value of US in at risk individuals without MSK symptoms appears to be limited.

Magnetic resonance imaging

One of the major benefits of MRI is its ability to provide highly sensitive multiplanar information on both the bone and soft tissue structures in and around the joints without using ionizing radiation. It has demonstrated superiority to US in detecting synovitis (**Figure 3**) and tenosynovitis in early RA and CSA (33, 35). This in addition to its unique ability to detect bone marrow edema, a potential precursor to erosions, makes its use in at risk individuals appealing (36). Despite this, MRI is not without its disadvantages; it is time-consuming, expensive and some patients struggle to tolerate it. Consequently US has generally gained more traction as the first line high resolution imaging assessment for synovitis in most rheumatology centers, with MRI often used as a second line investigation where required.

One specific concern with MRI in at risk individuals is that its high sensitivity for detecting inflammation may compromise specificity. MRI often detects inflammation in healthy, asymptomatic individuals without risk factors for RA (37, 38). One of the larger studies to investigate this performed contrast enhanced MRIs of the dominant metacarpophalangeal (MCP), wrist and metacarpophalangeal (MTP) joints of 193 symptom free persons. In this study, 72% of patients had at least one single inflammatory feature and 78% had one or more erosions. Inflammatory features and erosions were particularly prevalent in older age groups (39). In a small study of 28 patients with ACPA positive arthralgia, 93% of individuals had MRI synovitis with a Rheumatoid Arthritis Magnetic Resonance Imaging Score (RAMRIS) of 1. Forty-three percent of these patients went on to progress to IA and a RAMRIS score of 2 or above was associated with faster progression (40). Boer et al. created more specific parameters to define pathological MRI inflammation by comparison with a symptom free reference group. They demonstrated that by using a reference group MRI can be predictive in CSA and UA patients and the rates of false positives were reduced (41).

Larger studies of at risk individuals have demonstrated promising results in the predictive value of MRI. Van Steenbergen et al. looked at 150 patients with CSA of whom 46% had significant subclinical inflammation on MRI (synovitis, bone marrow edema or tenosynovitis) when scored against a healthy reference group. They followed up all patients up over a median of 75 weeks and 30% of patients developed IA. MRI inflammation was more positively associated with IA development than age, localization of initial symptoms and C-reactive protein level. Seventy-eight percent of the patients that had inflammation on MRI at baseline developed IA within a year compared with only 6% of patients without. Interestingly, tenosynovitis had the strongest independent association for progression to IA (HR = 7.56). Bone marrow edema and synovitis were also independently associated with progression but less strongly so (42).

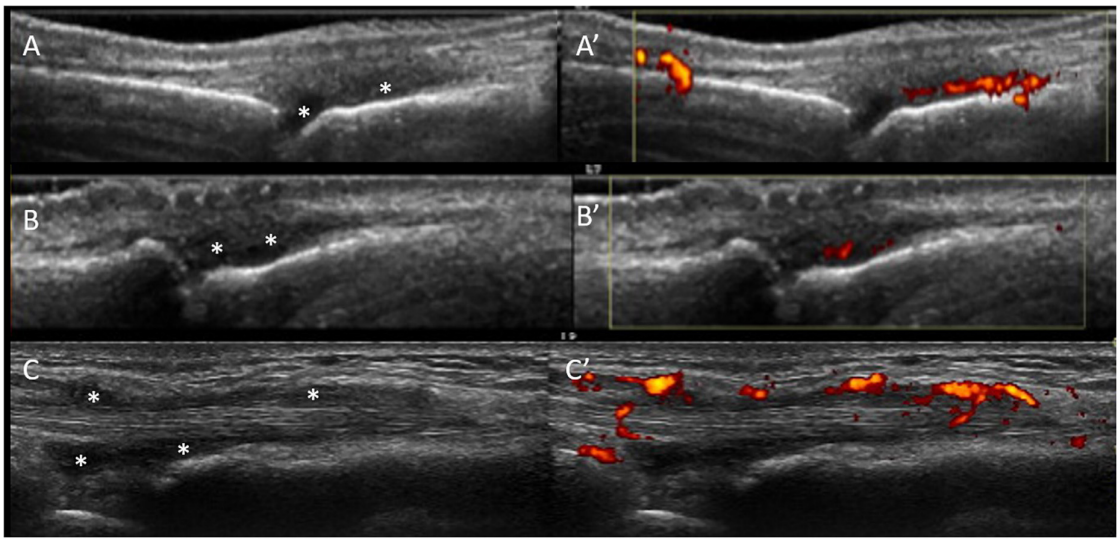

FIGURE 1
US sub-clinical synovitis and tenosynovitis in ACPA+ individuals with MSK symptoms. Gray scale **(A)** and power Doppler **(A')** positive synovitis of the 3rd MCP joint in a patient at-risk of RA high titre positive anti-CCP antibodies and non-specific musculoskeletal symptoms. Similar US findings are shown in the 2nd PIP joint in a different at-risk individual **(B,B')** with positive anti-CCP antibodies and rheumatoid factor, hands arthralgia. **(C,C')** Illustrate tenosynovitis of the 2nd extensor tendon compartment in a third individual at-risk of RA with high titre anti-CCP antibodies and clinically suspect arthralgia. All images were obtained using a longitudinal approach. Asterisks indicate synovial hypertrophy.

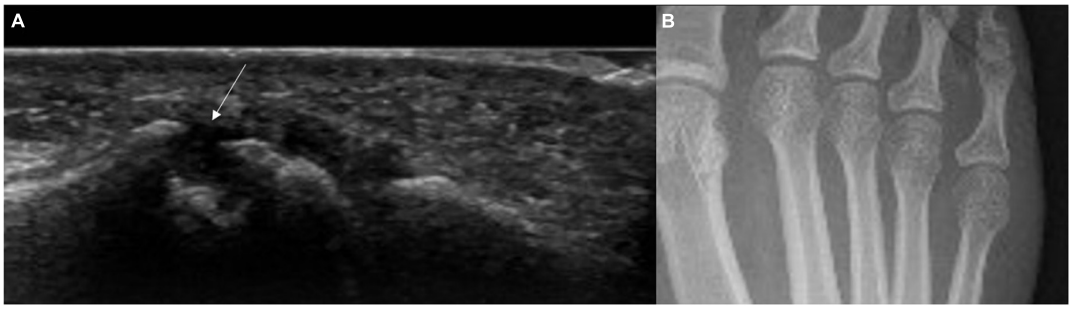

FIGURE 2
US bone erosion (not detected by x-rays) in the 5th MTP joint in an individual with high titre ACPA and non-specific MSK symptoms. **(A)** Longitudinal US scan of the lateral aspect of the 5th MTP joint. The white arrow indicates the presence of bone erosion. **(B)** Correspondent feet x-rays showing no bone erosions in the 5th metatarsophalangeal joint. This patient presented with non-specific musculoskeletal symptoms and high titre anti-CCP antibodies.

Overall the current evidence suggests that MRI may have a role in assessing at risk individuals. It may have particular value in delineating inflammation in extra-capsular structures in a sub groups of patients, which requires further exploration. For practical reasons, faster and cheaper MRI protocols are likely to be needed before the use of MRI in clinical practice becomes more widespread.

Positron emission tomography

Positron Emission Tomography (PET) is a nuclear imaging technique, which uses radioactive tracer drugs to detect metabolic cellular processes. It is used alongside another imaging technique, usually CT, to produce three dimensional functional imaging. PET-CT is able to detect synovitis and monitor treatment response in early RA (43). An important advantage is the ability to image the whole body in one acquisition unlike other more conventional imaging. Disadvantages include the high cost, limited availability (often restricted to large, specialist centers) and radiation dose. In addition, tracer uptake may not be specific to joint inflammation so specialist interpretation is required. Efforts are being made to improve safety; newer tracers have a much shorter half-life, which makes the radiation exposure similar to a standard CT scan (44). Moreover, the advent of PET MRI and the fact that

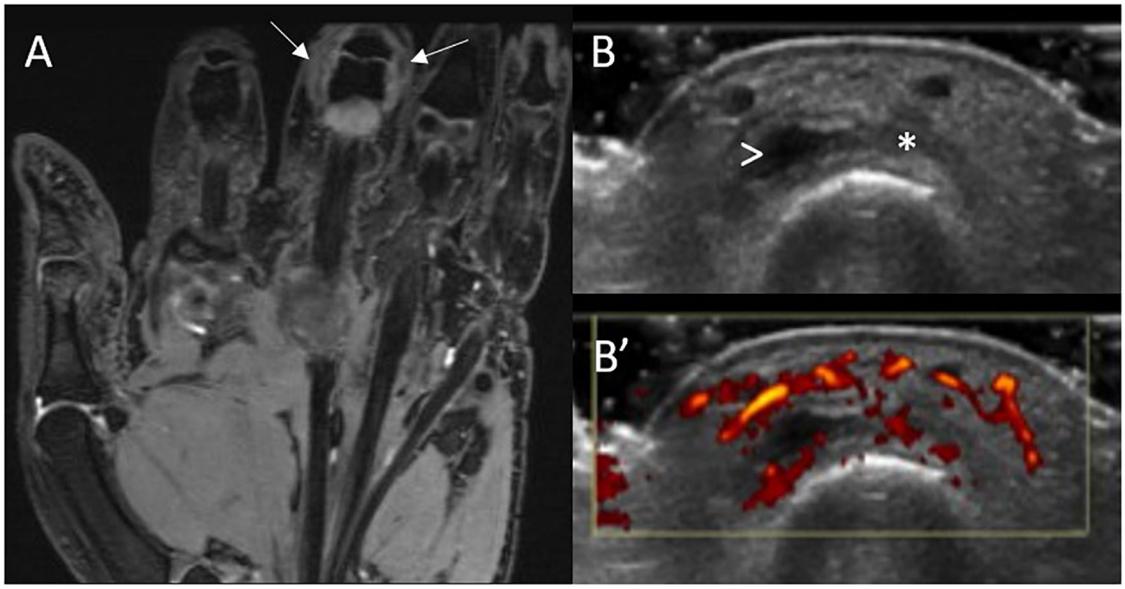

FIGURE 3
MRI and US sub-clinical synovitis in a patient with CSA and high titre ACPA. MRI **(A)** synovitis (white arrows) of the 3rd PIP joint in an individual at-risk of RA with corresponding gray-scale **(B)** and power Doppler **(B')** US scans. This individual had clinically suspect arthralgia and positive anti-CCP antibodies (high titre) and rheumatoid factor. These images were obtained 6 weeks before progression to RA. Asterisk indicates synovial hypertrophy, while the arrowhead a small joint effusion.

PET scans are becoming increasingly sensitive is also likely to lower radiation exposure.

In their small pilot study, Gent et al. used (*R*)-^{11}C-PK11195 PET to show that subclinical joint inflammation could be detected in 29 ACPA positive arthralgia patients. Hands and wrists were scanned at baseline and patients were then followed up over 24 months. Nine patients in total developed an IA. Four patients had a positive PET scan at baseline, all of whom went on to develop IA. Of the 5 patients who developed IA and had a negative scan at baseline, 3 of these patient developed inflammation in joints that were not scanned. These results of this preliminary study suggest that (*R*)-^{11}C-PK11195 PET may be useful in predicting IA development (45).

Nuclear medicine is an evolving area in RA imaging. The evidence from PET and the potential to develop new radiotracers that can highlight areas of inflammation at whole body level warrants further exploration in individuals at risk of RA.

Computed tomography

Unlike conventional radiography, CT provides three dimensional imaging of bone without projectional superimposition. However, unlike MRI, it has limited ability to assess soft tissues and is unable to detect inflammation. CT is also associated with ionizing radiation exposure, which, alongside the lack of information on soft tissue inflammation, has resulted in relatively little research into the use of CT in at risk individuals. There is evidence that changes in bone mineral density may begin in very early RA (46, 47). This has led to the question of whether some of these bone changes may occur in the "pre-RA" stage before the onset of clinical synovitis. HR-pQRCT is an imaging technique that was introduced over a decade ago and has shown promising use in individuals at risk of RA. One disadvantage is that it requires specialized technology that is not widely available. Kleyer et al. used a type HR-pQCT called microfocal CT (micro-CT) to investigate the association between ACPA and bone loss prior to the onset of inflammatory arthritis. They demonstrated that cortical bone thickness was significantly reduced in asymptomatic ACPA positive individuals compared to healthy controls (48). It is worth noting that cortical hand bone loss in early RA has been shown to predict radiographic hand joint damage (49). In contrast, in a separate study of 29 ACPA positive individuals trabecular bone was thinner when compared to controls but there was no significant difference with the cortical bone (50).

It is thought that erosions typically start in the "bare area" of a joint, which is not covered by articular cartilage. Simon et al. used HR-pQCT to investigate whether individuals at risk of RA have a higher frequency of cortical micro-channels (CoMiCs) at the bare joint areas. It was found that in 74 individuals, who were ACPA or anti-MCV positive, there were significantly more CoMiCs in the patients that progressed to RA and CoMiCs over metacarpal heads were associated with the development of RA (51). HR-pQCT scans have a higher spatial resolution

than conventional CT scans with a similar radiation dose. A disadvantage is that they can be prone to motion artifacts. Currently HR-pQCT scans are not widely available for research or clinical purposes but their promising initial results in pre RA does warrant further investigation. Further research is needed into the use of CT in other at risk groups such as CSA, including ACPA negative individuals.

Conventional radiography

Radiographs have been widely used in the initial work up of newly diagnosed RA patients and for the monitoring of disease progression. While they do not provide any information on soft tissues or synovial inflammation, they can detect structural joint damage. The benefits of radiographs include their low cost, accessibility and reproducibility for serial assessment. However, it has been shown that radiographs have limited ability in detecting bone erosions in early RA (52, 53). This clearly limits their use in predicting disease progression in at risk individuals. In a study of 418 ACPA positive at risk individuals only 4.1% had bone erosions on hand and feet radiographs and these did not predict progression to IA (54). This study suggests there is no value in routinely performing radiographs in individuals at risk of RA.

Should we image extra-capsular structures?

As discussed above, intra-articular joint inflammation identified on US, MRI and PET-CT in at-risk individuals is associated with progression to IA. However, it is not only the joints but also the structures outside the joint capsule that have shown interesting findings in individuals at risk of developing RA. MRI tenosynovitis is a particularly important finding as evidenced by Van Steenbergen et al. who found it to be the strongest independent predictive factor on MRI for the development of IA in patients with CSA (42). Further studies in ACPA positive individuals have also demonstrated that tenosynovitis is the strongest MRI predictor of progression to IA (55, 56). A recent study in CSA patients found that MCP-extensor peritendinitis, although infrequent, was strongly associated with IA development with a positive predictive value of 65% (57). Similarly, MRI interosseous tendon inflammation was identified in 19% of ACPA positive patients, 49% of early arthritis patients but no healthy controls (58). A histological study confirmed the absence of a tenosynovial sheath around the interosseous tendons, suggesting the MRI findings reveal a peri-tendinous inflammation rather than a genuine tenosynovitis. While US tenosynovitis has more mixed findings in predicting progression, it is important to note that when present it is highly likely to be pathological; it is infrequently seen in healthy individuals (59).

Other extracapsular structures are also of relevance in at risk individuals. Non synovial extra-capsular inflammation, in the absence of synovitis, represents a distinct phenotype in PR patients during flare (60). A very recent study found that inter-metatarsal bursitis may precede the development of RA. In this study, contrast enhanced MRI scans were performed in the forefoot, MTP and wrist joints of 577 CSA patients. The RAMRIS scoring system was used and intermetatarsal bursitis was only counted as being present if it would be uncommon in the same location in a healthy population. They found that 23% of CSA patients had intermetatarsal bursitis but this increased to 47% if only including the ACPA positive patients. In the ACPA positive patients, intermetatarsal bursitis was able to predict progression to IA (61).

Overall, these studies have demonstrated the relevance of MRI inflammation in extracapsular structures in at risk individuals. Although of pathobiological relevance, further research is required to determine if imaging these extracapsular structures adds additional value in predicting progression to RA in at risk individuals.

Can we image fewer joints?

Practically it is important to address how many and which joints should be scanned in individuals at risk of developing RA. To date, the majority of imaging studies in this cohort have used comprehensive imaging protocols that include a large number of joints. While this may be feasible in a research setting it is not usually practical in a clinical setting where time is limited.

One study that looked at a reduced subset of 30 unilateral RA specific MRI features in the wrist, MCP and MTP joints, as opposed to the 61 features in the RAMRIS scoring system, found that by using this smaller subset of measurements it was still possible to predict the development of arthritis in 225 CSA patients (62). In the Leeds cohort of ACPA positive patients with MSK symptoms, an US protocol of 32 joints was used to successfully predict progression to RA (28). Gray scale, PD and erosions were all shown to separately predict progression. In the first Leeds prediction model, presence of PD signal in 22 joints (the wrists, MCPJs and PIPJs only) was predictive of progression on multivariable analysis (27). This study demonstrated that an attenuated joint set of the hands and wrists only can have predictive value. van de Stadt et al. took a different approach in their study and only scanned tender joints and small joints directly adjacent and contralateral to the tender joints. It was found that in the 192 individuals with arthralgia and positive autoantibodies (RF and/or anti-CCP), only GS on US was predictive (29). As previously discussed, the different results in

these studies may also be partly explained by differences in the at risk cohorts.

To date, US studies in individuals at risk of RA have all used bilateral joint protocols. In established RA it has been shown that unilateral reduced scoring protocols of 7–9 joints were still able to capture 78–85% of the information from a full 36 joint protocol. This was, however, significantly less than the bilateral 7–9 joint protocols which captured 89–93% of the information (63). In contrast, MRI protocols in individuals at risk of RA have used the most symptomatic or dominant hand and wrist joints, as recommended in the RAMRIS scoring system (64). One concern with this approach is that synovitis does not always present symmetrically. In a study that looked at early RA patients it was shown that 21% of patients had unilateral synovitis in non-dominant joints (65). Furthermore, by just scanning the dominant hand and wrist joints it allows the potential of overuse tenosynovitis to influence findings (66). Despite these concerns, multiple MRI studies have demonstrated predictive value of imaging only the dominant hands in individuals at risk of RA (40–42).

RA is often considered a disease of the small joints, with large joints affected less frequently and later into the disease course (67, 68). This leads to the question of whether large joints should be included in imaging protocols of at risk individuals. Rogier et al. found that in 170 CSA patients scanning the shoulders did not predict the development of IA despite 50 patients showing abnormalities on the US scan. However, only 5% of shoulders scanned in this study were symptomatic (69). In an MRI study of 55 individuals with ACPA and/or RF antibodies it was found that MRI and synovial biopsy of the knee did not detect clear-cut inflammation in the 15 patients who went on to progress to RA (70). In contrast, when ACPA+ at risk individuals had symptomatic knees and shoulders, performing US in these areas added predictive power (28). As such, a pragmatic approach may be to scan all standard protocol small joints but only include the symptomatic large joints.

Overall, an attenuated US joint set and a reduced scoring system for MRI can have predictive value in individuals at risk of developing RA. Unilateral US protocols have not been investigated in at risk populations. However, given a significant amount of information is lost with unilateral protocols in established RA it seems likely that bilateral joint assessments should be retained. In MRI the use of the most symptomatic or dominant hand and wrist joints is effective in predicting progression in individuals at risk of RA. Scanning symptomatic large joints on US adds predictive power. Imaging techniques such as PET (45) and whole body MRI (WB-MRI) that are able to image the whole body in one acquisition may also aid in the dilemma of which joints to scan. As far as we are aware, WB-MRI is yet to be evaluated in at risk individuals but its ability to visualize total patient-level inflammatory burden may warrant further investigation in at risk individuals.

Hands, feet or both?

One limitation of US imaging of the feet in at risk individuals is that US abnormalities such as gray-scale synovial inflammation are fairly prevalent in the healthy population, particularly at MTPJ1 (25). The SONAR score includes the same joints as the DAS28 but excludes the thumbs, shoulders and also excludes the feet. Zufferey et al. found US to be predictive for IA development when using the SONAR score in 80 CSA patients (30). In contrast, Brulhart et al. did not find that a baseline SONAR US score predicted progression to RA. The cohort in their study, however, largely consisted of FDRs with mostly negative autoantibodies, and hence had a lower overall risk of progression, although interestingly 70% were symptomatic (23). Rakieh et al. also demonstrated that US of the hands and wrists alone can be predictive of progression in ACPA positive patients with MSK symptoms (27). Taken together, these studies demonstrate that in higher risk populations with MSK symptoms, US protocols that do not include the feet can still provide predictive information. However, it is not clear to what extent omitting the feet has an effect on predictive accuracy. For example, a recent study demonstrated useful additional information to be gained by including the feet in US protocols of individuals as risk of RA. A baseline US scan was performed in over 400 ACPA positive individuals to evaluate bone erosions in MCP2, MCP5 and MTP5 joints. The combination of bone erosions and synovial inflammation in MTP5 was the most successful in predicting RA development compared with the combination of synovial inflammation and erosions in either MCP2 or MCP5 (34).

One MRI study has addressed the importance of including the feet alongside the hands when imaging at risk individuals. Boer et al. performed contrast enhanced MRI of the hand (MCP2-5 and wrist) and foot (MTP1-5) in 357 CSA patients. Scans were scored for synovitis, osteitis and tenosynovitis. After 1 year follow up 18% of patients developed an IA. The investigators found that although tenosynovitis of the feet could independently predict IA it did not increase the overall predictive accuracy of MRI over the hands and wrists alone. Without including the feet, the overall predictive sensitivity remained at 77%, however, the specificity actually decreased from 66 to 62% (71).

In summary, there is evidence to suggest specific benefit from including the feet in US protocols for at risk individuals. Therefore, reducing the length of protocols by using a limited set of hand and foot joints may be the best approach for improving feasibility while retaining predictive accuracy. In MRI, unvalidated data suggests imaging the most dominant or symptomatic hand and wrist joints alone without the feet is sufficient to predict progression to RA. A summary of suggested structures to image for MRI and ultrasound is included in **Table 3**.

TABLE 3 A summary of which structures to image with MRI and US in individuals at risk of RA.

	Structures to image that add predictive value	Structures to image for diagnostic/Pathological value
US	• Bilateral attenuated subset of small joints (27, 28) • Bone erosions in the feet (34) • Symptomatic large joints (28)	• Extracapsular inflammation in PR (60) • Tendons (59)
MRI	• Most symptomatic or dominant hand and wrist joint (40–42) • Tendons of the hands (42, 55, 56) • Intermetatarsal bursae (61)	• Interosseous tendons (58) • Tendons of the feet (71)

The structures that add predictive value in ultrasound (US) include the small joints, which can be an attenuated subset, bone erosions in the feet and symptomatic large joints. US of tendons adds diagnostic and pathological value as does extracapsular inflammation in palindromic rheumatism (PR) patients. The structures that add predictive value in magnetic resonance imaging (MRI) include the most symptomatic or dominant hand and wrist joint, tendons of the hands and intermetatarsal bursae. MRI of interosseous tendons and tendons of the feet adds diagnostic/pathological value.

Which at risk populations should be imaged?

Populations who may be considered "at risk" of developing RA have now been defined by EULAR (6). These groups encompass a range of risk and symptom profiles, with some having a much higher risk of progression than others. Imaging can be time consuming and expensive, and also necessitates face to face clinical visits, so it is important to understand in which at risk populations it adds value.

Some people are at risk of developing RA despite having no MSK symptoms, e.g., asymptomatic genetically predisposed individuals. In terms of US studies, only 14.9–33% (27–29, 31) of patients with MSK symptoms have US PD on their baseline scan. This leads to the question of whether it is useful to image at risk individuals without MSK symptoms, as intuitively they may be even less likely to have subclinical inflammation on imaging. Only one study has looked at imaging individuals at risk of RA who do not have symptoms. Brulhart et al. performed US assessments using the SONAR score in 273 FDRs of RA patients of whom 8% were ACPA positive; 14% asymptomatic, 55% MSK had symptoms and 21% had UA. A positive US was defined as at least one joint with GS $\geq$ 2, or PD $\geq$ 1. US positivity was only found in the patients that had UA and not in the individuals that were asymptomatic regardless of their antibody status (23).

Seronegative patients with inflammatory symptoms (e.g., CSA) are a lower risk group for progression to RA than ACPA+ individuals with MSK symptoms. In CSA patients, MRI studies have shown that certain symptoms in particular are associated with subclinical inflammation. In their study of 575 CSA patients Krijbolder et al. found that the longer the duration of morning stiffness the more frequently subclinical inflammation was found on MRI (72). Only 14% of these patients were ACPA positive and 20% were RF positive. Further studies of MRI scans on CSA patients with similar antibody prevalence have shown that difficulty making a fist is associated with flexor tenosynovitis and a positive squeeze test is associated with subclinical synovitis (73, 74). Van der Ven et al.'s study included 143 CSA patients of whom only 13% were positive for ACPA and 26% for RF. In these patients the presence of US synovitis was still associated with IA development despite the lower antibody prevalence (30, 75). When patients do go on to develop RA around 25% of these patients are seronegative. These studies indicate the importance of imaging in patients who are seronegative, but have inflammatory MSK symptoms such as CSA.

Overall, it seems prudent to perform imaging preferentially in at-risk individuals who have MSK symptoms, even if they are autoantibody negative. Performing US scans in individuals without MSK symptoms may not add value, although US data is limited to a single study and it is unknown if this is the case with all imaging techniques. Clarity is also required on whether individuals with high autoantibody titres and non-MSK symptoms (e.g., fatigue) have subclinical inflammation on imaging in the absence of MSK symptoms such as joint pain and stiffness. A recent prospective observational study found that 21% of 92 asymptomatic ACPA positive individuals developed RA after an average of 10.7 months (76). This relatively high proportion of progression suggests that there may be value in imaging certain high risk asymptomatic individuals.

Palindromic rheumatism

Palindromic rheumatism (PR) is a syndrome characterized by interment flares of joint pain and swelling. Patients are asymptomatic between flares and many have positive autoantibodies with 42–67% ACPA positive and 42–82% RF positive (60, 77–80). PR was included in the EULAR defined at-risk populations as a significant number of patients with PR go on to progress to RA (79, 81).

Given flares of PR are transient and unpredictable, imaging can be practically challenging. A study that scanned 54 PR patients between flares found that only 7.4% had US subclinical synovitis in the asymptomatic phase (77). It is worth noting that the majority of PR patients in this study were not DMARD naïve which may have affected the imaging findings. However, a further study in DMARD naïve PR patients also did not find US inflammation between flares (60). In contrast when US scans were performed in symptomatic flares of 84 PR patients, 36% had synovitis on imaging (82). Seropositive patients were more likely to have US detected synovitis in flare. In this same cohort it was shown that US along with ACPA antibody status were able

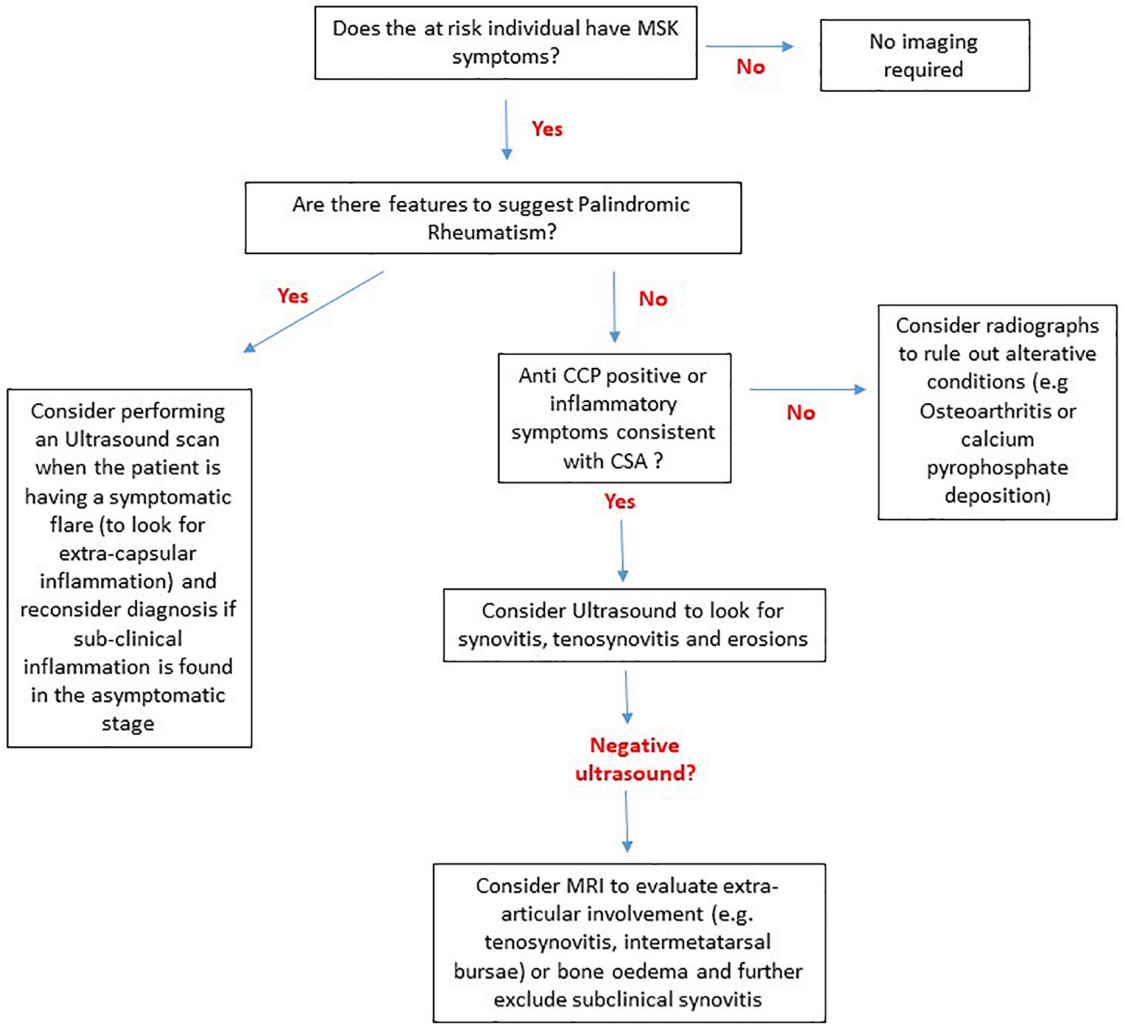

FIGURE 4
A suggested algorithm to guide the use of MRI, US and radiography in individuals at risk of RA without clinical synovitis based on current evidence. In patients that do not have any symptoms there is no evidence to suggest that any imaging techniques are of diagnostic or predictive value. For Palindromic rheumatism extracapsular inflammation can be captured on imaging during flare episodes and if subclinical inflammation is seen in the asymptomatic phase the diagnosis of palindromic rheumatism should be re-considered. For anti-citrullinated protein antibody (ACPA) negative individuals with inflammatory symptoms i.e., clinically suspect arthralgia (CSA) and ACPA+ individuals an ultrasound should be performed. If the ultrasound is negative MRI may be able to detect subtle sub-clinical inflammation, particularly in extracapsular structures. For at risk individuals such as first-degree relatives with non-inflammatory musculoskeletal (MSK) symptoms radiographs should be performed to look for alterative diagnoses.

to successfully predict RA development within 3 years, although it was the ACPA status that was the most predictive (83).

PR patients have a distinctive imaging phenotype during flare (60). In a study of 31 treatment naïve PR patients it was found that 61% of patients had extra-capsular inflammation during flares. In 39% of the patients there was extracapsular inflammation on imaging without associated synovitis. Only 23% had US detected synovitis during flare. This distinct imaging phenotype of isolated extracapsular inflammation may be particularly useful in differentiating PR from RA on clinical assessment. Overall, the current evidence suggests that PR patients should be imaged during a flare and not when they are in the asymptomatic phase.

Conclusion

The ability to study at risk individuals before they develop RA has opened up the possibility of a new and earlier "window of opportunity" for treatment. The implication of this is that there is now very real potential to treat prior to arthritis development with the prospect of halting disease progression. It is clear that

imaging has a role in this group of individuals in differential diagnosis and risk stratification.

So far, MRI and US have been the most investigated imaging techniques in individuals at risk of RA and studies have shown useful outcomes. MRI may be optimum for certain inflammatory parameters such as tenosynovitis, however, US represents the safest, cheapest and most practical imaging tool. Newer imaging techniques such as HR-pQRCT and PET have shown promising initial results and warrant further investigation.

Further work is needed to establish the optimum imaging protocols that give the most accurate and efficient results. Current studies have demonstrated that it is possible to design MRI and US protocols with reduced joint numbers. In US in particular there does appear to be additional benefit in imaging the feet and symptomatic large joints. Extra-articular structures can also provide additional information. In MRI, imaging the tendons and intermetatarsal bursa in particular can inform risk stratification. US extracapsular inflammation in PR patients may be beneficial in differentiating PR from early RA.

A careful clinical history in individuals at risk of RA is important to guide the use and timing of imaging. Symptomatic at risk individuals should be scanned preferentially regardless of their antibody status. In PR patients, it is more valuable to scan patients during a flare than in the asymptomatic phase. It should be noted that in certain lower risk groups such as CSA patients with low ACPA antibody prevalence, US inflammation appears to be less frequent and MRI may add more value. Further research is needed to establish whether there is value in imaging asymptomatic individuals with high antibody titres and other risk factors. A suggested algorithm to guide the use of imaging in at risk individuals is suggested in **Figure 4**.

With management strategies in early RA moving to a more personalized and preventative approach, risk stratification models which include serological, cellular and imaging biomarkers are being increasingly formulated. It is therefore essential that we continue to optimize the use different imaging techniques within this important cohort.

Author contributions

KH, AD, and KM contributed to the literature review and drafting of the manuscript. All authors contributed to the article and approved the submitted version.

Conflict of interest

The authors declare that the research was conducted in the absence of any commercial or financial relationships that could be construed as a potential conflict of interest.

Publisher's note

References

1. Silman AJ, Pearson JE. Epidemiology and genetics of rheumatoid arthritis. *Arthr Res.* (2002) 4:S265–72.

2. Hua C, Daien CI, Combe B, Landewe R. Diagnosis, prognosis and classification of early arthritis: results of a systematic review informing the 2016 update of the EULAR recommendations for the management of early arthritis. *Rheumatic Muscul Dis Open.* (2017) 3:e000406. doi: 10.1136/rmdopen-2016-000406

3. Barhamain AS, Magliah RF, Shaheen MH, Munassar SF, Falemban AM, Alshareef MM, et al. The journey of rheumatoid arthritis patients: a review of reported lag times from the onset of symptoms. *Open Access Rheumatol.* (2017) 9:139–50. doi: 10.2147/OARRR.S138830

4. Verstappen M, van Mulligen E, de Jong PHP, van der Helm-Van Mil AHM. DMARD-free remission as novel treatment target in rheumatoid arthritis: a systematic literature review of achievability and sustainability. *Rheumatic Muscul Dis Open.* (2020) 6:e001220. doi: 10.1136/rmdopen-2020-001220

5. Mankia K, Di Matteo A, Emery P. Prevention and cure: the major unmet needs in the management of rheumatoid arthritis. *J Autoim.* (2020) 110:102399.

6. Mankia K, Siddle HJ, Kerschbaumer A, Alpizar Rodriguez D, Catrina AI, Cañete JD, et al. EULAR points to consider for conducting clinical trials and observational studies in individuals at risk of rheumatoid arthritis. *Ann Rheumat Dis.* (2021) 80:1286–98.

7. van Steenbergen HW, Aletaha D, Beaart-van de Voorde LJJ, Brouwer E, Codreanu C, Combe B, et al. EULAR definition of arthralgia suspicious for progression to rheumatoid arthritis. *Ann Rheumat Dis.* (2017) 76:491–6.

8. van Steenbergen HW, van Nies JAB, Huizinga TWJ, Bloem JL, Reijnierse M, van der Helm-van Mil AHM. Characterising arthralgia in the preclinical phase of rheumatoid arthritis using MRI. *Ann Rheumat Dis.* (2015) 74:1225–32. doi: 10.1136/annrheumdis-2014-205522

9. Klarlund M, Østergaard M, Jensen KE, Madsen JL, Skjødt H, Lorenzen I. Magnetic resonance imaging, radiography, and scintigraphy of the finger joints: one year follow up of patients with early arthritis. *Ann Rheumat Dis.* (2000) 59:521–8.

10. Backhaus M, Burmester GR, Sandrock D, Loreck D, Hess D, Scholz A, et al. Prospective two year follow up study comparing novel and conventional imaging procedures in patients with arthritic finger joints. *Ann Rheumat Dis.* (2002) 61:895–904. doi: 10.1136/ard.61.10.895

11. Sugimoto H, Takeda A, Hyodoh K. Early-stage rheumatoid arthritis: prospective study of the effectiveness of MR imaging for diagnosis. *Radiology.* (2000) 216:569–75.

12. Garrigues F, Jousse-Joulin S, Bouttier R, Nonent M, Bressollette L, Saraux A. Concordance between clinical and ultrasound findings in rheumatoid arthritis. *Joint Bone Spine Revue Du Rhumat.* (2013) 80:597–603.

13. Stach CM, Bäuerle M, Englbrecht M, Kronke G, Engelke K, Manger B, et al. Periarticular bone structure in rheumatoid arthritis patients and healthy individuals assessed by high−resolution computed tomography. *Arthr Rheumat.* (2010) 62:330–9.

14. Fosse P, Kaiser M-J, Namur G, de Seny D, Malaise MG, Hustinx R. 18F-FDG PET/CT joint assessment of early therapeutic response in rheumatoid arthritis patients treated with rituximab. *Eur J Hybrid Imaging.* (2018) 2:6. doi: 10.1186/s41824-017-0022-y

15. Krijbolder DI, Verstappen M, van Dijk BT, Dakkak YJ, Burgers LE, Boer AC, et al. Intervention with methotrexate in patients with arthralgia at risk of rheumatoid arthritis to reduce the development of persistent arthritis and its disease burden (TREAT EARLIER): a randomised, double-blind, placebo-controlled, proof-of-concept trial. *Lancet.* (2022) 400:283–94. doi: 10.1016/S0140-6736(22)01193-X

16. Gerlag DM, Safy M, Maijer KI, Tang MW, Tas SW, Starmans-Kool MJF, et al. Effects of B-cell directed therapy on the preclinical stage of rheumatoid arthritis: the PRAIRI study. *Ann Rheumat Dis.* (2019) 78:179–85. doi: 10.1136/annrheumdis-2017-212763

17. Rech J, Ostergaard M, Tascilar K. Abatacept reverses subclinical arthritis in patients with high-risk to develop rheumatoid arthritis -results from the randomized, placebo-controlled ARIAA study in RA-at risk patients. *Am College Rheumatol Converg.* (2021). 73 (suppl 9).

18. Munn Z, Jordan Z. The patient experience of high technology medical imaging: a systematic review of the qualitative evidence. *Radiography.* (2011) 17:323–31.

19. Cate D, Luime JJ, Swen N, Gerards AH, de Jager MH, Basoski NM, et al. Role of ultrasonography in diagnosing early rheumatoid arthritis and remission of rheumatoid arthritis - a systematic review of the literature. *Arthr Res Ther.* (2013) 15:R4–R.

20. Rowbotham EL, Wakefield RJ. The technique and application of ultrasound in the diagnosis and management of inflammatory arthritis. *Sem Muscul Radiol.* (2012) 16:360–6.

21. Pentony P, Mankia K, Hensor EM, Nam JL, Hunt L, Garcia-Montoya L, et al. SAT0107 sequential ultrasound shows a late increase in inflammatory burden in anti-ccp positive patients with non-specific musculoskeletal symptoms just before progression to inflammatory arthritis. *Ann Rheumat Dis.* (2018) 77:916.

22. Di Matteo A, Duquenne L, Cipolletta E, Nam JL, Garcia Montoya L, Wakefield RJ, et al. Ultrasound subclinical synovitis in anti-CCP-positive at-risk individuals with musculoskeletal symptoms: an important and predictable stage in the rheumatoid arthritis continuum. *Rheumatology.* (2022) 61:3192–200. doi: 10.1093/rheumatology/keab862

23. Brulhart L, Alpízar-Rodríguez D, Nissen MS, Zufferey P, Ciubotariu I, Fleury G, et al. Ultrasound is not associated with the presence of systemic autoimmunity or symptoms in individuals at risk for rheumatoid arthritis. *Rheumat Muscul Dis Open.* (2019) 5:e000922.

24. Rogier C, Wouters F, van Boheemen L, van Schaardenburg D, de Jong PHP, van der Helm-van Mil AHM. Subclinical synovitis in arthralgia: how often does it result in clinical arthritis? Reflecting on starting points for disease-modifying anti-rheumatic drug treatment. *Rheumatology.* (2021) 60:3872–8. doi: 10.1093/rheumatology/keaa774

25. Padovano I, Costantino F, Breban M, D'Agostino MA. Prevalence of ultrasound synovial inflammatory findings in healthy subjects. *Ann Rheumat Dis.* (2016) 75:1819–23.

26. Mankia K, Briggs C, Emery P. How are rheumatologists managing anticyclic citrullinated peptide antibodies–positive patients who do not have arthritis? *J Rheumatol.* (2020) 47:305–6. doi: 10.3899/jrheum.190211

27. Rakieh C, Nam JL, Hunt L, Hensor EM, Das S, Bissell LA, et al. Predicting the development of clinical arthritis in anti-CCP positive individuals with non-specific musculoskeletal symptoms: a prospective observational cohort study. *Ann Rheumat Dis.* (2015) 74:1659–66.

28. Nam J, Hensor E, Hunt L, Conaghan P, Wakefield R, Emery P. Ultrasound findings predict progression to inflammatory arthritis in anti-CCP antibody-positive patients without clinical synovitis. *Ann Rheumat Dis.* (2016) 75:2060–7. doi: 10.1136/annrheumdis-2015-208235

29. van de Stadt LA, Bos WH, Reynders MM, Wieringa H, Turkstra F, van der Laken J, et al. The value of ultrasonography in predicting arthritis in auto-antibody positive arthralgia patients: a prospective cohort study. *Arthr Res Ther.* (2010) 12:R98. doi: 10.1186/ar3028

30. Zufferey P, Rebell C, Benaim C, Ziswiler HR, Dumusc A, So A. Ultrasound can be useful to predict an evolution towards rheumatoid arthritis in patients with inflammatory polyarthralgia without anticitrullinated antibodies. *Joint Bone Spine Revue Du Rhumat.* (2016) 84:299–303. doi: 10.1016/j.jbspin.2016.05.011

31. Ven M, van der Veer-Meerkerk M, Cate D, Rasappu N, Kok MR, Csakvari D, et al. Absence of ultrasound inflammation in patients presenting with arthralgia rules out the development of arthritis. *Arthr Res Ther.* (2017) 19:202. doi: 10.1186/s13075-017-1405-y

32. Molina Collada J, López Gloria K, Castrejón I, Nieto-González JC, Rivera J, Montero F, et al. Ultrasound in clinically suspect arthralgia: the role of power doppler to predict rheumatoid arthritis development. *Arthr Res Ther.* (2021) 23:299.

33. Ohrndorf S, Boer AC, Boeters DM, ten Brinck RM, Burmester GR, Kortekaas MC, et al. Do musculoskeletal ultrasound and magnetic resonance imaging identify synovitis and tenosynovitis at the same joints and tendons? A comparative study in early inflammatory arthritis and clinically suspect arthralgia. *Arthr Res Ther.* (2019) 21:59. doi: 10.1186/s13075-019-1824-z

34. Di Matteo A, Mankia K, Duquenne L, Cipolletta E, Wakefield RJ, Garcia-Montoya L, et al. Ultrasound erosions in the feet best predict progression to inflammatory arthritis in anti-CCP positive at-risk individuals without clinical synovitis. *Ann Rheumat Dis.* (2020) 79:901–7. doi: 10.1136/annrheumdis-2020-217215

35. Wakefield RJ, O'Connor PJ, Conaghan PG, McGonagle D, Hensor EMA, Gibbon WW, et al. Finger tendon disease in untreated early rheumatoid arthritis: a comparison of ultrasound and magnetic resonance imaging. *Arthr Rheumat.* (2007) 57:1158–64. doi: 10.1002/art.23016

36. Bøyesen P, Haavardsholm EA, Østergaard M, van der Heijde D, Sesseng S, Kvien TK. MRI in early rheumatoid arthritis: synovitis and bone marrow edema are independent predictors of subsequent radiographic progression. *Ann Rheumat Dis.* (2011) 70:428–33.

37. Parodi M, Silvestri E, Garlaschi G, Cimmino MA. How normal are the hands of normal controls? A study with dedicated magnetic resonance imaging. *Clin Exp Rheumatol.* (2006) 24:134–41.

38. Ejbjerg B, Narvestad E, Rostrup E, Szkudlarek M, Jacobsen S, Thomsen HS, et al. Magnetic resonance imaging of wrist and finger joints in healthy subjects occasionally shows changes resembling erosions and synovitis as seen in rheumatoid arthritis. *Arthr Rheumat.* (2004) 50:1097–106. doi: 10.1002/art.20135

39. Mangnus L, van Steenbergen HW, Reijnierse M, van der Helm-van Mil AHM. Magnetic resonance imaging–detected features of inflammation and erosions in symptom−free persons from the general population. *Arthr Rheumatol.* (2016) 68:2593–602. doi: 10.1002/art.39749

40. Gent Y, ter Wee MM, Ahmadi N, van Kuijk C, Voskuyl AE, van der Laken CJ, et al. Three-year clinical outcome following baseline magnetic resonance imaging in anti-citrullinated protein antibody-positive arthralgia patients: an exploratory study. *Arthr Rheumatol.* (2014) 66:2909–10. doi: 10.1002/art.38757

41. Boer AC, Burgers LE, Mangnus L, Ten Brinck RM, Nieuwenhuis WP, van Steenbergen HW, et al. Using a reference when defining an abnormal MRI reduces false-positive MRI results-a longitudinal study in two cohorts at risk for rheumatoid arthritis. *Rheumatology.* (2017) 56:1700–6. doi: 10.1093/rheumatology/kex235

42. van Steenbergen HW, Mangnus L, Reijnierse M, Huizinga TWJ, van der Helm-van Mil AHM. Clinical factors, anticitrullinated peptide antibodies and MRI-detected subclinical inflammation in relation to progression from clinically suspect arthralgia to arthritis. *Ann Rheumat Dis.* (2016) 75:1824–30. doi: 10.1136/annrheumdis-2015-208138

43. Roivainen A, Hautaniemi S, Möttönen T, Nuutila P, Oikonen V, Parkkola R, et al. Correlation of 18F-FDG PET/CT assessments with disease activity and markers of inflammation in patients with early rheumatoid arthritis following the initiation of combination therapy with triple oral antirheumatic drugs. *Eur J Nuclear Med Mol Imaging.* (2012) 40:403–10. doi: 10.1007/s00259-012-2282-x

44. Gent Y, Ahmadi N, Voskuyl AE, Hoetjes NJ, van Kuijk C, Britsemmer K, et al. Detection of subclinical synovitis with macrophage targeting and positron emission tomography in patients with rheumatoid arthritis without clinical arthritis. *J Rheumatol.* (2014) 41:2145–52.

45. Gent YYJ, Voskuyl AE, Kloet RW, van Schaardenburg D, Hoekstra OS, Dijkmans BAC, et al. Macrophage positron emission tomography imaging as a biomarker for preclinical rheumatoid arthritis: findings of a prospective pilot study. *Arthr Rheumat.* (2012) 64:62–6. doi: 10.1002/art.30655

46. Güler-Yüksel M, Allaart CF, Goekoop-Ruiterman YPM, de Vries-Bouwstra JK, van Groenendael JHLM, Mallée C, et al. Changes in hand and generalised bone mineral density in patients with recent-onset rheumatoid arthritis. *Ann Rheumat Dis.* (2009) 68:330–6. doi: 10.1136/ard.2007.086348

47. De Rooy DPC, KÄLvesten J, Huizinga TWJ, Van Der Helm-Van Mil AHM. Loss of metacarpal bone density predicts RA development in recent-onset arthritis. *Rheumatology.* (2012) 51:1037–41. doi: 10.1093/rheumatology/ker435

48. Kleyer A, Finzel S, Rech J, Manger B, Krieter M, Faustini F, et al. Bone loss before the clinical onset of rheumatoid arthritis in subjects with anticitrullinated protein antibodies. *Ann Rheumat Dis.* (2014) 73:854–60.

49. Hoff M, Haugeberg G, Ødegård S, Syversen S, Landewé R, van der Heijde D, et al. Cortical hand bone loss after 1 year in early rheumatoid arthritis predicts radiographic hand joint damage at 5-year and 10-year follow-up. *Ann Rheumat Dis.* (2009) 68:324–9. doi: 10.1136/ard.2007.085985

50. Keller KK, Thomsen JS, Stengaard-Pedersen K, Nielsen AW, Schiøttz-Christensen B, Svendsen L, et al. Local bone loss in patients with anti-citrullinated peptide antibody and arthralgia, evaluated with high-resolution peripheral quantitative computed tomography. *Scand J Rheumatol.* (2018) 47:110–6. doi: 10.1080/03009742.2017.1333629

51. Simon D, Kleyer A, Cong DB, Hueber A, Bang H, Ramming A, et al. Microstructural bone changes are associated with broad−spectrum autoimmunity and predict the onset of rheumatoid arthritis. *Arthr Rheumatol.* (2022) 74:418–26. doi: 10.1002/art.41229

52. Wakefield RJ, Gibbon WW, Conaghan PG, O'Connor P, McGonagle D, Pease C, et al. The value of sonography in the detection of bone erosions in patients with rheumatoid arthritis: a comparison with conventional radiography. *Arthr Rheumat.* (2000) 43:2762–70.

53. Rahmani M, Chegini H, Najafizadeh SR, Azimi M, Habibollahi P, Shakiba M. Detection of bone erosion in early rheumatoid arthritis: ultrasonography and conventional radiography versus non-contrast magnetic resonance imaging. *Clin Rheumatol.* (2010) 29:883–91. doi: 10.1007/s10067-010-1423-5

54. Di Matteo A, Mankia K, Nam JL, Cipolletta E, Garcia-Montoya L, Duquenne L, et al. In anti-CCP+ at-risk individuals, radiographic bone erosions are uncommon and are not associated with the development of clinical arthritis. *Rheumatology.* (2021) 60:3156–64. doi: 10.1093/rheumatology/keaa761

55. Hunt L, Nam J, Hensor EM, Mankia K, Rowbotham E, Grainger AJ, et al. OP0042 In acpa positive at-risk individuals, which mri and us findings best predict development of clinical synovitis? *Ann Rheumat Dis.* (2018) 77:72.

56. Kleyer A, Krieter M, Oliveira I, Faustini F, Simon D, Kaemmerer N, et al. High prevalence of tenosynovial inflammation before onset of rheumatoid arthritis and its link to progression to RA—a combined MRI/CT study. *Sem Arthr Rheumat.* (2016) 46:143–50. doi: 10.1016/j.semarthrit.2016.05.002

57. Matthijssen XME, Wouters F, Boeters DM, Boer AC, Dakkak YJ, Niemantsveriet E, et al. A search to the target tissue in which RA-specific inflammation starts: a detailed MRI study to improve identification of RA-specific features in the phase of clinically suspect arthralgia. *Arthr Res Ther.* (2019) 21:249. doi: 10.1186/s13075-019-2002-z

58. Mankia K, D'Agostino MA, Rowbotham E, Hensor EMA, Hunt L, Möller I, et al. MRI inflammation of the hand interosseous tendons occurs in anti-CCP positive at-risk individuals and may precede the development of clinical synovitis. *Ann Rheumat Dis.* (2019) 78:781–6. doi: 10.1136/annrheumdis-2018-214331

59. Trickey J, Sahbudin I, Ammitzbøll-Danielsen M, Azzolin I, Borst C, Bortoluzzi A, et al. Very low prevalence of ultrasound-detected tenosynovial abnormalities in healthy subjects throughout the age range: OMERACT ultrasound minimal disease study. *Ann Rheumat Dis.* (2021) 81:232–6. doi: 10.1136/annrheumdis-2021-219931

60. Mankia K, D'Agostino MA, Wakefield RJ, Nam JL, Mahmood W, Grainger AJ, et al. Identification of a distinct imaging phenotype may improve the management of palindromic rheumatism. *Ann Rheumat Dis.* (2019) 78:43–50. doi: 10.1136/annrheumdis-2018-214175

61. van Dijk BT, Wouters F, van Mulligen E, Reijnierse M, van der Helm-van Mil AHM. During development of rheumatoid arthritis, intermetatarsal bursitis may occur before clinical joint swelling: a large imaging study in patients with clinically suspect arthralgia. *Rheumatology.* (2021) 61:2805–14. doi: 10.1093/rheumatology/keab830

62. Aizenberg E, ten Brinck RM, Reijnierse M, van der Helm-van Mil AHM, Stoel BC. Identifying MRI-detected inflammatory features specific for rheumatoid arthritis: two-fold feature reduction maintains predictive accuracy in clinically suspect arthralgia patients. *Sem Arthr Rheumat.* (2019) 48:579–86. doi: 10.1016/j.semarthrit.2018.04.005

63. Aga A-B, Hammer HB, Olsen IC, Uhlig T, Kvien TK, van der Heijde D, et al. First step in the development of an ultrasound joint inflammation score for rheumatoid arthritis using a data-driven approach. *Ann Rheumat Dis.* (2016) 75:1444–51. doi: 10.1136/annrheumdis-2015-207572

64. Østergaard M, Peterfy CG, Bird P, Gandjbakhch F, Glinatsi D, Eshed I, et al. The OMERACT rheumatoid arthritis magnetic resonance imaging (MRI) scoring system: updated recommendations by the OMERACT MRI in arthritis working group. *J Rheumatol.* (2017) 44:1706–12. doi: 10.3899/jrheum.161433

65. Mo Y-Q, Yang Z-H, Wang J-W, Li Q-H, Du X-Y, Huizinga TW, et al. The value of MRI examination on bilateral hands including proximal interphalangeal joints for disease assessment in patients with early rheumatoid arthritis: a cross-sectional cohort study. *Arthr Res Ther.* (2019) 21:279. doi: 10.1186/s13075-019-2061-1

66. Anderson SE, Steinbach LS, De Monaco D, Bonel HM, Hurtienne Y, Voegelin E. "Baby wrist": MRI of an overuse syndrome in mothers. *Am J Roentgenol.* (2004) 182:719–24. doi: 10.2214/ajr.182.3.1820719

67. Zhao SS, Nikiphorou E, Young A, Kiely PDW. Large joints are progressively involved in rheumatoid arthritis irrespective of rheumatoid factor status—results from the early rheumatoid arthritis study. *Rheumatol Int.* (2021) 42:621–9. doi: 10.1007/s00296-021-04931-2

68. Scott DL, Coulton BL, Popert AJ. Long term progression of joint damage in rheumatoid arthritis. *Ann Rheumat Dis.* (1986) 45:373–8.

69. Rogier C, van der Ven M, van der Helm-van Mil AHM, de Jong PHP. Is shoulder involvement in clinically suspect arthralgia an early feature of rheumatoid arthritis? A longitudinal ultrasound study. *Rheumatology.* (2020) 59:2640–2. doi: 10.1093/rheumatology/keaa052

70. de Hair MJH, van de Sande MGH, Ramwadhdoebe TH, Hansson M, Landewé R, van der Leij C, et al. Features of the synovium of individuals at risk of developing rheumatoid arthritis: implications for understanding preclinical rheumatoid arthritis. *Arthr Rheumatol.* (2014) 66:513–22. doi: 10.1002/art.38273

71. Boer AC, Wouters F, Dakkak YJ, Niemantsveriet E, van der Helm van Mil A. Improving the feasibility of MRI in clinically suspect arthralgia for prediction of rheumatoid arthritis by omitting scanning of the feet. *Rheumatology.* (2020) 59:1247–52. doi: 10.1093/rheumatology/kez436

72. Krijbolder DI, Wouters F, van Mulligen E, van der Helm-van Mil AHM. Morning stiffness precedes the development of rheumatoid arthritis and associates with systemic and subclinical joint inflammation in arthralgia patients. *Rheumatology.* (2022) 61:2113–8. doi: 10.1093/rheumatology/keab651

73. Wouters F, van der Giesen FJ, Matthijssen XME, Niemantsverdriet E, van der Helm-van Mil AHM. Difficulties making a fist in clinically suspect arthralgia: an easy applicable phenomenon predictive for RA that is related to flexor tenosynovitis. *Ann Rheumat Dis.* (2019) 78:1438–9. doi: 10.1136/annrheumdis-2019-215402

74. Wouters F, Niemantsverdriet E, Van der Helm van Mil A. Ab1258 the value of the squeeze test for detection of subclinical synovitis in patients with arthralgia suspicious for progression to ra. *Ann Rheumat Dis.* (2020) 79:1920–1. doi: 10.1093/rheumatology/keaa082

75. Freeston JE, Wakefield RJ, Conaghan PG, Hensor EMA, Stewart SP, Emery P. A diagnostic algorithm for persistence of very early inflammatory arthritis: the utility of power doppler ultrasound when added to conventional assessment tools. *Ann Rheumat Dis.* (2010) 69:417–9. doi: 10.1136/ard.2008.106658

76. Mizuki S, Horie K, Imabayashi K, Mishima K, Oryoji K. POS0441 development of rheumatoid arthritis among anti-citrullinated protein antibodies positive asymptomatic individuals: a prospective observational study. *Ann Rheumat Dis.* (2021) 80:449–449.

77. Cabrera-Villalba S, Ramirez J, Salvador G, Ruiz-Esquide V, Hernandez MV, Inciarte-Mundo J, et al. Is there subclinical synovitis in patients with palindromic rheumatism in the intercritical period? A clinical and ultrasonographic study according to anticitrullinated protein antibody status. *J Rheumatol.* (2014) 41:1650–5. doi: 10.3899/jrheum.131545

78. Russell AS, Devani A, Maksymowych WP. The role of anti-cyclic citrullinated peptide antibodies in predicting progression of palindromic rheumatism to rheumatoid arthritis. *J Rheumatol.* (2006) 33:1240–2.

79. Tamai M, Kawakami A, Iwamoto N, Arima K, Aoyagi K, Eguchi K. Contribution of anti-CCP antibodies, proximal interphalangeal joint involvement, HLA-DRB1 shared epitope, and PADI4 as risk factors for the development of rheumatoid arthritis in palindromic rheumatism. *Scand J Rheumatol.* (2010) 39:287–91. doi: 10.3109/03009741003604534

80. Khabbazi A, Hajialiloo M, Kolahi S, Soroosh M, Esalatmanesh K, Sharif S. A multicenter study of clinical and laboratory findings of palindromic rheumatism in Iran. *Int J Rheumat Dis.* (2012) 15:427–30. doi: 10.1111/j.1756-185X.2012.01739.x

81. Emad Y, Anbar A, Abo-Elyoun I, El Shaarawy N, Al-Hanafi H, Darwish H, et al. In palindromic rheumatism, hand joint involvement and positive anti-CCP antibodies predict RA development after 1 year of follow-up. *Clin Rheumatol.* (2014) 33:791–7. doi: 10.1007/s10067-014-2569-3

82. Chen H-H, Lan J-L, Hung G-D, Chen Y-M, Lan HH-C, Chen D-Y. Association of ultrasonographic findings of synovitis with anti-cyclic citrullinated peptide antibodies and rheumatoid factor in patients with palindromic rheumatism during active episodes. *J Ultrasound Med.* (2009) 28:1193–9. doi: 10.7863/jum.2009.28.9.1193

83. Chen HH, Chen DY, Hsieh TY, Hung GD, Haw-Chang Lan H, Hsieh CW, et al. Predicting the progression of palindromic rheumatism to rheumatoid arthritis: the role of ultrasonography and anti-cyclic citrullinated peptide antibodies. *J Med Ultrasound.* (2010) 18:17–26.

frontiers | Frontiers in Medicine

TYPE Original Research
PUBLISHED 17 January 2023
DOI 10.3389/fmed.2022.1090468

OPEN ACCESS

EDITED BY
Anastasios E. Germenis,
University of Thessaly, Greece

REVIEWED BY
Dragana Lazarevic,
University Clinical Center Niš, Serbia
Fernando Saraiva,
Centro Hospitalar Universitário Lisboa Norte, Portugal
Georgios Filippou,
IRCCS Istituto Ortopedico Galeazzi, Italy

*CORRESPONDENCE
Andrea Di Matteo
andrea.dimatteo@hotmail.com

SPECIALTY SECTION
This article was submitted to Rheumatology, a section of the journal Frontiers in Medicine

RECEIVED 05 November 2022
ACCEPTED 29 December 2022
PUBLISHED 17 January 2023

CITATION
Di Matteo A, Moscioni E, Lommano MG, Cipolletta E, Smerilli G, Farah S, Airoldi C, Aydin SZ, Becciolini A, Bonfiglioli K, Carotti M, Carrara G, Cazenave T, Corradini D, Cosatti MA, de Agustin JJ, Destro Castaniti GM, Di Carlo M, Di Donato E, Di Geso L, Elliott A, Fodor D, Francioso F, Gabba A, Hernández-Díaz C, Horvath R, Hurnakova J, Jesus D, Marin J, Martire MV, Mashadi Mirz R, Massarotti M, Musca AA, Nair J, Okano T, Papalopoulos I, Rosa J, Rosemffet M, Rovisco J, Rozza D, Salaffi F, Scioscia C, Scirè CA, Tamas M-M, Tanimura S, Ventura-Rios L, Villota-Eraso C, Villota O, Voulgari PV, Vreju FA, Vukatana G, Hereter JZ, Zanetti A, Grassi W and Filippucci E (2023) Reliability assessment of ultrasound muscle echogenicity in patients with rheumatic diseases: Results of a multicenter international web-based study. *Front. Med.* 9:1090468. doi: 10.3389/fmed.2022.1090468

Reliability assessment of ultrasound muscle echogenicity in patients with rheumatic diseases: Results of a multicenter international web-based study

Andrea Di Matteo[1,2]*, Erica Moscioni[1], Maria Giovanna Lommano[1], Edoardo Cipolletta[1], Gianluca Smerilli[1], Sonia Farah[1], Carla Airoldi[3], Sibel Zehra Aydin[4], Andrea Becciolini[5], Karina Bonfiglioli[6], Marina Carotti[7], Greta Carrara[8], Tomas Cazenave[9], Davide Corradini[10], Micaela Ana Cosatti[11], Juan Josè de Agustin[12], Giulia Maria Destro Castaniti[13], Marco Di Carlo[1], Eleonora Di Donato[5], Luca Di Geso[14], Ashley Elliott[15], Daniela Fodor[16], Francesca Francioso[1], Alessandra Gabba[17,18], Cristina Hernández-Díaz[19], Rudolf Horvath[20], Jana Hurnakova[20], Diogo Jesus[21], Josefina Marin[22], Maria Victoria Martire[23], Riccardo Mashadi Mirza[24], Marco Massarotti[25], Alice Andreea Musca[26], Jagdish Nair[27], Tadashi Okano[28], Ioannis Papalopoulos[29], Javier Rosa[22], Marcos Rosemffet[9], João Rovisco[30], Davide Rozza[8], Fausto Salaffi[1], Crescenzio Scioscia[31], Carlo Alberto Scirè[8], Maria-Magdalena Tamas[32], Shun Tanimura[33], Lucio Ventura-Rios[19], Catalina Villota-Eraso[34], Orlando Villota[35], Paraskevi V. Voulgari[36], Florentin Ananu Vreju[37], Gentiana Vukatana[38], Johana Zacariaz Hereter[22], Anna Zanetti[8], Walter Grassi[1] and Emilio Filippucci[1]

[1]Rheumatology Unit, Department of Clinical and Molecular Sciences, "Carlo Urbani" Hospital, Polytechnic University of Marche, Ancona, Italy, [2]Leeds Institute of Rheumatic and Musculoskeletal Medicine, University of Leeds, Leeds, United Kingdom, [3]Hospital Provincial, Rheumatology, Rosario, Argentina, [4]Ottawa Hospital Research Institute, University of Ottawa, Ottawa, ON, Canada, [5]Internal Medicine and Rheumatology Unit, Department of Medicine, Azienda Ospedaliero-Universitaria di Parma, Parma, Italy, [6]Hospital das Clínicas da Faculdade de Medicina da Universidade de São Paulo, São Paulo, SP, Brazil, [7]Department of Radiology, Ospedali Riuniti, Università Politecnica delle Marche, Ancona, Italy, [8]Epidemiology Unit, Italian Society of Rheumatology, Milan, Italy, [9]Rheumatology Unit, Instituto de Rehabilitación Psicofísica, Buenos Aires, Argentina, [10]Rheumatology Unit, University Clinic AOU Cagliari, Monserrato, CA, Italy, [11]CEMIC, Centro de Educación Médica e Investigaciones Médicas "Norberto Quirno", Buenos Aires, Argentina, [12]Rheumatology Unit, Vall d'Hebron Hospital Universitari, Vall d'Hebron Barcelona Hospital Campus, Barcelona, Spain, [13]Department of Health Promotion, Mother and Child Care, Internal Medicine and Medical Specialties, Rheumatology Section, University of Palermo, Palermo, Italy, [14]Department of Internal Medicine, Ospedale Madonna del Soccorso, San Benedetto del Tronto, Marche, Italy, [15]Centre for Experimental Medicine, Queen's University Belfast, Belfast, United Kingdom, [16]2nd Department of Internal Medicine, "Iuliu Hatieganu" University of Medicine and Pharmacy, Cluj-Napoca, Romania, [17]Local Health Unit (ASL), Samugheo, OR, Italy, [18]Local Health Unit (ASL), Orosei, NU, Italy, [19]División de Reumatología, Instituto Nacional de Rehabilitación "Luis Guillermo Ibarra Ibarra", Mexico City, Mexico, [20]Department of Paediatric and Adult Rheumatology, University Hospital Motol, Prague, Czechia, [21]Department of Rheumatology, Centro Hospitalar de Leiria, Leiria, Portugal, [22]Hospital Italiano de Buenos Aires, Buenos Aires, Argentina, [23]San Roque Hospital, La Plata, Argentina, [24]Department of Radiology, A. O. Ospedali Riuniti Marche Nord, Pesaro, Italy, [25]Department of Rheumatology, University Hospitals Dorset NHS Foundation Trust, Christchurch Hospital, Christchurch, United Kingdom, [26]Department of Rheumatology, Colentina Clinical

Hospital, Bucharest, Romania, [27]Department of Rheumatology, Liverpool University Hospitals Foundation Trust, Liverpool, United Kingdom, [28]Department of Orthopedic Surgery, Osaka Metropolitan University Graduate School of Medicine, Osaka, Japan, [29]Department of Rheumatology, Clinical Immunology and Allergy, University Hospital of Heraklion, Heraklion, Greece, [30]Department of Rheumatology, Centro Hospitalar e Universitário de Coimbra, Coimbra, Portugal, [31]Rheumatology Unit, Department of Emergency and Organ Transplants (DETO), University of Bari, Bari, Italy, [32]Department of Rheumatology, "Iuliu Hatieganu" University of Medicine and Pharmacy, Cluj-Napoca, Romania, [33]Department of Rheumatology, Hokkaido Medical Center for Rheumatic Diseases, Sapporo, Japan, [34]IPS Servicio Integral de Reumatología e Inmunología Doctor Orlando Villota, Pasto, Colombia, [35]Division of Rheumatology, Fundación Hospital San Pedro, Pasto, Colombia, [36]Department of Rheumatology, School of Health Science, Faculty of Medicine, University of Ioannina, Ioannina, Greece, [37]Department of Rheumatology, University of Medicine and Pharmacy of Craiova, Craiova, Romania, [38]Rheumatology Unit, IRCCS Policlinico S. Orsola-Malpighi, Bologna, Italy

Objectives: To investigate the inter/intra-reliability of ultrasound (US) muscle echogenicity in patients with rheumatic diseases.

Methods: Forty-two rheumatologists and 2 radiologists from 13 countries were asked to assess US muscle echogenicity of quadriceps muscle in 80 static images and 20 clips from 64 patients with different rheumatic diseases and 8 healthy subjects. Two visual scales were evaluated, a visual semi-quantitative scale (0–3) and a continuous quantitative measurement ("VAS echogenicity," 0–100). The same assessment was repeated to calculate intra-observer reliability. US muscle echogenicity was also calculated by an independent research assistant using a software for the analysis of scientific images (ImageJ). Inter and intra reliabilities were assessed by means of prevalence-adjusted bias-adjusted Kappa (PABAK), intraclass correlation coefficient (ICC) and correlations through Kendall's Tau and Pearson's Rho coefficients.

Results: The semi-quantitative scale showed a moderate inter-reliability [PABAK = 0.58 (0.57–0.59)] and a substantial intra-reliability [PABAK = 0.71 (0.68–0.73)]. The lowest inter and intra-reliability results were obtained for the intermediate grades (i.e., grade 1 and 2) of the semi-quantitative scale. "VAS echogenicity" showed a high reliability both in the inter-observer [ICC = 0.80 (0.75–0.85)] and intra-observer [ICC = 0.88 (0.88–0.89)] evaluations. A substantial association was found between the participants assessment of the semi-quantitative scale and "VAS echogenicity" [ICC = 0.52 (0.50–0.54)]. The correlation between these two visual scales and ImageJ analysis was high (tau = 0.76 and rho = 0.89, respectively).

Conclusion: The results of this large, multicenter study highlighted the overall good inter and intra-reliability of the US assessment of muscle echogenicity in patients with different rheumatic diseases.

KEYWORDS

muscle echogenicity, musculoskeletal ultrasound, sarcopenia, reliability, rheumatic diseases

Introduction

Sarcopenia is a muscle disease that is characterized by low muscle mass (main criteria), reduced muscle strength and impaired physical performance (1, 2). Sarcopenia is regarded as the biological foundation of frailty. Both these conditions have been demonstrated to have an association with increased adverse health outcomes such as falls, hospital admission, and mortality (3). In a recent study on 400 patients with rheumatoid arthritis (RA), a significant association was found between sarcopenia and multiple RA-related comorbidities, including obesity, dyslipidemia, diabetes and chronic obstructive pulmonary disease (4).

While "primary" sarcopenia reflects age-related changes in muscle mass, strength and function, "secondary" sarcopenia may occur in relatively young patients with inflammatory diseases, such as RA, mainly as the consequence of chronic systemic inflammation, use of medications (e.g., steroids) and patients' reduced mobility (5–7).

Magnetic resonance imaging (MRI), computed tomography (CT), bioelectrical impedance analysis and dual-energy x-rays absorptiometry (DXA) are regarded as the reference imaging tests for the assessment of sarcopenia (8). Several studies have also highlighted the very promising role of ultrasound (US) as a reference method for the evaluation of sarcopenia-related muscle involvement in elderly populations (9) and, to a lesser extent, in patients with rheumatic

diseases (10). Muscle US based measurements have shown a strong correlation with MRI, CT and DXA based evaluations (11–13). In addition, US has been proven accurate for the evaluation of muscle quantity and quality in validation studies on cadavers (14, 15).

As acknowledged by the SARCopenia through UltraSound (SARCUS) working group (i.e., a Sarcopenia Special Interest Group of the European Geriatric Medicine Society), the use of US in sarcopenia is promising but limited mainly by lack of standardization and data supporting the reliability of this imaging tool (16).

The US measurement of muscle mass (i.e., muscle thickening) is regarded as the "traditional" US method for the diagnosis of sarcopenia (17). However, no clearly defined US cut-offs for the diagnosis of sarcopenia (neither for MRI nor CT) have been established (18). In addition, a reduction of muscle mass is only one of the aspects that characterize the process of sarcopenia-related muscle degradation, and arguably the one that is most influenced by aging (19).

Also "qualitative" changes of muscle architecture (i.e., increased muscle echogenicity due to fatty replacement or fibrosis of muscle tissue) have emerged as important US features of sarcopenia (20). Previous studies have demonstrated that an increased US muscle echogenicity, notwithstanding preserved muscle mass, is a relevant and accurate measure of sarcopenia-related muscle deterioration (i.e., reduced muscle quality) (21).

In last years, rheumatologists have been attracted by the promising role of US in the assessment of sarcopenia (or "sarcopenia spectrum") in patients with rheumatic diseases (22–25). The "early" detection of sarcopenia in patients with rheumatic diseases may raise important implications for the management of these patients, including the adoption of regular exercise and/or the use of medications and supplements (26).

In a very recent study, our research group has proposed a new US protocol for the evaluation of various aspects of sarcopenia-related muscle involvement ("multimodal ultrasound"), including muscle mass, muscle echogenicity/quality and muscle stiffness using shear-wave elastography (27). In this study, a four-grade US visual semi-quantitative scale for the assessment of muscle echogenicity was developed. Unlike the measurement of muscle mass, this US semi-quantitative scale showed the ability to discriminate between systemic lupus erythematosus (SLE) patients and healthy subjects. In addition, an increased US muscle echogenicity was significantly associated with patients' reduced muscle strength and low physical performance, thus emerging as a valuable tool for the early detection of muscle deterioration associated with sarcopenia in patients with SLE and, potentially, in patients with rheumatic diseases (27).

Beside the potential clinical implications of the recently proposed US semi-quantitative scale for muscle echogenicity, an equally important requisite for the application of this imaging method in clinical practice is the grade of consistency/agreement between different individuals (inter-reliability), and within the same individual on different occasions (intra-reliability), in the reading and interpretation of such scale.

Therefore, the main objective of the current study was to explore, in a large group of physicians (mostly rheumatologists) who routinely perform musculoskeletal (MSK) US, the inter and intra-reliability of the visual US semi-quantitative scale for muscle echogenicity which was recently developed by our research group. The inter and intra-reliability of a second quantitative visual scale for muscle echogenicity (from 0 to 100, VAS echogenicity) was also investigated, as well as the association between these two US visual scales and their correlation with an image-processing program that uses histogram analysis to calculate pixel gray scale intensity in a region of interest (ROI).

Materials and methods

Rheumatologists and MSK radiologists who had a training period in MSK US at the "Rheumatology Clinic" of the "Carlo Urbani" Hospital, Jesi, Ancona, Italy, were invited to participate in this web-based exercise. A detailed description of this research group has been recently published (28).

B-mode images and clips (5–10 s long) of the quadriceps muscle (i.e., rectus femoris and vastus intermedius muscles) were collected by 2 rheumatologists with 10 (ADM) and 4 years (GS) of experience in MSK US. The images and clips were obtained using a transverse approach in 64 patients with different rheumatic conditions (16 systemic sclerosis, 15 axial spondyloarthritis, 10 RA, 9 SLE, 6 osteoarthritis, 4 fibromyalgia, 2 gout, 2 calcium pyrophosphate deposition disease), with no current symptoms suggesting inflammatory myositis (nor a previous diagnosis of inflammatory myositis/neuromuscular disease), who attended the out-patient clinic of Rheumatology Unit, Jesi (Ancona), and 8 healthy subjects (staff members of the "Carlo Urbani" hospital). In 24 out of 64 rheumatic patients and in 4 out of 8 healthy subjects, a bilateral acquisition of the quadriceps muscle was obtained (left and right quadriceps muscle). Therefore, the images and clips composing the final US dataset were acquired from 100 different quadriceps muscles. Creatine phosphokinases were not systematically obtained in the current study. However, patients with an increased creatine phosphokinase recorded at least once in the 6 months preceding the enrollment, and patients/healthy subjects who had intense physical activity in the preceding 4 weeks, were excluded from the study. The mean age, gender, and body mass index (BMI) were 60.3 ± 13.7 years, 64.1% female, and BMI: 25.7 ± 5.4 in rheumatic patients and 37.2 ± 6.5 years, 50.0% females, and BMI: 24.6 ± 4.0 in healthy subjects. Fifteen out of 64 (23.4%) rheumatic patients were on corticosteroids (≥5 mg of oral prednisolone equivalents).

The final dataset included 80 static images and 20 clips. Images and clips were exported from the US machine and saved in JPEG and AVI format, respectively. The two rheumatologists (ADM and GS) developed the final images and clips dataset balancing the prevalence of the different grades of muscle echogenicity according to their evaluations (See **Supplementary Table 1**).

The US images and clips were obtained at the quadriceps muscle at the midpoint between the anterior superior iliac spine and the upper pole of the patella, as previously described (29). During clips acquisition, the probe was slowly moved 3 cm proximal and distal to the midpoint for a comprehensive exploration of the quadriceps muscle area. A MyLab C (Esaote Spa, Genoa, Italy) US system (frequency range 4–13 MHz, gain: 50 dB, depth 5 cm, or 6 cm in case of obese patients) and a MyLab9 XP (Esaote Spa, Genoa, Italy) broadband linear probe (frequency range 3–11 MHz, gain: 50 dB, depth 5 cm, or 6 cm in case of obese patients) were used for the acquisition of clips and images.

Participants, blinded to the patients diagnosis, were asked to score muscle echogenicity of quadriceps muscle (i.e., rectus femoris and vastus intermedius muscles) according to: (1) a visual semi-quantitative scale, recently developed by our research group (27)

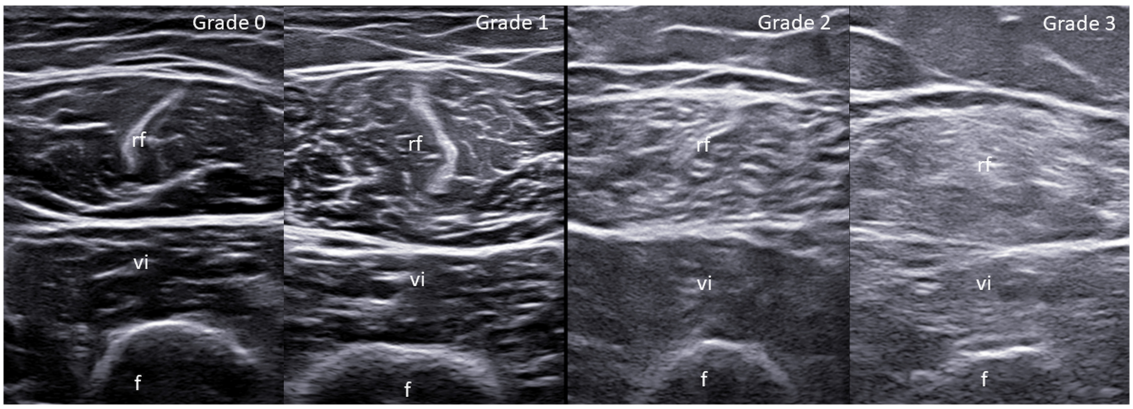

FIGURE 1
Visual semi-quantitative scale for the assessment of muscle echogenicity. Ultrasound (US) transverse scan images of the quadriceps muscle obtained at the midpoint between the anterior superior iliac spine and the upper pole of the patella. Grade 0 = normal (i.e., normal hypoechoic muscle); Grade 1 = mild (homogeneously distributed overall increase of the echogenicity involving ≤ one-third of the entire muscle tissue); Grade 2 = moderate (homogeneously distributed overall increase of the echogenicity involving > one-third but ≤ two-thirds of the entire muscle tissue); Grade 3 = severe (homogeneously distributed overall increase of the echogenicity involving > two-thirds of the entire muscle tissue). f, femur; rf, rectus femoris muscle; vi, vastus intermedius muscle.

which grades muscle echogenicity from 0 to 3, where 0 = normal (normal hypoechoic muscle), 1 = mild (homogeneously distributed overall increase of the echogenicity involving ≤ one-third of the entire muscle tissue), 2 = moderate (homogeneously distributed overall increase of the echogenicity involving > one-third but ≤ two-thirds of the entire muscle tissue) and 3 = severe (homogeneously distributed overall increase of the echogenicity involving > two-thirds of the entire muscle tissue) (see **Figure 1**); (2) a visual quantitative scale (VAS echogenicity) ranging from 0 (black) to 100 (white). The same evaluation was repeated ≥6 weeks after the first one to assess the intra-observer reliability in scoring US images and clips. The online scoring spreadsheet which was used in the study is shown in **Supplementary Figure 1**. The distribution of the different grades of muscle echogenicity in patients with rheumatic diseases and healthy subjects is illustrated in **Supplementary Table 2**.

Muscle echogenicity of quadriceps muscle was also calculated in the 80 static images using ImageJ (version 1.53e) by a research assistant (SF), blind to the participants assessment of images and clips. ImageJ is a public-domain Java-based image-processing program that calculates the mean pixel grayscale intensity in a ROI using histogram analysis (30). ImageJ values of grayscale intensity range from 0 (black) and 255 (white). The rectus femoris and vastus intermedius muscles were included in the ROI to determine the mean pixel gray scale intensity. Particular attention was paid to include in the ROI only muscle tissues (i.e., without the surrounding fascia or cortical bone). Inter-observer reliability of ImageJ assessment resulted to be optimal in a recent article published by our research group (27).

Statistical analysis

Prevalence of semi-quantitative rates was reported as counts and percentages. The inter and intra-rater reliability of the semi-quantitative scale was assessed by absolute agreement and Prevalence-Adjusted and Bias-Adjusted Kappa (PABAK), which was adopted to address prevalence imbalances in the rates. Intraclass Correlation Coefficient (ICC) was used to assess the inter and intra-reliability of VAS echogenicity. Kappa coefficients were interpreted according to Landis and Koch (31). The ICC was employed to inspect the association between the semi-quantitative scale and VAS echogenicity, whilst the Kendall's Tau and Pearson's Rho correlation coefficient were used for the correlation between semi-quantitative scale/VAS echogenicity and ImageJ.

Results

Forty-four physicians (42 rheumatologists from 33 rheumatology centers and 2 radiologists from 2 radiology centers) from 13 countries participated in the study (see **Table 1** for participants' information).

The prevalence of the different grades of muscle echogenicity, as determined by the mean prevalence observed across raters, is reported in **Table 2**.

Inter-reliability assessment

As showed in **Table 3**, the overall (i.e., all grades together) global (i.e., images + clips) inter-reliability of the semi-quantitative scale was moderate [absolute agreement = 0.68 (0.68–0.69), PABAK = 0.58 (0.57–0.59)]. No considerable difference was observed between the assessment of images and clips.

Lower reliability results (i.e., lower PABAK but absolute agreement consistent with the overall evaluation) were obtained when considering the single grades of the semi-quantitative scale separately. Grade 1 and grade 2 of the semi-quantitative scale showed the lowest absolute agreement and PABAK.

The reliability of VAS echogenicity was high, with no considerable differences between images and clips assessment [*images + clips* ICC = 0.80 (0.75–0.85); *images only* ICC = 0.80 [0.74–0.85]; *clips only* = ICC 0.84 [0.74–0.92]).

Since one of the possible reasons for the US changes of muscle quality is chronic inflammation, the inter reliability of

TABLE 1 Main information of the participants in the study (n = 44).

Study participants		
Female gender, n (%)		20 (45.4%)
Years of experience in MSK US, median (IQR)		10.2 (7–15)
MSK US scans/month, median (IQR)		77.5 (30–110)
US scans of muscles/month, median (IQR)		4 (2–10)
Have you ever performed a muscle US scan?	Yes	38 (86.4%)
Why do you scan muscles?	Clinical reasons	28 (73.7%)
	Research purposes	2 (5.3%)
	Both	8 (21.1%)
Country, n%	**Rheumatology centers (n = 33)**	**Radiology centers (n = 2)**
Italy	8 (24.2%)	2 (100.0%)
Argentina	5 (15.2%)	/
Romania	4 (12.1%)	/
United Kingdom	3 (9.1%)	/
Greece	2 (6.1%)	/
Japan	2 (6.1%)	/
Portugal	2 (6.1%)	/
Colombia	2 (6.1%)	/
Brazil	1 (3.0%)	/
Canada	1 (3.0%)	/
Czechia	1 (3.0%)	/
Mexico	1 (3.0%)	/
Spain	1 (3.0%)	/

IQR, inter-quartile range; MSK, musculoskeletal; US, ultrasound.

TABLE 2 Different grades of muscle echogenicity divided by images and clips as determined by the mean prevalence observed across raters.

All raters	Global (images + clips)	Images	Clips
Grade 0	18.3%	25.0%	18.2%
Grade 1	21.7%	23.8%	21.2%
Grade 2	27.5%	25.0%	25.2%
Grade 3	32.5%	26.2%	35.4%

Participants were asked to score a total of 80 images and 20 clips (global number of evaluations = 100).

US muscle echogenicity was also analyzed after excluding patients with osteoarthritis (n = 6) and fibromyalgia (n = 4). The inter-reliability of the semi-quantitative scale and VAS echogenicity without patients with osteoarthritis and fibromyalgia remained consistent with that of the whole population of rheumatic patients (see Supplementary Table 3).

Additional analyses were carried out including either the right or left side in patients in which a bilateral acquisition of the quadriceps muscle was obtained. The inter-reliability of the semi-quantitative scale and VAS echogenicity including such population resulted consistent with that of the total population (see Supplementary Tables 4, 5).

Finally, further analyses were performed by excluding those participants (i.e., raters) with no experience in the use of muscle US. This new analyses generated consistent results with those obtained in the whole group of raters (i.e., including those with no experience in the use of muscle US) (see Supplementary Table 6).

Intra-reliability results

As illustrated in Table 3, the overall (i.e., all grades together) global (i.e., images + clips) intra-reliability of the semi-quantitative scale was substantial [absolute agreement = 0.78 (0.76–0.80), PABAK = 0.71 (0.68–0.73)]. No remarkable difference was noted between the assessment of images and clips.

Moderate to substantial intra-reliability was obtained when the single grades of the semi-quantitative scale were considered. Grade 1 and grade 2 of the semi-quantitative scale showed the lowest intra-reliability.

The reliability of VAS echogenicity remained high in the intra-observer assessment [*images + clips*: ICC = 0.88 (0.88–0.89); *images only* = ICC 0.88 (0.88–0.89); *clips only* = ICC 0.88 (0.88–0.89)].

The intra-reliability of the semi-quantitative scale and VAS echogenicity remained consistent when patients with osteoarthritis and fibromyalgia were excluded (see Supplementary Table 3), when only the right or left quadriceps muscle where considered in patients in which a bilateral US acquisition of the quadriceps muscle was obtained (see Supplementary Tables 4, 5), and when raters with no experience in the use of muscle US were excluded from the analyses (see Supplementary Table 6).

Association between the semi-quantitative scale and continuous quantitative measurements for US muscle echogenicity, and their relationships with ImageJ

As shown in Figure 2, a substantial association was found between all participants' evaluations using the semi-quantitative scale and VAS echogenicity [ICC = 0.52 (0.50–0.54)]. This corroborates the high correlation between the two visual scales that was obtained when the evaluations of the two rheumatologists who developed the images and clips dataset were taken into account ("gold standard," t = 0.89, $p < 0.01$). For further details about numerical values see Supplementary Table 7.

In addition, a strong correlation was found between the participants evaluations using the semi-quantitative scale and VAS echogenicity and ImageJ analysis (t = 0.76 for the semiquantitative scale; r = 0.89 for VAS echogenicity). Similar good results were found when the "gold standard" assessment (i.e., the assessment of the two rheumatologists who developed the images and clips dataset) was considered (t = 0.76 for the semi-quantitative scale; r = 0.89 for VAS echogenicity).

Discussion

The results of the current study demonstrated the overall good inter and intra-reliability of the US assessment of muscle echogenicity

TABLE 3 Reliability assessment of the visual semi-quantitative scale for muscle echogenicity.

	Images + clips (n = 100)		Images (n = 80)		Clips (n = 20)	
	AA	*PABAK*	*AA*	*PABAK*	*AA*	*PABAK*
Inter-reliability assessment						
Overall	0.68 [0.68–0.69]	0.58 [0.57–0.59]	0.69 [0.68–0.69]	0.58 [0.57–0.59]	0.67 [0.66–0.68]	0.55 [0.54–0.56]
Grade 0	0.66 [0.65–0.67]	0.43 [0.41–0.44]	0.67 [0.66–0.68]	0.42 [0.41–0.44]	0.61 [0.60–0.63]	0.20 [0.18–0.22]
Grade 1	0.60 [0.60–0.61]	0.24 [0.22–0.25]	0.60 [0.59–0.61]	0.21 [0.20–0.23]	0.61 [0.60–0.63]	0.29 [0.26–0.31]
Grade 2	0.64 [0.63–0.65]	0.23 [0.21–0.24]	0.64 [0.63–0.65]	0.22 [0.21–0.24]	0.65 [0.63–0.66]	0.39 [0.37–0.41]
Grade 3	0.82 [0.81–0.83]	0.37 [0.35–0.40]	0.83 [0.82–0.84]	0.39 [0.37–0.42]	0.78 [0.76–0.80]	0.10 [0.08–0.12]
Intra-reliability assessment						
Overall	0.78 [0.76–0.80]	0.71 [0.68–0.73]	0.78 [0.76–0.80]	0.70 [0.67–0.73]	0.76 [0.69–0.81]	0.67 [0.60–0.74]
Grade 0	0.78 [0.74–0.82]	0.69 [0.63–0.74]	0.77 [0.73–0.81]	0.67 [0.61–0.74]	0.75 [0.69–0.81]	0.61 [0.50–0.71]
Grade 1	0.59 [0.51–0.66]	0.47 [0.39–0.56]	0.56 [0.48–0.63]	0.42 [0.33–0.51]	0.74 [0.65–0.82]	0.65 [0.54–0.75]
Grade 2	0.55 [0.47–0.64]	0.44 [0.34–0.53]	0.55 [0.46–0.63]	0.42 [0.32–0.52]	0.68 [0.61–0.75]	0.52 [0.41–0.62]
Grade 3	0.68 [0.55–0.79]	0.63 [0.51–0.75]	0.71 [0.59–0.82]	0.66 [0.54–0.78]	0.70 [0.59–0.79]	0.61 [0.48–0.75]

AA, absolute agreement; PABAK, prevalence-adjusted, bias-adjusted kappa.
Values in square brackets are the 95% confidence intervals.

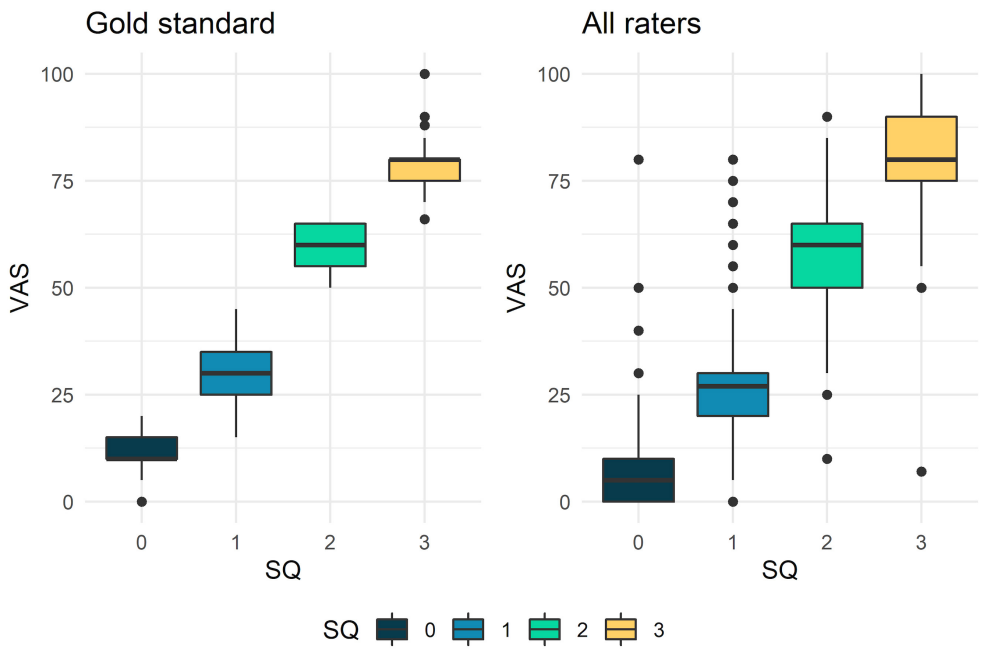

FIGURE 2
Boxplot of the joint semi-quantitative and quantitative (VAS echogenicity) ultrasound (US) scales distribution for muscle echogenicity. Box and whiskers plots showing the relationship between the semi-quantitative and the quantitative scores for muscle echogenicity. The upper and lower boundaries of the box represent the third and the first quartiles, respectively. The solid line in the box represents the median. Whiskers represent the maximum and the minimum values.

using an *ad hoc* developed dataset of US images and videos acquired in patients with rheumatic diseases.

This web-based exercise was carried out by a large group of rheumatologists and MSK radiologists who routinely perform US in their clinical practice, with a variable experience and training background in the US assessment of muscles (see Table 1).

The main objective of this study was to explore the reliability of two visual methods for the assessment of US muscle echogenicity, namely a semi-quantitative scale, which was recently developed by our research group (27), and a continuative quantitative measurement (VAS echogenicity), which was presented for the first time in this study. Both these two visual scales demonstrated an overall good inter and intra-reliability, with no remarkable difference between static images and clips assessment.

As shown in Table 3, variable grades of reliability were obtained when the single grades of muscle echogenicity of the semi-quantitative scale were evaluated. In the inter-reliability exercise, a grade 0 (i.e., normal muscle) and grade 3 (i.e., severe increase in muscle echogenicity) showed the highest, yet only moderate, degree of reliability. On the other hand, the intermediate grades

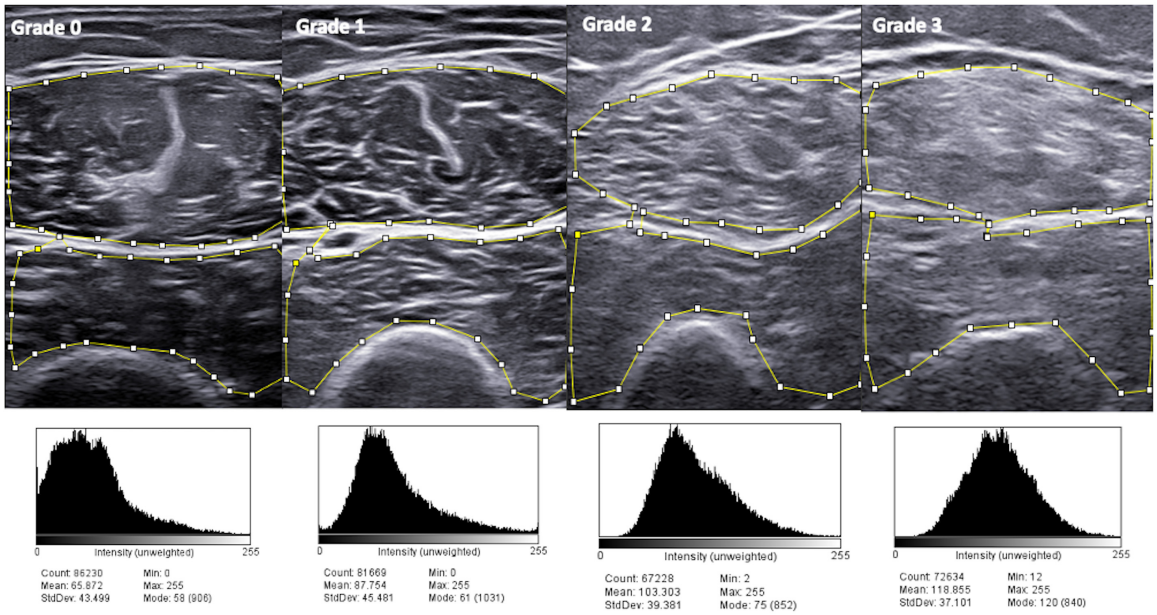

FIGURE 3
ImageJ analysis in patients with different grades of muscle echogenicity. Higher grades of the visual semi-quantitative scale for muscle echogenicity correspond to higher mean pixel analysis with ImageJ. During image analysis with ImageJ, particular attention was paid to include in the region of interest (ROI) only muscle tissues (i.e., without the surrounding fascia or cortical bone), which is the area included within the small squares and lines.

of muscle echogenicity (i.e., grade 1 and grade 2 of the semi-quantitative scale) showed the lowest degree of reliability. Such low reliability results might be at least in part explained by the relatively small number of images and clips available for each single grade of the semi-quantitative scale. Indeed, the absolute agreement of the single grades of the semi-quantitative scale was comparable with the absolute agreement of the overall evaluation (i.e., all grades together). However, we acknowledge that the distinction between the different grades of the semi-quantitative scale may be difficult in those patients with "borderline" muscle echogenicity (e.g., between normal and mild, or mild and moderate), especially in the assessment of the intermediate grades of such scale (i.e., grade 1 and 2).

On the other hand, an overall higher degree of reliability for all the single grades of the semi-quantitative scale was obtained in the intra-observer assessment (i.e., substantial reliability for grade 0 and grade 3, moderate reliability for grade 1 and grade 2).

A significant correlation was observed between the semi-quantitative scale and VAS echogenicity. Both these visual scales grade muscle echogenicity abnormalities based on extent of muscle involved as opposed to degree of echo-intensity changes, as is the custom for grading US muscle echogenicity in myopathies/neuromuscular disorders (32). While a multifocal increase of muscle echogenicity could be observed in several neuromuscular disorders, such as muscular dystrophies, motor neuron disease ("moth-eaten appearance") and inflammatory myositis, a homogeneous and broad involvement of muscle structures would be expected in patients with sarcopenia. For this reason, both the semi-quantitative scale and VAS echogenicity were developed by the current authors to score muscle echogenicity abnormalities as the extent of muscle area showing an increased echogenicity, rather than the degree of echo-intensity in a single "focal" area.

In addition, a significant association was found between both the semi-quantitative scale and continuous quantitative measurement and ImageJ (both with "all raters" and "gold standard" evaluations), which is a widely used software for processing and analyzing scientific images. Representative images of ImageJ analysis are reported in Figure 3. The main drawback of performing a software based evaluation is that this method is time consuming, other than being subjected to variations due to the fact that the areas of measurement (i.e., ROI) are defined by a human operator. In the current study, the software based evaluation with ImageJ required multiple steps: acquisition of US images on the US machine; upload of the US images from the US machine to a USB device and transfer to a computer/laptop; operator-based measurements of image echogenicity and acquisition of results. As described in the methods, the ImageJ operator of the current study included only muscle tissues in the ROI (i.e., without the surrounding fascia or cortical bone), which requires a careful and precise drawing of the borders defining the ROI (see Figure 3).

An increased muscle echogenicity is the result of the replacement of healthy muscle with fat (i.e., myosteatosis) rather than fibrosis and it is regarded as a reliable indicator of poor muscle quality (16). In addition, an increased US muscle echogenicity has been shown to be associated with muscle function and strength independently from a reduction of muscle mass, which is the main criteria for the diagnosis of sarcopenia (33–35). Therefore, US muscle echogenicity should be regarded as a reliable tool for the "early" detection of sarcopenia in patients with rheumatic diseases.

As acknowledged by the European Geriatric Medicine Society, US has a very promising role in the screening and "early" diagnosis of sarcopenia in patients susceptible to this condition (e.g., elderly populations, patients with chronic inflammatory diseases), given the ability of US to provide accurate assessment of muscle morphology and structure (i.e., muscle quality and muscle mass), good correlation

with other imaging tools which are regarded as "gold standard" for the assessment of sarcopenia (e.g., MRI, CT scan, or DXA), patient's bedside availability and relatively low costs (16, 19).

Imaging is one of the aspects that need to be considered in the diagnosis of sarcopenia. According to the European Working Group on Sarcopenia in Older People 2 (EWGSOP2), the diagnosis of sarcopenia should be made if loss of muscle mass (detectable with imaging) is accompanied by the reduction of patient's muscle strength and/or impaired physical performance (1). In this context, US may play a key diagnostic/screening role in the "early" phase of sarcopenia, potentially identifying those patients who require further investigations (e.g., grip strength test, short physical performance battery) and, when a status of sarcopenia is confirmed, a specific management (i.e., referral to dedicated physiotherapy programs, potential use of drugs and/or supplements).

In a recent systematic literature review, the Outcome Measures in Rheumatology (OMERACT) group has highlighted the need for more evidence supporting the validity, reliability, and feasibility of quantitative methods for the evaluation of US domains of muscle involvement, including muscle echogenicity (36).

Using four pre-defined categories (i.e., normal, mild, moderate, and severe), the semi-quantitative scale which was recently developed by our group allows for a quick and intuitive classification of muscle echogenicity abnormalities (27). The current results suggest that a continuous quantitative measurement (VAS echogenicity) may represent a valid option to be used in alternative or in association with the semi-quantitative measurement, especially in those patients without a normal or clearly abnormal muscle echogenicity (i.e., grade 1 and grade 2 of the semi-quantitative scale). Even if more time-consuming than a visual assessment, the use of ImageJ analysis should be considered to obtain an objective, precise and patient-targeted measurement of muscle echogenicity, especially in those patients with intermediate grades of muscle echogenicity according to the proposed semi-quantitative scale. The good correlation emerged in the current study between a visual assessment (both using a semi-quantitative scale and a quantitative continuous measurement) and a software based evaluation suggests the opportunity to consider implementation of a digital measurement into the US machine.

The sensitivity to change of the two visual scales evaluated in the current study (i.e., responsiveness to interventions, such as use of drugs and/or supplements and/or adoption of regular physical exercise), represents an important aspect that needs to be further investigated. In addition, whether the reliability results of the two scales evaluated in the current study would be obtained in the assessment of muscles with different architecture and US appearance in comparison to the quadriceps muscle (e.g., gastrocnemius muscle or upper limb muscles), should be further explored (37).

The main limitation of the current study is that participants were asked to assess muscle echogenicity on static images and clips but did not perform the US examinations by themselves. This is an important aspect to consider also in light of the fact that the US images and clips might lose important quality information when they are converted to JPEG or AVI format compared to a "live" assessment on the US screen. Therefore, further patients-based studies are desirable. In addition, the US dataset of images and clips was generated by two operators using only two different US machines; this may potentially reduce the inter-observer variations if compared with a dataset generated by multiple operators using different US machines, thus limiting the generalizability of our results. Furthermore, the lack of comparison with a reference imaging tool for the assessment of muscle involvement, such as MRI or CT, should be considered as another limitation of the study. Indeed, this could have provided insights into the understanding of the US findings (e.g., differentiation between subclinical myositis, steroid myopathy, or sarcopenia), thus improving their validity. In this context, exploring the possible correlation between the US findings and a clinical score for sarcopenia (e.g., SARC-F) or the individuals measures of such condition (e.g., grip strength, short physical performance battery, or timed up and go test), could have clarified further the clinical relevance of US muscle echogenicity in the current population of rheumatic patients. Another limitation of the study is that the reliability assessments were carried out not taking into account the disease duration of the included patients, their age, and time of corticosteroid exposure. Indeed, all these aspects might determine changes in muscle echogenicity.

This study provides evidence in support of the reliability of US muscle echogenicity in patients with rheumatic diseases. The inter and intra-reliability of two recently developed scales for muscle echogenicity was evaluated, as well as their association with ImageJ, which is a widely used software for image analysis and processing. Therefore, this novelty is the main strength of the study.

In addition, data are presented from a multicenter study, which involved many experts in MSK US from several international countries.

Conclusion

The results of this large, multicenter study support the reliability of US muscle echogenicity assessment in patients with rheumatic diseases, either using a visual semi-quantitative scale or a continuous quantitative measurement. US muscle echogenicity should be regarded as a reliable tool for the evaluation of changes of muscle quality in patients with rheumatic diseases, thus potentially representing a valuable tool for the "early" detection of sarcopenia in these patients.

Data availability statement

The raw data supporting the conclusions of this article will be made available by the authors, without undue reservation.

Ethics statement

The studies involving human participants were reviewed and approved by the local ethic committee (CERM n: 155/2021). The patients/participants provided their written informed consent to participate in this study.

Author contributions

ADM, WG, and EF established the cohort. ADM designed the study and wrote the first draft of the manuscript. ADM and GS prepared

the images and clips dataset. EM and ML developed the online exercise. GC, DR, CAS, and AZ carried out the statistical analysis. SF performed the ImageJ assessment. EC, CA, SA, AB, KB, MC, TC, DC, MAC, JA, GD, MD, ED, LD, ED, AE, DF, FF, AG, CH-D, RH, JH, DJ, JM, MVM, RM, MM, AM, JN, TO, JaR, MR, JoR, FS, CS, M-MT, ST, LV-R, CV-E, OV, PV, FV, GV, and JZH performed the reliability exercise. All authors contributed to revising the manuscript critically and approved the final version to be published.

Funding

RH and JH were supported by Ministry of Health, Czech Republic – conceptual development of research organization, Motol University Hospital, Prague, Czech Republic (00064203).

Conflict of interest

SA received honoraria from AbbVie, Celgene, UCB, Novartis, Janssen, Pfizer, and Sanofi. AB served as a speaker for AbbVie, Amgen, Sanofi-Genzyme, and UCB, outside the submitted work. EF had received speaking fees from AbbVie, Amgen, BMS, Janssen, Lilly, Novartis, Roche, Pfizer, and UCB, outside the submitted work. WG had received speaking fees from Celltrion and Pfizer, outside the submitted work.

The remaining authors declare that the research was conducted in the absence of any commercial or financial relationships that could be construed as a potential conflict of interest.

Publisher's note

Supplementary material

The Supplementary Material for this article can be found online at: https://www.frontiersin.org/articles/10.3389/fmed.2022.1090468/full#supplementary-material

References

1. Cruz-Jentoft A, Bahat G, Bauer J, Boirie Y, Bruyère O, Cederholm T, et al. Writing group for the European working group on sarcopenia in older people 2 (EWGSOP2), and the extended group for EWGSOP2. Sarcopenia: revised European consensus on definition and diagnosis. *Age Ageing.* (2019) 48:16–31. doi: 10.1093/ageing/afy169

2. Chen L, Woo J, Assantachai P, Auyeung T, Chou M, Iijima K, et al. Asian working group for sarcopenia: 2019 consensus update on sarcopenia diagnosis and treatment. *J Am Med Dir Assoc.* (2020) 21:300–7.e2. doi: 10.1016/j.jamda.2019.12.012

3. Cesari M, Landi F, Vellas B, Bernabei R, Marzetti E. Sarcopenia and physical frailty: two sides of the same coin. *Front Aging Neurosci.* (2014) 6:192. doi: 10.3389/fnagi.2014.00192

4. Shin A, Choi S, Han M, Ha Y, Lee Y, Lee E, et al. Association between sarcopenia defined as low lean mass by dual-energy X-ray absorptiometry and comorbidities of rheumatoid arthritis: results of a nationwide cross-sectional health examination. *Semin Arthritis Rheum.* (2022) 57:152090. doi: 10.1016/j.semarthrit.2022.152090

5. Therakomen V, Petchlorlian A, Lakananurak N. Prevalence and risk factors of primary sarcopenia in community-dwelling outpatient elderly: a cross-sectional study. *Sci Rep.* (2020) 10:19551. doi: 10.1038/s41598-020-75250-y

6. An H, Tizaoui K, Terrazzino S, Cargnin S, Lee K, Nam S, et al. Sarcopenia in autoimmune and rheumatic diseases: a comprehensive review. *Int J Mol Sci.* (2020) 21:5678. doi: 10.3390/ijms21165678

7. Salaffi F, Di Matteo A, Farah S, Di Carlo M. Inflammaging and frailty in immune-mediated rheumatic diseases: how to address and score the issue. *Clin Rev Allergy Immunol.* (2022) 21. [Epub ahead of print]. doi: 10.1007/s12016-022-08943-z

8. Tagliafico A, Bignotti B, Torri L, Rossi F. Sarcopenia: how to measure, when and why. *Radiol Med.* (2022) 127:228–37. doi: 10.1007/s11547-022-01450-3

9. Ticinesi A, Meschi T, Narici M, Lauretani F, Maggio M. Muscle ultrasound and sarcopenia in older individuals: a clinical perspective. *J Am Med Dir Assoc.* (2017) 18:290–300. doi: 10.1016/j.jamda.2016.11.013

10. Salaffi F, Carotti M, Di Matteo A, Ceccarelli L, Farah S, Villota-Eraso C, et al. Ultrasound and magnetic resonance imaging as diagnostic tools for sarcopenia in immune-mediated rheumatic diseases (IMRDs). *Radiol Med.* (2022) 127:1277–91. doi: 10.1007/s11547-022-01560-y

11. Reeves N, Maganaris C, Narici M. Ultrasonographic assessment of human skeletal muscle size. *Eur J Appl Physiol.* (2004) 91:116–8. doi: 10.1007/s00421-003-0961-9

12. Thomaes T, Thomis M, Onkelinx S, Coudyzer W, Cornelissen V, Vanhees L, et al. Reliability and validity of the ultrasound technique to measure the rectus femoris muscle diameter in older CAD-patients. *BMC Med Imaging.* (2012) 12:7. doi: 10.1186/1471-2342-12-7

13. Abe T, Loenneke J, Young K, Thiebaud R, Nahar V, Hollaway K, et al. Validity of ultrasound prediction equations for total and regional muscularity in middle-aged and older men and women. *Ultrasound Med Biol.* (2015) 41:557–64. doi: 10.1016/j.ultrasmedbio.2014.09.007

14. Martin D, Medri M, Chow R, Oxorn V, Leekam R, Agur AM, et al. Comparing human skeletal muscle architectural parameters of cadavers with in vivo ultrasonographic measurements. *J Anat.* (2001) 199:429–34. doi: 10.1046/j.1469-7580.2001.19940429.x

15. Kellis E, Galanis N, Natsis K, Kapetanos G. Validity of architectural properties of the hamstring muscles: correlation of ultrasound findings with cadaveric dissection. *J Biomech.* (2009) 42:2549–54. doi: 10.1016/j.jbiomech.2009.07.011

16. Perkisas S, Bastijns S, Baudry S, Bauer J, Beaudart C, Beckwée D, et al. Application of ultrasound for muscle assessment in sarcopenia: 2020 SARCUS update. *Eur Geriatr Med.* (2021) 12:45–59. doi: 10.1007/s41999-020-00433-9

17. Albano D, Messina C, Vitale J, Sconfienza L. Imaging of sarcopenia: old evidence and new insights. *Eur Radiol.* (2020) 30:2199–208.

18. Chianca V, Albano D, Messina C, Gitto S, Ruffo G, Guarino S, et al. Sarcopenia: imaging assessment and clinical application. *Abdom Radiol.* (2021) 23:1–12. doi: 10.1007/s00261-021-03294-3

19. Perkisas S, Baudry S, Bauer J, Beckwée D, De Cock A, Hobbelen H, et al. Application of ultrasound for muscle assessment in sarcopenia: towards standardized measurements. *Eur Geriatr Med.* (2018) 9:739–57. doi: 10.1007/s41999-018-0104-9

20. Albayda J, van Alfen N. Diagnostic value of muscle ultrasound for myopathies and myositis. *Curr Rheumatol Rep.* (2020) 22:82. doi: 10.1007/s11926-020-00947-y

21. Giovannini S, Brau F, Forino R, Berti A, D'Ignazio F, Loreti C, et al. Sarcopenia: diagnosis and management, state of the art and contribution of ultrasound. *J Clin Med.* (2021) 10:5552. doi: 10.3390/jcm10235552

22. Yoshida T, Kumon Y, Takamatsu N, Nozaki T, Inoue M, Nodera H, et al. Ultrasound assessment of sarcopenia in patients with rheumatoid arthritis. *Mod Rheumatol.* (2021) 13:roab049. doi: 10.1093/mr/roab049

23. Sari A, Esme M, Aycicek G, Armagan B, Kilic L, Ertenli A, et al. Evaluating skeletal muscle mass with ultrasound in patients with systemic sclerosis. *Nutrition.* (2021) 84:110999. doi: 10.1016/j.nut.2020.110999

24. Kaya A, Kara M, Tiftik T, Tezcan M, Ozel S, Ersöz M, et al. Ultrasonographic evaluation of the muscle architecture in patients with systemic lupus erythematosus. *Clin Rheumatol.* (2013) 32:1155–60.

25. Smerilli G, Castell S, Cipolletta E, Farah S, Carotti M, Salaffi F, et al. Ultrasound measurement of muscle thickness at the proximal forearm in a rheumatologic setting. *Clin Exp Rheumatol.* (2020) 38:985–8.

26. Cruz-Jentoft AJ, Romero-Yuste S, Chamizo Carmona E, Nolla J. Sarcopenia, immune-mediated rheumatic diseases, and nutritional interventions. *Aging Clin Exp Res.* (2021) 33:2929–39. doi: 10.1007/s40520-021-01800-7

27. Di Matteo A, Smerilli G, Cipolletta E, Wakefield R, De Angelis R, Risa A, et al. Muscle involvement in systemic lupus erythematosus: multimodal ultrasound assessment and relationship with physical performance. *Rheumatology.* (2022) 25:keac196. doi: 10.1093/rheumatology/keac196

28. Di Matteo A, Cipolletta E, Destro Castaniti G, Smerilli G, Airoldi C, Aydin S, et al. Reliability assessment of the definition of ultrasound enthesitis in SpA: results of a large, multicentre, international web-based study. *Rheumatology.* (2022) 16: keac162.

29. Smerilli G, Cipolletta E, Tanimura S, Di Battista J, Di Carlo M, Carotti M, et al. Ultrasound measurement of muscle thickness at the anterior thigh level in rheumatology setting: a reliability study. *Clin Rheumatol.* (2020) 40: 1055–60.

30. Schneider C, Rasband W, Eliceiri K. NIH Image to ImageJ: 25 years of image analysis. *Nat Methods.* (2012) 9:671–5. doi: 10.1038/nmeth.2089

31. Landis J, Koch G. An application of hierarchcal k-type statistics in the assessment of majority agreement among multiple observers. *Biometrics.* (1977) 33:363–74. doi: 10.2307/2529786

32. Heckmatt J, Leeman S, Dubowitz V. Ultrasound imaging in the diagnosis of muscle disease. *J Pediatr.* (1982) 101:656–60. doi: 10.1016/S0022-3476(82)80286-2

33. Buckinx F, Landi F, Cesari M, Fielding R, Visser M, Engelke K, et al. Pitfalls in the measurement of muscle mass: a need for a reference standard. *J Cachexia Sarcopenia Muscle.* (2018) 9:269–78. doi: 10.1002/jcsm.12268

34. Wijntjes J, van Alfen N. Muscle ultrasound: present state and future opportunities. *Muscle Nerve.* (2021) 63:455–66. doi: 10.1002/mus.27081

35. Casey P, Alasmar M, McLaughlin J, Ang Y, McPhee J, Heire P, et al. The current use of ultrasound to measure skeletal muscle and its ability to predict clinical outcomes: a systematic review. *J Cachexia Sarcopenia Muscle.* (2022) 13:2298–309. doi: 10.1002/jcsm.13041

36. Paramalingam S, Morgan K, Becce F, Diederichsen L, Ikeda K, Mandl P, et al. Conventional ultrasound and elastography as imaging outcome tools in autoimmune myositis: a systematic review by the OMERACT ultrasound group. *Semin Arthritis Rheum.* (2021) 51:661–76. doi: 10.1016/j.semarthrit.2020.11.001

37. Pillen S, van Alfen N. Skeletal muscle ultrasound. *Neurol Res.* (2011) 33:1016–24. doi: 10.1179/1743132811Y.0000000010

Frontiers in Medicine

Translating medical research and innovation into improved patient care

A multidisciplinary journal which advances our medical knowledge. It supports the translation of scientific advances into new therapies and diagnostic tools that will improve patient care.

Discover the latest Research Topics

See more →

Frontiers

Avenue du Tribunal-Fédéral 34
1005 Lausanne, Switzerland
frontiersin.org

Contact us

+41 (0)21 510 17 00
frontiersin.org/about/contact